The University of Leeds, School of Geography.

Characteristics of surge-type glaciers

Hester Jiskoot

October 1999

Submitted in accordance with the requirements for the degree of
Doctor of Philosophy.

Abstract

Glacier surging is an internally triggered oscillatory flow instability in which abrupt increases in flow velocity are accompanied by a downglacier transport of ice and often a marked frontal advance (Meier and Post, 1969). The exact mechanism(s) of surging and surge trigger(s) are still largely unknown as are the factors controlling surging. This PhD research explores and quantifies the relations between surge-type glaciers and glacial and environmental characteristics by isolating factors that discriminate surge-type glaciers from normal glaciers, hence the controls on surging. These controls are then used to verify proposed surge mechanisms. Further, variations in surge behaviour are used to distinguish between groups of surge-type glaciers and surge behaviour.

Through multivariate logit analysis, a set of glacial, mass balance related, geological, and thermal attributes of a glacier population in Svalbard were tested on the prevalence of surging. Long glaciers with steep slopes overlying fine-grained lithologies younger than Devonian and with orientations in a broad arc from NW to SE are shown to be more likely to exhibit surge behaviour. Further, polythermal regime and elevation span were found to be strongly related to the likelihood of surging. Residual analysis revealed a number of previously unidentified surge-type glaciers, as well as surge-type glaciers with uncommon characteristics. Glaciers in the Yukon Territory, Canada, were also analysed: long glaciers had increased surge probabilities. Fowler's index, an indication of a linked cavity surge mechanism, was only found to be significantly increasing the likelihood of surging for shorter glaciers. The findings of the logit analysis suggest that in Svalbard, Kamb's linked-cavity surge theory is not supported, but surges probably take place through a soft bed mechanism, with a possible thermal control. No significant relation between subglacial geological boundaries or mass balance attributes and surging was found. Possible causes of glacier length and substrate controls on surging are subglacial debris composition, longitudinal stress distribution and hydrological instability.

The surge history and behaviour of Sortebræ (68°45′N, 27°05′W), East Greenland was analysed and compared to surges in other regions. Sortebræ's western flow unit surged between 1933 and 1943 and the glaciers main flow unit surged between 1991 and 1995. Vertical and horizontal movements, as well as surface features of the 1990s surge, were analysed in detail using multi-model photogrammetry. The surge affected an area of 335 km^2 and resulted in an ice volume displacement of 18.6±0.4 km^3, causing a surplus calving flux of 2.3±0.1 to 5.9±0.4 $km^3\ a^{-1}$. In less than 2 years the tidewater front advanced 4-5 km. Sortebræ has a quiescent phase of at least 60 years and a surge phase of 2-4 plus years. The behaviour of this surge and others in East Greenland suggests that the surge mechanism in this region resembles that of Svalbard, rather than other regions. Observations of interacting flow units of Sortebræ suggest that restriction of outflow could be a major control on surging.

Table of Contents

Chapter 3: Review of Previous Research Isolating Surge Controls

Chapter 4: Methodologies: Logit Modelling and Multi-Model Photogrammetry

List of Figures

List of Tables

List of Symbols

a	exponents in the Boulton-Hindmarsh till rheology
a_c	fraction of debris supplied to accumulation area
A	constant in Boulton-Hindmarsh till rheology
A	glacier surface area (Chapters 5 and 7)
A^*	normalised glacier area, dimensionless
b	constant in the Boulton-Hindmarsh till rheology
b_i	constant in calculations of sedimentary bed index
B	temperature dependent constant from Glen's Law
c_1	constant in internal deformation velocity equation
C	cohesion of sediment (Chapter 2)
C	discriminant function (Chapter 3)
C_T	thermal constant
D	constant dependent on ice thickness
e_i	residual
f	shape factor, dimensionless
f^*	fractional area of the bed occupied by water film
F	glacier surface area
$\widetilde{F}$	Fowler's index: dimensionless product of glacier width squared and bed slope
$\widetilde{F}_{cat}$	categorical value for Fowler's index
g	the gravitational force, ≈9.8 m s^{-2}
h	depth of deformable layer
h_1	average pre-surge glacier thickness
h_2	average post surge glacier thickness
h_r	mean altitude range of mountains surrounding a glacier
H	ice thickness
H_1	highest measurement point
H_2	lowest measurement point
I	bed separation index
J	inclination of pro- and subglacial meltwater streams
$J_{S.x}$	fraction of multiple correlation unexplained by simple correlation
k	constant in sliding velocity equation
k^{-1}	fraction of total force acting parallel to the bed
l	length of the flowline
L	glacier length
m	contant in sliding velocity equation
M	Manning roughness
n	constant from Glen's Law
N^*	dimensionless effective pressure term
N_0	cohesion term
N_e	effective pressure
N_K	pressure at which linked-cavity drainage is stable
N_R	pressure at which conduit drainage is stable
p	precision

p_i ice overburden pressure
p_w water pressure
p_{crit} critical water pressure
P annual precipitation
P_i probability of an event occurring
P_s surge probability
q geothermal factor
Q ice flux
Q_c critical ice flux
r dimensionless bed roughness parameter
r^2 correlation coefficient
R sedimentary bed index
$R_{S.x}$ simple correlation to surging
$R_{S.123\ldots m}$ multiple correlation to surging
s bed-smoothness measure
s_{max} maximum value in ice flux curve
S flux shape factor (Chapter 2)
S assigned surge index (Chapter 3 and onwards)
S_{NEW} updated surge index
$\hat{S}$ fitted value in logit models
u_2 horizontal surge velocity
U^* dimensionless velocity term
U_- velocity of lower (slow) branch in Fowler's surge theories
U_+ velocity of upper (fast) branch in Fowler's surge theories
U_b bed deformation velocity component
U_d internal deformation velocity component
U_s sliding velocity component
U_s* increased sliding velocity
V net basal motion (Chapter 2)
V volume (Chapter 7)
w surge front propagation velocity
W average glacier width
$\widetilde{W}$ dimensionless average glacier width
X_i parameter value
Z elevation
Z^* normalised glacier elevation, dimensionless
α angle of average ice surface slope
α base estimate or offset (Chapter 4)
α^* dimensionless parameter of self similar beds
β_b bed geometry factor
β cavitation term (1 for cavitation, 2 for no cavitation)
β_s steepest angle between stoss face of bed obstacles and mean bed slope
β_k parameter estimates
γ amplitude of bed irregularities
δ degree of cavitation

$\dot{\varepsilon}$	shear strain rate
ε	error term
ε_T	total absolute error
η	ice viscosity
κ	flow parameter in Fowler's theories
κ_c	critical flow parameter for transition from conduit to linked-cavity drainage
λ	orifice wavelength
λ_i	wavelength of bed irregularities
Λ	controlling obstacle size (Chapter 2)
Λ	maximum likelihood (Chapter 4)
Λ'	finite thickness of water film
Λ_b	hydraulic length of the cavities
μ_1,μ_2	dimensionless parameters related to bed roughness
o	orifice amplitude
Ξ	orifice melting stability parameter for step orifices
Ξ'	orifice melting stability parameter for wave orifices
ρ	ice density, ≈900 kg m^{-3}
σ	effective pressure
τ	basal shear stress
τ^*	dimensionless stress term
τ_0	sediment yield stress (or yield strength)
Φ	balance flux per width
ϕ	friction lubrication factor
ϕ_s	sediment friction angle
$\tilde{\chi}$	ten times bed slope in radians (often substituted by surface slope)
ω	orifice tortuosity

Acknowledgements

*"Although all glaciologists are **in** ice, they are not all **of** ice"*

Glaciology can sometimes be a lone struggle or a lone triumph, but it is a field where collaboration with others is vital. I have had the opportunity to meet many inspiring people in the broad field of glaciology. First I am indebted to my supervisor, Tavi Murray, who stimulated me to start the PhD on glacier surging, kept me focussed and was always available to give critical feedback and support. She further gave me many opportunities to contribute to national and international conferences and invited me to take part in fieldwork on Bakaninbreen, Svalbard. The freedom that Tavi gave me during my PhD was much appreciated.

Paul Boyle, Mike Kirkby and Stan Openshaw, my Research Support Group, are thanked for their critique and suggestions on route to this thesis. Paul is in particular thanked for his help with logit modelling. Present and past members of the Leeds Glaciology Group are thanked for sharing good and bad times (and coffees) and for having many a discussion. Andy Evans, Phil Porter and John Woodward are thanked for reading manuscripts and providing feedback. I thank Seraphim Alvanides for his help with Arcinfo and other GISish. Further I acknowledge the technical and support staff at the School of Geography for their help and assistance.

Due to the nature of the research, visits to glacier data archives were indispensable. In total, six weeks were spent at the Norsk Polarinstitutt (NPI), Oslo, and four months at the Geological Survey of Denmark and Greenland (GEUS), Copenhagen. Unlimited access to the NPI aerial photograph archive and map collection was provided by Trond Eiken, Bjørn Barstad and Bjørn Lytskjold, electronic map and inventory data were made available by Torstein Berge and Geir Anker, and Jostein Amlien provided satellite images. Brit Luktvasslimo is thanked for putting me up in Oslo in 1996 and Bjørn Lytskjold for lending me his bike in 1998. Also 'tusind takk' to Harald Aas and other members of the Mapping Department of the NPI for their help and hospitality. At GEUS, Carl Bøggild, Henrik Højmark Thomsen and Wolfgang Starzer gave logistic, scientific and amiable support, and are thanked for every aspect. Anker Weidick's Greenland glacier archive at GEUS was indispensable. I also warmly thank Anker his office at GEUS and for provided much appreciated feedback. Tapani Tukiainen is thanked for his help with satellite images. The Department of Hydrology and Glaciology under Bjarne Madsen are thanked for their hospitality and making me feel part of the team even before I spoke Danish. I thank Asger Ken Pedersen and Lotte Melchior Larsen for the Danish Lithosphere Centre stereo photographs of East Greenland and for spending much time on getting the right copies. I also owe Asger 'mange tak' for his help with photogrammetric measurements at the Institute of

Surveying and Photogrammetry, Technical University of Denmark. Fleming Bernth at Kort & Matrikelstyrelsen is thanked for his assistance with the Greenland aerial photographs. Tak for hjælpen allesammen!

I would like to thank David Bahr, Helgi Björnsson, Garry Clarke, Jon-Ove Hagen, Chris Haggerty, Martin Hoelzle, Jaçek Jania, Thomas Jóhannesson, Barclay Kamb, Vladimir Konovalov, Shawn Marshall, Jaap van der Meer, Anne-Marie Nuttall, Simon Ommanney, Veijo Pohjola, Viktor Popovnin, Oddur Sigurðsson and David Sugden for their exchange of ideas and material. Jeffrey Schmok is thanked for GLADYS, the Canadian Glacier Inventory. Very helpful institutions were CRELL, NSIDC, SPRI and WGI. Many thanks to Dick van der Wateren who made me keen on ice in the first place, while teaching Geography back in 1981.

Brian Davison, Tavi Murray, Andy Smith and John Woodward taught me to skidoo, bear polar, frostnip, and further initiated me in GPR, seismics, hot water drilling, and cold temperature engineering during the spring fieldseason on Bakaninbreen. They are all thanked for sharing five weeks of small world in a vast whiteness.

The hospitality and help of friends abroad is much appreciated. Jon Haber put me up in Oslo and showed me Gaustatoppen. Kalle & Line Vestman Hansen are thanked for sharing their house in Copenhagen and their friendship with me. Andreas Ahlstrøm is thanked for discussions and essential library searches. Other friends I would like to thank for good times, help and support are Σεραφειμ Αλβανιδης, for being a perfect office mate, Gill Black, Julia Bottomley, Covadonga Escandón, Heather Eyre, Steffen Fritz, Sarah Fuller, Nicola Gamble, Vicky Hipkin, Ian Jones, Tobias Kerzenmacher, Wouter Knap, Catherine McKinna, Paul Norman, Mike Nuttall, Claire Prospert, Linda See, Andy Turner and Tom Wilson. It's great to have people like you around!

The School of Geography is thanked for providing the PhD scholarship and for additional logistic and financial support. Further support was through an EU-Leonardo placement scheme to work at GEUS, for which I also thank Martine Peers at the European Office. ESF-EISMINT funded two valuable learning experiences: the 1997 Summerschool on modelling of glaciers and ice sheets in Karthaus, Italian Alps, and the 1998 workshop on Vatnajökull in Iceland. For these I would also like to thank Hans Oerlemans and Helgi Björnsson. The Bakaninbreen research was funded by NERC grants (GR3/R9757 and GR3/R9031).

Last, but should come first, are my family and friends whose love and letters always seem to find me, whether in +45°C in the Israeli desert or in -35°C in the Arctic one. Iedereen bedankt!

CHAPTER 1:
Glacier Surging and Surge-Type Glaciers

The principal task for the glaciologist is an investigation into the variations in the rapidity of motions of glaciers within a restricted area, for the purpose of throwing light on the differences between "living" and "dead" ice

Gabel-Jørgensen (1940, p. 139)

1.1 Introduction and thesis aims

Glacier surging is an internally triggered recurring ice flow instability, accompanied by a downglacier transport of ice and often, but not necessarily, a marked terminus advance (Meier and Post, 1969). In glaciers that experience surging, *surge-type glaciers*, long periods of quiescence, in which the ice flow is virtually stagnant, are alternated with short periods of surge, in which the flow velocity increases abruptly and where fast flow is maintained over some time. Although surging is only observed in a small percentage of glaciers world-wide, it is a key topic in the study of ice flow dynamics. Despite field observations and physical modelling of surges, the surge mechanism(s) and trigger(s) still remain obscure and the controls on surging are still incompletely understood. A number of surge models have been developed but because of the small number of well-documented glacier surges, it is difficult to test the global validity of these models. Information on surge controls might be concealed in glacier characteristics that distinguish surge-type glaciers from normal glaciers. In addition, there might be information on surge controls in the spatial distribution of surge-type glaciers, which is markedly non-uniform, both on a global and a local scale (Post, 1969; Clarke *et al.*, 1984). However, no single characteristic has been found that explains the distribution of surge-type glaciers and it has therefore been suggested that a combination of factors control surging (Glazyrin, 1978; Clarke, 1991; Hamilton and Dowdeswell, 1995). Therefore, the topic of this thesis will be to assess surge controls through multivariate analysis of glacial and environmental attributes that discriminate surge-type glaciers from normal glaciers and from comparing surge behaviour in different regions. The specific research aims of this thesis are:

- To provide a method to test and validate existing theories on the mechanisms of glacier surging by means of isolating environmental and glacier related factors responsible for the distribution of surge-type glaciers,
- To identify diagnostic characteristics of surge-type glaciers by discriminating surge-type glaciers from non-surge-type glaciers,
- To develop a method that can be used to predict if glaciers are of normal type or of surge-type,
- To assess whether there are distinct classes of surge-type glaciers and of surge behaviour.

1.2 Research approach

In order to achieve the thesis aims the following research approach will be implemented:

1. From theories on surge mechanisms and ice flow instabilities and from previous research into the controls on surging, a set of key variables (or 'explanatory' variables) will be selected to test their relationship with glacier surging,
2. With these key variables, or derivatives, a glacier inventory of surge-type and normal glaciers will be developed,
3. A multivariate data analysis will be selected that is capable of analysing the independent and combined effects of explanatory variables on the incidence of glacier surging and of predicting surge probabilities for individual glaciers,
4. Testing and validating of existing theories on the mechanism(s) of glacier surging will be realised by means of relating environmental and glacial characteristics of surge-type glaciers to the hypotheses on surge mechanisms,
5. The surge behaviour in different regions will be compared and will be analysed with respect to possible multiple surge mechanisms.

The construction of a glacier inventory (step 2) is greatly facilitated by the availability of data from the world glacier inventory and local glacier inventories (e.g. Ommanney, 1980; IAHS(ICSI)/UNEP/UNESCO. 1989; Hagen *et al.*, 1993). However, the data available in electronic glacier databases is limited and additional glacial and environmental data need to be collected from maps, aerial photographs, publications and other sources in order to obtain a complete dataset appropriate for the intended analysis. In the scope of a PhD research it would be impossible to collect additional data from all regions with surge-type glaciers. Therefore, a key study area, Svalbard, has been selected on which data analysis will be performed. In addition, the surge characteristics and impact of the 1990s surge of Sortebræ, East Greenland, will be analysed and compared to surge behaviour of other surge-type glaciers, particularly those in Svalbard.

1.3 Glacier surging

A glacier is a large body of ice and firn that is in motion due to gravitational forces. However, the actual ice flow velocity can vary from glacier to glacier. Variations in glacier motion are measured between the extremes of slow flow (~5 m a^{-1}) for Ice Stream C, Antarctica, to extremely fast flow (20 km a^{-1}) during the surge of Variegated Glacier, Alaska (Clarke 1987). Average flow conditions for valley glaciers are in the order of 10^1-10^2 m a^{-1}, whereas for fast flowing outlet glaciers velocities are in the order of 10^3 m a^{-1} (Paterson, 1994). Most glaciers have small seasonal velocity fluctuations, with the fastest velocities occurring in the meltseason

(e.g. Iken, 1981). Theoretically, ice fluxes in glaciers should discharge the accumulated ice volume downglacier in order to maintain a steady-state glacier profile: this is the balance flux. The corresponding velocity, the balance velocity, is controlled by mass balance conditions and glacier geometry and can be calculated when mass balance conditions and glacier depths are known or can be estimated (e.g. Clarke, 1987a; Budd and Warner, 1996). Most glaciers have actual flow velocities very close to their balance velocity. However, some glaciers behave in a pulsating manner, resulting from flow instabilities. In these glaciers the ice flow can suddenly switch between slow flow and fast flow and the actual flow velocities are dissimilar to the balance velocities. Examples of pulsating glaciers are unstable tidewater glaciers, oscillating between one stable position and another, while constrained by fjord geometry, and ice streams, which have been inferred to switch on and off, oscillating between fast flowing modes and slow flowing modes (e.g. Clarke, 1987a; Meier and Post, 1987; Alley *et al.*, 1989; Alley and MacAyeal, 1994). Glacier surging is a specific type of pulsating flow behaviour, in the sense that it is internally triggered and has a semi-regular cyclic recurrence period (Meier and Post, 1969; Clarke, 1987a; Raymond, 1987). The surge cycle involves long periods (15-100 yr) of quiescence, with slow flow velocities of up to a few hundreds metres per year and much lower than the balance velocity, interspersed with short active, or surge, periods (1-10 yr), in which a 10-100 fold increase of flow velocity results in average velocities of more than 1000 m a^{-1}, greatly exceeding the balance velocity (Meier and Post, 1969; Clarke, 1987a; Dowdeswell *et al.*, 1991). Glaciers showing surge evidence are called surge-type or surging glaciers, yet, the last term is usually restricted to the period when a glacier is in its surge phase.

Surge behaviour has been identified and reported since the early 20th century (e.g. Tarr and Martin, 1914) and occurs in a wide variety of glacier types and sizes. By integrating common patterns from observations of a large number of surge-type glaciers a generalised description of glacier surging has been developed that should encompass all surge-type glaciers, although individual surge behaviour can vary. Every surge-type glacier can be divided into a reservoir zone, in which ice accumulates during the quiescent phase, and a receiving zone, which is undernourished and depleted in quiescence (Dolgoushin and Osipova, 1975). These zones do not necessarily coincide with the accumulation and ablation areas of a glacier, instead, the location or zone where the outflow is restricted determines the boundary between these zones (Clarke *et al.*, 1984). During surge, a large volume of ice is transported from the reservoir zone to the receiving zone. Dolgoushin and Osipova (1975) divided the surge cycle into three phases:

1) *The build-up phase*, where the glacier profile steepens as a result of a restricted outflow and a vertical accretion, and can be steeper than its lateral trimlines (Meier and Post, 1969). In this phase, the glacier is on the verge of flow instability and basal shear stress is maximal. Short periods of speed-ups, called mini-surges, can appear, in conjunction with basal water

pressure fluctuations and vertical uplifts and drops in the glacier surface (Kamb and Engelhardt, 1987; Harrison *et al.*, 1994). Further, a marked ramp of ice, a surge bulge, up to tens of metres in height can form at the boundary between the reservoir and receiving zones (Dolgoushin and Osipova, 1975; Clarke *et al.*, 1984).

2) *The surge phase*, where the ice is transported from the reservoir zone to the receiving zone, and ice velocity increases abruptly. A surge often initiates in the upper regions and propagates downglacier as a surge-front. Above the surge font, the ice flow is extensional, resulting in transverse crevassing, while downglacier of the surge front the flow is compressive. A glacier in full surge, is often completely crevassed (see Section 1.4.2). When the surge front reaches the terminus region a marked frontal advance can take place (Meier and Post, 1969). During surge the glacier profile becomes rapidly shallower due to the rapid down-draw in the upper region and a thickening of the lower region. The surge phase usually terminates abruptly with a sudden slowdown to pre-surge velocities, often accompanied by a measurable drop in the ice surface and outburst floods (e.g. Kamb *et al.*, 1985; Fleisher *et al.*, 1995).
3) *The stagnation and depletion phase*, where the glacier is virtually stagnant, a rapid depletion of the lower regions occurs and crevasses close slowly. The glacier surface often looks irregular and pitted (Liestøl *et al.*, 1980; Sturm, 1987; Weidick, 1988). The ice may also become covered in moraine material and medial moraines in the lower zone tend to tower above the depleted glacier surface (Dolgoushin and Osipova, 1975).

Surface velocity of glaciers is the result of three components: internal deformation, basal sliding and bed deformation (see Section 2.3). These components contribute in various degrees to the net glacier movement. The sudden changes in velocity during surge indicate that critical thresholds in ice flow dynamics exist where the ratio of flow mechanisms can change. This change in ratio can be derived from velocity profiles across the width of a glacier. In quiescence the profiles are hyperbolic with the highest velocity in the centre of the glacier, whereas during surge the profiles are more ‘block-like’ and the velocity distribution is equal over the width of the glacier. This ‘block-schollen’ flow indicates that the influence of valley wall drag is confined to a narrow shear margin and that the glacier is decoupled from its bed (Paterson, 1994). Observations and measurements of surge-type glaciers during both surge and quiescent phases, provide a basis for the development of theories and models of glacier surging. Observational evidence during the active phase of surging glaciers demonstrates that fast flow during surges results from motion at the glacier bed rather than creep instability within the glacier ice. Fast flow during surging is facilitated by water trapped at pressure beneath the ice and sudden variations in subglacial water pressure could play a crucial role in the surge instability (Clarke *et al.*, 1984). Dichotomous views of the process of fast flow have emerged,

dependent on whether the glacier is underlain by hard and impermeable bedrock or soft and permeable sediments (e.g. Boulton, 1979; Kamb, 1987). Subsequently, three different mechanisms of instability have been suggested to control glacier surging: *i.e.* thermal, hydrological and substrate instability. However, after years of research on surging it still remains unclear which physical processes cause the periodic flow switches characteristic for glacier surging. Details of surge mechanisms and connected controls on surging are discussed in detail in Chapter 2.

1.3.1 Why study surge-type glaciers?

Apart from glaciologists being excited about the enigma of surging and the dramatic impact of surges, glacier surging holds crucial information on ice flow dynamics and can have important environmental implications. Surging of glaciers can be viewed as a small-scale analogues for unstable ice stream behaviour. Surges of ice sheets could have catastrophic effects discharging very large volumes of ice into the ocean and on land over one or more years (e.g. Radok *et al.*, 1987). Surging could also be important in the reconstruction of the behaviour of Pleistocene ice sheets such as the Laurentide ice sheet, producing the repetitive glaciomarine layers in Pleistocene ocean cores known as Heinrich events (Alley, 1991). Furthermore, glaciers are commonly used to derive long term climate signals. However, this signal may be obscured or even non-existent in surge-type glaciers (Jóhannesson and Sigurðsson, 1998). It is therefore critical to realise from which type of glaciers the climate signal is derived and for this purpose surge-type glaciers would be inappropriate. Also, methods such as tracing equilibrium line altitudes from concave to convex contour-line change (concave in the accumulation area and convex in the ablation area) can be problematic for surge-type glaciers, since a sudden redistribution of ice in surge can obscure this contour-line pattern (Wilbur, 1988). Switches between normal and fast flow in surge-type glaciers provide important information on glacier dynamics. Research involving surge mechanisms and triggers thus provide important information for the development of physical laws used in glacier and ice sheet modelling (e.g. Lliboutry, 1968; Bindschadler, 1982; Mazo and Salamatin, 1986; Fowler, 1989; Alley, 1992; Marshall and Clarke, 1997). Further, glacier surging has been treated as equivalent to thrust sheet emplacement (Sharp *et al.*, 1988), and could be seen as metaphors for other processes such as turbidite formation, hill slope instablity and ice- and snow avalanches. Although exact processes might be different, a cross fertilisation of state-of-the-art knowledge on these subjects could help in solving the enigma of surging. This task is however beyond the scope of this thesis.

Surging is also associated with natural hazards such as outbursts of glacier-dammed lakes in the Central Andes, and the trapping of sea animals caused by the surging Hubbard Glacier damming a fjord in Alaska (e.g. Anonymous, 1986; Bruce *et al.*, 1987; Lliboutry, 1998). In 1985, artificial drainage of a glacier-dammed lake on the depleted surface of quiescent Bogatyr Glacier, Tien Shan, was needed in order to prevent flooding of downstream areas (Nurkadilov *et al.*, 1986). Furthermore, the 'Alaska Pipeline' passes through a region where glacier surging is frequently observed and it is possible that a surge advance could damage the pipeline and cause a major environmental hazard. Further, surges of tidewater glaciers can discharge large numbers of icebergs in a short period of time. This can have major effects on shipping routes, exploration of oil/gas, *etc.* (Dowdeswell, 1989; Lefauconnier and Hagen, 1991). Predictions of glacier surges and surge models could be useful tools to alleviate the effects of these natural hazards.

1.3.2 The spatial distribution of surge-type glaciers

Surge behaviour has been identified and reported since the early 20th century (e.g. Tarr and Martin, 1914) and occurs in a wide variety of glacier types and sizes. However, the spatial distribution of surge-type glaciers is non-uniform on both a global and regional scale (Clarke *et al.*, 1986). In most areas there are no surge-type glaciers, but clusters of surge-type glaciers exist in Alaska, Canada, the Central Andes, Tien Shan, Pamir, Kamchatka, Karakoram, Iceland, Greenland and Svalbard and the Russian High Arctic (Paterson, 1994; Dowdeswell and Williams, 1997) (Figure 1.1 and Table 1.1).

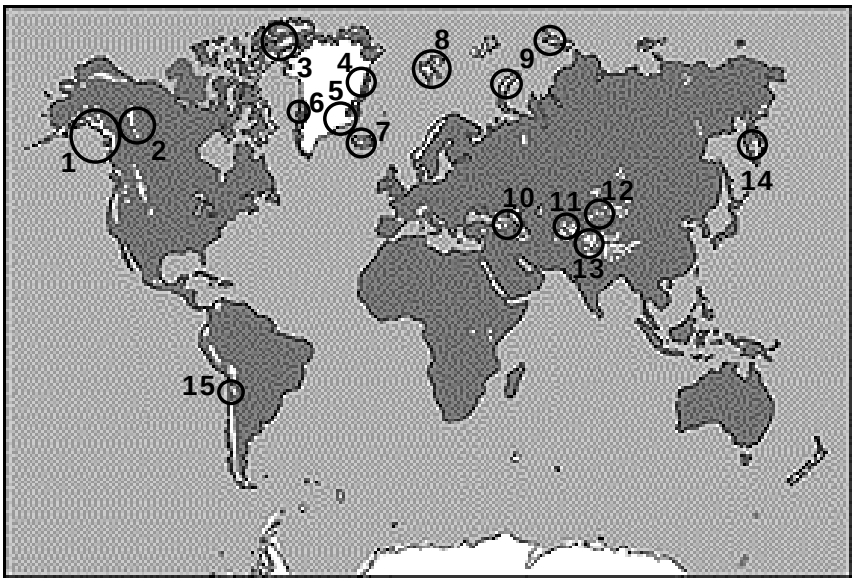

Figure 1.1: *Distribution of surge-type glaciers world-wide. All white shaded areas are glaciated. Cluster regions of surge-type glaciers are circled and numbered: 1=Western North America, 2= Yukon Territory, 3= Canadian High Arctic, 4=NE Greenland, 5=E Greenland, 6=W Greenland, 7=Iceland, 8=Svalbard, 9= Russian High Arctic (two circles), 10=Caucasus, 11=Pamir, 12= Tien Shan, 13=Karakoram, 14=Kamchatka, 15=Central Andes (Source basemap: USGS, 1994).*

In some regions, for example Antarctica (Wellman, 1982); Tibet (Zhang Wenjing, 1992) and Patagonia (Rivera *et al.*, 1997), a number of glaciers exhibit characteristics of surge-type glaciers but observations of true surges are lacking: these regions are excluded from the list of cluster regions. The catastrophic advances of Vernagtferner, Austrian Alps, between 1599 and 1845 are generally considered as surges (Finsterwalder, 1897; Hoinkes, 1969), but the Alps are (at present) considered as a region devoid of surge-type glaciers as this glacier is the single example of internally triggered surging in this region and has since ceased its activity. The pattern of clustering in certain regions and complete absence from others implies that environmental conditions control surging (Post, 1969). Despite various regional studies into this subject, it still remains obscure what controls the distribution of surge-type glaciers and which environmental conditions control surging (Post, 1969; Glazyrin, 1978; Clarke *et al.*, 1984; Wilbur, 1988; Clarke 1991, Hamilton, 1992; Hamilton and Dowdeswell, 1995). In Chapter 3 of this thesis a complete account of the research into the controls on surging is given.

Sharp (1988a) estimated that 4% of glaciers world-wide were of surge-type. However, the actual numbers of surge-type glaciers (Table 1.1) suggest that this is an overestimation of about 2000 glaciers. In Table 1.1, the total numbers of surge-type glaciers are a combination of figures from references in the right hand column, while the total for Antarctica is estimated by extrapolating Greenland's data (Weidick *et al.*, 1992), while taking into account the difference in size and assuming that the glacier density in Antarctica is half that of Greenland as there is hardly any local ice. The total number of glaciers world-wide is calculated by adding published total numbers of glaciers from different regions (Kotlyakov, 1980; Shih Ya-feng *et al.*, 1980; Chinn, 1989; IAHS(ICSI)/UNEP/UNESCO, 1989; Weidick *et al.*, 1992). The estimate of 157122 glaciers world-wide is in agreement with a recently published estimate of 160000 glaciers world-wide (Bahr and Dyurgerov, 1999). If 'true' glaciers are defined as the glacier population in which surge behaviour is possible, following the procedures of Clarke *et al.* (1986) (*i.e.* excluding all glacierets, névés, rock glaciers, snow patches, niches and ice aprons), Weidick *et al.* (1992) or Hagen *et al.* (1993) (i.e. exclude all glaciers smaller than 1 km^2), then it is estimated that about 50% of all glaciers world-wide are true glaciers. Therefore, even if the percentage of surge-type glaciers is calculated as fraction of the true glacier population, 717/78561= 0.91%, which is less than 1% of total glacier population. (Table 1.1). However, ongoing research to surge-type glacier slowly adds small numbers of surge-type glaciers to the existing lists (e.g. pers. comm., Weidick, 1997; Hewitt, 1998). In cluster regions, surge-type glaciers have been estimated to count between 1 and 7% of the total regional glacier populations, and locally even more (Clarke *et al.*, 1986; Hamilton and Dowdeswell, 1995; Kotlyakov *et al.*, 1997; Jiskoot *et al.*, 1998).

DISTRIBUTION OF SURGE-TYPE GLACIERS WORLD-WIDE					
Geographical Area	**Number of surge-type glaciers[1]**	**Number of observed surging glaciers[2]**	**Total number of glaciers[3]**	**% of surge-type glaciers**	**References**
Svalbard	146	104	2128	6.9 %	1+2: Liestøl, 1969; Schytt, 1969; Robin and Weertman, 1973; Clapperton, 1975; Hagen, 1987; Croot, 1988; Dowdeswell, 1989, Hodgkins and Dowdeswell, 1989; Dowdeswell *et al.*, 1991; Lefauconnier and Hagen, 1990 and 1991; Hamilton, 1992; Hagen *et al.*, 1993; Liestøl, 1993; Dowdeswell *et al.*, 1995 ; 3: IAHS(ICSI)/UNEP/UNESCO, 1989
Iceland	15		330	4.5 %	1: Thorarinsson, 1969. 3: Williams, 1983
Greenland	71	18	14585*	0.5 %	1+2: Higgins and Weidick, 1988; Weidick, 1983, 1988, 1995. 3: Weidick *et al.*, 1992 (5297 in West Greenland); IAHS(ICSI)/UNEP/UNESCO, 1989; Reeh *et al.*, 1994;
Western North America	152	37	>8000	1.3 %	1: Horvath and Field, 1969; Post, 1969; Clarke *et al.*, 1986
Yukon Territory and Canadian High Arctic	153	38	100 000 (4681)	0.2 %	1: Hattersley-Smith, 1964; Jeffries, 1984; Clarke *et al.*, 1986; 3: IAHS(ICSI)/UNEP/UNESCO, 1989
Central Andes	9	11		<1%	1: Corte, 1980; Bruce *et al.*, 1986; Leiva *et al.*, 1989; Lliboutry, 1998
Caucasus	7		1791	0.4%	1: Paterson, 1994. 3: IAHS(ICSI)/UNEP/UNESCO, 1989
Kamchatka	1		405	0.3%	1: Paterson, 1994. 3: IAHS(ICSI)/UNEP/UNESCO, 1989
Tien Shan	21		20609	0.1%	1: Paterson, 1994; 3: Liu Chaohai and Ding Liangfu, 1986 (China); IAHS(ICSI)/UNEP/UNESCO, 1989 (CIS).
Pamir	120	60	5400	2.2%	1+2: Kotlyakov, 1980; Kotlyakov *et al.*, 1997. 3: IAHS(ICSI)/UNEP/UNESCO, 1989
Russian High Arctic	5		1965	0.3%	1: Dowdeswell and Williams, 1997
Karakoram	17				1: Hewitt, 1969; Wang Wenying *et al.*, 1984; Gardner and Hewitt, 1990; Wake and Searle, 1992; Hewitt, 1998.
World Wide	717		157122**	0.5%	3: Shih Ya-feng *et al.*, 1980; IAHS(ICSI)/UNEP/UNESCO, 1989; Weidick *et al.*, 1992

***Table 1.1**: Numbers of surge-type glacier in cluster regions and percentage of surge-type glaciers of the estimated total number of glaciers world wide. Numbers are subject to interpretation. Numbers marked * and ** are extrapolated estimates. Further explanation of figures is given in the text.*

1.3.3 Variations in surge behaviour

There appears to be a large variability in the duration of quiescent phases and surge phases and in the actual velocity development during surges. Although for individual glaciers the phases and surge propagation are very similar, for example: Variegated Glacier surges about every 20 years and the surge extent of different surges is very similar (Lawson, 1996), Bering Glacier also surges about every 20 years (Muller and Fleisher, 1995) and Medvezhiy Glacier about every 15 years (Dolgoushin and Osipova, 1975), large variations occur both between regions and within regions. Two surge-type glaciers originating from the same icefield or sharing accumulation areas do not necessarily surge simultaneously: Black Rapids and Susitna Glacier, central Alaska Range, surged in 1936-37 and 1953 respectively (Paterson, 1994). Dowdeswell *et al.* (1991) compared the surge duration of Svalbard glaciers with that in other regions and found that in Svalbard the active surge phase lasts 3-15 years whereas in other regions surges commonly last only 1-2 years. However, for regions in East Greenland, surge durations of up to 7 years have been inferred as well (Rutishauser, 1971; Weidick, 1988). Furthermore, from three Svalbard glaciers with multiple observed surges with quiescent periods of 40, 70 and 110 years, and from estimated durations for other Svalbard glaciers, Dowdeswell *et al.* (1995) concluded that the recurring period of surges is much longer in Svalbard than in other regions: 50-500 years instead of 15-50 years (Meier and Post, 1969; Dowdeswell *et al.*, 1995). Given that surge duration is mainly controlled by surge dynamics and quiescence duration by mass balance conditions (Robin and Weertman, 1973), the long surge duration in Svalbard is believed to result from a distinct surge mechanism operating in the Svalbard region, which is thought to be related to basal processes, or to a combination of basal processes and thermal regime (Dowdeswell *et al.*, 1991; Murray *et al.*, in review). The prolonged quiescent phase is however ascribed to a slower mass accumulation in the Svalbard region, where the net accumulation is often only 0.3-0.6 m a^{-1} (Dowdeswell *et al.*, 1995). This could be indicative for durations of quiescent phases in other High Arctic regions as well. Indeed, Svalbard is not the only region with long quiescence periods, because surge-type glaciers in East and Northeast Greenland have recurrence periods of the order of 70 years, and certain Alaskan glaciers, e.g. Black Rapids Glacier, have similar estimated recurrence periods (Colvill, 1984; Reeh *et al.*, 1994; Heinrichs *et al.*, 1996). Furthermore, for most surge-type glaciers in Greenland it is difficult to infer a semi-regular periodicity of surging, as the quiescent phase is longer than the period of observation. In contrast, surging glaciers in West Greenland conform to the 'norm' with surge durations of 1-2 years and recurrence periods of 30-50 years (Weidick, 1988).

It has also been suggested that, in Svalbard, surges occur less frequently than in the past: with the decrease in numbers of surge-type glaciers occurring over the last 50-60 years being related

to a change in mass balance (Dowdeswell *et al.*, 1995). However, for three snapshot periods, defined by aerial photograph coverages in 1936/38, 1969-71 and 1990, with surging glacier observations of 18, 10 and 5 respectively, and with at least five more surges since 1990 (see Section 5.2.6), the statistics behind Dowdeswell *et al.*'s hypothesis are not convincing. Opposing views exist on the influence of climate dependence on changes in surge cycles or in the spatial variations in surging. Post (1969) argues that given glacier surging is an internally triggered instability it would bear no direct relation to climate perturbations. However, climate affects the rate of mass accumulation during quiescence and has as such an effect on the geometrical evolution of a glacier, which is in turn one of the driving forces of the surge evolution (Raymond, 1987). In Iceland, an increase in surge activity in the late 1960s was ascribed to a preceding period of increased precipitation (Thorarinsson, 1969). Hence, climate deterioration, resulting in a more negative net mass balance, may cause the length of the quiescent phase to shorten and amelioration of climate, resulting in a more positive net mass balance, may cause the length of the quiescent phase to lengthen or may even lead to the cessation of surge activity at particular glaciers (Dowdeswell *et al.*, 1995). However, some argue that meltwater production is the driving force for glacier response to climate. The increased amount of meltwater at the glacier bed during climate warming could trigger surges, despite the decrease in glacier volume by the same climate perturbation (Jania, 1988; Jania *et al.*, 1996). More details on the complex link between mass balance and glacier velocity and response are given in Section 2.3 of this thesis.

Apart from a long surge phase and a long quiescent phase, Svalbard surge-type glaciers have an overall 'sluggish' character, with less than a ten-fold increase in flow velocity and a slow and indistinct surge termination (Dowdeswell *et al.*, 1991; Murray *et al.*, 1998). Some surging outlet glaciers in Greenland are suggested to have a 'periodic' surge on top of a 'permanent' surge, for which the velocity increase is also less than ten-fold (Weidick, 1988). In addition, there are observations of very short pulses in flow velocity, usually up to a few weeks, resembling surges. These pulses are classified as 'mini-surges' because the pulse periods are too short, the velocity increase is not large enough, and no major ice redistribution takes place. However, observations on the dynamics of mini-surges has showed a strong similarity to the surge dynamics in real surges. Furthermore, mini-surges may precede a major surge (Kamb et al, 1985), but this is not necessarily the case (Joughin *et al.*, 1996). Hence, since the behaviour of surge-type glaciers is so diverse there seems to be a wider range of surge phenomena and it might be necessary to redefine the classical concept of glacier surging (e.g. Rototayev, 1986; Weidick, 1988; Kotlyakov *et al.*, 1997). However, it should be kept in mind that a good definition of glacier surging provides a tool that enables us to distinguish between 'specific' surging behaviour and other pulsating behaviour.

1.4 How do we recognise surge-type glaciers?

Because the work undertaken for this thesis included the verification of surge evidence by means of aerial photograph interpretation and interpretation of other photographic and satellite derived imagery, it is necessary to explain which criteria were used to distinguish surge-type from normal glaciers. The strongest evidence for surging, *direct evidence,* is the observation of a surge, either in person or from historic reports. However, some frontal advances and active termini are the response of a climatic signal, and surge advances could coincide with an overall pattern of glacier advance, for example at the end of the Little Ice Age around 1850 (e.g. Lefauconnier and Hagen, 1991). This implies that even direct evidence is sensitive to interpretation. Direct evidence of a surge is also possible from analysis of time sequences of aerial photographs or satellite imagery, where a glacier in pre-surge condition can be compared to the same glacier in surge- or post-surge condition. From time series of overlapping images, not only changes in the nature of glacier surfaces and termini can be observed, but also surface velocities can be measured using moving surface features like lakes, crevasses and pothole-fields. Measurements of horizontal and vertical displacements of glaciers in West Spitsbergen, the documentation of Medvezhiy glacier, Pamir, and of West Fork Glacier, Alaska are good examples of this technique (Liestøl, 1969; Osipova and Tsvetkov, 1991; Harrison *et al.*, 1994; Kotlyakov *et al.*, 1997). From Landsat MMS and TM images at scale 1:24000, terminus positions and advances, patterns of medial moraines and formation of ice-dammed lakes were documented in detail for surging glaciers in Iceland (e.g. Rundquist *et al.*, 1978; Ferrigno and Williams, 1980). Further, repeat-pass SAR interferometry is increasingly being used to determine ice flow properties and flow instabilities in regions where ground-based measurements are problematic (e.g. Joughin *et al.*, 1996; Fatland and Lingle., 1998; Mohr *et al.*, 1998; Joughin *et al.*, 1999).

Indirect evidence for surge behaviour exists in the form of a glacier's appearance. Because of their distinct dynamic behaviour, surge-type glaciers show distinctive morphological and surface characteristics resulting from the changes taking place in surge-type glaciers both during the active and quiescent phase in the surge cycle. Also the proglacial landscape can display signatures of surging. Post (1969, 1972) frequently detected evidence for surging by aerial photograph reconnaissance in Alaska. Studies of surge-type glaciers for which direct surge evidence is lacking include Bjørnbo Glacier and other Greenland glaciers (e.g. Rutishauser, 1971; Weidick, 1988). ERS-1 SAR observations were used for the determination of surface features on glaciers in Alaska (Josberger *et al.*, 1994). In Section 1.4.1 to 1.4.5 morphological and surface characteristics of surge-type glaciers will be explained and illustrated.

1.4.1 Surface gradient and geometry of surge-type glaciers

A surge is usually the main means of transporting a large 'surplus' volume of ice from the reservoir to the receiving area (see Section 1.3). At the end of the quiescent phase the surface gradient of a surge-type glacier is markedly steeper than its trimlines or lateral moraines, while the end of the surge phase is characterised by a very low surface slope (Figure 1.2). Both end-members are an indication of the fact that surge-type glaciers have no steady state profiles (Meier and Post, 1969; Paterson, 1994). Profile steepening during the quiescent phase results from the progressive thickening of the upper and middle parts of the glacier and thinning of the lower part. For Variegated Glacier in Alaska this steepening started to take place only one year after the termination of the surge, but the process is probably slower for larger glaciers and glaciers with a longer surge-period (Kamb *et al.*, 1985). Most surge-type glaciers show a rapid downwaste of the frontal area just after surging and extensive stagnant tongues during the rest of the quiescent phase (Clapperton, 1975; Meier and Post, 1969). During the surge phase, the glacier gradient is subject to a rapid change due to the down-draw of the upper part of the glacier and a thickening and potential advance of the lower part due to the transport of large volumes of ice down-glacier. During the 1982-83 surge of Variegated Glacier, the upper part of the glacier thinned by 50 m, while the lower part thickened by 100 m (Kamb *et al.*, 1985). Similarly, during a surge of the Usherbreen in Svalbard the mean surface slope decreased from 3.3° to 1.8° (Hagen, 1987; Dowdeswell, 1991).

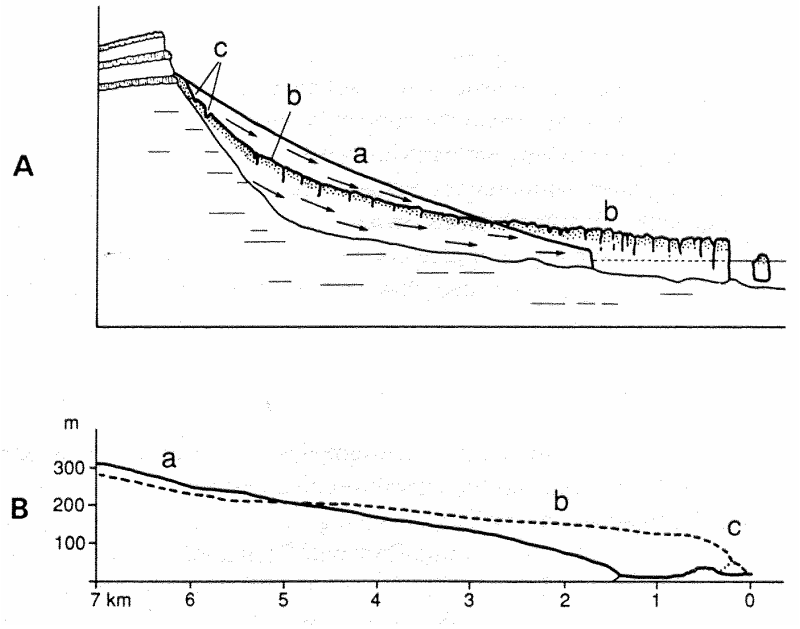

Figure 1.2: a) *Longitudinal profile change during a surge of a calving glacier with a: pre-surge surface, b: post-surge crevassed surface and c: concentric crevassing close to the rock wall.* ***b)*** *longitudinal profile of a surge of a land-based glacier (Usherbreen, Spitsbergen) with a: pre-surge surface, b: post-surge surface and c: the marked convex glacier margin (From: Lefauconnier and Hagen, 1991).*

In some surging glaciers, a ramp of steep gradient, often described as surge-bulge or surge-front, has been observed to propagate as a wave down-glacier. The ramp usually steepens with time, resulting in a sharp distal side (e.g. Kamb *et al.*, 1985). The surge-bulge of Bakaninbreen, Svalbard, with a maximum height of 60 m, steepened its average distal gradient from 6° to 11º while propagating with an average speed of 3.5 m d^{-1} (Murray *et al.*, 1998). Variegated Glacier's surge front propagated down-glacier with a velocity of 40 m d^{-1}, which was roughly double the velocity of the ice (Kamb *et al.*, 1985). A maximum speed of 80 m d^{-1} was measured at the surge-front of Bering Glacier, Alaska (Fleisher *et al.*, 1995). Whilst on Variegated Glacier the ice compression below the surge bulge resulted in the formation of thrust faults, on Bakaninbreen a pronounced fore-bulge developed (Sharp *et al.*, 1988; Murray *et al.*, 1998).

If the surge front reaches the glacier margin, the glacier tongue steepens with time and becomes well-marked convex (Hagen, 1987; Raymond, 1987). This convex front is typical for surging glaciers ending on land (e.g. Donjek Glacier, Canada, Usherbreen (Figure 1.2) and Marmorbreen, Svalbard, and the 20-50 m steep front of Bruárjökull, Iceland (Thorarinsson, 1969; Johnson, 1972, Lefauconnier and Hagen, 1991; Hagen *et al.*, 1993). Calving and tide-water glaciers generally develop an almost vertical ice cliff during the surge (Hagen, 1987) (Figure 1.2). A considerable frontal advance can occur if the surge-front reaches the glacier margin (Meier and Post, 1969), but surges do not always result in an advance of the glacier tongue (Paterson, 1994). The highest advance velocities, 12 km a^{-1} with average velocities of 35m/d, were recorded during the 1935-36 surge of the Negribreen (Liestøl, 1969). The largest ever recorded advance of the terminus position of approximately 21 km was observed during a surge of the Bråsvelbreen (Schytt, 1969). Both Negribreen and Bråsvelbreen are calving glaciers in the Svalbard archipelago. Also outside Svalbard dramatic advances have been recorded, for example; 10 km advance in one year of Bruárjökull, Iceland; 9 km advance in nine months during a surge of Bering Glacier, Alaska; and advance of more than 10 km between 1978 and 1984 of the calving front of Storstrømmen, NE Greenland (Thorarinsson, 1969; Molnia, 1994; Reeh, *et al.*, 1994). The advance of the glacier tongue during a surge can result in an increase of the total glacier length with approximately 10-50%. Further, complex lobating of the glacier front and spreading of the glacier tongue as a droplike accumulation cone have been associated with surges (Johnson, 1972; Kotlyakov, 1980; Weidick, 1988). Occasionally thrusting of a glacier tongue over others takes place (e.g. Kotlyakov, 1980; Raymond *et al.*, 1987; Sharp *et al.*, 1988). There are some references to an increase in ice volume during a surge phase (Dolgoushin and Osipova, 1975; Raymond, 1987), but this is possibly due to the opening of crevasses during surge and it is better to talk about a redistribution of ice volume (Murray *et al.*, 1998). The above mentioned vertical and horizontal displacements can be observed on aerial photographs and satellite images. Remnants of snow, ice and debris left hanging on valley walls are an

indication of the drop in glacier surface during the surge. In 1952, Nansen Glacier showed remnants of landfast ice after the surge between 1946-48 as a result of a drop in surface elevation (Liestøl, 1969). At Bering Glacier, previous winter snow was left hanging on the valley wall during its surge of 1993-94, marking a down-draw of the glacier surface by approximately 25 m (Molnia, 1994). On Bruanglacier in the Karakoram, a double cone-shaped avalanche-snow deposit marks a drop in the glacier surface. The upper cone coincides with a higher glacier level and the lower (superimposed) cone coincides with a lowered glacier surface (Gardner and Hewitt, 1990). Truncated tributary glaciers and hanging tributaries are also an indication of the drop in surface and the increased velocity during the active phase (e.g. Meier and Post, 1969; Clapperton, 1975; Raymond, 1987). There are even observations of isolated tongues of tributary glaciers which have been cut off and moved down-glacier (Johnson, 1972). Changes in the marginal position can be detected from time series of photographic material and from map documentation in archives (e.g. van der Meer, 1992).

1.4.2 Surface features of surge-type glaciers

A range of surface features are indicative for surge-type glaciers. In this section the development and characteristics of both surface features (crevasses, medial moraines, supraglacial lakes and debris, pothole fields) and proglacial features associated with surging glaciers (frontal moraines, proglacial drainage system and iceberg production) will be illustrated. The majority of these surface features can be observed during any time in the surge-cycle, however, the features are best developed during and just after a surge.

Crevasse patterns

Crevasses form when stresses at the glacier surface exceed the tensile strength of glacier ice (Paterson, 1994). As a crevasse is orientated perpendicular to the direction of the principal extending stress, crevasse patterns can be deduced from the direction of the principal stresses. Transverse crevasses form as a result of longitudinal extending stresses/tectonics and longitudinal crevasses result from longitudinal compressive stresses/tectonics (Hodgkins and Dowdeswell, 1994). Characteristic crevasse patterns, fractured and pinnacled ice and the evolving change in pattern of surface crevassing during the active phase have been observed on numerous surging glaciers (e.g. Meier and Post, 1969; Post, 1969; Johnson, 1972; Dolgoushin and Osipova, 1975; Kotlyakov, 1978; Hagen, 1987; Dowdeswell *et al.*, 1991; Lefauconnier and Hagen, 1991; Hamilton, 1992; Herzfeld and Mayer, 1997). Due to the abnormal distribution of velocity and glacier movement in surging glaciers, chaotic crevasse patterns develop during the surge phase: often affecting the entire glacier basin (Meier and Post, 1969). The orientations of crevasses have been used to investigate tectonic processes in glacier surges recorded by

repeated aerial photography and satellite imagery (e.g. Sharp *et al.*, 1988; Hodgkins and Dowdeswell, 1994; Rolstad *et al.*, 1997). Peak crevasse density is often found at the surge-front or 'nucleus'. The mixed longitudinal and transverse crevassing behind the propagating surge-front indicates a changing stress field, with a strong compression as the front arrives and extension as it is passing (Echelmeyer *et al.* 1987). This phenomenon is also described in models by McMeeking and Johnson (1986). Some tidewater glacier in Svalbard experience very rapid terminus advances. Crevasse patterns suggest that this frontal advance is related to the propagation of strain waves in connection with the location of a surge front relative to a low effective pressure zone (Sharp et al., 1988; Hodgkins and Dowdeswell, 1994). The propagation of a compressive wave in the ice just above the surge front causes a 'push from behind' mechanism: the rate of terminus advance increases dramatically when this surge front enters the zone of low effective pressure (Hodgkins and Dowdeswell, 1994: see Section 2.3 for effective pressure). The steady mode of surge front propagation prior to entering the low effective pressure zone is the 'push' whereas the rapid propagation afterwards is the 'rush'. Thorarinsson (1969) distinguished different crevasse patterns in the accumulation area and the ablation area of Brúarjökull, Iceland. In the accumulation area, longitudinal parallel crevasses developed at right angles to the glacier movement. In the ablation area, however, a criss-cross pattern of crevasses appeared, in some parts polygon jointed like basalt. Raymond *et al.* (1987) described the development of crevasse zones on Variegated Glacier during its 1983-84 surge. In the lower zone of the glacier microcracking appeared, followed by a zone of buckling and longitudinal cracking higher up. In the upper zone of the glacier, longitudinal crevasse growth was predominant. Sharp *et al.* (1988) related these crevasse patterns to tectonic processes and inferred that extensional tectonics in the upper part of the glacier lead to transverse crevassing; that in the zone of the surge front, superimposed extensional and compressional tectonics lead to intersecting transverse and longitudinal crevasses, while compressional tectonics (below the velocity peak) in the terminus area lead to longitudinal crevassing. Transverse crevasses ('bergschrund') near steep mountain slopes in the upper basin are associated with the depression of the glacier surface during surge (Lefauconnier and Hagen, 1991) (Figure 1.2). Sheared margins, wrench faults and marginal faults suggest active marginal shear, which is related to the block-like flow (Post, 1969; Kotlyakov, 1980; Kamb *et al.*, 1985; Reeh *et al.*, 1994). Such marginal shearing is also suggested by small shear planes on sandur surfaces and slickensides and grooved marginal ice surfaces down-glacier from contacts with the valley wall (Hagen, 1987; Gardner and Hewitt, 1990). Transverse crevasses over the width of the glacier separate the stagnant upper part of the glacier from the lower surging part of the glacier. Up to 30 metres vertical displacement has been measured in these cross-glacier crevasses (Gardner and Hewitt, 1990).

Looped and contorted medial moraines

Probably the most spectacular surface features of surge-type glaciers are peculiar folded medial moraines, which are considered as being diagnostic for surging (Meier and Post, 1969). However, surge-type medial moraines can only develop if two important factors in medial moraine development are met: moraine material must be available and tributary glaciers or confluent ice streams must be present. Due to the alternating velocity in surge-type glaciers, from rapid flow in the active phase to normal flow in the quiescent phase, a distinct medial moraine pattern is formed in surge-type glaciers. End moraines of tributaries protrude onto the surface of the stagnant trunk and form moraine loops. These moraine loops are extended and transported downglacier during surges of the trunk and are transformed into elongated 'tear-shaped' medial moraines (Figure 1.3). This can clearly be seen on Abrahamsenbreen, Svalbard (Figure 1.4).

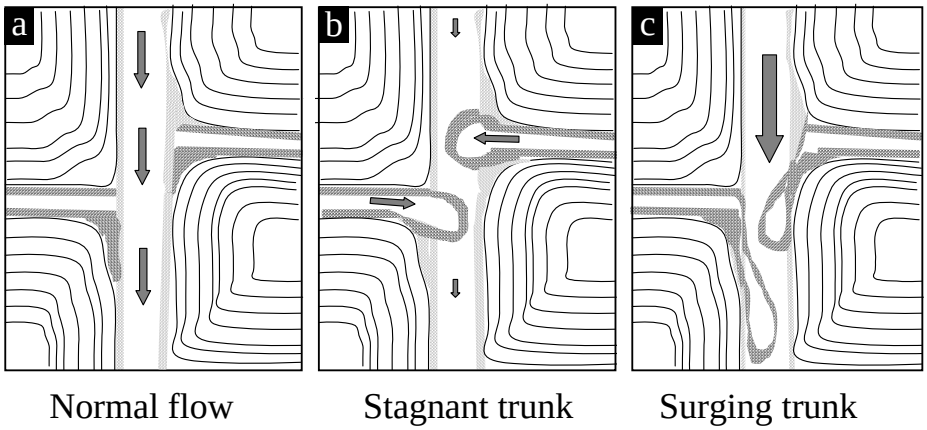

Figure 1.3: *The formation of 'tearshaped' elongated moraine loops (After: Gripp, 1929; Croot, 1988)*

a **b**

Figure 1.4: *Elongated moraine loops and crevasses on Abrahamsenbreen, Svalbard, which surged around 1978.* ***a)*** *1969: pre-surge,* ***b)*** *1990: post-surge. (Aerial photographs S69 1493 and S90 3134, ©Norsk Polarinstitutt)*

Sometimes the looped moraines are being transformed into tight folds ('accordion' like folds) during the surge phase (e.g. Post, 1972: Figure 1.5), but this feature has also been observed in non-surge-type piedmont glaciers and appears to be controlled by contrasting rheological properties of moraine and ice and occurs when the ice flow meets resistance (Ramberg, 1964). The development of tight folds towards the glacier terminus during a surge probably results from compressional ice flow along the flowline of the terminal lobe and extensional flow (radial spreading) in transverse direction (Paterson, 1994). Folded medial moraines are transported down-valley by further surge advance and stand as prominent ridges above the ice surface of the wasted glacier tongue in the (late) quiescent phase. Loops, folds and irregularities in medial moraines are recorded in numerous surging glaciers, but with emphasis in the surge regions in western North America, Svalbard and East Greenland (Meier and Post, 1969; Post, 1972; Clapperton, 1975; Kotlyakov, 1980; Raymond, 1987; Lefauconnier and Hagen, 1991; Weidick, 1995). One of the best known glaciers for its beautifully contorted moraine is Susitna Glacier, Alaska (Figure 1.5).

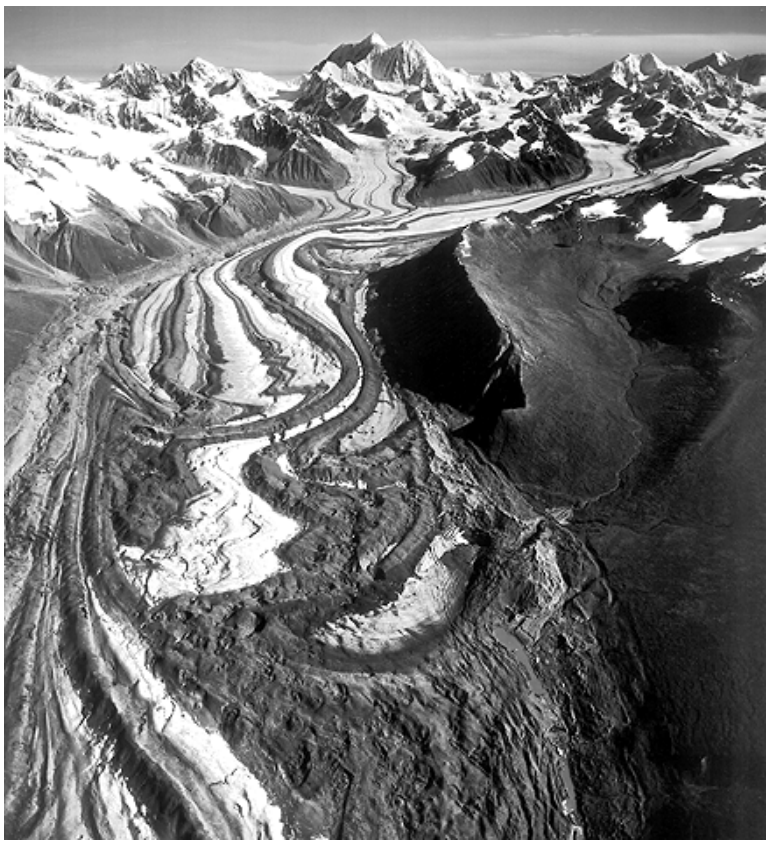

Figure 1.5: *Contorted moraine loops on Susitna Glacier, Eastern Alaska Range. Photo by Austin Post,US Geological Survey, 3/9/1970. Photograph from the American Geographic Society Collection archived at the National Snow and Ice Data Center, University of Colorado at Boulder and obtained from the Internet at http://www-nsidc.colorado.edu on 13/8/99.*

Undulations, lakes and pothole fields

Due to the irregular undulating glacier surface of surge-type glaciers there is a relatively high frequency of depressions and associated supraglacial lakes (Liestøl *et al.*, 1980). These depressions, also called potholes or pits, are usually 10-100 m across and circular to elliptical in plan view (Sturm, 1987). Meier and Post (1969) suggested that potholes were a criterion for identifying surge-type glaciers in their quiescent phase. Indeed, pothole fields are most frequently detected on surging glaciers. Whereas potholes generally develop near the equilibrium line on normal glaciers, potholes on surge-type glaciers are found far down into the ablation area and often over the entire glacier surface (Meier and Post, 1969; Sturm, 1987; Wilbur, 1988; Harrison *et al.*, 1994). This gives a glacier the appearance of a 'Swiss Cheese' (pers.comm., Weidick, 1997).

The critical conditions required for pothole development are not clear but it is suggested that pothole fields could be related to the presence of crevasses and glacier lakes in a surge type glacier and thus require special supra and englacial hydrological conditions (Sturm, 1987). Supraglacial lakes also develop in the surge phase: on Bering Glacier, numerous supraglacial lakes were observed during the 1993-94 surge (Molnia, 1994). These lakes are often not permanent, but drain annually. After the annual drainage of the supraglacial lakes on Storstrømmen, NE Greenland, the pressure ridges formed from these lakes by katabatic wind were passively transported down-glacier and eventually deposited on the glacier surface as a series of curved ridges. These annual ridges were subsequently used to estimate surge velocity (Reeh *et al.*, 1994). Further, the development of ice marginal and ice-dammed lakes is also associated with surging (e.g. Rundquist *et al.*, 1978; Kotlyakov, 1980; Hagen, 1987). The marginal lake that developed during the surge of Variegated Glacier drained during the termination of the surge-phase (Kamb *et al.*, 1985). Jökulhlaup features and staircases of strandlines, also visible on aerial photographs are remnants from the sudden drainage of these lakes (Sugden and John, 1976; Sharp, 1988b).

1.4.3 Proglacial features of surge-type glaciers

Icebergs

The surge cycle has several consequences relevant to iceberg production and dimensions. In the quiescent phase, the ice flux is so low that surge-type glaciers have an iceberg production which is lower than that of normal calving glaciers (Dowdeswell, 1989). In surge, the iceberg production is enhanced due to an increase in ice flux and the advance of the glacier terminus into the water, which increases floating conditions (Dowdeswell, 1989). This increased iceberg production has frequently been observed during surges of calving glaciers in Svalbard, but also

during the 1993-94 surge of Bering Glacier, Alaska, releasing large volumes of ice into Lake Vitus (Lefauconnier and Hagen, 1991; Lingle *et al.*, 1993). The surge of Storstrømmen, Northeast Greenland, released icebergs with a calving rate of about 10.8 km^3 a^{-1} into the fjord and coastal waters (Reeh *et al.*, 1994). Dowdeswell (1989) argues that chaotic crevassing and close spacing of crevasses in surging glaciers enhance the disintegration of ice near the glacier margin, resulting in the reduction of the dimensions of icebergs produced by surging glaciers. However, Storstrømmen, Northeast Greenland produced large tabular icebergs with tidal cracks (Reeh *et al.*, 1994). This difference could be due to fact that most Svalbard tidewater glaciers are grounded, whereas Storstrømmen is free floating over an area of about 100 km^2 (Reeh *et al.*, 1994).

The proglacial drainage system

Rapid changes in discharge and fluvial geometry occur during a surge (e.g. Thorarinsson, 1969; Johnson, 1972; Raymond, 1987; Lefauconnier and Hagen, 1991; Hamilton, 1992). Associated with surges are: an increase in the turbidity of glacier water and rapid changes in sediment discharge. Release of large quantities of turbid water at the glacier margins and debris-laden floods (muddy waters) are recorded in conjunction with the surge termination in many surging glaciers (Kamb *et al.*, 1985; Echelmeyer *et al.*, 1987; Hagen, 1987; Raymond, 1987; Sharp, 1988b; Molnia, 1994). These events cause changes in the proglacial glaciofluvial system. Scours of alluvial deposits and cut accumulation cones below glacier tongue were remnants of a surge of the Medvezhiy Glacier, Pamir (Dolgoushin and Osipova, 1975). There is also evidence of triggering of landslides and mudflows by glacier surges in the Pamir and Karakoram regions (Kotlyakov, 1980; Gardner and Hewitt, 1990). Erosion of alluvial fans is one of the morphological effects of a surge of the Donjek glacier, Alaska (Johnson, 1972). In Svalbard, icings in the proglacial area have been associated with surge-type glaciers in quiescence, but are most probably really associated with warm-based glaciers (Liestøl, 1977: see Section 5.2.5). Most of these features in the proglacial drainage system can be observed on aerial photographs.

Frontal moraines and till features

Several components are useful in distinguishing between frontal moraines of normal and surging glaciers. Croot (1988) proposed a correlation between glaciotectonics and surging, based on evidence of 29 composite ridges (push moraines) on West Spitsbergen. These push moraine complexes consist of a series of arclike ridges, marking the position of a glacier margin and thus the limit reached during a surge advance (Croot, 1988). The process of glaciotectonic deformation in push moraines requires special hydrological, tectonical and lithological conditions, but above all a rapid advance (Croot, 1988; van der Wateren, 1995). Also in other regions, push moraine complexes have developed in front of surging glaciers (Rutter, 1969;

Schytt, 1969; Thorarinsson, 1969; Clapperton, 1975; Sharp, 1988b). Of particular note are the frontal moraines of the "Usherbreen type" with marked concentric moraine crests (Lefauconnier and Hagen, 1991). Here, old terminal ridges were pushed forward (resulting in folds and thrust faults) and Usherbreen gradually moved over the old ridges (Hagen, 1987). This overriding and reincorporating of dead ice from previous surges is observed in other regions as well (Paterson, 1994). In some proglacial areas of surge-type glaciers, the marginal zone of dead ice is overlain by till, evolving into chaotic hummocky topography (Sharp, 1988b). On this till surface, distinctive rectilinear pattern of till ridges can be observed. These till ridges or debris bands are crevasse fillings, reflecting the orientation of crevasses in the tongue of a surging glacier (Johnson, 1972; Sharp, 1988b). Crevasse-fill ridges at Eyjabakkajökull, Iceland, are aligned normally to obliquely (Sharp, 1985).

Push moraine complexes and till ridges are distinct features on aerial photographs. However, some push moraine complexes were formed during frontal advances in response to climate and simply indicate the position of the glacier margin during the last glacial maximum (Lefauconnier and Hagen, 1991). Smaller scale features such as drumlins and eskers, are also related to surging and fast flow, but these are sometimes hard to detect from remote sources.

1.4.4 Summarising diagnostic features

From the preceding exposition it could be concluded that distinguishing surge-type from normal glaciers from aerial photographs is a simple procedure. This is partly true, for those glaciers with clear development of surface features diagnostic for surging. These diagnostic features include:

- a surge advance,
- elongated 'tearshaped' moraine loops,
- strandlines of former ice surface hanging above the present ice surface,
- a marked surge-bulge,
- a completely crevassed glacier.

However the decision of classifying a glacier as being surge-type must be based on at least a number of features and many glaciers are lacking clear evidence for surging. Therefore, the Canadian Glacier Inventory developed a surge probability index according to the number and type of observed surge-type features (Ommanney, 1980; see also Table 3.1, Section 3.2.2). In summary, a glacier with four or more observed features diagnostic for surge behaviour, has a surge probability high enough to be classified as a surge-type glacier.

1.5 Concluding remarks

As the major data source for detecting glacier surges in remote Arctic places is aerial photography (and in recent years also satellite imagery) the detection of a surge is subsequently dependent on the image coverage. We should be aware of a possible bias in the detection of surges and surge-type glaciers introduced by the availability of aerial photographs as morphological evidence of a surge fades with the years and it is more likely to detect surges that occurred in a period of about 5 years before the aerial photograph coverage than those in preceding periods. Since the surge cycle in certain regions is longer than the period of observation (about one century) and the surge duration is shorter than the period between subsequent aerial photograph coverage it is often problematic to time surges accurately. This predicament will be of lesser concern when considerable time series of satellite images becomes available, particularly from High Arctic locations.

CHAPTER 2:
Theoretical Framework: Possible Controls on Surge Mechanisms

It unlink'd itself and with intended glides did slip away

Shakespeare (As you like it: Act 4, Scene 3)

2.1 Introduction

In this chapter current surge theories are presented in conjunction with the possible controlling factors of surging. The questions, surge theories and instability mechanisms presented in sections 2.2 to 2.4 form a mathematical-physical basis of the variables that will be tested for their relation to glacier surging and form the theoretical foundation of the data analysis in Chapters 5 and 6. Relating environmental and glacial characteristics of surge-type glaciers derived from these analyses to the hypotheses on surge mechanisms provides a method for testing and validating existing theories on the mechanism(s) of glacier surging.

Ever since the first identification of surge behaviour as anomalous to 'normal' glacier flow, theories have been developed to try and explain the mechanisms of surging (e.g. Tarr and Martin, 1914). After it became evident that surges were internally triggered, surge-type glaciers were considered as physical systems out of balance with their environment, where flow instabilities can be triggered by internal feedback mechanisms (e.g. Meier and Post, 1969; Bindschadler, 1982; Clarke, 1987a). The development of theories on surge mechanisms has particularly benefited from advances in the physical-mathematical modelling of surges (e.g. Robin, 1955; Lliboutry, 1968; Clarke, 1976; Weertman, 1979; Bindschadler, 1982; Fowler, 1987a) and from field measurements and observations on glaciers in surge and in quiescence (e.g. Liestøl, 1969; Harrison, 1972; Clarke, *et al.*, 1984; Kamb *et al.*, 1985; Osipova and Tsvetkov, 1991; Harrison, *et al.*, 1994). Today these two approaches are interlinked. Field measurements are critical to the testing of theories on surge mechanisms and surge dynamics and to determine model parameters and to provide new ideas on surge mechanisms (Clarke *et al.*, 1984; Kamb *et al.*, 1985; Echelmeyer *et al.*, 1987; Murray *et al.*, in review). Moreover, surge models can be used to predict expected trends in field measurements and to indicate which types of measurements should be performed (e.g. Bindschadler, 1982; Kamb, 1987; Fowler, 1989).

Observations on different surging glaciers have led to a suite of ideas on how and when surges are triggered as well as on the mechanisms of surge propagation and termination. Ideas developed using data from one glacier must however be tested using data derived from

measurements on other glacier surges (Echelmeyer *et al.*, 1987). An intrinsic problem of using the few measured glacier surges to explain glacier surging is the difficulty of ensuring to what extent the developed surge theories are universally applicable: they might only hold for a particular surging glacier, certain classes of surges, or in certain regions. It is therefore necessary to verify surge mechanisms on a wider dataset of surge-type glaciers (Clarke, 1991). If surge-type glaciers are considered a separate class of glaciers, or as an extreme end member in a continuous spectrum of possible pulsating flow, then surge-type glaciers can be distinguished from other ('normal') glaciers on the basis of certain characteristics (Raymond, 1987). Given that the distribution of surge-type glaciers is markedly non-random, some of these characteristics could be environmentally controlled (Post, 1969). Specific characteristics that distinguish surge-type glaciers from normal glaciers can thus act as benchmark data to test surge theories and to identify boundary conditions for surging.

2.2 The essential questions on glacier surging

Over recent decades two groups of essential questions were put forward that theories on surge mechanisms and theories on triggering of surging must address (e.g. Meier and Post, 1969; Weertman, 1969; Raymond, 1987; Sharp, 1988a; Paterson, 1994):

1. Specific questions related to surge behaviour

- What causes the restriction of ice flow during the quiescent phase?
- What is the surge trigger?
- Which flow instabilities can cause an increase in flow velocity of one to two orders of magnitude?
- Is the flow instability at the surge initiation the inverse of the process at the surge termination?
- How are high sliding velocities maintained over a period of time, while glacier geometry and thus internal stresses change gradually?
- Which factors determine the duration of the surge cycle?
- Are local conditions at the surge front more important in triggering and maintaining a surge than larger-scale conditions such as average surface slope?
- Are specific stress distributions conducive to surging?

2. Generic questions related to glacier flow and distribution of surge-type glaciers

- Is glacier surging a distinct class of flow behaviour or is it part of a continuum from normal (slow) glacier flow to fast glacier flow?
- Can individual glaciers pass into and out of surge-type behaviour or is glacier surging a permanent state: do glaciers transgress from normal to surge-type and *vice versa*?

- Is there one surge mechanism that can explain surges in all settings and thermal conditions or are there a range of surge mechanisms?
- What is the nature of the relationship between flow velocity, stresses and hydrostatic pressure in a glacier?
- What is the role of the hydrological system in glacier flow?

Field and theoretical research has contributed to the development of conceptual hypotheses on ice flow instabilities, surge mechanisms and surge triggers. Some of these postulates provide answers to the above questions and have resulted in forward leaps in the process of solving the surge-enigma. It has for example been postulated that two sets of boundary conditions are needed to calculate the velocities within a glacier: one set matching the slow flow conditions (10^1-10^2m a^{-1}) observed in the majority of the valley glaciers and ice sheets and one set matching the fast flow conditions (10^2-10^3m a^{-1}) observed in some outlet glaciers, ice streams and during glacier surges. Tidewater glaciers, surge-type glaciers and ice streams are the only glacier types that switch between slow and fast flow and conditions in and around these glaciers should match the two sets of boundary conditions (Raymond, 1987). The two-phase velocity regime of these glaciers indicates that different processes control slow and fast flow and that critical thresholds exist at which flow can become unstable (Clarke, 1987). An essential observation is that fast flow during a surge is caused by decoupled motion; either by basal sliding or by a combination of sliding and bed deformation (Boulton and Hindmarsh, 1987; Clarke, 1987a; Raymond, 1987). As decoupling only occurs under low effective pressures, fast flow would require an inefficient drainage system and either a smooth, hard bed (fast sliding) or a soft sedimentary bed (deformation) (Alley *et al.*, 1989). Budd (1975) suggested that the boundary condition controlling flow dynamics is the product of glacier slope and balance flux over width (see section 2.4.6). For surge-type glaciers this product would be constant, irrespective of glacier geometry (Budd, 1975). Conversely, instead of classifying surge-type glaciers as a separate class of glaciers in terms of dynamic behaviour, surging could be viewed as part of a spectrum of pulsating behaviour in the continuum from normal to fast flowing glaciers, with surge-type glaciers being an extreme manifestation of pulsating behaviour (Raymond, 1987). Though, even for this continuum there must be critical geometries for initiation and termination of surges (Raymond, 1987).

There still remain a large number of unresolved questions in the understanding of surge behaviour (see Raymond, 1987). The three key questions are: (1) what controls the boundary conditions of fast flow and slow flow; (2) what are the triggers of the flow instabilities leading to surges and; (3) which factors control surge initiation, propagation and termination? The surge

theories and possible controls on surging presented in this chapter have been an attempt to provide some answers to these questions.

2.3 Glacier flow: processes and instabilities

Glacier flow occurs when driving force (gravity) overcomes the resisting forces (both within the glacier and at the ice-bed interface). The rate of flow can be expressed as a function of the internal stresses and the stresses at the glacier-bed interface. For an ice mass with a surface slope greater than zero, the downstream component of the force of the ice is balanced by the basal shear stress. If the longitudinal stresses are very small, the shear stress τ (in Pa) at the base of a rectangular section in a glacier equals

$$\tau = f\rho g H \sin\alpha, \tag{2.1}$$

where ρ is the density of ice, g the gravitational force, H the ice thickness (m), α the ice surface slope (dH/dx) and f a dimensionless shape factor related to the glacier profile and valley shape (Paterson, 1994). In regions where longitudinal deviatoric stresses (due to the pushing or pulling of the up and dowstream ice) are large compared to the basal shear stress a correction term must be added to equation 2.1 (e.g. McMeeking and Johnson, 1985).

The empirical flow law for ice, *Glen's Law,* provides the relation between shear strain rate $\dot{\varepsilon}$ and shear stress τ in a steady-state flow of ice and is expressed as:

$$\dot{\varepsilon} = B\tau^n, \tag{2.2}$$

where B is a factor depending on ice temperature, hydrostatic pressure and activation energy according to the Arrhenius relation (Glen, 1955). B ranges from 10^{-14} to 10^{-17} $s^{-1}kPa^{-3}$ and decreases log-linearly with temperature for temperatures well below the melting point but at a higher rate close to the melting point (Paterson, 1994). The exponent n is a constant with values between 1.5 and 4.2 and a mean of about 3 for temperate glaciers (Paterson, 1994). The temperature dependence of B and n indicate that at lower temperatures the ice is stiffer (*i.e.* cooling ice from -10°C to -25°C reduces the internal deformation by a factor 5 (Paterson, 1994)). On a local scale, variations in deformation of ice can take place through variations in grainsize and water content and by inclusion of debris or impurities (Souchez and Lorrain, 1991).

Three components can contribute to the overall surface velocity of a glacier: internal deformation (U_d), basal sliding (U_s) and bed deformation (U_b). The relative contributions of the different terms to the total glacier surface motion is variable and is controlled by ice and bed properties, particularly temperature and hydrostatic pressure and by variations in local conditions such as valley shape (Paterson, 1994). Flow laws have been developed for each of the above mentioned flow components, with the ultimate purpose of deriving a quantitative description of glacier velocity from glacier geometry (Bindschadler, 1983).

The vertically averaged horizontal deformation flow velocity (U_d) can be described as:

$$U_d = c_1 H \tau^n , \tag{2.3}$$

where the constant c_1 depends on the values for B and n from Glen's Law (equation 2.2), H is ice thickness, τ is basal shear stress (equation 2.1) (Kamb and Echelmeyer, 1987). The geometrical controls in this relationship are clear: steeper and thicker glaciers have a larger internal deformation rate than thin ones with shallow slopes.

Basal boundary conditions for the sliding velocity (U_s) are the basal shear stress (equation 2.1) and the effective pressure (N_e), which is the difference between ice overburden pressure ($p_i = \rho g H$) and water pressure (p_w). Water pressure is dependent on the pressure-flux relations in the subglacial drainage system (see Section 2.4.5). The lower the effective pressure the lower the basal drag thus the higher the sliding velocity. At water pressures exceeding the overburden pressure the glacier can start to 'float', which means that complete ice-bed decoupling takes place and theoretically the sliding velocity can increase infinitely. The flow law for sliding is more controversial than that for basal deformation; while most scientists agree that a pressure term has to be included, some suggest a multivalued sliding law (Lliboutry, 1968; Iken, 1981; Bindschadler, 1983; Fowler, 1987a). A general form for the sliding velocity flow law is:

$$U_s = \frac{k \tau^m}{N_e} \tag{2.4}$$

where k and m are constants ($m>n$) and N_e is the effective normal pressure (N_e) (Bindschadler, 1983). For a multivalued sliding law, k and m could have one value matching the conditions for sliding without cavitation and one for sliding with cavitation (Fowler, 1987b; Lliboutry, 1968; Röthlisberger, 1972). An additional exponent could be added to N_e in equation 2.4, for sudden and large changes in the effective pressure (Bindschadler, 1983). Basal sliding is in nature a

stick-slip behaviour rather than a continuous sliding movement: the actual ice motion behaves in a jerky fashion. This could be the result of a spatially variable basal drag which can be hypothesised as the theoretical concept of 'sticky-spots' (Alley, 1993; Blake *et al.*, 1994: see also section 2.4.12).

At locations where glaciers overlie unconsolidated sediments, shear deformation of the substrate can contribute significantly to the ice surface flow (Boulton *et al.*, 1974). Boulton and Hindmarsh (1987) established a constitutive relation ('the B-H rheology') for till, which was restructured by Fowler and Walder (1993) as the following power law:

$$\dot{\varepsilon} = A \frac{(\tau - \tau_0)^a}{(N_e + N_0)^b}, \tag{2.5}$$

where a and b are constant exponents with values of respectively 1.33 and 1.8 when the critical shear stress is not exceeded, A = 400 kPa^{b-a}y^{-1}, $\dot{\varepsilon}$ is the shear strain rate, τ is the shear stress, τ_0 the yield stress (or yield strength) of the sediments (usually defined as $\tau_0 = N_e \tan\phi_s + C$, where $\tan\phi_s$ is the internal friction and C the cohesion of the sediment), N_e is effective pressure and N_0 a cohesion term which prevents infinite deformation at zero effective pressure (Alley, 1989; Fowler and Walder, 1993; Murray, 1998). A common equation for effective pressure in soft sediments is given by Alley (1989) as $N_e = C/(1 - \tan\phi_s)$. However, effective pressure can also be expressed as a function of the bed geometry and stresses as $N_e = \beta_b \tau / f^*$, where β_b is a bed geometry factor, τ is basal shear stress and f^* the fractional area of the bed occupied by a water film. Thus, effective pressure in a water film overlying sediments is proportional to basal shear stress but inversely proportional to the area of the bed that is occupied by a water film (Alley, 1989).

Hence, till deformation only occurs if the shear strength of the sediment is exceeded (*i.e.* $\dot{\varepsilon}$ = 0, if $\tau \leq \tau_0$), which depends on porosity, temperature and water content of the substrate (Boulton and Jones, 1979; Clarke, 1987b). Using equation 2.5 a sliding law can be constructed, including bed deformation: for steady flow of a glacier coupled to its bed it has the form:

$$U_b = Ah \frac{(\tau - \tau_0)^a}{(N_e + N_0)^b}, \tag{2.6}$$

where h is the depth of the deformable layer and A, a and b are constants from the adjusted B-H rheology (equation 2.5) (Fowler *et al.*, 1994). However, shear strength and deformation rate of

till can vary spatially and temporally: for example, (partly) frozen till is less likely to deform than unfrozen till, though partly frozen sediment can show evidence of bed deformation (Boulton and Hindmarsh, 1987; Echelmeyer and Wang Zhongxiang, 1987). In this respect, the interaction between the basal drainage system and till deformation is of importance as till deformation can both create and destroy drainage paths (Clarke *et al.*, 1984; Murray and Dowdeswell, 1992). The leakage of the bed and impact of soft bed deformation on the overall flow regime of the glacier depends on the size of the glacier (Boulton and Jones, 1979; Boulton and Hindmarsh, 1987; Alley, 1989). Thus, bed deformation is dependent on basal hydrology, distribution of subglacial permeability, the pressure dependence of the flow law and the extent of a glacier (Boulton and Dobbie, 1993; Boulton *et al.*, 1995). For a more sophisticated flow law for glaciers overlying soft deformable sediments we therefore ideally need both the dynamic equations for till rheology, including the processes causing variations in till properties and a term related to the decoupled motion (Fowler *et al.*, 1994).

For a steady-state glacier (constant geometry) the ice flux is governed by the accumulation and ablation rates averaged over a period. This flux is used to transport the excess volume of ice from the accumulation area to the ablation area and is referred to as the 'balance flux': the corresponding ice velocity is the 'balance velocity' (Clarke, 1987a). The concept of balance flux would suggest a direct relation between mass transfer and glacier velocity via the 'activity index' (Meier, 1962) or 'energy of glaciation' (Schumskii, 1964): the steeper the mass balance gradient at the equilibrium line (expressed as mm mass loss/gain per m elevation change) the faster the ice flows. The activity index is related to continentality and latitude (for example, high polar glaciers have a typical activity index of 1 mm m^{-1} and temperate maritime glaciers of 10 mm m^{-1}), indicating that the distribution of glacier velocity could be geographically controlled (Andrews, 1975). Conversely, measured velocities show that the system is complicated by feedback mechanisms related to glacier geometry and local flow conditions and that changes in mass budget do not result in instantaneous changes in ice velocity, but via a glacier-specific response time (Clarke, 1987a; Oerlemans, 1996). Comparison of actual flow and balance flow gives a measure of the state of imbalance of a glacier: when the balance flux is higher than the actual (measured) flux, positive feedback mechanisms in the glacier system could trigger surges (Meier, 1965; Clarke, 1987a; Fowler, 1987a). Figure 2.1 (overleaf) is an example of a positive feedback mechanisms that could trigger a surge.

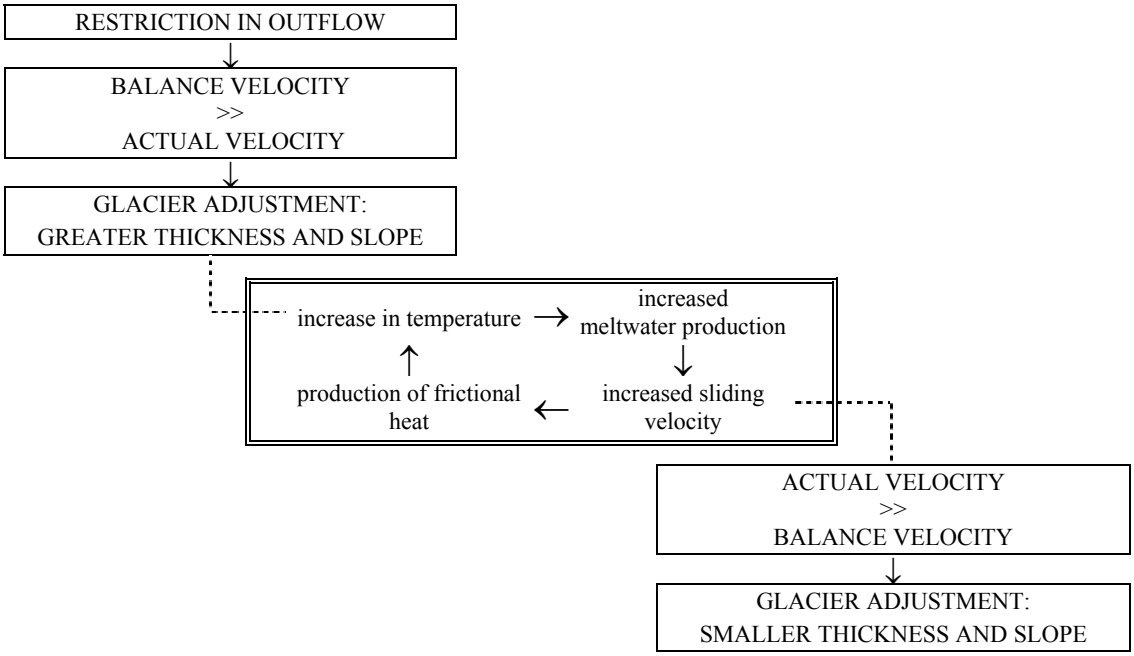

Figure 2.1: *An example of a positive feedback mechanism (lubrication: centre box) in the glacier system of a surge-type glacier (After: Meier, 1965; Sugden and John, 1976; Paterson, 1994).*

Deviations from balance velocity result from deviations in the balance between the driving forces and the resisting forces. Small perturbations in accumulation rate, water pressure and non-uniformities in the deformation rate, due to for example formation of crevasses, can initiate stress irregularities which may lead to short term perturbations in flow speed (Hutter, 1983). Temporal variations in the driving forces are related to variations in mass balance. As the adjustment to mass balance changes is not instantaneous, occurring according to a specific response time, glaciers are constantly adjusting to the large scale mass balance conditions and are in dis-equilibrium with their present mass balance conditions (Oerlemans, 1989). However, short term perturbations in mass balance, for example excess accumulation, can be transmitted downglacier more rapidly in the form of waves of increased velocity known as 'kinematic waves' (Bindschadler, 1982; Clarke, 1987a; Paterson, 1994). The response time appears to be related to the glacier size, but the exact form of relation is a subject of debate (Bahr *et al.*, 1998; Jóhannesson *et al.*, 1989; Oerlemans, 1989). Temporal variations in the resisting forces are primarily due to changes in hydrostatic pressure. These can occur periodically, due to diurnal or seasonal variations in meltrate, temperature and adjustment of the drainage system (Iken, 1981; Iken and Bindschadler, 1986; Alley, 1989), or in response to isolated events such as heavy rainfall or release of trapped water (Hooke *et al.*, 1989; Fountain and Walder, 1998).

2.4 Surge theories and boundary conditions

The occurrence of surging in a wide range of glaciers and environments (see Section 1.3.2) indicates that flow instabilities could occur in different elements that control glacier flow. Each time a positive feedback mechanism, or instability, can be detected in the physical laws describing ice motion, a surge theory can be developed to describe the switch between slow (normal) flow and fast flow (Hutter, 1983). Since the 1970s glaciologists have focused on three broad groups of ideas about the instability mechanisms:

1. *Thermal instability*
2. *Hydrological instability of the subglacial drainage system*
3. *Instability of a deformable substrate*

These mechanisms reflect the different types of glaciers that have been observed surging: glaciers overlying soft and hard beds, as well as polythermal and temperate glaciers. In order to understand and verify these potential instabilities it is necessary to identify the boundary conditions related to proposed instability conditions. The most plausible causes of instability that might lead to surging include creep instability, thermal instability, critical shear stresses or shear stress gradients, changes in subglacial drainage systems and unstable bed deformation (Clarke, 1987a; Raymond, 1987; Sharp, 1988a). Most scientists take a hydro-mechanical approach to explain surge instability. These include surge theories based on variations in longitudinal stress gradients (Budd, 1975; McMeeking and Johnson, 1987), kinematic wave propagation (Palmer, 1972); multivalued sliding/shear stress and water pressure relations (Mazo and Salamatin, 1986; Fowler, 1987a) and variations in water lubrication (Weertman, 1969) and water pressure (Kamb, 1987). Based on observations of bed deformation under fast flowing glaciers, unstable soft bed deformation has been proposed as a possible surge mechanism (Boulton and Jones, 1979; Clarke *et al.*, 1984; Alley, 1989). Others focus on the thermal approach and explain surge behaviour by thermal instability over space (Schytt, 1969) or time (Clarke, 1976). Only the multivalued sliding law theory depends on thermal and hydraulic conditions (Fowler and Johnson, 1995) and includes a combined thermo-mechanical approach.

2.4.1 First and untenable theories

Some pioneering studies of surge-type glaciers already recognised the fundamental issues of glacier surging: (1) surge-type glaciers are not in balance with their climatic environment, and (2) a surplus volume in the upper glacier basin causes a critical condition at which the surge is triggered (De Geer, 1910; Tarr and Martin, 1914).

On the basis of observations on the surge of Sefströmbreen, West Spitsbergen, De Geer (1910) postulated that surges relate to mass balance conditions. Glaciers for which the average accumulation rate is too small to maintain a balance velocity would build up a reservoir of ice. The load of ice accumulated in this reservoir zone over several years might overpass a limit in which a phase of active movement is started (De Geer, 1910; Lamplugh, 1911). Although the idea that climate is the primary control for surging is now abandoned (Meier and Post, 1969), some of De Geer's concepts were adopted to explain surges as well as postulated changes in surge behaviour (e.g. Budd, 1975; Dowdeswell *et al.*, 1995)

Tarr and Martin (1914) observed that earthquakes in the Yukatan Bay region, Alaska, caused an increased avalanche activity resulting in a surplus mass in the upper regions of glaciers and subsequently developed the *earthquake advance theory*: the surplus snow mass would trigger glacier surges with response times related to the size of the glaciers. The surge propagation was explained as a *glacier flood hypothesis*: the surge would propagate downglacier as a wave-like thrust increasing the viscosity of the lower ice layers and resulting in a rapid increase in ice motion (Tarr and Martin, 1914). However, Post (1967) observed that renewed earthquake activity in Alaska did not result in surging behaviour.

It has now been generally accepted that surges are not externally triggered because surges are observed in different geographical regions with a wide range of geologic and local climatic conditions and appear to be unrelated to any kind of external activity. Moreover, surging glaciers have individual semi-regular surge periodicities and asynchronous surging of neighbouring glaciers can occur (Sharp, 1988a). Instead, surging exemplifies imbalance and instability through an episodic self-regulating process, which can be perfectly explained by system-specific periodic oscillation (Miller, 1973; Fowler, 1987a)

2.4.2 Stress distribution and glacier surging

Longitudinal profiles of surge-type glaciers are unstable: during quiescence the profile steepens due to a thickening in the reservoir zone and a depletion of the receiving zone, while the downglacier transport of volume during the surge results in a decreasing overall surface slope and a rapid shallowing of the reservoir zone (Meier and Post, 1969). This suggests that during quiescence the basal shear stress would gradually increase (see equation 2.1). A surge would start when a critical basal shear stress was reached (Meier and Post, 1969). Indeed, shear stresses in surging glaciers are on average 20-50% higher than for the same glaciers in quiescence (Bindschadler, 1982; Osipova and Tsvetkov, 1991; Harrison *et al.*, 1994; Murray *et al.*, 1998). Although Dolgoushin and Osipova (1975) argue that enhanced deformation or faulting could be

a mechanism for surging, Meier and Post (1969) suppose that surge propagation must be maintained through decoupled motion under large longitudinal stresses. Further, as shear stress decreases during surge, water flotation would be essential for rapid sliding, although a surge would terminate when the total basal shear stress falls below the critical shear stress again. In addition, Meier and Post (1969) state that critical boundary conditions for the initiation of surge instabilities would only occur on beds with specific properties: the geographical distribution of these properties would thus be governing the geographical distribution of surge-type glaciers. However, Post (1969) showed that it is not obvious which specific bed conditions are conducive to surging.

The initiation of a surge often involves a compressive front: the surge bulge (see Section 1.4.1). While for normal glaciers average compressive strain rates of less than 0.1 per year are common, at the surge bulge of Variegated Glacier extremely large rates of 0.2 per day were inferred from the longitudinal gradient in the flow velocity (Kamb *et al.*, 1987). Given that surge-type glaciers have distinct zones of compressive and extensional flow, the longitudinal stress component cannot be ignored (Budd, 1975; McMeeking and Johnson, 1986). By comparing basal shear stresses with calculated required stresses for a number of surging glaciers, it was inferred that basal shear stress only partly supports the forces acting in the glacier (McMeeking and Johnson, 1986). This means that longitudinal stresses are comparable or larger than basal shear stresses in surging glaciers. Furthermore, continuous fast flow and surge front propagation are driven by longitudinal stresses in addition to the basal shear stress (Sharp *et al.*, 1988; Hodgkins and Dowdeswell, 1994).

Maybe even more important in surge dynamics is the local stress gradient, which can be very sharp at the vicinity of the surge front (e.g. Clarke *et al.*, 1984; Blatter *et al.*, 1998; Rolstad *et al.*, 1997; Murray *et al.*, 1998). According to a model by McMeeking and Johnson (1986), surges would initiate at the region of discontinuity between high and low drag regions because that is where the largest stress concentrations occur. After surge initiation the low drag region would spread rapidly up and downglacier and the surge would continue until the basal stress (including the longitudinal stress term) falls below a critical value (McMeeking and Johnson, 1986). Although this model is constructed to describe general surge features for all glaciers types, the stress concentrations could be translated into local effects of thermal (e.g. failure of frozen base), hydrological (e.g. damming of water or destroying of drainage paths) and substrate character (e.g. shear rupture). Although advantageous in terms of universal applicability, McMeeking and Johnson's model fails to provide a physical framework of surge processes.

In conclusion, if surge-type glaciers were to surge as an effect of stress distribution only, they would be steeper and deeper in their late quiescent phases than normal glaciers. Furthermore, local geometry anomalies such as icefalls or pronounced bed and surface undulations would be expected to occur more frequently on surge-type glaciers than on normal glaciers.

2.4.3 Thermal controls on surging and thermal instability mechanisms

The distribution of temperature within a glacier is fundamental to its motion and *vice versa*. Both internal deformation and sliding potential are temperature dependent (Paterson, 1994, see also Section 2.3). Moreover, glacier hydrology and debris entrainment are closely related to temperature in the ice and at the ice-bed interface (Clapperton, 1975; Boulton, 1996; Hodgkins, 1997; Fountain and Walder, 1998). Even if no glaciers surge by thermal instability, thermal processes must influence the timing of the surges in subpolar surge-type glaciers, because a glacier in surge cannot be frozen to a large fraction of its bed (Clarke, 1976; Clarke and Blake, 1991). Furthermore, it is postulated that one of the triggers or at least controlling factors of surges in subpolar glaciers can be the englacial thermal variability and the coupled hydrological and rheological properties (Robin, 1969; Clarke, 1976; Baranovski, 1977; Fowler and Johnson, 1995).

The analysis of thermal controls on flow instabilities is very complex because of the interdependence of a large number of processes determining the heat budget in a glacier. Shear heating (increasing temperature resulting in increased internal deformation) has been found to play a role in the thermo-mechanical behaviour of a glacier, but this mechanism is not likely to act as a surge trigger (Clarke *et al.*, 1977). Frictional heating is more likely to be related to flow instabilities as it can induce thermally regulated hydraulic-runaway surge mechanism (Fowler and Johnson, 1995). The frictional heat produced at the glacier bed due to sliding permits a positive feedback mechanism: frictional heat produces meltwater at the glacier bed, which reduces friction and enhances sliding. A negative feedback mechanism caused by the extension of a glacier as it advances prevents sustained sliding. As a result of extension and thinning during surge the temperature gradient at the ice-bed interface increases and the thermal flux away from the bed causes the glacier to refreeze at the bed (Robin, 1955; Clarke, 1976). As this process prevents sliding by dissipating water and possibly by thermal re-coupling it could be a possible relaxation mechanism in a surge cycle (Murray *et al.*, in review). Thus, when the glacier bed is at the pressure melting point the heat flux at the ice-rock interface may become discontinuous: this imbalance of flux is accounted for by melting basal ice or refreezing basal water (Clarke, 1976).

The initiator of the thermal instability theories, Robin (1955), argued that surges could be explained by the oscillation of the basal temperature between sub-freezing conditions where there is no sliding possible and melting conditions which are accompanied by rapid sliding. With increasing ice thickness during quiescence the basal shear could exceed the required shear stresses for ice movement at this temperature and this would lead to enhanced ice deformation. This state is unstable because deformation produces more heat. Further increase of ice velocity could raise the ice temperature to the pressure melting point, at which sliding can take place and a surge could start. Thinning of the glacier during a surge would lead to refreezing of the base to the substrate. Although Robin (1955) argues that this chain of events could be cyclic with a long period, Clarke (1976) found that the surge periodicity based on this mechanism is much longer than observed surge periods.

Thermal effects have been identified as possible controls on surge behaviour in subpolar glaciers. Schytt (1969) observed that subpolar surging glaciers in Nordaustlandet, Svalbard have a so-called 'cold ring' thermal regime. Cold ring glaciers have a polythermal structure with an inner core of warm ice at the pressure melting point throughout, surrounded by an annulus of cold ice frozen to bedrock. In years with enhanced melting in spring, water would trickle down and release latent heat to the cold ice below. This process could make the winter cold wave disappear completely and result in a glacier surge when the warm ice breaks through the barrier of cold ice. However, Schytt (1969) fails to explain the cause of the failure of the cold ring and it is unclear which boundary conditions are required for the breakthrough.

Similar cold ring thermal regimes have also been found in a number of subpolar surge-type glaciers in the Yukon-Alaska region (Collins, 1972; Clarke and Jarvis, 1976; Clarke *et al.*, 1984). One of these, Trapridge Glacier, has been intensely instrumented and monitored over several decades by Clarke and co-workers. From the Trapridge Glacier observations a number of thermally based surge mechanisms were developed and tested. Clarke (1976) proposed a surge mechanism based on thermally controlled glacier geometry: the improved version would later be known as 'thermal run-away' (Clarke *et al.*, 1977 and 1984). In order to maintain the velocity rate from a zone with sliding to a zone without, the internal deformation must increase, thus so must the basal shear stress (Clarke, 1976). A small rise in temperature would increase the internal deformation, leading to a further rise in temperature, *etc.*. Surge motion starts when the basal ice temperature reaches the pressure melting point, due to the combined effects of surface accumulation (thickening) and compressive glacier flow (Clarke *et al.*, 1977).

The polythermal structure of glaciers could also act as a cold-dam preventing the discharge of subglacial water (Clarke and Jarvis, 1976). The pressure increase caused by this trapped water

could eventually trigger the surge, particularly during periods of enhanced melting in spring. The balance between the frictional heat source and the advective heat sink caused by extension and thinning of the glacier would control the duration of the active sliding phase. Eventually, the thermal flux away from the ice-rock interface exceeds the generation of frictional heat and the glacier refreezes to its bed and the surge terminates. However, field observations have not been able to identify locally trapped water under Trapridge Glacier or Variegated Glacier (Bindschadler *et al.*, 1977; Clarke *et al.*, 1984).

A common feature on subpolar surge-type glaciers is the development of a surge bulge in the late quiescent phase (Dolgoushin and Osipova, 1975; Clarke *et al.*, 1984; Murray *et al*, 1998). In the initial stages of the surge, this bulge causes an uplift of the glacier surface at the location where the surge starts. Both the formation and propagation of the surge bulge are believed to be intimately related to the thermal regime of a glacier: a surge bulge commonly initiates at the boundary between warm-based ice and cold ice with permafrost underlying the glacier from the bulge downstream (Clarke *et al.*, 1984; Clarke and Blake, 1991; Murray *et al.*, in review). Initially, it was suggested that a thermal boundary was the primary control on the ice flow and the initiation of a surge. But, as no thermal instability was found near the Trapridge's surge bulge it was suggested that downstream resistance to sliding might be a controlling factor to surging, as it divides the glacier into a reservoir and a receiving area (Clarke *et al.*, 1984). Increased ice thickness and surface slope would decrease both the stability of the substrate and of the subglacial drainage system, increasing the hydrostatic pressure at the glacier bed. Because the geometry of the glacier changes during the surge, the system stabilises again and the drainage system can be re-established. By inference from the above, variations in water pressure due to water storage, were proposed to play a more essential role in surging than the thermal regime of the glacier (Clarke *et al.*, 1984). These findings support Clarke's initial statement that 'thermal regime would be more of a regulatory effect on glacier surging than a causative one' (Clarke, 1976). Indeed, at a later date it was observed that the surge bulge propagated as an overthrust incorporating the cold-ice downglacier of the bulge, while not raising the temperature of this ice (Clarke and Blake, 1991). The ice flow on Trapridge Glacier is thus apparently not primarily thermally controlled.

More recently, studies on Bakaninbreen, Svalbard, have revived the theories of thermal controls on glacier surging (Murray *et al.*, 1998; Murray *et al.*, in review). Bakaninbreen is a polythermal surge-type glacier overlying a soft deformable bed of 1-3 m thickness (Porter *et al.*, 1997). The surge of Bakaninbreen has been characterised by a long duration, low shear stresses and a slow and indistinct surge termination (Murray *et al.*, 1998). Radar and basal instrumentation suggested that the propagation of the surge bulge coincided with the propagation of a thermal

boundary, where warm-based ice occurs above the surge front and cold-based ice overlying permafrost below the surge front (Murray *et al.*, in review). Because the surge front propagated downglacier at a faster rate than the permafrost layer could be warmed, it was suggested that fast movement took place as a result of sliding over the bed or bed deformation of only the top layer of the substrate (Murray *et al.*, in review). Surge propagation would then be facilitated by the high-pressure basal water trapped between the fast moving ice and the permafrost layer beneath it. The surge termination would result from the slow dissipation of the high basal water pressure, where the water would evacuate from the high pressure layer through processes of refreezing and leaking downwards to the bed and upwards through the glacier (Murray *et al.*, in review). Both propagation and termination of the surge of Bakaninbreen would thus be thermally regulated. This mechanism for thermal relaxation could possibly explain the gradual and indistinct surge termination of other Svalbard glaciers (Drewry and Liestøl, 1985; Hagen, 1988).

The major weakness of the thermal surge mechanism is that it does not explain surges of temperate glaciers. Moreover, no satisfactory explanations of thermal character have been developed to explain the commonly observed sudden termination of glacier surges (see Section 1.3.3). However, it was not until 1976 that the existence of a temperate thermal regime in a surge-type glacier was confirmed by temperature measurements (Bindschadler *et al.*, 1976). This observation was of vital importance to the development of surge theories other than only thermally or stress based. Whereas glaciers that are temperate throughout cannot surge by a thermal instability mechanism, thermal conditions can however still play a role in the timing and development of a surge (Clarke, 1976; Clarke *et al.*, 1984).

2.4.4 Testing factors related to thermally controlled glacier surging

If thermal instability were the controlling mechanism of surges, regional variations in geothermal heat flux, permafrost conditions, bed roughness, permeability and erodibility, accumulation rate and a mass balance function related to bed- and glacier geometry could be controlling the geographic distribution of surge-type glaciers (Robin, 1955; Clarke, 1976; Clarke *et al.*, 1984). High accumulation rates will increase the downward heat flux as well as the rate of thickening of the glacier in the reservoir area and could possibly accommodate conditions favourable to surging.

It is also suggested that subpolar glaciers with a polythermal regime are more inclined to surge, as these have a markedly different hydrological regime from temperate and polar glaciers (Baranovski, 1977; Hodgkins, 1997). In Svalbard, a trend in the geographical distribution of glaciers with internal reflection horizons (continuous IRHs are indicators of a polythermal

regime: see Section 5.2.5) can be observed (Macheret and Zhuravlev, 1982; Bamber, 1987). This trend is suggested to be related to the distribution of surge-type glaciers (Hamilton and Dowdeswell, 1996) or to the distribution of climate variations over the archipelago (Bamber, 1987). Statistical testing of the relationship between polythermal regime and surge potential in specific regions could elucidate to what extent thermal regime is related to surging. In this respect, it is also important to consider glacier size in conjunction with thermal regime, as it is argued that the presence of a polythermal regime is directly related to glacier thickness: the thinner a subpolar glacier the more likely that it is cold throughout (Hagen *et al.*, 1993). Thick glaciers in subpolar areas would therefore be more likely to have a polythermal regime (Jiskoot *et al.*, in review). Furthermore, although retreating glaciers with basal sliding switched off have generally steeper surface slopes than retreating glaciers with a sliding component, surge-type glaciers with a thermally 'blocked' outflow must be even thicker and steeper in their quiescent phase than normal retreating glaciers (Clarke *et al.*, 1984; Schwitter and Raymond, 1993). Controlling factors on surge initiation would therefore be ice thickness and surface slope, while a positive mass balance is necessary.

2.4.5 Hydrological controls on surging and hydrological instability mechanisms

As thermal theories are unable to explain surges in temperate glaciers, alternative surge theories have been developed for temperate (and polythermal) surge-type glaciers. As the base of a temperate glacier is at the pressure melting point, a thin layer of water can form at the ice-bed interface (Weertman, 1979). When water volume increases either an interconnected conduit system or a linked-cavity system will develop, dependent on subglacial topography, water flux and hydrostatic pressure (Lliboutry, 1969; Weertman, 1972; Walder, 1982; Kamb *et al.*, 1985). A conduit system consists of a major network of tunnels, mostly parallel to the ice flow direction and arborescent in configuration (Fountain and Walder, 1998). A linked-cavity-system is an ensemble of cavities and orifices of different shapes and sizes. The water flow in this system is determined by the size of the orifices (generally <0.1m), where the general flow direction is transverse to the ice flow (Kamb, 1987). A linked-cavity-system is characterised by a long retention time of water and high basal water pressures reducing the friction at the glacier bed and enhancing sliding (Lliboutry, 1968; Kamb, 1987). Unconsolidated permeable beds can also drain a proportion of the subglacial water in the substrate. Because the permeability of subglacial sediment is limited, the influx water into the bed will rapidly exceed the water evacuation capacity, which is limited by the hydrostatic pressure. As a result, the subglacial water pressure will rise unless a drainage system can develop in the substrate (Alley, 1989; Murray and Dowdeswell, 1992; Ng and Fowler, in review). Through the year the drainage systems can

evolve with a more efficient (conduit) draining system generally developing during the melt season (Fountain and Walder, 1998).

Subglacial drainage systems can be distinguished by two types of pressure-flux relations: one in which water discharge and water pressure are inversely related (e.g. conduit system) and one in which water discharge and water pressure are directly related (e.g. linked-cavity-system). These relations are important as basal motion and the hydrological system are closely related. Surge-mechanisms related to the subglacial drainage system are based on disruption of the normal subglacial hydrology and the related effects on sliding (Paterson 1994). Although hydrological instability mechanisms are build on the assumption of a hard bed, the mathematical treatment could be the same for hard and for soft beds (Fowler, 1987b). There are two main processes that might explain the appearance of surges due to the nature of the subglacial hydrology system: lubrication (Lliboutry, 1968; Weertman, 1969; Budd, 1975) and flotation (uplift of the glacier from its bed caused by high effective pressures) (Kamb *et al.*, 1987; Harrison *et al.*, 1994; Iverson *et al.*, 1995). Both processes reduce the friction at the glacier bed and enable fast sliding: the first results in sliding without cavity formation and the second in sliding with cavity formation. Sliding without cavity formation can be translated into 'Weertman-type' linear or non-linear sliding laws where sliding velocity is a direct function of basal shear stress, whereas sliding with cavitation is described in 'Lliboutry-type' sliding laws where sliding velocity is a multivalued function of basal shear stress and where the magnitude of the effective pressure is critical (Fowler, 1987b).

2.4.6 Water lubrication mechanisms

For the water lubrication surge mechanism it is assumed that the subglacial drainage is through a distributed system consisting of a water film of variable thickness (Weertman, 1969). If this water layer was to reach a certain thickness it could submerge bed obstacles, reduce friction and enhance sliding (Weertman, 1969). For a bed with juxtaposed series of obstacles of different sizes, there will be a specific obstacle size would give the most resistance to sliding. This 'controlling obstacle size' Λ can be expressed as (Weertman, 1969):

$$\Lambda = C_T \left(\frac{\beta^n k^{n-1}}{B s^{2n-2} \tau^{n-1}} \right)^{\frac{1}{2}}, \tag{2.7}$$

where C_T is a constant for thermal conditions at the ice-bed interface, β is a term related to cavities behind the obstacle (1 when there is, 2 when there is not), B and n are the constants from

Glen's Law, s is a bed-smoothness measure related to the average obstacle size, τ is basal shear stress and k^{-1} is the fraction of the total force acting parallel to the bed as a result of the basal shear stress (Weertman, 1969). For a jagged (rough) bed, s is small and thus Λ is large, hence smooth beds would be conducive to surging. The controlling obstacle size was estimated to be 3-6 mm for an average glacier, but later estimates vary range from 1 to 100 mm, with regelation inferred to be most effective at obstacle sizes shorter than 10 mm (Weertman, 1967; Weertman, 1969; Alley, 1989; Paterson, 1994; Hubbard and Hubbard, 1998). Average water-film thickness is expected in the order of 0.5-1 mm, hence for an exceptionally smooth glacier bed with obstacle sizes in the order of 1-2 mm, the water film thickness could become more than 0.1 times the controlling obstacle size (Weertman, 1969). This results in the increase of sliding velocity as:

$$U_s^* = \frac{10\Lambda'}{\Lambda} U_s \,, \tag{2.8}$$

where U_s* is the increased sliding velocity, Λ' the finite thickness of the water film, Λ the controlling obstacle size and U_s the normal sliding velocity (Weertman, 1969). Increasing ice thickness during quiescence raises basal shear and results in a reduction in the controlling obstacle size. A surge would be triggered when the ice thickness reaches a critical value, possibly related to the passage of a kinematic wave through the glacier (Weertman, 1969). Once the glacier surges, the melt rate at the glacier bed would increase and fast sliding velocities could be sustained over a considerable time. This is a type of 'hydraulic run-away' (Fowler and Johnson, 1995).

Finite water layer thickness calculated as a function of melt rate at the glacier bed, inverse water pressure and glacier length show that the longer the glacier, the greater the thickness of the water film that can develop (Weertman, 1969). Longer glaciers would thus have higher probabilities of being surge-type: Weertman (1969) found that the highest probabilities of glaciers being surge-type are found in glaciers over 30 km in length with a 'smooth bed' with controlling obstacle size of about 1-2 mm.

Apart from lubrication being distributed over a large subglacial area, a negative gradient in basal shear stress could cause water to be trapped, lubricating a local trigger zone (Robin and Weertman, 1973). As yet, field evidence does not support this theory as no negative gradients in water pressure have been measured at the (alleged) locations of surge initiation (Bindschadler *et al.*, 1977; Clarke *et al.*, 1984).

Naturally glacier beds are more complicated than envisaged by Weertman (1969): a more realistic bed would have larger obstacles covered with smaller ones (Lliboutry, 1967). Instead of developing a continuous water layer, pockets (cavities) of water could fill in the lee-side of large-size obstacles (Lliboutry, 1968). Furthermore, Walder (1982) proved that a continuous sheet of water is not stable as water pressure increases and instead, with increasing water pressure, conduits in the ice or in the substrate develop. A permeable bed that allows water to leak away would also prevent the development of a water film at the glacier bed. Another major drawback of Weertman's lubricating mechanism is that it fails to explain the termination of surges.

Budd (1975) suggested a more generic type of lubrication as a control of surges. He argues that fast sliding would be made possible by a localised excess of meltwater, reducing the basal shear stress. Budd (1975) expressed this as a 'friction lubrication factor', ϕ, and an additional 'geothermal factor', q, for regions with a higher than average geothermal heat flux. If ϕ or q reach a critical value, the shear stress at the base of the glacier would be lowered so much that very fast flow is made possible. Given that ϕ is directly related to the energy dissipation by basal motion (τV), the lubrication increases with increasing velocity. The total energy dissipation can be defined as:

$$\tau V = S\rho g \alpha \Phi , \tag{2.9}$$

where S is flux shape factor (0.5<S<1), ρ ice density, g gravitational acceleration, α surface slope and Φ balance flux per width for a given flux shape factor (Budd, 1975). Thus, the lubrication factor is directly related to the surface slope and balance flux (equation 2.9 can be simplified as $\tau V \equiv \alpha \Phi$). Evidently, balance flux is related to the accumulation rate over the catchment (Clarke, 1987a).

Using existing glacier data in this model, Budd (1975), concluded that glaciers could be divided into three groups (see Figure 2.2): (1) slow/normal flowing glaciers with low fluxes and lower than critical lubrication factors, (2) continuously fast flowing glaciers with fluxes that are high enough to have a permanently lowered basal shear stress (lubrication factors higher than critical), and (3) surge-type glaciers that switch between the two modes. The critical lubrication factor, separating surge-type glaciers from normal and fast flowing glaciers, can be approximated as:

$$\Phi \tilde{\chi} = \mathrm{O}\left(10^5\right) m^2 a^{-1} , \tag{2.10}$$

which is the product of balance flux divided by width (Φ) and ten times surface slope in radians ($\tilde{\chi}$) (Budd, 1975; Fowler, 1989). Surge-type glaciers would only build up to this critical stage after a number of years of accumulation and a steepening during quiescence. When the critical value (equation 2.10) is reached a surge would start through lubrication of the base, but the accumulation rate would be too low to maintain this fast mode. With changing geometry the glacier would switch back into the slow mode again. However, the geographical distribution of surge-type glaciers in Alaska cannot be explained by the mass balance-slope relationship alone (Wilbur, 1988: see Section 3.3.7).

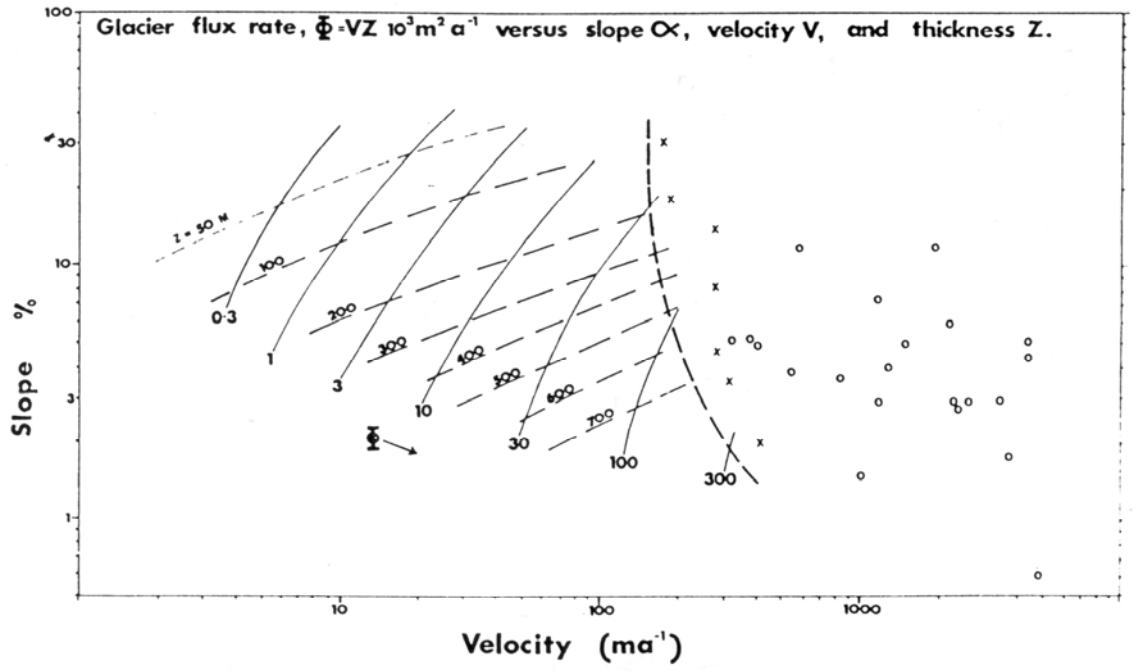

Figure 2.2: *Budd's diagram, showing the critical product of* $\Phi\tilde{\chi}$ *as a heavy broken line. Crosses in this diagram are surge-type glaciers and circles are fast flowing glaciers (From: Budd, 1975).*

According to Budd (1975), the surge velocity would be dependent on the lubrication factor ϕ and the ice viscosity η (see Figure 2.3). The lower the viscosity the faster the flow that is possible. Ice viscosity is temperature and stress dependent: cold glaciers have lower flow velocities as their viscosity is about 2 times higher than that of temperate glaciers. Viscosity would also be lowered under large longitudinal stresses: this suggests that large bed undulations have a direct effect on the flow velocity. Hence, according to Budd's theories, surge-type glaciers would not be a distinct category of glaciers, but glaciers would be able to pass from one state into another, just by changing mass balance conditions. The changing character of surges in Svalbard as postulated by Dowdeswell *et al.* (1995) would conform to this idea.

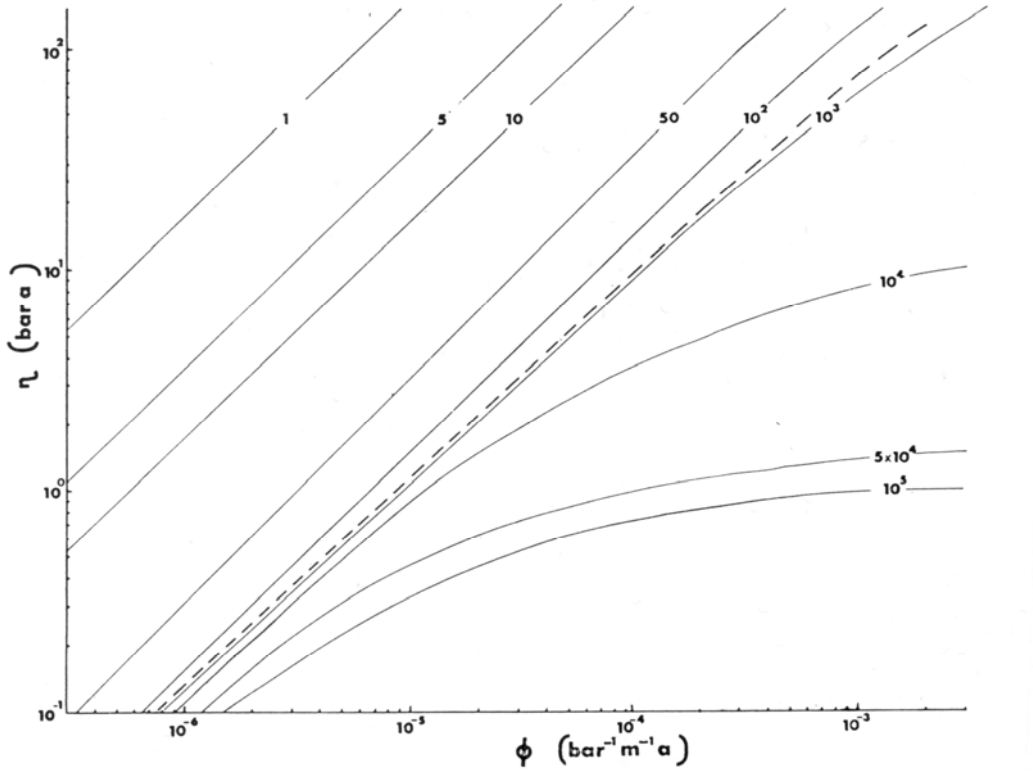

Figure 2.3: *Variations in maximum sliding speed (m a^{-1}) over different values for viscosity (η) and lubrication (ϕ). The dashed line is the division between steady-state glaciers, to the left, and surge-type glaciers, to the right. Temperate ice has a lower viscosity than cold ice, thus temperate glaciers would be more likely to reach higher sliding speeds (From: Budd, 1975).*

2.4.7 Testing factors related to lubrication controlled glacier surging

For Weertman lubrication, surge-type glaciers should be longer than normal glaciers and overlie smooth impermeable beds, where the obstacles are in the order of 1-2 mm (Weertman, 1969). This implies that surge-type glaciers would overlie lithologies with small grainsizes and low permeabilities. Instead, Budd (1975) considers accumulation rate and bed profile as primary controls on glaciers surging, whereas other factors (such as bed smoothness, geothermal heat flux, *etc*.) are secondary. The proposed critical lubrication factor can be tested in geometrical terms as the product of accumulation rate and slope have to be high. Steep mass balance curves, high accumulation area ratios (AARs) and steep surface slopes would thus be typical for surge-type glaciers in their late quiescent phase.

Characteristic glacier hypsometry curves are related to characteristic net mass balance curves and accumulation area ratios, while glacier hypsometry is also important in regulating glacier flow (Furbish and Andrews, 1984). One of the most powerful feedback mechanism between glacier geometry and mass balance is the 'altitude mass balance feedback': a rise in the overall

glacier elevation results in a larger net balance (Oerlemans, 1996). The strength of this relation depends on the rate at which glacier thickness increases with glacier size and is most effective for glaciers resting on flat beds and for keyhole-shaped glaciers (glaciers with a large accumulation area and a narrow glacier tongue) (Oerlemans, 1989). The rate of change of AAR due to changes in the equilibrium line elevation is therefore mainly controlled by the glacier hypsometry. Besides, the altitude-mass balance feedback mechanism causes a nonlinearity in glacier flow: for a glacier with a reversed bed slope (overdeepening) it is possible to have two stable geometry solutions for the same mass balance (Oerlemans, 1989). Thus, in support of Budd's theories, glaciers with top-heavy hypsometries (e.g. keyhole-shaped glaciers) in combination with large AARs would be more likely to surge.

2.4.8 The linked cavity configuration surge mechanism

Field observations suggested basal friction is not simply reduced by the presence of subglacial water but rather by bed separation and the storage of pressurised water (Lliboutry, 1968; Kamb, 1970; Iken, 1981). The lubrication mechanisms of Weertman (1969) and Budd (1975) are therefore not sufficient to explain surge velocities, unless their sliding laws are supported by a pressure term, in which the relationship between sliding velocity and subglacial water pressure is quasi-continuous (Lliboutry, 1968; Bindschadler, 1983; Fowler, 1987b). The fundamental question is what causes the storage of water and the high water pressures (Raymond, 1987). For surge-type glaciers blockage or collapse of passageways could result in an imbalance of in and outflow of water, leading to high effective pressures and subsequent bed separation (Röthlisberger, 1969; Iken, 1981; Clarke *et al.*, 1984; Kamb, 1987).

The importance of cavitation (bed separation) in controlling sliding velocity has been emphasised by Lliboutry (1968, 1969). He postulated that glacier sliding would be a multivalued function of the basal shear stress and effective pressure. Given the pressure-flux relation of conduit systems is inverse and that of linked-cavity systems is direct, the effective pressures are generally low in conduit systems, but can be close to overburden pressure in linked-cavity systems (Kamb, 1987). Figure 2.4 shows a general multivalued sliding law for which two branches of stable sliding velocity exist: a 'slow branch' for drainage through conduits (R-channels) and a 'fast branch' for drainage through linked cavities. At critical values for τ and N_e, sliding could become unstable and switch to the next branch (Lliboutry, 1969; Fowler, 1987a; Kamb, 1987; Fowler and Johnson, 1995). For surges, drastic changes in the ice-bed coupling must occur, thus only if the jump from one branch to the other is large enough might this explain mathematically the flow instability that occurs in glacier surges (Fowler, 1987a; Kamb, 1987).

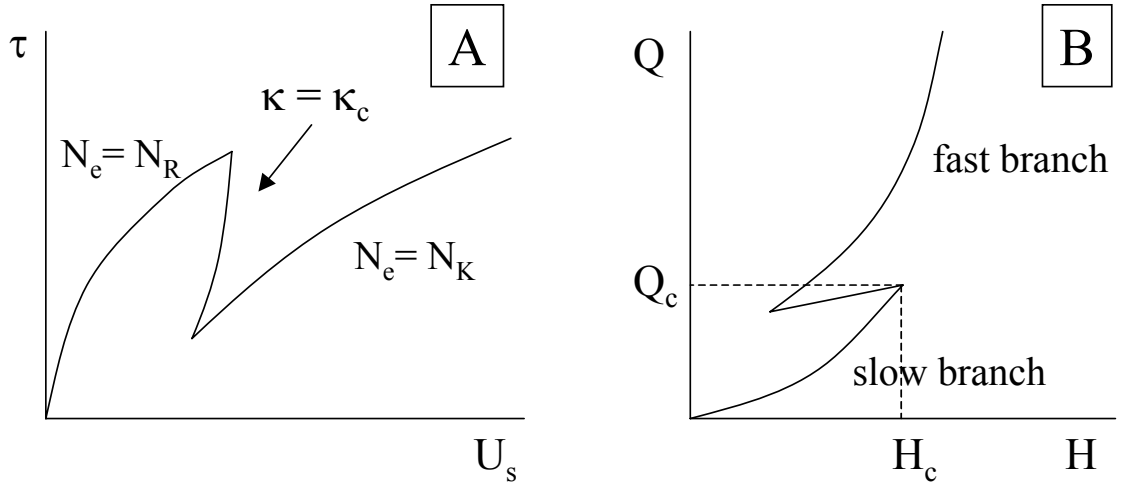

Figure 2.4: a) *Multivalued sliding law relation between basal shear stress and velocity. N_e is the effective pressure, N_R is the pressure at which channels are stable and N_K where a linked cavity system is stable,* ***κ*** *is a flow parameter: at* ***κ*** *=* ***κ***$_c$ *there is a transition from conduit drainage to linked cavity drainage;* ***b)*** *multivalued flux (Q)/depth (H) relation. At a critical depth and corresponding critical flux the ice flow jumps from the slow branch to the fast branch (After: Fowler, 1987a and Fowler, 1997).*

Field observations on relations between ice-bed separation and ice velocity suggest that velocity is highest at the early stages of cavity growth, in transient rather than stable conditions (Iken, 1981). A critical water pressure where sliding would become unstable was derived:

$$p_{crit} = p_i - \frac{\tau}{\tan \beta_s}, \tag{2.11}$$

where p_i is ice overburden pressure (ρgH), τ basal shear stress and β_s the steepest angle between the stoss faces of bed obstacles and the mean bed slope (Iken, 1981). If subglacial water pressure exceeds p_{crit} the glacier is pushed upwards as a rigid body along the stoss face of the bed waves, a phenomenon that is also know as the 'hydraulic jack effect' (Röthlisberger and Iken, 1981). This would suggest that ice-bed separation is more common in thick glaciers with steeper slopes overlying rugged beds.

The effect of pressurised water on the sliding process was subsequently examined through a 'bed separation index' (Bindschadler, 1983). The bed separation index

$$I \equiv \frac{\tau}{N_e}, \tag{2.12}$$

is dependent on τ (basal shear stress) and N_e (effective pressure). Bed separation can occur when I exceeds zero but there is no strict quantitative relationship between I and U_s, because bed separation is not proportional to the increase in I and is moreover dependent on the bed roughness (Bindschadler, 1983). However, if N_e is zero the glacier is afloat and I tends to infinity (Bindschadler, 1983). As the distribution of water pressure is strongly dependent on glacier geometry, it is likely that surge-type glaciers have more extreme values for I than normal glaciers. Bindschadler's bed separation index would predict that surge-type glaciers are thicker and steeper than normal and would have higher hydrostatic pressures.

Observations before and during the 1982-83 surge of Variegated Glacier, Alaska, inspired the development of a detailed linked-cavity configuration surge mechanism (Kamb *et al.*, 1985; Kamb, 1987). Bindschadler (1983: see above) had already suggested that bed separation and high effective pressures were promoting the fast flow during the surge. By combining the signals of water pressure and water retention with the observations on geometric adjustment and timing of the surge, Kamb *et al.* (1985) developed a more detailed picture of processes of bed separation and pressure-flux relationships.

Variegated Glacier's surge activity started with frequent icequakes in winter (January 1982) and terminated at the height of the meltseason (mid-July 1983). The surge occurred in two phases, where for each phase the peak velocities occurred in mid-to-late June (see Figure 2.5). During the surge, 95% of the flow velocity was due to basal sliding, while only 5% was due to internal deformation. Dye trace experiments, borehole measurements and proglacial hydrological observations revealed that before the surge the water drained subglacially in an effective low pressure conduit system, while during the surge consistently high water pressures around overburden pressure occurred and the basal water flow was retarded and laterally dispersed (Kamb *et al.*, 1985). Peaks in water pressure coincided with oscillatory pulses in glacier movement and sudden increases in horizontal flow were accompanied by vertical uplifts of the glacier surface. Surge termination was marked by a drop in the ice surface and coincided within days with a massive outburst flood. After the surge termination, the effective low pressure drainage system was re-established (Kamb *et al.*, 1985).

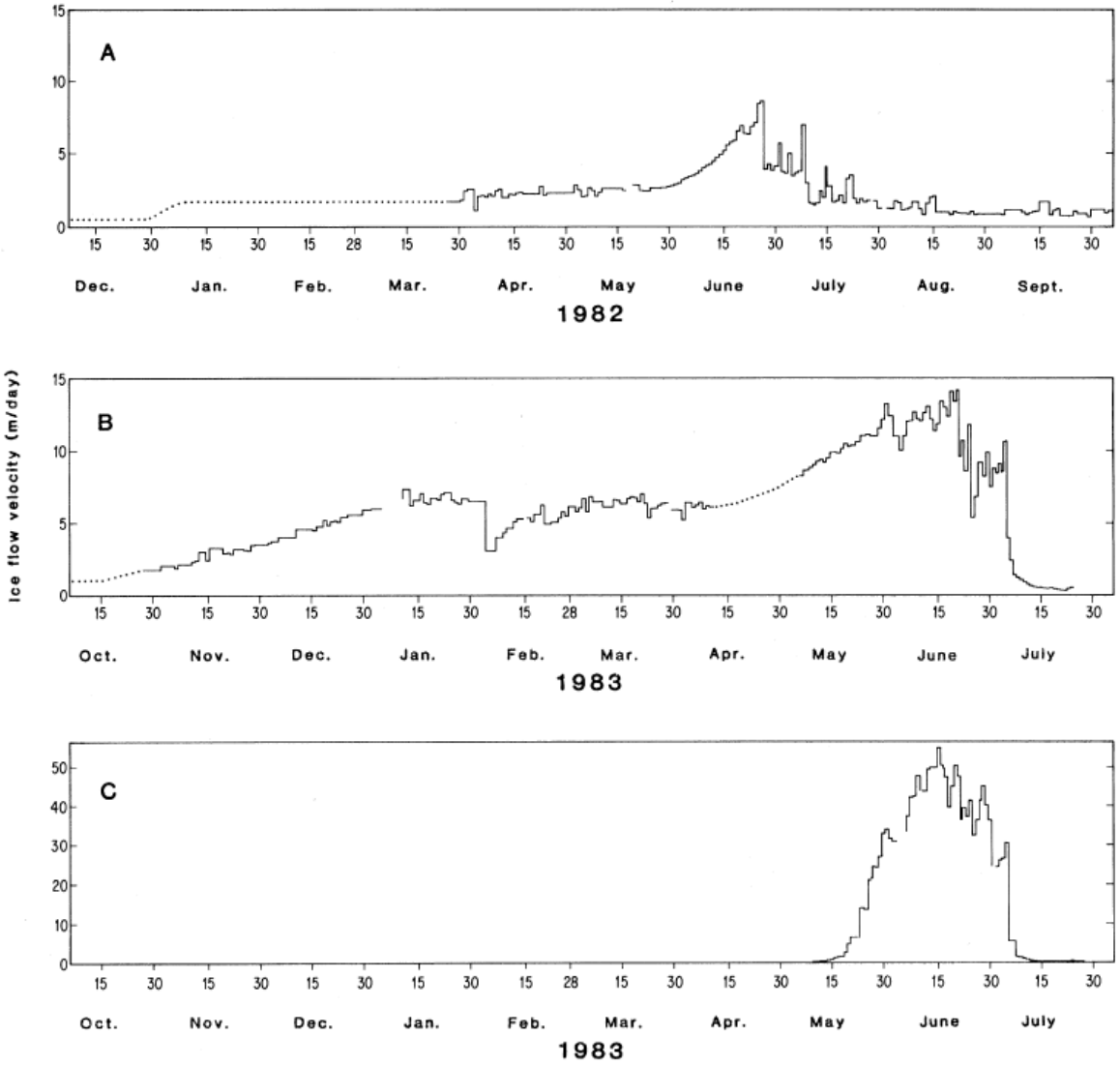

Figure 2.5: *Surge velocities of Variegated Glacier. A and B are measured in the upper 8 km of the glacier, while C is measured at 15 km from the head (4-5 km from the margin) (From: Kamb et al., 1985).*

Kamb *et al.* (1985) postulated from the link between vertical and horizontal velocity that fluctuations were caused by the process of ice-bedrock separation or basal cavitation. The surge trigger would coincide with a sudden switch in the subglacial drainage system from a conduit-dominated system to a linked-cavity-system (Kamb *et al.*, 1985). This shift would occur when the main tunnel in the conduit system outgrows itself, de-stabilises and collapses (Kamb, 1987). The process of bed separation, enhanced by a sudden increase in water pressure would then lead to the development of a linked-cavity-system (Iken, 1981; Bindschadler, 1983; Kamb, 1987).

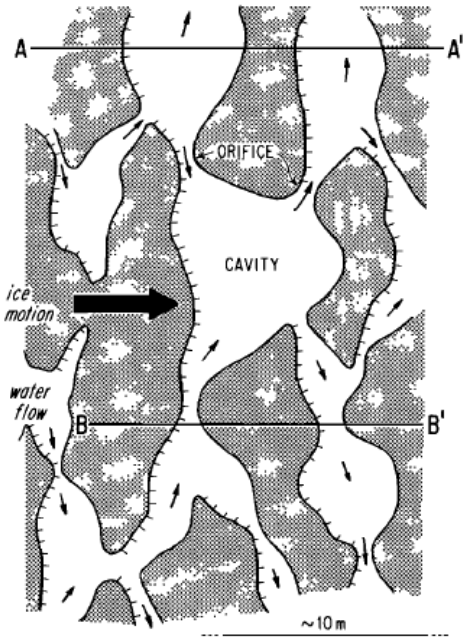

Figure 2.6: *Linked cavity system with glacier flow from left to right (From: Kamb, 1987)*

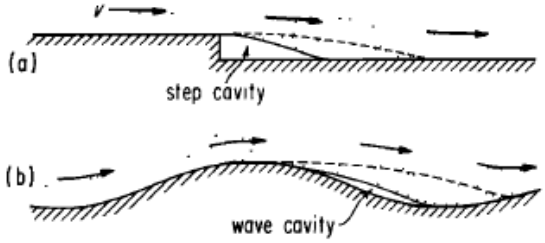

Figure 2.7 a) *Step and* ***b)*** *wave geometry cavities. The dashed line gives the configuration of the cavity roof for increasing sliding velocity or increasing effective pressure (From: Kamb, 1987).*

Bed separation can result in two main geometry types of cavities and orifices: a step geometry and a wave geometry (see Figure 2.7). Cavities and orifices are held open by the melting of the glacier roof (meltback rate) and tend to close as a result of ice flow (gap-closure) (Kamb, 1987). The flow of water through a linked-cavity-system appears to be sensitive to the geometry of orifices rather than that of cavities (Kamb, 1987). For a given bed roughness, water pressure, ice overburden pressure and sliding velocity, a particular orifice geometry is determined by cavitation processes. The discharge of water flow is determined by the geometry of orifices and cavities and the hydraulic gradient. As flowing water generates heat by viscous dissipation, the orifice roof is melted back, increasing the orifice diameter and thus increasing the drainage capacity and water flux. If meltback-rate and gap-closure-rate are balanced, cavities and orifices are stable. Kamb (1987) expresses this balance by an orifice melting stability parameter: Ξ for step orifices and Ξ' for wave orifices. The stability parameters are expressed as:

$$\Xi = \frac{2^{1/3}}{\pi^{1/2}} \frac{\alpha \Lambda_h / \omega}{DM} \left(\frac{\eta}{V \sigma_R} \right)^{1/2} H^{7/6} \left(\frac{\tau_R}{\tau} \right)^{3/2} \tag{2.13}$$

and

$$\Xi' = 0.162 \frac{(\alpha \Lambda_h / \omega)^{3/2}}{DM} \frac{\lambda o^{3/2}}{V_R} \left(\frac{\tau}{\tau_R} \frac{\sigma}{\sigma_R} \right)^3 \left(1 - \frac{\sigma^2}{\Sigma_0{}^2} \right)^{11/6} . \tag{2.14}$$

In equations 2.13 and 2.14, α is glacier surface slope, Λ_h the hydraulic length of the cavities (length of cavity/length of orifice parallel to the water flow), ω orifice tortuosity, D a constant dependent on ice thickness, M Manning roughness, η ice viscosity, V ice velocity, σ effective pressure, H glacier thickness, λ and o are the orifice wavelength and amplitude, Σ is a wave cavitation parameter that increases with velocity as $V^{1/3}$ (Kamb, 1987). A linked-cavity system would be stable for $\Xi<1$ or for $\Xi'<1.5$ (Kamb, 1987). Thus, for glaciers in quiescence the values for Ξ and Ξ' would be higher than these critical values. A surge would start when the linked cavity system at the start of the meltseason is stable and remains stable when the water flux increases: high water pressures would then reduce the basal friction and fast sliding is promoted. A surge would terminate when the stability parameters fall below the critical value and the linked-cavity-system degenerates into a tunnel system (Kamb, 1987). An unsolved problem is how the cavity system and high sliding velocities could be maintained over periods of 2-3 years.

Because Ξ and Ξ' vary with surface slope as $\alpha^{3/2}$, given other variables in equations 2.13 and 2.14 are held constant, low slopes would be related to stable linked-cavity-systems (Kamb, 1987). However, stabilisation of the linked cavity system is not only promoted by low slopes, but also by high sliding velocities and large basal shear stresses (thus increased glacier thickness) (Kamb, 1987). Surges are therefore likely to start at locations in the reservoir area where the glacier depth has increased, but where the surface slope has not increased during quiescence. This slope dependence of the orifice stability parameters implies that low slope is conducive to surging (Clarke, 1991). Furthermore, the larger a glacier, the more vulnerable its subglacial drainage system to instability and collapse (Clarke *et al.*, 1986). Therefore, long glaciers with low slopes are more likely to conform to a linked-cavity-configuration surge mechanism than short steep or long steep ones.

Other physical-mathematical theories describing cavity formation in relation to surging include Fowler (1987a) and Fowler (1989). Based on two central relations in the general sliding law function: $\partial \tau / \partial U_s > 0$ and $\partial \tau / \partial N_e > 0$, Fowler (1987a) postulated that the ice flux, Q, is multivalued depending on the ice depth, H (Figure 2.4). If the ice flux reaches a critical value Q_c,

the switch from normal flow (lower branch) to surge flow (upper branch) occurs. From the general steady state relation $Q = s(x)$, in which $s(x)$ is a concave profile, Q_{max} must coincide with s_{max}, so Q_c is first reached at s_{max} (Fowler, 1987a).

Fowler (1987a) describes an irregular bed with cavitation as a self-similar bed:

$$\gamma \approx \lambda_i^{\alpha^*/2}, \tag{2.15}$$

where γ is the amplitude and λ_i the wavelength of the irregularities in the bed, α^* is a dimensionless parameter with $2 < \alpha^* < 2\left(\frac{n+2}{n-1}\right)$ (if regelation is ignored), where n is the constant from Glen's Law (equation 2.2). Geologically 'young' beds are somewhat jagged and have small amplitudes, thus small values of α^*, whereas older beds would be expected to be more eroded and have longer amplitudes and larger values for α^* (Fowler, 1987a). The multivalued sliding law for these irregular beds is mathematically expressed as:

$$\tau^* = k\left(\mu_2 N^*\right)^a \left(U^* \mu_1^{-1}\right)^{(1-r)n^{-1}}, \tag{2.16}$$

where τ^*, N^* and U^* are dimensionless stress, effective pressure and velocity measures, k is a measure for the bed profile; r, μ_1 and μ_2 are dimensionless parameters related to bed roughness where r is defined by Fowler (1987) as:

$$r = 1 - n\left(\frac{\alpha^* - 2}{4 - \alpha^*}\right), \tag{2.17}$$

where for $n = 3$, $2 < \alpha^* < 2.5$ and $0 < r < 1$. The surge is triggered when τ^* is at its maximum.

From the multivalued sliding law and a tunnel stability term related to water pressure and degree of cavitation, Fowler (1987) derived an expression for the ratio of quiescent and surge velocities, U_- and U_+, corresponding to the velocities of the lower and upper branch in Figure 2.4. This ratio is expressed as:

$$U_+ / U_- = (1/\delta)^{nr/(1-r)}, \tag{2.18}$$

where δ is the degree of cavitation and depends on the number of cavities across the width of a glacier, the area fraction of bedrock free of cavities and the cavity tortuosity and the value of *n*, while *r* is bed roughness (equation 2.17) (Fowler, 1987a).

Based on the above summarised theory, Fowler (1987a) outlined a number of possible glacial and environmental controls on surging:

- As s_{max} must be greater than Q_c before the switch from the lower to the higher sliding velocity branch can take place, a glacier must be deep enough and thus the accumulation rate in a region with surging glaciers must be relatively high.
- As surge velocities are 100-1000 times higher than quiescent phase velocities, U_+/U_- ratios must be 2 to 3. As this ratio is inversely related to α* and a small value for α* is related to a rough bed (equation 2.17), surge-type glaciers must have rougher beds than non-surge-type glaciers. Younger beds are generally rougher, thus glacier surging would occur preferably on geological young lithologies.
- Because the U_+/U_- ratio is inversely related to δ, surging would be promoted if δ is small, implying that the number of cavities across the glacier width must be smaller for surging glaciers than for non-surge-type glaciers.
- Tunnels in a conduit system only become unstable if the tunnel stability parameter reaches a critical value and only then a transition to the linked-cavity-system can appear. This means that the effective pressure must reach a certain value. As the effective pressure is dependent on depth and slope of a glacier, these two variables should have critical values or ratios in surge-type glaciers as well.

Fowler (1989) subsequently suggested an instability parameter representing a substantial difference between the ice velocity branch for subglacial channels from the velocity–pressure branch for cavities. The difference would correspond to the velocity variations that are found in surge-type glacier. Fowler's instability parameter (or *Fowler's index*) can be defined as:

$$\widetilde{F} = \widetilde{\chi}\widetilde{W}^2, \tag{2.19}$$

which is the product of dimensionless bed slope ($\widetilde{\chi}$ = 10 times the average bed slope in radians) and width-squared ($\widetilde{W}$ = dimensionless average glacier width (width in km/1km) (Fowler, 1989). For surge-type glacier Fowler's index would be smaller than the order of one: narrow glaciers with low average surface slopes would thus be more likely to be of surge-type (Fowler, 1989). $\widetilde{F}$ is a purely geometrical term making it particularly suitable for statistical testing of glacier population characteristics.

In addition, timing of surges is critical for testing theories on surge mechanisms (Raymond, 1987). For example, the periodicity of surges is dependent upon the length of time which it takes for the surge instability to develop, while the duration of a surge depends on the time which it takes until the critical conditions have ceased and the glacier system crosses an instability threshold (Sharp, 1988a). Indeed, Lawson (1997) found that the behaviour and geometric evolution of subsequent surges of Variegated Glacier was largely similar. For the linked cavity configuration surge theories the initiation of surges should coincide with appropriate geometric configuration and with low water input into the system, when the configuration of the subglacial drainage system is not yet fully developed and is draining water ineffectively (Kamb *et al.*, 1985). Raymond (1987) suggested a winter-initiation, but the concept 'winter' could be expanded to 'the time that surface water is absent' (Harrison *et al.*, 1994). For the Northern Hemisphere, surge initiation could then be any time between August (early end of meltseason) and June (late start of meltseason). This would only leave surge initiations in July not applicable for a surge with the hydrological instability mechanism.

Although Kamb's surge theory was developed for temperate glaciers resting on hard beds or soft beds with immobile clusters of unconsolidated rock debris, recent observations on the surge of Skeiðararjökull suggest that this theory could apply to deformable soft-bedded glaciers as well (Björnsson, 1998). Furthermore, there is some evidence that Variegated Glacier itself is underlain by a weak deformable layer (Richards, 1988). Observations on the surge of Peters Glacier, Alaska, are also consistent with Kamb's surge mechanism as the surge initiation was related to the development of high subglacial water pressure in a distributed subglacial drainage system during the season of low surface water input (Raymond and Harrison, 1988). It is however hard to explain how the orifice stability parameters in these glaciers were low whereas the glacier was somewhat oversteepened and overthickened at the onset of the surge (Raymond and Harrison, 1988). Furthermore, it was unclear if the high water pressures induced rapid sliding or rapid deformation of a saturated substratum (Echelmeyer *et al.*, 1987).

2.4.9 Testing factors related to stability of linked cavities and conduits

According to Kamb's surge mechanism, surge-type glaciers could be distinguished from normal glaciers by specific ranges of basal shear stress, water pressure and ice overburden pressure. In addition, surge-type glaciers would require specific dimensions and spatial arrangement of bed roughness features. Bedrock lithology and glacier geometry would thus be key factors in testing Kamb's linked cavity surge theory. According to the definition of the orifice melting stability parameters (see equations 2.13 and 2.14), low slope would be conducive to surging. Yet, as glacier inventories only list average surface slope, which by definition is at its maximum at the

end of the quiescent phase, giving high orifice stability parameters and thus contradicting Kamb's postulate that linked-cavity-systems are stable only when the orifice stability parameter is low. However, as surges initiate locally, the overall surface slope of glaciers could not be the appropriate surface slope measure, but instead, local variations of slope should be taken into account.

2.4.10 The deformable bed surge mechanism

The preceding surge mechanisms have all been developed with the assumption of hard rocky beds. Yet, a large number of surge-type glaciers can be found in young mountain ranges which are subject to rapid erosion and low lying sediment-rich terrain (Post, 1969). This causes material to be available for the development of subglacial till and indeed, actively deforming beds are known or believed to exist beneath for example the surge-type glaciers Bakaninbreen, Breiðamerkurjökull, Peters Glacier, Trapridge Glacier, Variegated Glacier and West Fork Glacier (Boulton *et al.*, 1974; Clarke *et al.*, 1984; Harrison *et al.*, 1986; Echelmeyer *et al.*, 1987; Harrison *et al.*, 1994; Porter, 1997). Furthermore, sediment content and morphology of surge-type glaciers in Svalbard and Iceland differs from that of normal glaciers (Boulton, 1971; Clapperton, 1975; Sharp, 1985; Croot, 1988). Further, surge behaviour in regions with extensive deformable beds (such as Svalbard) disagrees with the 'classic' surge behaviour of glaciers overlying hard beds (Hagen, 1988; Dowdeswell *et al.*, 1991: see Section 1.3.3). This field evidence suggests that glaciers overlying deformable beds could have distinct surge mechanisms. Unfortunately measurements and understanding of the mechanisms of bed deformation are inadequate to develop rigorous physical theories explaining glacier surging by unstable bed deformation.

Till characteristics of Breiðamerkurjökull and Eyjabakkajökull, Iceland, as well as Sefströmbreen, Svalbard, suggest that bed deformation was a major contributing component to the fast movement during the surges of these glaciers (Boulton and Jones, 1979; Sharp, 1985; Boulton *et al.*, 1996). It is also hypothesised that many of the Laurentide Icesheet lobes and some of the Fennoscandian lobes may have been produced by surges resulting from pervasive bed deformation (Boulton and Jones, 1979; Alley, 1991; Alley and MacAyeal, 1994). However, the thickness of the deformable layer and the reconstructed shape of the fast flowing ice lobes dispute pervasive deformation (Boulton and Jones, 1979; Clayton *et al.*, 1989). Moreover, recently observed bed deformation during the surge of Bakaninbreen, Svalbard, as well as during fast flow periods of Ice Stream B, Antarctica, and Storglaciären, Sweden, discloses that major bed deformation only occurs in an upper shear zone (up to a few decimetres thick) and thus that partial decoupling instead of pervasive deformation takes place (Iverson *et al.*, 1995;

Engelhardt and Kamb, 1998; Murray *et al.*, in review). Nevertheless, deforming beds should be considered as one of the variables that are potentially favourable to surging (Clarke *et al.*, 1984; Clayton *et al.*, 1989).

Till is inhomogeneous and can alter its properties through time as a result of the compression history, sediment transport, dilatancy and communition (Dreimanis and Vagnes, 1972; Clarke, 1987b; Hooke and Iverson, 1995). Pore pressure, total pressure, shear stress, porosity and volume fraction of the fine-grained solids determine the till rheology (Boulton and Paul, 1976; Clarke, 1987b). Forcings such as basal shear stress, water flux and overburden pressure can result in changes in the deformability of a till (Clarke, 1987b). Enhanced bed deformation, or pervasive shearing, is made possible by the existence of high pore water pressures reducing the strength of the substratum (Boulton *et al.*, 1974; Clarke, 1987b). According to the B-H rheology for till (equation 2.5), instabilities occur at locations where the yield strength of the till is exceeded and very low effective pressures maintained. These effective pressures must be smaller than $(\tau - C)/\eta$, a term related to the porosity of the sediment and basal shear stress (Boulton and Jones, 1979). As effective pressure is the difference between ice overburden and hydrostatic pressure, the stability of sediments is directly related to the subglacial hydrology. Soft bed instability is therefore controlled by local increases in subglacial water pressure, variations in permeability, the position of the glacier margin and variations in local mass balance which, by changing glacier slope and thickness, may lead to high local shear stress and overburden stress in the sediment (Boulton and Hindmarsh, 1987).

Surges on deformable beds might be triggered in the region where shear stresses build up during quiescence or by the destruction of subglacial drainage paths or drainage paths in the subglacial sediment (Boulton and Jones, 1979; Clarke *et al.*, 1984). This leads to the trapping of water and an increase in the till deformability, resulting in increasing flow velocities. If the deformation is inhomogeneous, then local differences in hydraulic conductivity will give rise to differences in water content and even trapping of water. This process could potentially destabilise the sediment and induce a surge (Murray and Dowdeswell, 1992). However, it is clearly possible for a stable water system to exist in deforming sediments, as no trapped water was found underneath Trapridge Glacier, despite its deforming bed (Clarke, 1987b). As ice advances and thins during the period of enhanced bed deformation, both the normal and shear stress as well as hydrostatic pressure diminish and deformation of the mobile bed will eventually return to normal (Boulton and Hindmarsh, 1987). Moreover, as till is dilatant (*i.e.* deformation increases permeability), deformation of the till layer increases the effectiveness of subglacial water discharge (Clarke, 1987b). The experimental work of Murray and Dowdeswell (1992) also shows that sediment

deformation can enhance drainage patterns. The process of piping particularly reduces the water pressure and restores the sediment stability (Boulton and Hindmarsh, 1987; Clarke, 1987b).

Because not all glaciers overlie deformable beds it is important to identify which factors control the distribution of sedimentary beds. Based on observations in the Swiss Alps, Haeberli (1986) developed an index describing whether a glacier rests on a predominantly rocky bed or a sedimentary bed. The index is denoted as:

$$R = a_c h_r \Big/ PFJ^{b_i} l \,, \tag{2.20}$$

where l is length of the flowline, $a_c h_r$ stand for debris supply and PFJ^{b_i} for meltwater transport capacity (a_c is a factor describing what part of the debris is supplied to the accumulation area, h_r is the mean altitude range of the mountains surrounding the glacier, P is annual precipitation, F surface area of the glacier, J inclination of the pro- and subglacial meltwater stream and $b_i \approx 1.6$) (Haeberli, 1986). Thus, smaller, narrower glaciers surrounded by rugged topography, in a relatively dry climate and with gently sloping meltwater channels would overly the most extensive sedimentary beds. Additionally, most calving glaciers are assumed to rest upon sedimentary beds in their lower regions (Haeberli, 1986).

Potential sediment instability is strongly related to till composition. Fine-grained sediments on impermeable rocks are thought to be especially sensitive to changes in pore water pressure, grain-size distribution and mineralogy (Boulton, 1979). Furthermore, it is physically reasonable that matrix-rich tills are more easily deformable than clast-rich tills (Clarke, 1987b). The dynamic equilibrium of glaciers resting on fine-grained sediments may thus be very unstable and may result in surging behaviour. The overall geological controls on bed deformability and erodibility are a function of geological maturity and lithology (Clarke *et al.*, 1984). Dreimanis and Vagnes (1972) found that the grainsize of the till matrix is dependent on the terminal grades of the minerals in the bedrock and on the length of the flowpath. Most igneous and metamorphic lithologies will produce sandy to silty tills, for limestone and dolostone it is predominantly silty with a little sand and clay and shales produce predominantly clay-rich tills (Dreimanis and Vagnes, 1972). The longer the transport path, the larger the percentage of terminal grade fraction (till-matrix) as compared to the clasts fraction, thus long glaciers would overly predominantly matrix-rich tills, while for shorter glaciers the tills would be clast-rich (Figure 2.8). Moreover, till thickness increases from the head of a glacier to the margin, because deformation moves sediments downglacier and additional tectonic processes during surges may stack thick layers of till and of sediment-rich ice close to the margin (Boulton, 1971; Sharp, 1988). Yet, the actual till

composition can be complicated by pre-deposited sediments, localised redistribution by meltwater, clustering together of different grainsizes, lithological pluriformity and local (often in the marginal regions) intensity of crushing processes (Boulton *et al.*, 1974; Clarke, 1987b).

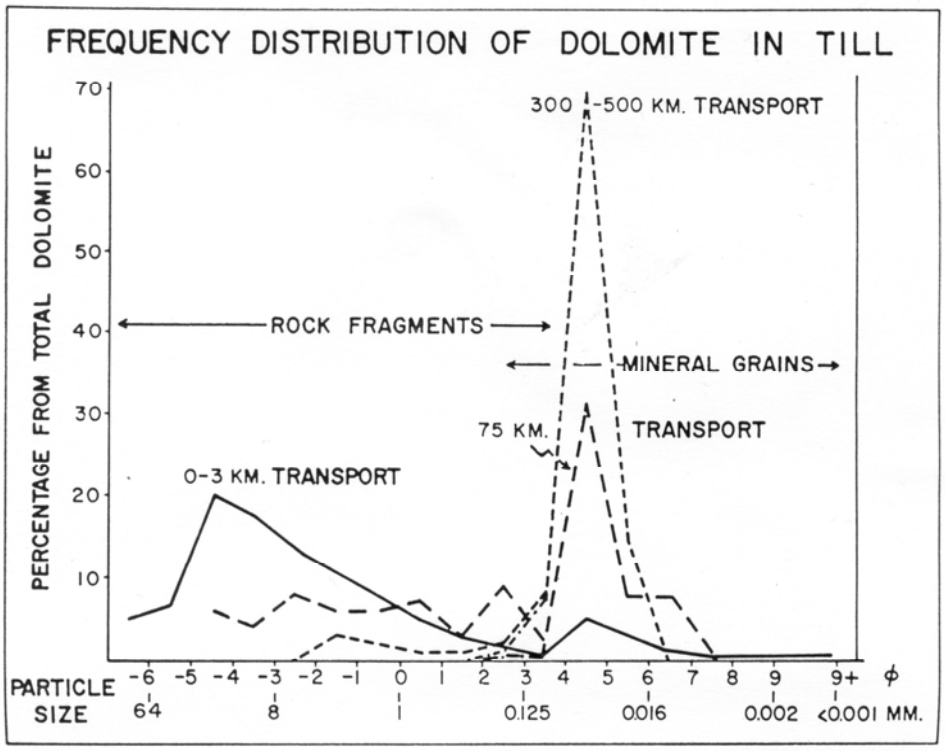

Figure 2.8: *Frequency distribution of dolostone-dolomite till samples taken at three locations in SE Canada, showing the progressive transport and communition (From: Dreimanis and Vagners, 1972).*

2.4.11 Testing factors related to substrate instabilities

The process of bed deformation requires a potentially deformable subglacial layer of a minimum thickness. Depending on the grain-size distribution and the properties of the underlying bed, this deformation is potentially unstable. It appears that fine-grained sediment underlain by an aquitard is most likely to deform in an unstable manner as required for surge activity (Boulton, 1979). This means that the lithology types in a cluster region of surge-type glaciers must be very erodible and preferably produce fine-grained sediments, while the bedrock underlying the soft bed must be impermeable (e.g. shales) (Dreimanis and Vagners, 1972; Freeze and Cherry, 1979). Furthermore, glaciers overlying more than one type of bedrock and in complex geological settings should have an increased surge potential, as changes in substrate properties could result in local hydrostatic pressure differences and thus lead to unstable bed deformation (Clarke, 1991; Harrison *et al.*, 1994). It has been suggested that the fault generated geometry and weak bedrock type along the tectonically active Denali fault zone may be correlated with the large number of surging glaciers in Alaska (Post, 1969; Echelmeyer *et al.*, 1987). Thus, bed roughness, erodibility, porosity, permeability, deformability and homogeneity

are of crucial importance for the subglacial hydrological processes and the flow dynamics (Boulton, 1979; Weertman, 1979; Sharp, 1988a; Souchez and Lorrain, 1991; Marshall *et al.*, 1996). As these data are difficult to obtain and only available for a handful of glaciers, lithology, regional geologic activity and geological boundaries can be used as proxies for these bed characteristics.

2.4.12 Factors controlling the outflow during quiescence and the termination of surges

The return period of surges is dependent upon the time it takes to build up the instability, while the duration of the surge depends on the time it takes for the system to adjust until the instability is revoked again. It would therefore be possible that the response time of surge-type glaciers changes with changing mass balance conditions (e.g. Dowdeswell *et al.*, 1995). However, disregarding external changes, the conditions within the glaciers system can change gradually with time and could control the duration of quiescent and surge phase of individual glaciers.

Clarke *et al.* (1984) proposed that downstream resistance to sliding is the cause for surge-type glaciers to have an unstable flow behaviour. Given that surge-type glaciers experience restricted outflow they should have overall steeper slopes than normal glaciers, particularly in the late quiescent phase. Restriction in outflow could be thermally controlled but could also be caused by enhanced friction or blocking of the outflow (Stanley, 1969; Colvill, 1984; Clarke, 1987a; Raymond and Harrison, 1988; Heinrichs *et al.*, 1996; Nuttall *et al.*, 1997). Factors enhancing the friction at the bed can include: bed roughness ('ruggedness' and bed geometry), roughness of the basal ice layer (e.g. sandpaper friction), low temperatures, no free water at the bed, low hydrostatic pressure and a (partly) frozen substrate. Furthermore, a downstream increase in drainage effectivity and subsequent reduction of hydrostatic pressure towards the terminus can generate a downstream increase in sliding resistance (Clarke *et al.*, 1984). This last process implies that the longer a (temperate) glacier is, the more likely it is to experience downstream resistance to sliding.

Higher than average bed friction could be related to an abundance of 'sticky spots'. These are locations of high basal drag where the friction exceeds the average friction of the bed (Alley, 1993). Ideas about the nature of 'sticky spots' range from bedrock protuberances, cavities, thermal lows and local pressure dips in hard beds, to absence of a water film and locally increased stiffness of the substrate in deformable beds (Lliboutry, 1967; Alley, 1993; Blake *et al.*, 1994; Smith, 1997; Fisher *et al.*, 1999). However, Iverson *et al.* (1995) postulate that deformable beds may not provide the principal resistance to motion, but rather that this resistance occurs at places where the till is absent. Some consider 'sticky spots' to be ephemeral

in nature, *i.e.* that they can be created and destroyed in response to variations in subglacial water pressure (e.g. Fisher *et al.*, 1999). It would thus be possible that restricted outflow is related to the ephemeral nature of sticky spots. On a larger scale, bedrock sills and marked subglacial protuberances are known to restrict flow be it mechanically, thermo-mechanically or because the bed characteristics above and below the bedrock protuberance are different (Hoinkes, 1969; Drewry and Liestøl, 1985). It is noteworthy that both the surge bulges on Finsterwalderbreen and Trapridge Glacier and the zone of anomalous velocity at the start of the surge of Variegated Glacier coincide with the location of a topographic anomaly on the glacier bed (Raymond and Harrison, 1988; Clarke and Blake, 1991; Nuttall *et al.*, 1997). Whereas specific types of topographically-controlled channel curvature (e.g. sharp bends) could conceivably obstruct glacier flow, this factor appears to have no effect on the likelihood of surging in Spitsbergen (Hamilton, 1992).

Blocking of outflow is possibly related to the occurrence of tributaries. Tributaries joining a surge-type glacier often form a bulge and an accompanying moraine loop on the surface of the quiescent trunk: this process could block the flow of the trunk at the point of confluence. This phenomenon has been observed at Roslin glacier, East Greenland, and at Black Rapids Glacier, Alaska (Colvill, 1984; Heinrichs *et al.*, 1996). The reverse process was observed at Steele Glacier and its tributary Hodgson Glacier, where the latter started surging about a year after having been blocked by the raised surface of the surging trunk (Steele Glacier) (Stanley, 1969).

Surge instabilities have to be self-limiting and encompass negative feedback mechanisms as well as the initial positive feedback mechanism. Because sliding causes erosion of the bed, a sliding glacier at least partly determines the shape and roughness of its bed, while it is suggested that glaciers will erode those wavelengths that offer most resistance to sliding (Weertman, 1979). If bed roughness is indeed a function of sliding and if the sliding rate is not constant with time, this might give clues to the timing of surges. It is however difficult to establish how this erosion mechanism would explain the cyclic nature of surging. Drewry (1986) and Sharp (1988a) suggest that glaciers in surge are more geomorphologically competent as they dissipate more energy in a short period than normal flowing glaciers. As a linear relation between speed and erosion rate exists (the ratio 'metres eroded from the bed' to 'metres sliding' is about 10^{-4}), it is not surprising that the erosion rate of Variegated Glacier in surge was calculated as 400 mm a^{-1}, while in quiescence it is only 3 mm a^{-1} (Humphrey and Raymond, 1994). The process of plucking would be particularly enhanced during surges (Röthlisberger and Iken, 1981; Drewry, 1986). Further, as meltwater is distributed over a larger area during surge than during quiescence (see sections 2.4.6 and 2.4.8) evacuation of fine debris from the ice-bed interface is facilitated during surge (Sharp, 1988b). Thus, both roughening of the bed and net coarsening of

basal debris take place during surges (Sharp, 1988b). The former increases obstacle size and the latter reduces bed deformability (see section 2.4.10). If during quiescence a gradual smoothening of the bed and net fining of the substrate occurs and the reverse during surge, then the duration of surge and quiescent phase could not only be controlled by mass balance conditions, glacier geometry and hydrology but also by geomorphic processes.

Surge termination either requires dissipation of high basal water pressures or a substantial reduction in basal shear stress (Murray *et al.*, in review). Although surge initiation is always rapid and catastrophic, the termination of surges can be divided into two categories: (1) a rapid and distinct end of the surge (sometimes within hours) and (2) a slow undetermined end of a surge where it is difficult to tell when the surge proper ends. Processes in thermally regulated surges occur at a 'controlled' slow rate, as compared to the hydrologically regulated surges where sudden termination of surges are often accompanied by outburst floods and a measurable surface drop (Kamb *et al.*, 1985; Echelmeyer *et al.*, 1987; Lingle *et al.*, 1993; Molnia, 1994). For the slow terminations it is suggested that slower and more gradual processes remove water from the ice-bed interface such as 'leaking' of water through the bed or refreezing of basal water (Murray *et al.*, in review). Thus thermal properties, local shear pressure, glacier geometry and substrate properties are important in the termination of surges.

2.5 Summary and listing of variables that can be used to test surge theories

Raymond (1987) suggests that the geometrical evolution of a glacier is the overriding control on the occurrence of surging: there must be critical geometries for initiating and terminating of surges. The surge theories outlined in this chapter indicate that variables related to glacier geometry could indeed distinguish surge-type glaciers from normal glaciers. Furthermore, mass balance characteristics in relation to the glacier geometry as well as substrate and topographical conditions are likely to be different for surge-type glaciers and can be tested through glacier population analysis. These controls fundamentally cover the whole range of dependent (glacier system related) and independent (environmentally related) variables that were postulated by Sugden and John (1976) to relate to the distribution of glaciers and to affect glacier movement.

Three broad hypotheses can be deduced from the theories presented in this chapter:

- The surge potential is controlled by a combination of glacier geometry, local climate and substrate conditions, while the primary control is possibly mass balance.
- The duration of the quiescent phase is primarily controlled by mass balance conditions
- The duration and character of the surge phase is primarily controlled by the environmental setting (substrate, topography and local climate).

Specific glacial and environmental controls relating to the different surge theories are listed in Table 2.1. Only few of these are unique controls and give definite support for a single theory: the majority are controls across a number of theories. However, unique combinations of controlling factors (Table 2.1) could also be used to verify specific surge theories.

CONTROLS ON SURGE THEORIES AND INSTABILITY PARAMETERS												
Surge theories and instability indices →		Stress instability	Thermal instability	Lubrication instability *Weertman*	Lubrication instability *Budd*	Linked-cavity-system *Kamb*	Linked-cavity-system *Fowler's index*	Bed separation index *Iken*	Bed separation index *Bindschadler*	Bed deformation *B-H rheology*	Bed deformation *Haeberli's index*	Blocking or restricting
Controls ↓		2.5.2	2.5.3	2.5.6	2.5.6	2.5.8	2.5.8	2.5.8	2.5.8	2.5.10	2.5.10	2.5.12
Glacier length	long		+	+		+				+		+
	short											
Glacier area	large											
	small										+	
Glacier width	wide											
	narrow						+				+	
Glacier slope	high	+			+			+	+			
	low					+	+				+	
Glacier thickness	large	+	+					+	+			
	small											
Fowler's index	low						+					
Channel curvature	high	+										+
Tributaries	present											+
Lithology	young		+				+			+		
	fine grained			+						+		
	impermeable			+	+							
Geological boundaries	present					+				+		
	absent			+								
Geothermal heat	high		+		+							
Subglacial topography	rugged >50cm				+							+
	smooth <8cm					+	+					
AAR	large	+			+							
Hypsometry	top-heavy	+			+							+
Equilibrium line	low				+							
Accumulation	high	+			+							
	low										+	
Polythermal glacier			+									
Temperate glacier				+	+	+	+					
Tide-water glacier										+		

Table 2.1: *Controls on the different surge theories. Unique controls are in grey shaded cells, all others are controls across a number of different theories.*

CHAPTER 3:
Review of Previous Research Isolating Surge Controls

We in your motion turn, and you may move us

Shakespeare (Comedy of errors: Act 3, Scene 2)

3.1 Introduction

The distinct non-random distribution of surge-type glaciers on both on a global and regional scale must conceal information about controls on glacier surging (Post, 1969; Clarke *et al.*, 1986). Some of controls could be external or *environmental controls* on surging, for example climate, geology and topography, while others could be *glacial controls*, such as geometry and thermal regime. Given that surge-type glaciers and normal (non-surge-type) glaciers are distinct groups (see Section 1.3.3 for a discussion) these environmental and glacial controls may well emerge from analysing glaciers in cluster regions of surge-type glaciers, whereby characteristics of surge-type glacier are contrasted to those of normal glaciers. The concentration of surge-type glaciers in certain geographical areas could thus be a function of the distribution of glaciers with characteristic attributes (Hamilton, 1992). Studies of the interaction between fast glacier flow or glacier instabilities and substrate, stress distribution, glacial hydrology and thermal regime are predominantly of a combination of process studies and physical-mathematical modelling (e.g. Weertman, 1969; Boulton, 1979; Boulton and Jones, 1979; Raymond and Malone, 1986; Boulton and Hindmarsh, 1987; Echelmeyer and Kamb, 1987; McMeeking and Johnson, 1986; Alley, 1989, 1991; Boulton and Dobbie, 1993; Iverson *et al.*, 1995; Jackson and Kamb, 1997; Blatter *et al.*, 1998; Murray *et al.*, in review). However, these studies are based on field observations of a relatively small number of glaciers although they have produced a large number of surge theories and theories on surge instabilities. In order to test if the proposed controls on flow instabilities, surging and fast flow are universally applicable to surge-type glaciers it is necessary to try and match certain controls with populations of surge-type glaciers.

In Section 3.2 of this chapter the previous regional geographical studies are introduced alongside their methodologies and the results of these studies are discussed in Section 3.3, while Section 3.4 summarises the conclusions from the studies. Glaciological implications of the possible controls on surging are outlined Section 3.5. Finally, Section 3.6 lists the recommendations that will be adopted and taken further in Chapters 5 and 6 of this thesis.

3.2 Previous research to the controls on surging

The regional geographical studies of the controls on the distribution of surge-type glaciers cover glacier populations of western North America, the Yukon Territory, Central Asia and Svalbard. Some of these studies used qualitative observations (Post, 1969), others univariate statistical analysis (Glazyrin, 1978; Clarke *et al.*, 1986; Wilbur, 1988; Hamilton, 1992; Hamilton and Dowdeswell, 1996) and multivariate statistical analysis (Clarke, 1991; Marshall *et al.*, 1996). A multivariate study by Marshall *et al.* (1996) used geologic and topographic influences on the facilitation of large-scale fast flow and surging in Canada and western North America.

3.2.1 Research approaches and details of investigated regions

Post (1969) qualitatively tested environmental and glacier attributes that might influence the spatial distribution of 204 surging glaciers in western North America. The percentage of surge-type glaciers for the entire region is about 2.5%, but as the surge-type glaciers are all located in five mountain ranges the concentration is locally higher. No evidence of surging in western North America is detected outside these mountain ranges. Within the mountain ranges, the distribution of surge-type glaciers is also non-random: the majority of surge-type glaciers are clustered in specific regions, with the most renowned cluster occurring along the Denali Fault in the Alaska range (Post, 1969).

Glazyrin (1978) analysed a group of 62 glaciers in the Pamir, Central Asia, of which 43 surge-type and 19 normal. By finding correlations between glacio-morphometrical characteristics and glacier surging using this group, the distribution of the same surge-type and normal glaciers was reproduced. In total, 12 glacier attributes were tested using two pattern classification methods, including glacier dimensions, presence of an icefall and mass balance related attributes.

Clarke *et al.* (1986) examined population statistics of 2356 glaciers in the St. Elias Mountains, Yukon Territory, Canada. Data were derived from the Canadian Glacier Inventory (CGI) including all glaciers in the Yukon Territory. From the total 4675 entries in the CGI, Clarke *et al.* (1986) rejected all rock glaciers, glacierets and glaciers without a special features code assigned to them, leaving about 50% of all glaciers for the data analysis. A six-point surge index (Table 3.1) was assigned by the close examination of available aerial photographs, publications and scientific reports and historic evidence. The Yukon glaciers are located in 55 drainage basins, which were used as regions for geographical analysis. Surge probabilities for the different drainage basins ranged from 0.5% to a maximum of 23.8%. Basins with surge probabilities higher than the primary dataset (6.4%: see Table 3.2) have high concentrations of

surge-type glaciers. Three drainage basins having extremely high surge probabilities (>20%) are located in three separate regions of overall higher than average surge probabilities (>7%) (Clarke *et al.*, 1986). From these data Clarke *et al.* (1986) concluded that the spatial variation of surge probability appeared to have a large-scale pattern, as well as a regional one. Using Laplacian probability methods, Clarke *et al.* (1986) tried to isolate glacier attributes that would explain this geographical distribution. Analysis was performed on the glacier attributes length, slope, elevation, orientation and tributaries. A few years later, Clarke (1991) performed a multiple correlation analysis on a number of these attributes, in order to disentangle the causal relationships between length, slope, glacier width, Fowler's index and the surge probability. As a result of the available data, only 1754 of the 2356 earlier analysed Yukon glaciers were used in the multivariate analysis.

Wilbur (1988) performed statistical analysis on 146 glaciers from 11 mountain ranges in western North America. The glacier population overlaps the glaciers studied by Post (1969). According to location and behaviour, the 146 glaciers were classified into six glacier types:

1. coastal normal-type
2. coastal intermediate-type
3. coastal surge-type
4. interior normal-type
5. interior intermediate-type
6. interior surge-type.

Details on surge classification, counts and surge probabilities in the data are given in Table 3.1 and 3.2. Wilbur concentrated his research on finding systematic differences in hypsometry and balance-related-geometry between normal and surge-type glaciers and between coastal and interior type glaciers and used nine testable parameters: (1) glacier-type (one to six above), (2) hypsometry group, (3) average surface slope, (4) glacier width, (5) balance related depth, (6) balance related velocity, (7) basal shear stress, (8) Budd's parameter (Φ = balance flux/width) and (9) glacier area. Four tests were used to evaluate Budd's parameter, ratios of parameters and optimal combinations of variables distinguishing glacier types and to determine whether surge-type and normal glaciers had different hypsometry curves (Wilbur, 1988). Analysis methods included visual analysis of dataplots, analysis of ratios and multiple discriminant functions.

Hamilton (1992) studied the environmental controls on surge-type glaciers in Spitsbergen by means of a statistical probability analysis. Glacier data were selected from ten topographic colour maps at scale 1:100000 (Hamilton, 1992). As a result of this selection method, the area covered was only about 50% of the island Spitsbergen. Hamilton disregarded glaciers less than 1 km, partly covered glaciers on map edges and plateau ice caps. The remaining 615 glaciers

cover about 30% of the total glacier population in Svalbard. Data for these glaciers were collected from maps, aerial photographs, geology maps and publications. From the sample population of 615 glaciers, 224 were estimated to be surge-type, which represents a surge possibility of 36.4% for this primary population. Probability statistics of the primary dataset are shown in Table 3.2. From geographical analysis, Hamilton (1992) found that surge probability of the ten individual map sheets varied from 15.8% to 46.8%. Maps sheets with higher surge probabilities than the surge probability of the whole dataset (36.4%) have higher than average concentrations of surge-type glaciers. It was found that three map sheets had a higher concentration of surge-type glaciers than the average. Hamilton concluded from this result that the clustering of surge-type glaciers on global scale also occurs on a regional scale within Svalbard.

To build upon the assumption that large-scale surging and ice streaming behaviour must have similar flow mechanisms and experience similar terrain control, Marshall *et al.* (1996) developed a numerical ice sheet model, which was capable of generating subgrid ice stream and surge lobe dynamics. With this model it was suggested that spatial variations in ice-bed coupling, imposed by bed geology and topography, could explain the distribution of ice streams in the Laurentide and Cordilleran ice sheets as found from glacio-geologic evidence. Multivariate factor analysis and discriminant analysis techniques were used to find optimal combinations of nineteen geology and terrain characteristics. Terrain characteristics included measurements of elevation, slope, aspect, terrain roughness and terrain hypsometry, and geologic characteristics included measurements or estimates of fractional bedrock exposure, average sediment depth, water storage capacity and hydraulic conductivity (Marshall *et al.*, 1996). From parameter optimisation of a set of 49 surge control points and 11 non-surge control points the spatial distribution of ice stream location for the remaining 3438 terrestrial cells was predicted.

3.2.2 The surge index and surge probabilities

The purpose of analysing glacier populations is both to describe datasets of (surge-type) glaciers in order to find clusters with similar properties and to discover conditional relationships and associations between surge characteristics and various glacier attributes. In order to analyse surge-type and normal glaciers statistically, a value (surge index *S*) representing the likelihood that a particular glacier is of surge-type has to be assigned to each glacier in the sample population (Hamilton, 1992). The Canadian Glacier Inventory (CGI) established a five digit special features code additional to the basic 6 digit classification code of the World Glacier Inventory (Ommanney, 1980; IAHS(ICSI)/UNEP/UNESCO, 1989). This special features code

(*S* in Table 3.1)) was used to identify for example rock glaciers as well as evidence for surging. Surging in the special features code was based on the presence of surface features such as contorted medial moraines, sheared margins, bulging terminus and pothole fields (see Section 1.4.2). The CGI code was directly used as a surge-index by Clarke *et al.* (1986) and Wilbur (1988), although the latter restricted the assignment of S=5 only to surge-type glaciers which have shown large magnitude surges in the past and reduced the final category description to three classes (see Table 3.1). Hamilton (1992) used a 4-point surge index, which he adjusted from the 6-point surge index of Clarke *et al.* (1986). Instead of using a dichotomous variable with a value 0 for normal glacier and 1 for surge-type, Clarke (1991) used a measure of surge probability denoted as $P_s=p(P_s=1/S)$: the probability that a glacier is surge-type give that its surge index is S.

CLASSIFICATION OF SURGE-TYPE GLACIERS				
S	CGI (Ommanney, 1980) Clarke *et al.* (1986)	Wilbur (1988)	Clarke (1991)	Hamilton (1992)
0	very probably normal: no special surging glacier features	non surge-type	P_s = 0.005	glacier most likely to be normal (non surge-type)
1	uncertain surge characteristics: possibly by association with surging glaciers		P_s= 0.02	glacier possibly surge-type (1-2 surge-type features)
2	possible surge characteristics: one or two surging glacier features	intermediate type	P_s = 0.03	glacier probably surge-type (>2 surge-type features)
3	probable surge characteristics: several surging glacier features		P_s = 0.2	glacier most likely to be surge-type: observed surge (s))
4	very probable surge characteristics: diagnostic surging features: strong surface evidence	surge- type	P_s = 0.8	
5	definite surge characteristics: historical or corroborative evidence of a surge		P_s = 0.95	

Table 3.1: *Classification of surge-type glaciers according to surge-indexes (S). P_s is the probability of coming upon a surge-type glacier in that particular surge index.(After: Clarke et al.,1986; Wilbur, 1988; Clarke, 1991; Hamilton, 1992).*

Clarke *et al.* (1986) mention that surge indices should be assigned by one person in order to avoid inconsistency in the surge classification. This indicates that the classification of surge-type glaciers is a rather subjective business and prone to possible disputes about exact numbers of surge-type glaciers in a region (e.g. Glazyrin, 1978; Hamilton, 1992; Jiskoot *et al.*, 1998). It is therefore important to properly define diagnostic criteria of surge-type glaciers as compared to characteristics suggestive for surging but possibly resulting from 'normal' dynamic behaviour. When assigning surge indices to glaciers from interpretation of aerial photographs, maps or historical reports it should always be recorded which surge criteria were used and from which source(s) this information has been derived (e.g. Jania, 1988; Lefauconnier and Hagen,

1991; pers. comm. G. Hamilton to T. Murray, 1995). However, until the identification of surge-type glaciers can be automated, the surge classification will strongly depend on the subjective view of the researcher.

Much of the statistical methodology to analyse environmental controls on glacier surging is based on Laplacian probability (Clarke *et al.*, 1986; Clarke, 1991; Hamilton, 1992). For this methodology surge probability of a primary dataset (the complete region) is compared to the surge probability of certain subsets. The surge probability P_s of a primary dataset could simply be calculated as the percentage of surge-type glaciers in the entire population. However, in order to measure the probability that a particular glacier classified as S-type is of surge-type it is necessary to quantify the surge index by giving it a weighting coefficient (Clarke *et al.*, 1986). This weighting factor is the surge-probability in each class of the surge index. Thus, the number or percentage of mis-classified glaciers in each class has to be estimated. The percentage of misinterpretations is dependent upon the size of the population, the duration of the quiescence period (Hamilton, 1992), the distinction between the different surge indexes, the available glacier data and the accuracy of the scientist. There are two ways to estimate surge probability in each class: (1) by estimating the number of possible misinterpretations and (2) by simply estimating the percentage of possible misinterpretations. The latter case will result in a surge probability for each surge index of more 'round' numbers. See for example Table 3.2, where Hamilton (1992) used the first approach and Clarke *et al.* (1986) the second. The main aim of these procedures is to prevent over-estimation of statistical results.

SURGE PROBABILITIES												
	Clarke *et al.* (1986)				Hamilton (1992)				Wilbur (1988)			
S	n_S	P_s	$p_{s\|S}$	$n_{s\|S}$	n_S	p_s	$P_{s\|S}$	$n_{s\|S}$	n_S	P_s	$p_{s\|S}$	$n_{s\|S}$
0	1926	0.8175	0.005	9.6	393	0.639	0.051	20	23	0.1437	0.005	0.1
1	129	0.0548	0.020	2.6	141	0.229	0.894	126	28	0.1750	0.020	0.6
2	77	0.0327	0.030	2.3	26	0.042	0.923	24	28	0.1750	0.030	0.8
3	82	0.0348	0.200	16.4	55	0.089	0.980	154	30	0.1875	0.200	6.0
4	104	0.0441	0.800	83.2					29	0.1813	0.800	23.2
5	38	0.0161	0.975	37					22	0.1375	0.975	21.5
	2356	1.0000	6.42%	151.2	615	1.0000	36.4%	224	160	1.0000	32.6%	52.2

Table 3.2: *Surge indexes and calculated probability schemes for the primary datasets of Clarke et al. (1986), Hamilton (1992) and Wilbur (1988). S is surge index, n_S the number of glaciers in that surge index, P_s the probability of coming upon a surge-type glacier in a surge index and nS\|S the number of surge-type glaciers to be found in the group of glaciers classified with that surge index. The percentages in the P_s\|S column indicate the overall surge probability in the corresponding region or selection.*

Subsets of the primary dataset can be selected according to geographical region, glacier attributes (e.g. length, width, slope, orientation, tributaries) and environmental attributes (e.g. geology or climate). A sensible way to select subsets is to start with a hypothesis resulting from physical theories of surging (Clarke, 1991; Hamilton, 1992). The specific aim of geographical analysis is to distinguish regions where surge-type glaciers are concentrated and then seek possible environmental influences on surging (Clarke *et al.*, 1986). These regions can for example be represented by map sheets or drainage basins. Regions having a greater than average concentration of surge-type glaciers, have surge probabilities exceeding the surge probability of the complete dataset (Clarke *et al.*, 1986).

By comparing the surge probability of subsets, the *attribute predicted surge probability*, with the surge probability of the primary dataset, the influence of an attribute to surging can be calculated. For surge probabilities significantly higher than the surge probability of the primary dataset, the attribute will be strongly related to surge-type glaciers and might be a controlling factor of glacier surging. This relation is generally expressed by the probability ratio: the ratio of the probability of surging in a subset over the surge probability in the primary dataset. Subsets consisting of continuous data (length, slope, altitude, etc.) are for this purpose commonly divided into 'bins' (e.g. Clarke *et al.*, 1986; Hamilton and Dowdeswell, 1995). Calculating the probability ratios of surge probability in a particular length bin over surge probability of the primary dataset or with that of a particular subset (for example drainage basin or map sheet), can reveal if these factors are related to glacier surging. However, the boundaries of these bins were often arbitrarily chosen (e.g. Clarke *et al.*, 1986; Hamilton and Dowdeswell, 1995). For log-normally distributed attributes it would perhaps be more justifiable to divide the length bins accordingly, thus with equal intervals on the logarithmic scale. In this case the conclusions drawn from observed trends are more likely to have a physical validity.

3.2.3 Bivariate correlations: conditional surge probabilities

If surface slope decreases with increasing glacier length and if length is related to surge probability, the analysis of the influence of slope on surging is confused, because length is also influencing the surge potential. Similarly, if length has a hidden influence on glacier orientation (e.g. longer glaciers are more likely to flow north), the surge probability for glacier orientations is biased. Because of these mutual conditional relationships between attributes, it is necessary to remove the influence of one to the other and to calculate unbiased surge probabilities. This can be done by calculating the attribute predicted surge probability for a second attribute. Length influence on surface slope can be removed by dividing, for each length bin, the slope into two different subsets, for example (α+) slope exceeding the median slope in that length bin and (α-)

slope below the median slope for that subset. The probability that a glacier belongs to subset α+, given that it is surge-type and in a certain length-bin is calculated from Bayes' theorem for posterior probability (Clarke *et al.*, 1986). If length has a hidden influence on glacier orientation (e.g. longer glaciers were more likely to flow north), the surge probability of glaciers in an octant can be compared to the length predicted surge probability for that octant (based on a length distribution into 10 length bins): the probability ratio is then a measure for the deviation of surge probability from length predicted surge probability. If there is no deviation, then the probability ratio is one, any deviation from this indicates that surge-type glaciers are more or less likely to have orientations in a particular octant. Both Hamilton (1992) and Clarke *et al.*, (1986) used these probability techniques to disentangle bivariate correlations between possibly correlated subsets.

3.2.4 Multivariate correlations: multiple correlation techniques

The aim of multiple correlation analysis is to derive which correlations between surge tendency and glacier/environmental attributes are primary and which are secondary so as to disentangle which attributes are explanatory factors in the surge mechanism(s) (Clarke, 1991). Each variable or attribute in a multiple correlation analysis can be considered as a function of any other variable in the population or subset. The problem is how to determine the influence of each variable on the surging potential. These complicated relationships between glacier attributes can be tackled by postulating linear relationships between attributes. The correlation between pairs of continuous (log-) normally distributed attributes such as length, width, slope, elevation, orientation and surge-index can be expressed by covariance, which can be qualitatively visualised by scatter diagrams or quantitatively in covariance and correlation matrices. Correlation values vary between –1, indicating a perfect negative correlation between two attributes and 1, indicating a perfect positive correlation between two attributes. All diagonal elements in a correlation matrix equal one, expressing the correlation of an attribute with itself.

The purpose is to find a maximum correlation between surge potential and a set of attributes. Multiple correlations between surge- and other attributes can be calculated from breaking down the correlation matrix (R) into parts of correlations between each single attribute and the surge potential, the *simple correlation* $R_{S.x}$ (where x can be length, slope, width or Fowler's index in the example of Clarke (1991)) and the correlations between the attributes and the surge potential, or the *multiple correlation* $R_{S.123\ldots m}$. The simple correlation which most approximates the multiple correlation can be interpreted as the primary correlation between the surge potential and an attribute. This factor can be quantified by calculating the fraction of the multiple correlation that is unexplained by the simple correlation, expressed as:

$$J_{Sx} = \frac{R_{S.123...m} - R_{Sx}}{R_{S.123...m}} . \quad (3.1)$$

Hence, the attribute that is the primary control on surging would have the smallest fraction of the multiple correlation unexplained, thus the largest fraction of the multiple correlation would be explained by the simple correlation between the surge potential and the primary controlling attribute (Clarke, 1991).

Other methods that have been used to analyse multiple correlations between surging and a set of attributes include multiple discriminant analysis and correspondence analysis (Wilbur, 1988; Marshall *et al.*, 1996). A multiple discriminant analysis can be used to determine which combination of variables optimally discriminates surge-type glaciers from normal glaciers (Davis, 1986). In this procedure the original set of parameters (attributes/variables) is transformed into a discriminant score or function, which collapses the multivariate problem into one or two canonical variables (Wilbur, 1988). An optimal discriminant function is one that best separates the population of surge-type glaciers from normal glaciers, using the smallest number of variables, where its statistical significance is tested by means of F values (Davis, 1986). When a single variable emerges as defining the best discriminant function then this attribute is optimally related to glacier surging. Advantages of discriminant analysis are that from the discriminant functions both the proportional contributions of variables emerge and their type of relationship (direct or inverse). Correspondence analysis is a type of principal component analysis, which combines the factor analysis between components with factor analysis between grid cells (Davis, 1986; Marshall *et al.*, 1996).

3.3 Results from previous research

In this section the results from previous research to the controls on glacier surging are presented. The structure of the subsections is such that some of the variables introduced on their own and others in groups of associated variables.

3.3.1 Length and tributaries

Post (1969) found that surging appeared in all shapes and types of glaciers, whereby length of surge-type glaciers in western North America ranges from 1.7 to 200 km and area ranges from 4 to 5800 km. From these figures Post (1969) concluded that no special shape or size is required for surging. These findings are however not unequivocally confirmed by subsequent research. Clarke *et al.* (1986) found the glacier length distribution for the Yukon glaciers to be log-

normally distributed and subsequently divided length into 10 length bins of variable size containing approximately equal numbers of glaciers. A steady increase in surge probability was found with increasing glacier length, with a maximum surge probability (65.1%) in the length bin for longest glaciers (15-75 km) (see Figure 3.1). All glaciers over 4 km in length appeared to have surge probabilities above the average. Similar results were found for Spitsbergen, where glacier length ranges from 0.9 km to 35 km (Hamilton, 1992). Dividing length into 9 length bins with variable length limits (similar to Clarke *et al.*, 1986), it emerged that glaciers in general have the largest probability, about 25%, of falling into the length range of 2 to 3 km and this probability steadily decreases with the increase in length. However, an almost monotonic increase of the surge probability with increasing length can be found. The surge probabilities range from 20.4% for glaciers in the lowest length bin (0-1 km) to 75.1% for glaciers in the highest length bin (Figure 3.1). These trends suggests that long glaciers have a higher surge probability than short ones, but these findings finding seems to be stronger for the Yukon Territory than for Spitsbergen (Clarke *et al.*, 1986; Hamilton, 1992). Because the average length of glaciers with tributaries exceeds the length of glaciers without tributaries, tributary glaciers were removed from the analyses. However, length influence on surge probability is obvious, whether tributary glaciers are included or not.

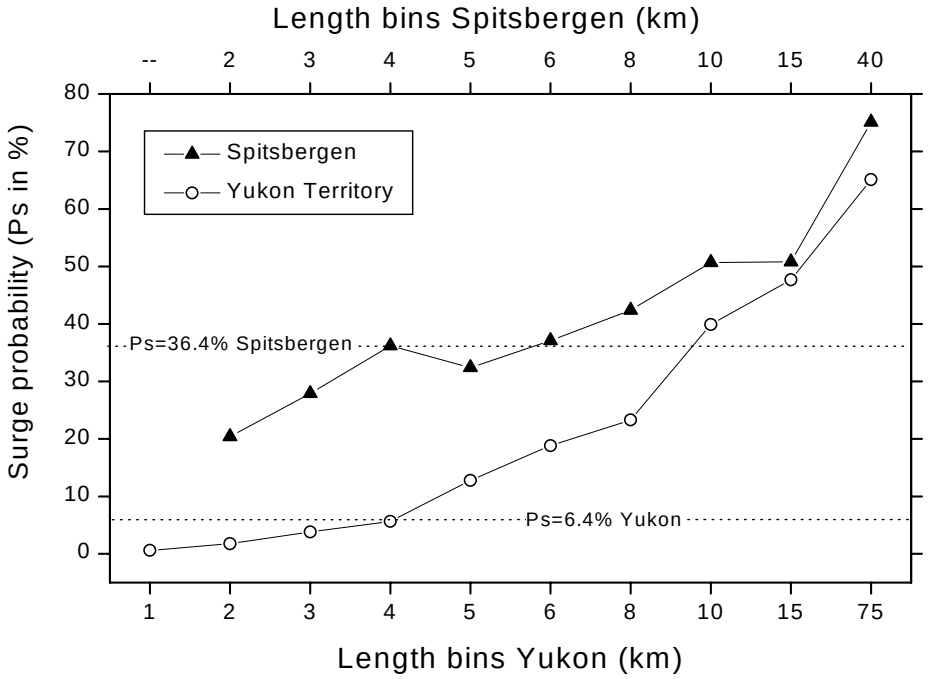

Figure 3.1: *Surge probability per length bin for Yukon Territory and Spitsbergen glaciers. Length on the x-axis gives the maximum length in km for each bin. Yukon Territory glaciers over 4 km in length have surge probabilities exceeding that of the primary dataset (6.4%) and Spitsbergen glaciers over 6 km in length have surge probabilities exceeding that of the primary dataset (36.4%) (After: Clarke et al., 1986; Hamilton and Dowdeswell, 1995).*

Could the non-random geographical distribution of surge-type glaciers in the Yukon territory and Spitsbergen be explained by the distribution of glacier lengths over the drainage basins/map sheets? Clarke *et al* (1986), found by comparing the actual distribution of surge-type glaciers with the length predicted distribution of surge-type glaciers that the geographical distribution of surge-type glaciers over the drainage basins in the Yukon Territory could not be fully explained by the length predicted surge probability. Although three main regions with highest length predicted surge probabilities are the same as the three regions with the higher observed surge probabilities, there is some reorganisation of the overall geographical pattern (Clarke *et al.*, 1986). By calculating the length-predicted surge probability for each of the ten map sheets in Spitsbergen, Hamilton (1992) found the opposite result: length was unable to explain the geographical distribution of surge-type glaciers over the map sheets. Because even length, having the strongest impact on surge probability, cannot explain the distribution of surge-type glaciers, both Clarke *et al.*, (1986) and Hamilton and Dowdeswell (1995) concluded that surging is probably controlled by a combination of variables.

It would be possible that surge-type features on small glaciers are less obvious and hence are more difficult to distinguish, hence short glaciers could easily be missed as their surge evidence is harder to detect (Post 1969; Clarke *et al*., 1986). This effect would bias the distribution of surge-type glaciers over the different length bins. However, when surge-probabilities found for the largest length bins in the Yukon territory (P_s>40%) would count for the entire population it would imply that more than 40% of the total glacier population would be of surge-type. This would be a huge overestimation of the total number of surge type glaciers as instead of the 151 glaciers which have been calculated to be of surge-type (Table 3.2), 942 glaciers would be so. Therefore, Clarke *et al.* (1986) concluded that longer glaciers have significantly higher surge probabilities than short glaciers. Nevertheless, Hamilton (1992) suggested that the relation between length and surging may be the result of the sampling technique. On Svalbard, surge-type features on glaciers shorter than 6 km would easily be overlooked on aerial photographs (Hamilton, 1992).

By analysing two subsets of the primary datasets, one with *tributaries* (T-subset) and one *without tributaries* (NT-subset), Clarke *et al.* (1986) and Hamilton (1992) explored whether glaciers with tributaries are more likely to be of surge-type than glaciers without tributaries. Surge probabilities Yukon Territory varied from 4.3% for the NT-subset to 23.1% for the T-subset (compared to 6.4% for the primary dataset) and for Spitsbergen between 31.5% for NT-subset and 39.3% for T-subset (as compared to 36.4 for the primary dataset). This indicates glaciers with tributaries are more likely to be of surge-type than glaciers without tributaries. However, the average length of glaciers with tributaries is greater than that of glaciers without

tributaries and hence, the length influence on the surge probability has to be estimated. Although for the Yukon territory the surge probability for tributaries controlled for length is considerably lower than the original T-subset surge probability (9.5% as compared to 23.1%), it is still higher than the surge probability of the primary dataset thus indicating that tributary glaciers are more likely to be of surge-type (Clarke *et al.*, 1986). For Spitsbergen length did not influence the surge probability of the NT- and T-subsets, but analysis of the ranking order of map sheets for the primary dataset and the NT-subset by means of the Spearman's rank correlation coefficients indicated that the datasets were statistically identical. Thus, although glaciers without tributaries had a slightly higher probability of being surge-type in Spitsbergen, the geographical distribution of surge-type glaciers seems to be unrelated to that of glaciers with tributaries (Hamilton, 1992).

The relation between surging and the presence of tributaries could be explained by the fact that surges in tributary glaciers can trigger surges in the trunk and *vice versa.* Clarke *et al.*, (1986) called these 'contagious' surges and argued that trunks are more likely to trigger surges in their tributaries than reverse. Therefore, trunk glaciers and their tributaries would not only have an internal surge trigger, but occurrence of a surge could also be related to an external triggering through the surge of a trunk or a tributary.

3.3.2 Slope and elevation

Although Post (1969) found that the topography of regions with surging glaciers does not differ obviously from that of regions without surging glaciers, Clarke *et al.* (1986) found that surge-type glaciers occur generally at higher altitudes. Furthermore, elevation span increases with glacier length from 400 m for small glaciers to 2250 for long glaciers, while median slope decreases monotonically with glacier length from 25° for short glaciers to 4° for long glaciers. Because length and slope as well as length and elevation are interdependent subsets, Clarke *et al.* (1986) therefore calculated length-controlled surge probabilities both for elevation and slope. Surge probability is larger for glaciers with steep overall median slopes and steep median slopes of the accumulation zone, whereas median slopes of the ablation zone are less than average. This is also reflected in the geographical distribution: regions with the highest surge probabilities also have higher average elevations (Clarke *et al.*, 1986). This association of altitude with surging could be explained by the increased likelihood of undernourishment at lower elevations (Clarke *et al.*, 1986).

Hamilton arranged his dataset of Spitsbergen glaciers so that for each length bin, the median maximum elevation and median minimum elevation were calculated. Median slope for the

primary dataset was 6.3º. Hamilton (1992) found that as length increases, there is an increase in elevation span, but a decrease in median slope. However, while controlling for glacier length, he found the tendency for surge-type glaciers to have surface slopes steeper than the median not statistically convincing.

3.3.3 Is length, width, slope or Fowler's index a primary control on surging?

Because there are strong correlations expected between glacier length, width and slope, Clarke (1991) performed additional multiple correlation analysis to the same data in order to disentangle which relationships between attributes and surge tendency are primary and which are secondary. With this approach two surge theories predicting that certain glacier geometries could be conducive to surging could be tested (Kamb, 1987; Fowler, 1987a, 1989). Kamb (1987) predicts that low slopes are conducive to surging by proposing a dimensionless stability parameter Ξ, whereas Fowler's index $\widetilde{F}$ is dependent on slope as well as width of the glacier (see Sections 2.5.7 and 2.5.8). The multivariate analysis performed by Clarke (1991) was used to find observations supporting or rejecting these theories.

By introducing logarithmic transformations to obtain approximate Gaussian distributions for length, slope and Fowler's index, Clarke (1991) could calculate sample means and variances. Covariance and correlation matrixes of these Yukon data show that the surge-length correlation is strongest (R_{SL}= 0.47), surge-width correlation is weaker (R_{SW}= 0.25) and surge-slope correlations are weaker and inverse ($R_{S\alpha}$ = -0.28) and the weakest correlation is that between surge tendency and Fowler's parameter ($R_{S\,\widetilde{F}}$ = 0.11). The strongest (inverse) correlation of all is that between length and slope ($R_{L\alpha}$= -0.67), which indicated that long glaciers have low slopes (Clarke, 1991). Further, the length-width correlation (R_{LW}= 0.54) indicates that long glaciers tend to be wide and the width-slope correlation ($R_{W\alpha}$= -0.47) indicates that wide glaciers have low slopes (Clarke, 1991). From these results it cannot be derived whether strong correlations between length and other attributes could explain part of the strong surge-length correlation. To disentangle which attribute is the explanatory factor in surging, Clarke (1991) performed multiple correlation analysis. Multiple correlation between surge tendency and attributes ($R_{S.LW\alpha}$= 0.47) was compared to the simple correlations ($R_{S.L}$, $R_{S.W}$, $R_{S.\alpha}$ and $R_{S\,\widetilde{F}}$). It followed that more than 99.68% of the multiple correlation between surge tendency and attributes is explained by the simple correlation between surge tendency and length, while only more than 60.6% of $R_{S.LW\alpha}$ is explained by $R_{S.\alpha}$ while 53.3% is explained by $R_{S.W}$. Further, the simple correlation between surge potential and Fowler's parameter only explains 23.3% of the multiple correlation.

Thus, virtually all multiple correlation between surge tendency and glacier attributes is explained by the simple correlation between surge tendency and glacier length (Clarke, 1991). This is not consistent with Kamb's prediction that the correlation between surge tendency and slope should be the controlling relationship (Clarke, 1991). Although statistical testing shows a possible discrepancy between sample slope values and population slope values, the conclusion that the multiple correlation coefficient by the simple correlation between surging and lenth is not being rejected. Clarke (1991) concluded from the multiple correlation analysis that length is a primary explanatory attribute of surging. As a result, Kamb's theory predictions are not supported, while Fowler's prediction is completely rejected. However, Clarke (1991) argued that Kamb's theory is a local one and might thus be valid for glaciers with specific geometries and bed configurations. Length, on the other hand, is a global control.

3.3.4 Orientation and channel curvature

For western North America there appears to be no particular glacier orientation dominant for surging glaciers (Post, 1969). For Spitsbergen, the dominant flow directions for both the upper and lower zone are NW and NE (Hamilton, 1992). Spitsbergen glaciers with the highest (unconditioned) surge probability were those with upper zones orientated N and SE and lower zones orientated SE and W. However, length predicted surge probabilities resulted in a different pattern: highest surge-probability values for the upper zones with orientation S and SE and for the lower zones orientated SE. Because these surge probabilities were not significantly higher than the surge probability of the primary dataset, Hamilton concluded that in Spitsbergen, orientation could not be a controlling factor to surging.

Because there could be a hidden influence of glacier orientation on glacier length (Kasser, 1980), probability ratios of orientation and glacier length were calculated (Clarke *et al.*, 1986). In the Yukon Territory, orientation- length ratios exceeding 100% were found in the SE and E octants whereas ratios smaller than 100% occurred in the W and SW octants. This suggests that both accumulation and ablation areas of surge-type glaciers are more likely to have aspects in E and SE octants and less likely in the W and SW. This is in contrast to the overall trend: Clarke *et al.* (1986) noted that the majority of glaciers in the Yukon dataset flow to the north and fewest to the south, which could be explained by the decreased radiation on north orientated slopes in the northern hemisphere (Clarke *et al.*, 1986). A probable explanation is that long glaciers are also most concentrated in the E and SE and least in the W and SW octants (Clarke *et al.*, 1986). A drawback of the locality of the study areas that W flowing glaciers are likely to be underestimated, because the Yukon territory is situated on the East flank of St. Elias Mountains.

In addition, Spitsbergen glaciers were divided into four groups according to different channel curvatures, measured by the difference between the orientation of the upper part and lower part of the glacier (Hamilton, 1992). The curvature groups range from almost straight (curvature ≅ 0º) to curved (>90º) and the surge probabilities range from 34.5 to 40.6%. As the variability in surge probability between categories is small and not significantly different from that of the primary dataset, channel curvature appears to have little to no effect to the surge tendency. Hamilton (1992) nevertheless argues that there could be a hidden channel curvature influence on surging, but that this could not be revealed by this analysis as data from only upper and lower glacier orientations do not fully describe the actual channel curvature of the flowline.

Hence, although glaciers with E to SE orientations were found to have increased probabilities of surging in the Yukon Territory, statistical analysis of Spitsbergen glaciers did not reveal strong controls of orientation on glacier surging (Clarke *et al.*, 1986; Hamilton, 1992). Moreover, channel curvature of glaciers in Spitsbergen was not found to be related to surge potential whatsoever.

3.3.5 Terrain, geology and substrate

From geological maps, Post (1969) observed that surging glaciers are not related to a single type of bedrock since surging occurs on sedimentary and volcanic as well as metamorphic rock. However, non-surge-type glaciers were observed in the granitic Coast Mountains and the sedimentary formations of the Rocky Mountains. From the presence of many surging glaciers on severe deformed bedrock and in some fault-related areas, Post (1969) postulated that bed roughness or unusual bed permeability might be a controlling factor of glacier surging. The presence of many surging glaciers along the Denali fault in the Alaska Range suggests that surging might be due to fault displacement and related deformation, but the total absence of surging in other active fault areas with greater displacement rates contradicts this theory. Furthermore, many clusters of surging glaciers in other regions are found in localities without tectonic activity, such as The Yukon Territory and West and East Greenland. Thus, no direct relations between earthquakes, avalanches or volcanic activity and surging were found, but geological controls in terms of substrate conditions were suggested by Post (1969) to play a role in glacier surging. However, rough comparison of surge probability variations between Yukon Territory drainage basins with geology maps revealed no correlation of surge potential with lithology, geological age, regional tectonics, seismicity or physiographic boundaries (Clarke *et al.*, 1986). Nevertheless, the global distribution of surge-type glaciers reveals that the majority of surging glaciers occur in young mountain ranges undergoing rapid erosion (Paterson, 1994).

For geology as a parameter, Hamilton found the highest surge probability (39.8%) for glaciers overlying sedimentary rocks, a lower probability on metamorphic rock (27.5%) and the lowest surge probability on igneous rocks (5.1%). A possible explanation for sedimentary rocks having the highest surge probability is that sedimentary rocks may be better suitable for the formation of sedimentary and potentially deformable beds (Hamilton, 1992). This may be misleading because 80% of the total glacier database overlies sedimentary rocks. But, petrological class alone was unable to identify geographic distribution of surge-type glaciers, hence geology was divided into individual rock types. For sedimentary rock types, the surge probability ranged from 62.5% for limestone to 35% for conglomerate, with a standard deviation of 18.4%. So, surge probability based on *lithology* is slightly more effective than the *geology*-based probability.

Marshall *et al.* (1996) found that seven geological and terrain parameters optimally predicted the distribution of surge and non-surge outlets of the Laurentide ice sheet. These are: areal fraction of bedrock outcrop, average sediment thickness, upstream area, terrain curvature, terrain hypsometry, cell elevation range and standard deviation of slope aspect. Of these, low basal coupling strength (small fraction of bedrock outcrop) results in fast flow and high basal coupling (topographically or geologically controlled) results in slow flow. However, the simulated effect predicted fast flowing icestreams over a much larger extent than inferred from the geological evidence and Marshall *et al.* (1996) subsequently noted the possible influence of the position of ice divides, thermal regime, permafrost conditions and subglacial drainage characteristics. In conclusion, Marshall *et al.* (1996) mention that extensive areas with low bed coupling are inducive to the development of fast flow ice streams and might control the distribution of surge-type glaciers.

3.3.6 Thermal regime

Post (1969) as well as Clarke *et al.* (1986) found that regions with clusters of surge-type glaciers appear to be topographically high compared to other regions. One possible explanation could be that high glaciers are more likely to have subpolar thermal regimes, which may be favourable (but not necessary) to surging. In addition, Macheret (1990) and Bamber (1987) found a clear geographical trend in the distribution of internal reflection horizons (IRH) over the Svalbard archipelago, which could possibly be connected to the distribution of surge-type glaciers in the region. Using a dataset of 136 Spitsbergen glaciers with recorded radio echo-sounding data, Hamilton (1992) analysed the probability of glacier surging given a glacier is of a specific thermal regime, which was classified as cold, polythermal (specified as presence of an IRH), relatively warm (equivalent to temperate) and not specified. The surge probability of the

'adjusted' primary dataset of 136 Svalbard glaciers is 23.5%. Hamilton (1992) found that two layered thermal structure glaciers have the highest probability (45.7%) of being surge-type and cold glaciers the second highest probability (13.2%), but he ignored in his argument the 'not specified' thermal regime group with a surge probability of 17.2%. Because the surge classification of the RES dataset was assigned by the Soviets it did not include surge probabilities for the surge indices. Due to this uncertainty and moreover, due to differences between this dataset and the primary dataset of 615 Spitsbergen glaciers, no rigid statistical analysis could be performed by Hamilton and possible length bias was not removed (Hamilton and Dowdeswell, 1995). More importantly, some of the thermal classes contained small numbers of surge-type glaciers (once one count and twice five counts) and the author of this thesis is sceptical about the statistical significance of this test of control of thermal regime.

3.3.7 Glacier hypsometry

Glacier hypsometry is closely related to mass balance conditions and glacier dynamics (Furbish and Andrews, 1984; Oerlemans, 1989) and could thus be a control of glacier surging (see Section 2.5.7). Based on 'established' glacier and hypsometry classification schemes by Ahlmann (1948) and Furbish and Andrews (1984), Wilbur (1988) classified the 146 surge-type glacier and normal glaciers in western North America into six hypsometry curve groups: (1) top-heavy mountain valley group, (2) bottom-heavy mountain valley group, (3) top-heavy icecap group, (4) bottom-heavy icecap group, (5) equi-dimensional group. Of these, bottom-heavy glacier hypsometry appeared to be most successful in discriminating between surge-type and normal glaciers: 77% of surge-type glaciers were bottom-heavy, whereas only 22% of the normal glaciers were bottom-heavy (Wilbur, 1988). Thus, surge-type glaciers typically have long, narrow and steep upper valleys and wide and flat tongues. This could be partially derived from terrain hypsometry (Marshall *et al.*, 1996)

Wilbur (1988) tested whether this preferential hypsometry was a cause or effect of surge behaviour. He suggests that three principal factors influence glacier hypsometry: valley shape, topographic relief and ice volume. The first two factors remain constant over the surge cycle, whereas ice volume indicates the long-term climatic trend (Wilbur, 1988). Hypsometry changes are primarily caused by the redistribution of ice in a glacier, resulting in major advances or rapid ablation of the lower part of a glacier. Wilbur (1988) argued that because for large surge-type glaciers only slope and depth change significantly as a result of a surge: this has only minor effects on the curve shapes. From observations on small surge-type glaciers, showing dramatically advancing termini during surge and wasting tongues during quiescence, Wilbur (1988) concluded that smaller glaciers will have a greater tendency to change their hypsometry

curves than larger glaciers. As other research (Clarke *et al.*, 1986; Clarke, 1991; Hamilton, 1992) suggests that surging is more probable for long glaciers, which are less likely to change their hypsometry curves, hypsometry would indeed establish surge potential and not *vice versa*. However, Wilbur (1988) based this hypothesis on a very small sample of surging glaciers and many records of dramatically advancing large surging glaciers are known in other regions (e.g. Liestøl and Hagen, 1991; Molnia, 1993; Reeh *et al.*, 1994; Thorarinsson, 1969). Moreover, the hypothesis of small glaciers changing their surge potential over time and large glaciers having a fixed surge potential, is contradictory to the regular surge periodicity of both small and large surging glaciers, provided hypsometry is controlling surge potential.

3.3.8 Climate, balance flux and Budd's index

In respect of climate, surging glaciers occur most from sub-maritime to continental conditions and surging glaciers seem to include both temperate and subpolar glacier types (Meier and Post, 1969). Furthermore, the exchange (sum of accumulation and ablation) of surging glaciers varies between great extremes, hence no specific climate conditions seem to be in favour of surging (Post, 1969). Budd (1975) however, concluded (see Section 2.5.6) that normal glaciers would have a low product of balance flux and slope and fast flowing glaciers a high product. From the position of surge-type glaciers in Budd's diagram it appears that surge-type glaciers must have critical balance flux-slope products ($\Phi\tilde{\chi}$: see equation 2.10). Wilbur (1988) plotted adjusted Budd diagrams for the interior and coastal subsets of his analysis and found no critical zone exclusively for surge-type glaciers. Subsequently Wilbur (1988) warned of the danger of jumping to conclusions on the basis of small sample sizes, as the hypothesis proposed by Budd (1975) was based only based on seven surge-type glaciers defining a critically high product.

A different set of climate related factors were analysed by Wilbur (1988) from visual examination of bivariate plots. Investigated factors include ratios of slope, width, balance-related depth, balance-related velocity and basal shear stress. Weakly discriminating balance-related geometry relationships were found for width:depth ratios smaller than 4:1, balance velocity:width ratios higher than 1:10, balance velocity:depth ratios larger than 4:1 and high basal shear stress at low width:depth ratios, but these relations did not hold for the smaller glaciers. Moreover, balance depth was calculated by assuming a parabolic valley shape and balance flux conditions (Wilbur, 1988), which is a method ignoring the possibly fundamental differences in depths between surge-type and normal glaciers. Glazyrin (1978) found that for the Pamirs, ratios of accumulation to ablation area alone were not successful in predicting the distribution of surge-type and normal glaciers, yet accumulation area over width of the glacier

tongue was more successful, suggesting that keyhole shaped glaciers are more likely to be of surge-type. The latter result would suggest a hypsometric control on glacier surging.

Discriminant analysis revealed an optimal discriminant function of the form C=3.7(logW)-1.4(logA)-1.3(logΦ)-7.1, where W is average glacier width, A glacier area and Φ balance flux, was fairly successful for discriminating normal glaciers from surge-type glaciers (Wilbur, 1988). This suggests a surge relation proportional to $W^a / A^b \Phi^c$, with a, b and c exponents to be estimated (Wilbur, 1988). In total, 73.2% of the surge-type glaciers in western North America were identified correctly and 65.4% of normal glaciers. However, the main failures occurred in discriminating small surge-type glaciers and the large normal glaciers (Wilbur, 1988). It was notable that an inverse relation between W and Φ was part of the discriminant function for surge-type and normal groups, which is contrary to the direct relation between W and Φ for the coastal and interior groups (Wilbur, 1988). Narrow glaciers with high balance fluxes would thus have a higher likelihood to be of surge-type, again suggesting a hypsometric control in combination with climate.

3.4 Conclusions from previous research

From most studies (Clarke, 1991; Hamilton, 1992, 1996; Marshall *et al.*, 1996) glacier length and specific substrate conditions emerge as factors of greatest association to the distribution of surge-type glaciers and as controls of fast flowing ice streams. Long glaciers have high probabilities of being surge-type and short glaciers have high probabilities of being normal. Further, sedimentary bedrock in young active mountain ranges could be favourable to surge activity (Paterson, 1994). However, none of the analysed variables satisfactorily explains the distribution of surge-type glaciers or reveals explicit controls on surging. This implies that surging is probably a product of more than one environmental condition, but also raises the issue of whether the correct (combination) of variables are being analysed (Clarke *et al.*, 1986; Marshall *et al.*, 1996).

Glacier hypsometry emerges as a fairly good discriminator of surge-type and normal glaciers (Glazyrin, 1978; Wilbur, 1988). From these results the most significant conclusion is that environmental factors, possibly mountain geometry and geology are controlling the non-random distribution of surge-type glaciers. Post (1969) suggests that (1) subglacial temperature anomalies (related to groundwater temperatures and geothermal heat), (2) bed roughness or (3) permeability of the glacier bed, or a combination of these factors, might be creating conditions which make surge activity possible. The problem of these environmental attributes is that their measurement is difficult and data were consequently insufficient at that time to prove any

relationship. Marshall *et al.* (1996) suggested that water storage capacity and hydraulic conductivity were probably less important than the actual subglacial distribution of water, in controlling the locations of fast flow.

None of the tested critical parameters from surge theories: Budd's critical product of balance flux and slope (Budd, 1975); Kamb's slope relation in the cavity stability parameter (Kamb, 1987); nor Fowler's index (Fowler, 1989), were found significantly related to glacier surging in the investigated regions. Furthermore, the length related surge probability results for the Yukon Territory and Spitsbergen give no reason for the existence of two or more distinct surge mechanisms as there is a monotonic increase in surge probability with glacier length. Two or more separate surge mechanisms would probably result in a two or more peaked surge probability for certain glacial or environmental attributes (Clarke *et al.*, 1986). However, no two distinct populations of surge-type glaciers have been detected from previous research.

3.5 Implications from detected controls on surging

Conclusions from previous research possibly raise more questions about surging that it provides answers. Some of these questions suggest that specific further analysis is needed to test if hypotheses are supported or rejected by common characteristics of surge-type glaciers. Below we present the most important hypotheses developed to explain the glaciological implications of detected (possible) controls on glacier surging.

3.5.1 What is the significance of increasing surge probability with increasing length?

The larger a glacier becomes the more vulnerable its subglacial drainage system is to instability and collapse (Clarke *et al.*, 1986). Long glaciers have greater likelihood of traversing lithological boundaries and thus experiencing a change in substrate, which in its turn could effect the stability of the subglacial drainage system. Further, glacier length could be a proxy for other factors such as mass balance (Miller, 1973; Budd, 1975; Raymond, 1987), hypsometry (Glazyrin, 1978; Wilbur, 1988), subglacial conditions (Post, 1969; Clarke, 1991) or thermal conditions (Clarke, 1976; Baranovski, 1977; Kotlyakov and Macheret, 1987; Raymond, 1987; Fowler and Johnson, 1995). Moreover, the direct relation between surge probability and glacier length has interesting implications for the stability of large ice sheets and ice caps: these would be predicted to have high surge probabilities (Clarke *et al.*, 1986). There are however several problems connected with the length related surge probability. Some of the significant and unresolved questions in this respect are:

- If long glaciers have such a high surge probability, why are not all glaciers above a certain length in a cluster region of surge-type?
- Do small surge-type glaciers have separate surge controls from large surge-type glaciers?
- Which specific conditions are required to make some very small glaciers surge?

3.5.2 What is the significance of increasing surge probability with increasing elevation?

Firstly, high glaciers are more likely to have subpolar thermal regimes, which may be favourable (but not necessary) to surging (see next section). Secondly, higher elevations possibly reflect higher tectonic uplift rates and geomorphologically younger terrain, which favours the production and availability of subglacial debris (Clarke *et al.*, 1986). Thirdly, glaciers at lower elevations could be more likely to be undernourished (Clarke *et al.*, 1986). This could mean that build-up to a surge cannot be realised.

3.5.3 What is the significance of increasing surge probability with presence of an internal reflection horizon?

This is probably one of the most difficult questions as both temperate and surge-type glaciers have been observed to surge. Circumstantial evidence (e.g. Dowdeswell *et al.*, 1991; Murray *et al.*, 1998) suggests that polythermal glaciers could perhaps have a different surge control from glaciers of other types of thermal regime. Moreover, internal drainage of polythermal glaciers is different from that of temperate or cold glaciers and bed rheology as well as hydraulic conductivity of (partly) frozen sediments is different from conditions where which free water is present (e.g. Hodgkins, 1997; Porter, 1997). The main issue is whether glaciers surge by thermal instability or whether thermal regime only controls the propagation of the surge-front (e.g. Murray *et al.*, in review). Further is it not clear if a polythermal regime is the (possible) cause or the effect of glacier surging (Hamilton and Dowdeswell, 1995).

3.5.4 What is the significance of increasing surge probability for certain glacier orientations?

Orientation of glaciers is first of all controlled by the terrain topography and drainage basin configuration allowing or obstructing glaciers to flow in certain directions. Further, there could be a hidden global and local climate control in glacier orientation in the form of differences in received radiation, accumulation patterns, shade effects, *etc.*. Related is the possible difference

in terrain shape ratio (elevation:area) between different mountain faces (Sugden and John, 1976). However, for some glacier types (e.g. ice caps and ice plateaux) it is difficult to define what the actual direction of flow is, as a number of different flow lines can be selected which represent different flow directions.

3.5.5 What is the significance of increasing surge probability for bottom-heavy hypsometries?

Glacier hypsometry is intimately related to the relative amount of advance or retreat to regional changes in equilibrium line altitude, thus contrasting hypsometric shapes will have intrinsically different response times and some hypsometry types could promote extreme differences between balance fluxes and actual fluxes (Furbish and Andrews, 1984). Further, different glacier hypsometry types result in distinct balance flux and balance flux per width distributions over the longitudinal glacier profile (Wilbur, 1988). This can effect the flow and stress regimes in these glaciers and possibly result in regions of anomalous stress. Further, glacier hypsometry is influence by three principal factors: valley shape, topographic relief and ice volume (Wilbur, 1988). Marshall *et al.* (1986) found that terrain hypsometry and curvature indeed appears to be related to the occurrence of fast flowing ice streams and thus the spatial configuration of elements controlling ice-bed coupling could play a direct role in the controls on glacier surging.

3.5.6 What are the major constraints of analysis methods used in the past?

Although geographical studies were based on extensive glacier inventories, the analysis were limited in the number and type of attributes. For example, Clarke's (1991) study included only four glacier geometry-attributes: glacier length, width, average slope and Fowler's parameter (Fowler, 1989). Besides, the use of area statistics in the studies of Clarke *et al.* (1986) and Hamilton (1992) did not allow the contribution of individual glaciers to the overall statistical model to be verified. Multivariate studies using similar glacier data and attributes could reveal additional significant associations between parameters. However, no explicit multivariate analysis has been performed including both continuous and categorical data. Further, by constraining selected glacier populations to arbitrary boundaries (e.g. map sheets, political borders) a bias can be introduced in the studied glacier population. It is therefore better to select the glacier population from for example a complete mountain range, island or archipelago, where the boundaries of glaciation are physical boundaries.

3.6 Which recommendations will be adopted in this thesis?

The purpose of the research into controls on glacier surging is in the testing of physically based hypotheses on the surge mechanism(s) and flow instabilities (see Chapter 2). On the basis of results and recommendation from former research into the controls on glacier surging the following additional aspects of methodology and glacier and environmental features will be investigated in Chapters 5 and 6 of this thesis.

The analysis method(s) on controls on glacier surging has to be capable of:

- simultaneously assess the influence of a combination of glacial and environmental attributes, in order to explicitly account for the confounding effects of the attributes,
- discriminating between primary and secondary controls on surging,
- generating a function or algorithm which can be used to predict the surge probability of individual glaciers,
- analysing individual glaciers instead of discrete groups of the glacier population.

The selected cluster region of surge-type glaciers has to:

- be defined according to physical boundaries,
- include a large number of surge-type and normal glaciers of different types and dimensions situated in a variety of different environmental settings.

Apart from the previously analysed set of glacial and environmental variables, the following attributes will be analysed in detail:

- climate related factors,
- geological boundaries,
- geological controls,
- thermal regime.

CHAPTER 4:
Methodologies:
Logit Modelling and Multi-Model Photogrammetry

In geomorphological systems the ability to measure may always exceed the ability to forecast or explain

Leopold and Langbein (1963)

4.1 Introduction

In this methodological chapter two different methods are presented that were used for the glacier data analysis presented in Chapters 5 and 6. In Sections 4.2 to 4.6 the method of *logit regression modelling* is presented. This statistical data analysis technique can be used to distinguish characteristics of surge-type glaciers from those of non-surge-type glaciers. Logit models enable exploration of the type and strength of relationships between a range of environmental and glacial variables and the distribution of surge-type glaciers in a regional glacier population, while controlling for interactions between variables. Subsequent to the establishment of variables distinctive for surge-type glacier the model performance for individual glaciers in the glacier population can be analysed to identify 'unusual' normal and surge-type glaciers. Section 4.6 contains a case-study of glaciers in the Yukon Territory, Canada, demonstrating the advantages of logit modelling over other data analysis techniques. The part on logit modelling is then concluded by a critical review of the benefits and drawbacks of the method in section 4.7. Part of the logit methodology has already been published in Atkinson *et al.* (1998), Jiskoot *et al.* (1998) or is in review in Jiskoot *et al.* (in review), while aspects of the case-study on Yukon Territory glaciers has already been published in Atkinson *et al.* (1998). In sections 4.8 to 4.10 a different method: the *multi-model photogrammetry* is presented. This is an advanced and accurate method that enables us to measure glacial features from photographs in three-dimensions. Application of this method in combination with the available imagery allowed the author to accurately measure and analyse an actively surging glacier and compare the surge characteristics of this glacier to other surging glaciers.

4.2 Background and purpose of logit regression modelling

The aim of statistical modelling is the quantitative representation of the relationship between a response variable to one or more explanatory variables, while giving a measure of uncertainty in this relationship. The products from a statistical model are the provision of a concise summary of the relationship in the form of a regression equation and a tool allowing the prediction of values of the response variable based on values of the explanatory variables. Statistical black box approaches, such as ordinary least square (OLS) multiple regression analysis (Davis, 1986),

have often been used as an explanatory tool to aid our understanding of processes in geomorphology. However, there are a number of limitations to the applicability of classical statistical techniques to geographical systems. Some of the most severe limitations are that the techniques are only applicable to continuous data types, and that assumptions must be made about the statistical distribution of the data and error terms (Atkinson *et al.*, 1998). In Generalised Linear Modelling (GLM) the conventional linear relationships of multiple regression are generalised to permit a much broader class of linear additive relationships between response and predictor variables of mixed types which can include both continuous and categorical variables. Moreover, there are no restrictions on the distribution of the data and the non-linear probability distribution implemented in GLM is more realistic than the linear one in traditional OLS regression (Wrigley, 1985).

GLM has been applied in biostatistics since the 1940s, and more recently in medical statistics, econometry, medical geography and population geography. However, the technique has received little use in geomorphology (e.g. Uno *et al.*, 1994; Siegel *et al.*, 1995; Atkinson *et al.*, 1998). In other fields such as medical research GLM is used primarily for prediction. In geomorphology, the cause and effect relation between response and explanatory variables is less clearly defined. Further, there are often many errors and much uncertainty in geomorphological primary (field) and secondary data, and outliers in the data are common. Therefore, while prediction remains the ultimate goal of GLM, one of the most important uses of GLM in geomorphology is as a means to quantify and explore the relations between response and explanatory variables with the eventual goals of understanding such relations and gaining insight into the geomorphological processes (Atkinson *et al.*, 1998). For the research presented in this thesis it is of primary importance to test hypotheses on which characteristics distinguish surge-type glaciers from normal glaciers with the ultimate aim of determining which of these characteristics are fundamental to the process of glacier surging and which characteristics are secondary (Clarke *et al.*, 1986; Clarke, 1991).

For the glacier population data analysis *logit regression models* were used and fitted as Generalised Linear Models (GLM). Logit models allows the relation of a binary response variable (surge-type versus normal glaciers) to a variety of explanatory variables and their interaction terms. Logit modelling of surge-type glaciers is therefore a statistical data analysis technique relating the likelihood that a glacier is of surge-type to one or more glacial and environmental characteristics. Further the technique can be used both as an exploratory and as a predictive technique by focussing on the residuals calculated for each individual glacier (Section 4.4 including subsections and Section 4.6.3).

4.3 Theory of logit regression models

The logit technique models the log-odds of an *event* occurring in a *population*, based on a number of *explanatory variables*. The *event* is defined by a binary (dichotomous) response variable: S=1 for 'presence' of a surge-type glacier and S=0 for 'absence' of a surge-type glacier. The *explanatory variables* are the set of selected glacial and environmental characteristics, which can be of mixed continuous and categorical types. The relation between the log-odds of an event, commonly written as *logit(P_i)* can be expressed as:

$$P_i = \frac{e^{f(X_i)}}{1+e^{f(X_i)}}, \tag{4.1}$$

where P_i is the probability of an event occurring for a given observation *i* (Wrigley, 1985). In this context, logit(P_i) is logit(P_s): the log-odds of the probability that the glacier is of surge-type. Logit(P_s) can alternatively be expressed as $\ln\frac{P_s}{1-P_s}$. The logit link function *f(X_i)* in equation 4.1 can be expressed as the linear predictor function or 'logistic regression function':

$$f(X_i) = \alpha + \sum_{k=1}^{n} \beta_k X_{ik}, \tag{4.2}$$

where α is the 'base estimate' or offset, $ß_k$ are the n 'estimates' or coefficients to be calculated in the model and X_{ik} are the *n* values for each of the explanatory variables. For X_{ik} being a mixture of continuous and categorical variables the $ß_k$ estimates are commonly being optimised through a maximum likelihood procedure (Wrigley, 1985). Although a logit regression function links the explanatory variables in a linear additive way, the underlying probability model is not linear, but has a logistic curve (an S-shaped cumulative probability distribution) and is strictly bounded such that if $X_{ik}=-\infty$, then *logit(Pi)*=0 and if $X_{ik}=+\infty$, then *logit(Pi)*=1 (Wrigley, 1985). The choice of an S-shaped cumulative probability distribution resulted from empirical observations showing that for probabilities close to zero and one a unit change in X_{ik} value had a substantially smaller effect on the probability change than a unit change in X_{ik} variable at probabilities in the middle ranges (Wrigley, 1985). The model formed is a logistic regression of success or failure of a given binary variable (presence or absence of a surge-type glacier) on the explanatory variables (Atkinson *et al.*, 1998). Because logit models give log-odds ratios, which can be converted into probabilities they are suitable to test hypotheses on the effects of the explanatory variables on the occurrence of surge-type glaciers (Francis *et al.*, 1993).

4.3.1 Data and sampling

Input data for a logit model include a response variable (or dependent variable) and a series of explanatory variables. In an object-orientated approach the response and explanatory variables are averages for whole units. For example, glaciers in certain geographical regions can be taken as 'units', with the binary response variable being the dichotomous surge index (S=0 for normal glaciers and S=1 for surge-type glaciers), and the explanatory variables can include glacial and environmental characteristics. A consequence of this object-orientated approach is that each unit is given the same weight regardless of the size or shape of the unit, unless specific weights are introduced (Atkinson *et al.*, 1998). To produce an optimal model it is best to use the complete population of surge-type and non-surge-type glaciers in the logit model.

For logit regression it is not problematic if explanatory variables are correlated because the model can separate the influence of both individual variables and also assess the combined effect of the variables on the response, whether the explanatory variables are of the same type or of mixed types.

4.3.2 Model fitting, model significance and significance terms

A multivariate logit model is usually fitted in a step-wise manner. First a *null model* is established which includes an intercept effect, no explanatory variables, and effectively treats the estimated value for each case as average for the whole dataset. The intercept is the constant that best fits the average response of the data. The deviance *D* that results in this model is a baseline against which the improvement of the model fit can be determined for the addition of each explanatory variable that corresponds with the loss of degrees of freedom (d.f.) through the addition of the variable. The degrees of freedom in a GLM model is the number of measurements (units) minus the number of parameters (variables) included in the model. For a null model this is the total number of glaciers in the model minus one d.f. (for the intercept). Each additional continuous variables will take one d.f. and categorical variables take the number of categories minus one (Crawley, 1993). Model deviance (D) is strictly speaking a measure for the unexplained part of the model and is expressed as:

$$D = -2\left[\ln \Lambda_c - \ln \Lambda_f \right], \tag{4.3}$$

where Λ_c is the maximum likelihood of the current model and Λ_f the maximum likelihood of the full model, which includes all variables (Wrigley, 1985). Although the aim is to minimise the model deviance, *D* cannot be used directly as an indicator of goodness-of-fit since one cannot

compare the fitted probabilities and the binary observations. However, since the deviance reduction for a given difference in degrees of freedom between separate models can be approximated to have a Chi-squared distribution, the reduction in model deviance can be used as an indicator of the significance of each term added to the model (Wrigley, 1985; Francis *et al.*, 1993). Furthermore, model deviances exceeding the value of degrees of freedom in the model can be considered as failing to satisfactory link the explanatory variables to the response variable.

Because goodness-of-fit can be assessed through a given reduction of deviance and degrees of freedom, terms are normally added to the model in a stepwise fashion, checking the significance of each term at each step. Using this approach, the effect of individual variables, combinations of variables and interaction terms between variables can be assessed logically. Only those terms which are significant at a given confidence level should be retained. In all the models a confidence level of 95% was used, and Chi-square values were derived from standard statistical tables. Once a term has been checked as significant, the calculated estimate (or estimates in case of categorical terms, β in equation 4.2) must be tested for significance against its standard error using the student t-test. With a null hypothesis (H_0) stating that 'the estimate is not significantly different from zero' and an alternative hypothesis (H_1) stating that 'the estimate is significantly different from zero', the t-value can be calculated by dividing the estimated coefficient by its standard error (Wrigley, 1985). For a large sample size (over 120) the critical Student t-value at the 95% significance level is 1.96. H_0 is accepted if the calculated t-value is smaller than the critical t-value, while H_0 is rejected and H_1 accepted if the calculated t-value is larger than the critical t-value. Using the 5% rule of the thumb a coefficient is therefore significant when it is greater than approximately twice the standard error (Wrigley, 1985).

Logit analysis is usually performed in two stages (Atkinson *et al.*, 1998). First a univariate stage, where the relationship between each variable and the incidence of surging is examined individually. Then a step-wise multivariate stage, where the combined effects of variables on glacier surging are examined simultaneously. When a factor has not been found significant in the univariate stage it should generally not be included in the multivariate stage. Because interaction between the terms of explanatory variables may be significant, it is common to test the significance of interaction terms (the product of the main terms). At each step in the multivariate stage the interaction terms between the variables can be explored and, if found to be significant, added to the model. Thus, each new variable is modelled while controlling for the effects of variables included previously. Eventually, no further variables will be significant at the chosen confidence interval. At this stage the *optimal model* is reached, in which the combination of variables is inferred to optimally discriminate between surge-type and normal

glaciers. The optimal model is build upon the underlying concept of parsimony, which means that with a simple model, most of the variance in the data is explained, instead of explaining all the variance with a more complicated model (Francis *et al.*, 1993). Instead of optimal logit model, some say therefore parsimonious logit model.

The testing of interaction terms for models including three or more terms or more than one categorical variable can be complex. For example, when a third main term is added to a model, the interaction between the three combinations of two terms and the interaction between the three terms should be checked. Clearly, the number of interaction terms grows exponentially with the number of main terms, and interaction terms between three or more variables can be difficult to interpret. Further problems arise for interaction terms between categorical variables. These categorical variables may be divided into several binary terms, and so the number of interaction terms may become large. For these reasons interaction modelling is usually limited to the two-way interaction terms and in addition categorical variables are usually aggregated into fewer, coarser classes.

Standard logit modelling procedures introduce a complication for the fitting of categorical variables by so called 'intrinsic aliasing' (Francis *et al.*, 1993). This means that the first class of the categorical variable is omitted from the model and fitted as base in univariate models or included in the intercept in multivariate models. The parameter estimates for this base are automatically set to zero and estimates of all other classes are compared to this 'reference level' (Francis *et al.*, 1993). This process saves time and enables the analysis of the main classes. In logit modelling it is therefore recommended that the right base class or reference level is selected: this is usually the class that is expected to have the least effect on the occurrence of the response variable.

In some cases (where non-linear relationships are expected) transformation of a continuous variable causes a much larger reduction in model deviance than the non-transformed variable and can consequently improve the model significantly. Therefore, where sensible, logarithmically transformed and normalised variables were also experimented with in order to obtain the best model fit. There are also cases where 'fully subdivided' categorical variables give standard errors that are much larger than the parameter estimate: here the counts in each category are too small to give significant correlations. It is then good practice to reduce the number of categories by means of aggregating the categorical variable data into larger, fewer groups (Wrigley, 1985). These procedure were implemented for the majority of categorical variables in the glacier databases of the Yukon Territory (Section 4.6 and subsections) and Svalbard (Chapters 5 and 6).

4.3.3 Model interpretation

Interpreting logit models is quite straightforward. When an optimal model has been obtained and the estimates have been found significant, one can start to interpret what effects the explanatory variables have on the response variable. For categorical variables, a positive sign of the estimate implies an above average correlation and a negative sign implies a below average correlation. For continuous variables, positive signs imply direct correlations and a negative value imply inverse correlations, while the magnitude of the estimate relative to the base estimate gives the strength of the correlation. Thus, positive signs suggest the likelihood that a glacier is of surge-type increases with the level or presence of the variable, with the other variables held constant, depending if the variable is continuous or categorical (Liao, 1994). However, the exact value of the estimate does not directly represent the magnitude of effect on the change in likelihood of surging. Interpretation of interaction terms is less straightforward and has to be viewed in terms of pre-determined physical relations in the glacier system.

A more meaningful way of interpretation of an estimate value is achieved by transforming this value into the probability that an event (presence of a surge-type glacier) is occurring ($P_{(S=1)}$). This can be expressed as:

$$P_{(S=1)} = \frac{e^{\beta_k X_k}}{1 + e^{\beta_k X_k}} \tag{4.4}$$

where $ß_k$ is the estimate calculated in the model and X_k is the parameter value (0 or 1 in the case of categorical variables and a continuous range in the case of continuous variables) (Liao, 1994). A probability larger than 0.5 indicates and increased chance of a surge-type glacier occurring and a probability smaller than 0.5 indicates a decreased chance of a surge-type glacier occurring. Comparison of this estimate probability to that of the other significant estimates in a model gives a measure for the marginal effect of a unit change or the presence or absence of a variable on the probability of fitting a surge-type (S=1). The advantages of this procedure is that the variables can be ranked in order of effect on glacier surging, irrespective of the sign of the estimate, and that the estimate probability represents the magnitude of effect on changing the likelihood of surging (Liao, 1994; Downs, 1995). Although this procedure will only be explained for the multivariate logit modelling results of the Yukon Territory glaciers case-study in Section 4.6.2, it will be implemented throughout the logit modelling results sections in Chapters 6 and 7.

4.3.4 Model predictions

An optimal logit model can be utilised as a predictive tool by means of the obtained logit regression equation. By filling-in values for the explanatory variables (X_{ik} in equation 4.2) the model returns the fitted value for that glacier. However, predicting a glacier's fit would be biased if this glacier were included in the training set of glaciers for the optimal logit model. For prediction proper the glacier(s) to be predicted can be excluded from the optimal model, thus running a separate optimal model using only part of the complete glacier population. Prediction is then simply done by applying the logit regression equation from the optimal model. Using the attribute values for that particular glacier in this equation returns the predicted value for the response variable ($\hat{S}$) for that glacier.

Through this method of prediction, it is also possible to experiment with a 'virtual' glacier by gradually changing the value of one of its explanatory variables (while keeping the others fixed) and examining its effect on the likelihood that a glacier is of surge-type. This enables information to be obtained on how much a certain increase or decrease of the explanatory variable changes the likelihood of the response. Further, it is possible to explore if cut-off values or specific ranges exist where the likelihood of surging changes from low to high. This procedure could thus be useful for the testing of critical ranges of variables related to specific surge theories (see Chapter 2).

4.4 Goodness-of-fit and accuracy assessment

Although a number of measures for goodness-of-fit are available (see Wrigley, 1985), the most reliable method for verifying the model performance is in the analysis of residuals and comparison of the predicted probability with the associated binary observation of the response variable (see Section 4.6.3). Plotting of residuals against explanatory variables may lead to the identification of outliers. Outliers may indicate unusual cases that are not covered by the set of explanatory variables used in the model, or they may be mis-classified units, such as a surge-type glacier that is incorrectly classified as a normal glacier.

4.4.1 Residual analysis

A residual (e_i) is a measure of the discrepancy between the fitted ($\hat{S}$) and observed response variable (S). Instead of using raw residuals ($e_i = S - \hat{S}$), which are statistically incomparable, GLM uses modified Pearson's residuals that are standardised to have a mean of zero and a unit

variance (Wrigley, 1985; Francis *et al.*, 1993). The standardised residuals e_i for each glacier is calculated as:

$$e_i = \frac{(S - \hat{S})}{\left\{\hat{S}(1-\hat{S})\right\}^{1/2}}, \qquad (4.5)$$

where S is the assigned binary surge index and $\hat{S}$ is the fitted value in the model (Jiskoot *et al.*, in review). Large residuals indicate failure of the model to fit well for the corresponding glacier. A perfect model would give fitted values close to one for all surge-type glaciers and fitted values close to zero for all normal glaciers.

Logit models intrinsically produce a systematic pattern in the distribution of residuals (Wrigley, 1985). Large residuals are generally found in the low and high fitted values - this is inherent to the dichotomous nature of the logit regression (Aitkin *et al.*, 1989). This means that common statistical residual analysis techniques for least square regression cannot be applied in logit models and residual analysis is mainly through visual interpretation of residual plots.

There are two causes of large residuals: (1) mis-specification of observed values for the response variable S to glaciers in the population and (2) the occurrence of aberrant observations, distorting either the probability distribution or the parameter estimates for the model (after Aitkin *et al.*, 1989). Hence, the model can be used to both detect mis-classifications and to locate 'unusual' surge-type glaciers that are not well described by the general statistical model. Visual interpretation of residual plots on pronounced patterning can then help to understand what is distinctive about these glaciers. If a systematic pattern occurs, for example high or low residuals only occurring on certain lithologies, it can be detected if the model 'overpredicts' or 'underpredicts' surging on that lithology. Furthermore residual patterns can suggests introduction of a new explanatory variable that might be a control on surging.

4.5 The GLIM software

Logit regression models were fitted as generalised linear models using the UNIX operated Generalised Linear Interactive Modelling (GLIM4) software system (Francis *et al*, 1993). GLIM is an interactive statistical analysis program with its own (Unix-based) syntax. Standard procedures in GLIM include data input, model specification, model fitting, data display and data manipulation. The logit models presented in this thesis were run on the Cray Superserver CS6400 at the Manchester Information Datasets and Associated Services server (formerly MIDAS, now MIMAS) based at the Manchester Computer Centre. A standard publication on

the GLIM4 software package is Francis *et al.* (1993), although good descriptions of its capabilities and applications can be found in Aitkin *et al.* (1989) and Crawley (1993).

4.6 Application of logit models to Yukon glacier data

A case-study of Yukon glacier data was implemented in order to demonstrate the strength of logit modelling as compared to conventional multiple regression as applied by Clarke (1991) (see Section 3.2). Data for the analysis were selected from the Yukon Glacier Inventory, a component of the Canadian Glacier Inventory (Ommanney *et al.*, 1973). Following Clarke (1991), all rock glaciers, remnants and non-real glacier features were excluded as well as most tributary glaciers from the 4675 entries in the Yukon Glacier Inventory. This procedure leaves a total of 1726 glaciers that were used to optimise logit models. Clarke (1991) used 1754 non-tributary glaciers for his analysis derived in a similar manner. The difference is the result of an additional exclusion of a number of non-real glaciers from this case-study. The Yukon Glacier Inventory includes a surge index related to observed surges and morphological evidence of surging (Ommanney *et al.*, 1973). Each glacier is assigned a code from 0 (no surge features) to 5 (definite surge evidence). Based on the surge probability schemes published in Clarke *et al.* (1986) the glaciers were divided into non-surge-type (digits 0-3) and surge-type (digits 4 and 5) (see Section 3.2.2). The estimated probability of mis-classifying a surge-type glacier as a non-surge-type glacier, or *vice versa*, is less than 20% for digits 3 or 4, and for the other digits smaller than 5% (Clarke *et al.*, 1986). From the total of 1726 glaciers in the data set, 69 (4%) glaciers were classified as surge-type. The purpose of Clarke's (1991) multivariate analysis was to find observations supporting or rejecting the surge theories of Kamb (1987) and Fowler (1989) (see Section 2.4.8). For that reason, Clarke (1991) used four variables: glacier length, average glacier width, average surface slope and Fowler's index (see Section 3.2.1). To compare the performance of logit modelling to standard multiple regression modelling a similar set of glaciers and variables were used, but with type of glacier front and an additional categorical variable for Fowler's index added, to illustrate the power of logit models. Further, variables for maximum and one for minimum elevation were introduced in order to test Clarke *et al.*'s statement that regions with clusters of surge-type glaciers appear to be topographically high compared to other regions (Clarke *et al.*, 1986).

A logit analysis is started by assigning a response variable and a number of explanatory variables. The response variable in the Yukon Territory logit model is the dichotomous surge index, S, with S=1 for surge-type glaciers and S=0 for non-surge-type glaciers. The logit model was fitted for a set of continuous variables, that is, glacier length, mean glacier width, average surface slope, minimum and maximum glacier altitude, Fowler's index ($\widetilde{F}$) and two factors: type of glacier

front and a categorical version of Fowler's index ($\tilde{F}_{cat}$). The parameters glacier length, width and surface slope are log-normally distributed (see Clarke, 1991) and so are $\tilde{F}$, maximum and minimum altitude. Because the logarithmic transformed variables sometimes resulted in a better linear fit, these log-transformed data were used as separate parameters in the model (see Table 4.2).

$\tilde{F}$ is the dimensionless product of glacier width squared and bed slope (Fowler, 1989), where average surface slope can be substituted for bed slope. It is hypothesised that this index is smaller than the order of one for surge-type glaciers (Fowler, 1989: see also Section 2.4.8). For this purpose, $\tilde{F}_{cat}$ was divided into three categories (1) $\tilde{F}$ <0.5, (2) $0.5 \leq \tilde{F} \leq 2$, and (3) $\tilde{F}$ >2. These categories represent the values for $\tilde{F}$ smaller than the order of one, of the order of one, and larger than the order of one. According to Fowler (1989), the first category would contain the majority of surge-type glaciers, the second category would be a transitional category, and the third category would contain no surge-type glaciers. The data presented in Table 4.1 shows no clear agreement with this hypothesis. The numbers of surge-type glaciers in the three categories demonstrate no negative trend, while the values for normal glaciers demonstrate that the majority of normal glaciers fall into the range of Fowler's index smaller than the order of one. This would contradict Fowler's hypothesis. The logit analysis will enable quantitative exploration of the relationship between Fowler's index and surge-type glacier as well as of the correlations between Fowler's index and other glacier characteristics.

CATEGORIES OF FOWLER'S INDEX			
	$\tilde{F} < O(1)$	$\tilde{F} = O(1)$	$\tilde{F} > O(1)$
Normal glaciers	710	775	172
Surge-type glaciers	14	42	13

Table 4.1: *Count of surge-type and normal glacier in categories of Fowler's index.*

The logit analysis was performed in two stages. First, univariate models were fitted to explore the relationships between the individual parameters and glacier surging (Table 4.2). As this approach ignores the confounding effects of other variables, the second stage involved fitting multivariate models where each variable is incorporated in a step-wise fashion, so that the effect of each variable on surging can be explored while controlling for the effects of other variables (Atkinson *et al.*, 1998). While fitting multivariate models the two-way interaction terms of the explanatory variables were also included in the analysis. Significant multivariate models are presented in Table 4.3.

4.6.1 Univariate logit models of Yukon glaciers

Conforming to the logit modelling procedures explained in Section 4.3 and subsections a so-called null model was fitted (Table 4.2). This model fits only an intercept, and gives identical fitted values for all glaciers, which is equal to the dataset's mean value for *S*. With 69 glaciers in the class S=1 (surge-type glaciers) and 1677 glaciers in the class S=0 (normal glaciers) this mean value equals 0.04 (*i.e.* ((69×1)+(1677×0))/1726). This fitted value ($\hat{S}$ =0.04) is close to the observed value of normal glaciers (*S*=0), but for surge-type glaciers it is very different from the observed value (*S*=1). All normal glaciers have therefore small standardised residuals (-0.2) but all surge-type glaciers have large standardised residuals (+4.9) (see Section 4.4.1). The purpose of including explanatory variables in the model is to reduce the residuals significantly.

The null model has a model deviance of 579.49 for 1725 degrees of freedom. Because the model deviance is much smaller than the total degrees of freedom, a large part of the data can be explained by just fitting an intercept. However, as the model deviance is much larger than one, much of the data still remains unexplained. By adding, one-by-one the variables length, width, slope, Fowler's parameter, highest and lowest elevation and type of glacier front to the model, the variables can be explored which explain the occurrence of surge-type glaciers better and result in a better fit for both surge-type glacier and normal glaciers. At the 95% significance level, the critical χ^2 value for a loss of 1 d.f. is 3.84, for 2 d.f. it is 3.22, for 3 d.f. it is 4.64 and for 7 d.f. it is 9.80. This means that continuous variables (taking one d.f.) only improve the model significantly if inclusion reduces the model deviance by more than 3.84. Inclusion of a categorical variable with 8 classes (e.g. type of glacier front) results in a loss of 7 d.f. (the number of categories minus one, see section 4.3.2) and the model is only significant when the reduction in model deviance is more than 9.80.

Table 4.2 presents the results of the univariate models. Of all the variables added to the null model, log-length gives the greatest reduction in deviance: 265 for 1 d.f.. The estimate for this log-length parameter is significant and positive (5.84) indicating that surge-type glaciers in the Yukon Territory tend to be longer than normal glaciers. The estimate for logarithmically transformed glacier width is also significant and positive (4.24), although the relationship is somewhat weaker. On the contrary, the estimate for surface slope (-0.39) indicates that surface slope has a significant, but negative, relation to glacier surging. Here, the untransformed variable caused a greater reduction than the log-transformed variable. The model including the untransformed Fowler's index is not significant as inclusion of $\tilde{F}$ only caused a reduction in deviance of 0.92. Conversely, the logtransformed variable causes a reduction in deviance of 14

and from the estimate of 0.496 it appears that that log-$\widetilde{F}$ is positively related to surge-type glaciers. This finding contradicts Fowler's hypothesis (Section 2.4.8). Moreover, the model results for $\widetilde{F}_{cat}$ support this finding, as glaciers with $\widetilde{F}$ exceeding the order of one are more likely to be of surge-type (based on an estimate of 1.3 for $\widetilde{F} > 2$). With a parameter estimate of 0.002, maximum glacier altitude is positively related to surging suggesting that surge-type glaciers tend to initiate at higher altitudes. Minimum altitude is also significant but the parameter estimate is negative (-0.001), so, according to the univariate analysis, surge-type glaciers tend to have their terminus at low altitude. Type of glacier front reduces the deviance by 72 for a loss of 7 d.f.. This result is significant at the 95% significance level. The front types piedmont, expanded, stagnant and ice-cored moraine have a strong positive correlation to surging (Table 4.2). Yet, as some classes contain less than 10 glaciers (resulting in a large s.e.) these were combined to form fewer, larger classes. Consequently, piedmont and expanded were combined, confluent and stagnant/wasted remained individual classes and the remainder of frontal types were included in the class of normal/miscellaneous frontal types. Non-significant estimates in this collapsed model are not the result of a statistical deficiency, but are related to the nature of the data. Thus, only piedmont/expanded and stagnant/wasted glaciers have a significantly higher likelihood to be of surge-type than other glaciers.

However, many glacier characteristics are dependent on glacier type (see Figure 4.1), and in order to distinguish glacier front type as a factor related to glacier surging a multivariate analysis is necessary. Furthermore, Clarke (1991) and Jiskoot *et al.* (1998) already demonstrated that some of the continuous glacier variables are log-linearly correlated (see Figure 4.2). For example, glacier length and width have a strong positive correlation, and glacier length and slope a strong negative correlation (Clarke, 1991; Jiskoot *et al.*, in review). Therefore, long glaciers tend to be large, and thus wide and have low slopes, and so multivariate analysis is necessary to disentangle these multiple correlations.

UNIVARIATE LOGIT MODELS					
Variable	***Subgroup***	***Estimate***	***Standard error***	***Deviance***	***Degrees of freedom***
Null model	intercept	-3.179	0.1228	579.49	1725
L	base	-4.249	0.1963	428.32	1724
	L	0.2143	0.0256		
	base	-6.795	0.4306	314.00	1724
	log-L	5.841	0.4990		
W	base	-4.119	0.1940	516.14	1724
	W	1.2866	0.1710		
	base	-2.343	0.1341	489.37	1724
	log-W	4.240	0.4538		
α	base	1.489	0.3583	383.13	1724
	α	-0.392	0.0375		
	base	4.819	0.6415	387.37	1724
	log-α	-7.577	0.6593		
max	base	-8.321	0.6800	504.67	1724
	max	0.0022	0.0003		
	base	-44.44	5.239	509.12	1724
	log- *max*	5.319	0.668		
min	base	-1.297	0.3585	554.04	1724
	min	-0.0014	0.0003		
	base	-3.466	1.569	560.31	1724
	log- *min*	-0.926	0.221		
$\tilde{F}$	base	-3.207	0.1262	578.56	1724
	$\tilde{F}$	0.02245	0.01949		
	base	-3.061	0.1235	561.81	1724
	log- $\tilde{F}$	0.4958	0.01151		
$\tilde{F}_{cat}$	base ($\tilde{F}$ <0.5)	-11.29	1.104	563.43	1723
	$0.5 \leq \tilde{F} \leq 2$	1.011	0.314		
	$\tilde{F}$ >2	1.344	0.3928		
Front	base	-4.237	0.252	506.56	1718
	piedmont	2.627	1.124		
	expanded	5.153	0.874		
	lobed	-3.328	10.890		
	calving	-3.328	26.670		
	confluent	1.292	1.056		
	stagnant/wasted	1.799	0.296		
	ice-cored-moraine	3.544	1.250		
Frontx	base	-4.183	0.239	515.61	1722
	piedmont+expanded	4.029	0.606		
	confluent	1.239	1.054		
	stagnant/wasted	1.746	0.286		

Table 4.2: *Significant univariate logit models for glacier surging with the reduction in model deviance for loss of degrees of freedom, parameter estimates and standard errors. L=glacier length, W=mean glacier width, α=surface slope, $\tilde{F}$ =Fowler's index, max=maximum altitude, min=minimum altitude, Front=type of glacier front, Frontx=reclassified glacier front with base class containing normal and miscellaneous, calving, lobed and ice-cored-moraine frontal types. (After: Atkinson et al., 1998).*

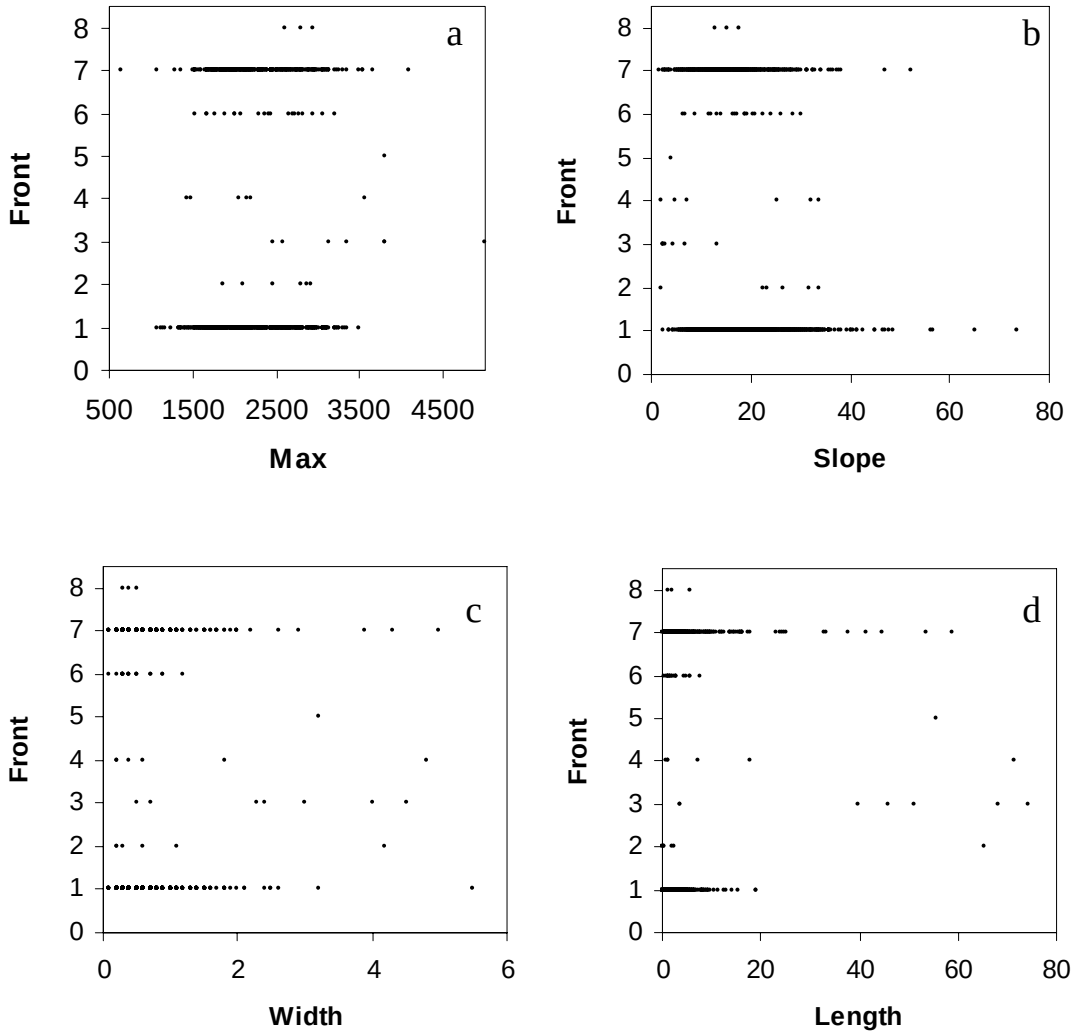

Figure 4.1: *Bivariate scatter plots of categorical vs continuous data of 1726 glaciers in the Yukon dataset.* ***a)*** *Maximum altitude (m asl) vs frontal type,* ***b)*** *Average slope (degrees) vs frontal type* ***c)*** *Average width (km) vs frontal type* ***d)*** *Length (km) vs frontal type. Frontal type is classified as: 1=normal/miscellaneous; 2=piedmont; 3=expanded; 4=lobed; 5=calving; 6=confluent; 7=stagnant/wasted and; 8= ice-cored-moraine. (After: Clarke, 1991).*

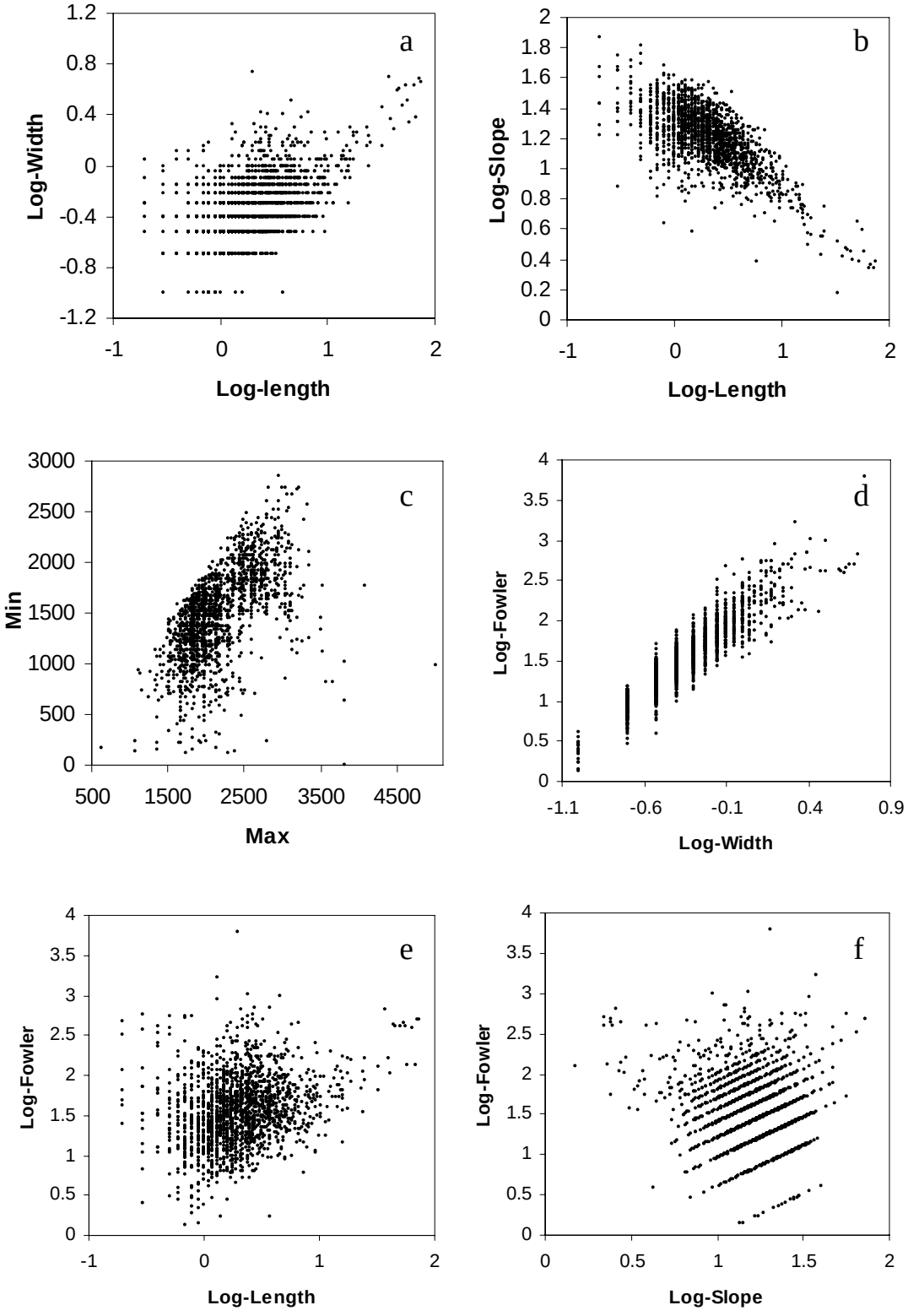

Figure 4.2: *Bivariate scatter plots of continuous data of 1726 glaciers in the Yukon dataset.* ***a)*** *Length vs width,* ***b)*** *Length vs slope* ***c)*** *Maximum altitude vs minimum altitude* ***d)*** *Width vs Fowler's index* ***e)*** *Length vs Fowler's index* ***f)****. Slope vs Fowler's index (After: Clarke, 1991).*

4.6.2 Multivariate logit models of Yukon glaciers

Because the model for log-transformed glacier length was the most significant univariate model all other variables were added to this model in a step-wise fashion to detect which variables led to a significant improvement. Each additional variable to the model was accompanied by a test of the interaction terms of the variables. All variables were tested, but only significant parameters are shown in Table 4.3.

MULTIVARIATE LOGIT MODELS						
Variable	***Subgroup***	***Estimate***	***Standard error***	***Probability***	***Deviance***	***Deg. of Freedom***
Null model	intercept	-3.179	0.1228	0.04	579.49	1725
L+W	base	-8.148	0.7302	**0.00**	306.84	1723
	log-L	7.027	0.7131	**1.00**		
	log-W	-2.338	0.8924	**0.09**		
L+ $\tilde{F}$	base	-7.128	0.4853	**0.00**	293.82	1723
	log-L	7.046	0.6284	**1.00**		
	log- $\tilde{F}$	-0.5718	0.1327	0.36		
L+[1] $\tilde{F}_{cat}$	base	-7.096	0.5103	**0.00**	300.50	1722
	log-L	6.593	0.5871	**1.00**		
	0.5 <= $\tilde{F}$ <=2	-0.1479	0.3674	0.46		
	$\tilde{F}$ >2	-2.342	0.7527	**0.09**		
L+[2] $\tilde{F}_{cat}$	base	-9.438	0.9895	**0.00**	300.50	1722
	log-L	6.593	0.5871	**1.00**		
	0.5 <= $\tilde{F}$ <=2	2.194	0.6785	**0.90**		
	$\tilde{F}$ <2	2.342	0.7527	**0.91**		
L+*max*	base	-9.487	0.9342	**0.00**	300.69	1723
	log-L	5.739	0.5271	**1.00**		
	max	0.00116	0.00032	**0.50**		
L+ *min*	base	-11.16	1.072	**0.00**	284.68	1723
	log-L	7.820	0.7195	**1.00**		
	min	0.00215	0.00042	**0.50**		
OPTIMAL MULTIVARIATE LOGIT MODEL						
L + $\tilde{F}$ + min	***base***	***-11.24***	***1.091***	***0.00***	***267.69***	***1722***
	log-L	***8.928***	***0.8285***	***1.00***		
	$\tilde{F}$	***-0.5623***	***0.1449***	***0.36***		
	min	***0.0020***	***0.0004***	***0.50***		

Table 4.3: *Significant multivariate logit models for glacier surging with the reduction in model deviance for loss of degrees of freedom, parameter estimates and standard errors. L=glacier length, W=mean glacier width,* $\tilde{F}$ *=Fowler's index,* [1] $\tilde{F}_{cat}$ *=categorical version of Fowler's index with 1st class* $\tilde{F}$ <O(1) and *3rd class* $\tilde{F}$ >O(1), [2] $\tilde{F}_{cat}$ *= categorical version of Fowler's index with 1st class* $\tilde{F}$ >O(1) and *3rd class* $\tilde{F}$ <O(1), *max=maximum altitude, min=minimum altitude (After: Atkinson et al., 1998).*

It is notable that when glacier width is fitted in the univariate model (Table 4.2) its estimate is positive, while in combination with length, the sign changes to negative (Table 4.3), indicating that long glaciers with relatively narrow width are more likely to surge. The parameter that causes the greatest reduction in model deviance in combination with log-length is the minimum altitude, indicating that long glaciers with their margins at slightly higher altitudes are likely to be of surge-type.

Adding Fowler's index to the length model also causes a large reduction in model deviance (21). In this model, the estimate for log-transformed length becomes more positive, whereas the estimate for Fowler's index is negative, but still significant as the standard error is less than half the value of the estimate. To test Fowler's hypothesis quantitatively $\tilde{F}$ was replaced by $\tilde{F}_{cat}$. According to this model, glaciers with a Fowler's index larger than the order of one are less likely to be surge-type (see ${}^{1}\tilde{F}_{cat}$) and glaciers with a Fowler's index smaller than the order of one are more likely to be of surge-type (see ${}^{2}\tilde{F}_{cat}$). However, the validity of Fowler's hypothesis is dependent on glacier length: for short glaciers the models agree with Fowler's hypothesis but for longer glaciers the statement that surge-type glaciers have $\tilde{F}$ values smaller than the order of one is rigid.

The optimal logit model, with a reduction in model deviance of 316.6 for a loss of 3 degrees of freedom, indicates that the strongest correlation between glacier surging and the set of glacier parameters tested consists of three parameters: glacier length, Fowler's index and minimum altitude (Table 4.3). The parameter estimates for length and minimum altitude are positive, while Fowler's index has a negative estimate. These model results suggest that a long, low altitude glacier with small values for Fowler's index are is most likely to be of surge-type. The hypothesis that surge-type glacier should have values smaller than the order of one for Fowler's index is valid for small glaciers, but for longer glaciers this hypothesis is too rigid.

4.6.3 Model performance

The model performance can be explored by examination of the residuals. Therefore, the model outputs (fitted values) were calculated for each individual glacier. For a perfect model the response variable would be one for every surge-type glacier and zero for every non-surge-type glacier. In reality the response variable is continuous, with range 0-1, and its value corresponds to the predicted probability that the glacier is of surge-type. For the optimal model of the Yukon glaciers the model was not actually expected to have very successful fits for individual glaciers as this model only includes three factors that might be related to glacier surging.

From the graphical relationship between the original data and the model output (Figure 4.3) it can be seen that the multivariate model generally results in a good match between the observed surge index and the modelled fitted values. Overall, the fraction of glaciers classified as surge-type increases with higher fitted values, although the number of surge-type glaciers in the intermediate bin ($0.4 < \hat{S} < 0.6$) is somewhat lower than expected. However, there are still 35 surge-type glacier with fitted values below 0.4 (thus predicted to be normal) and 5 normal glaciers with fitted values above 0.6 (thus predicted to be of surge-type). This overall picture suggests that the optimal model predicts better for normal glacier than for surge-type glaciers.

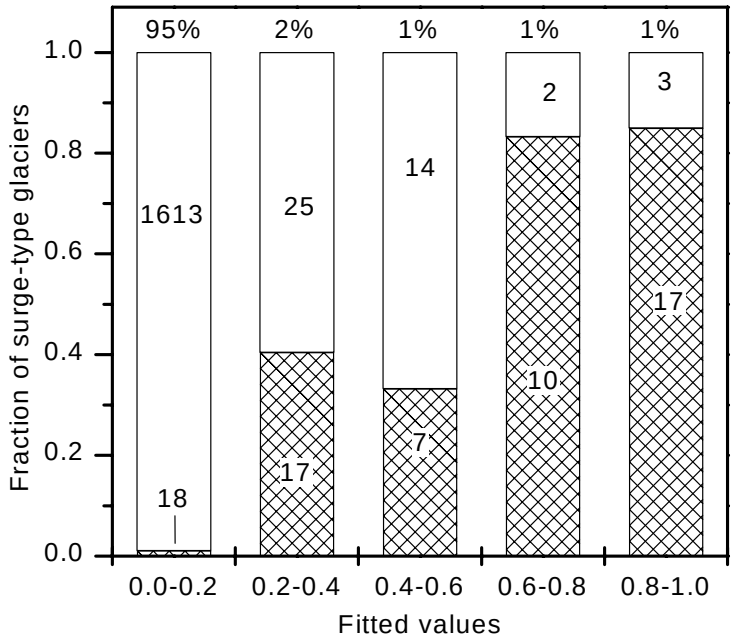

Figure 4.3*: Bar chart showing the fraction of observed surge-type (hatched) and non-surge-type (white) glaciers in each of five output classes. These output classes represent the predicted probabilities that the glacier is of surge-type from 0 (normal) to 1 (surge-type). The values above the bars give the percentage of total number of glaciers covered by each class. The values in the bars give the number of normal and surge-type glaciers in that category (After: Atkinson et al, 1998).*

To examine what might cause the poor fit of these surge-type glaciers a number of residual plots were created (Figures 4.4 and 4.5). Positive residuals represent surge-type glaciers (S=1) with fitted values lower than one and negative residuals represent normal glaciers (S=0) with fitted values larger than zero. The higher the residual the poorer the model fit for that glacier. From Figure 4.4 it can be seen that the model failed to fit well for smaller size surge-type glaciers: especially for glaciers smaller than 10 km. This reflects the weight of the positive estimate for the length variable in the multivariate model (Table 4.3).

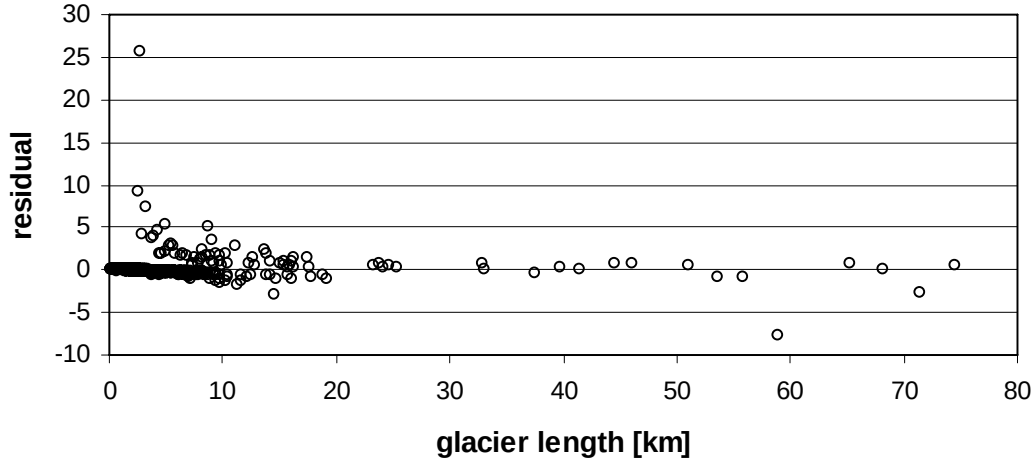

***Figure 4.4**: Residual plot of residual value vs glacier length.*

Plotting residuals against drainage basin number (Figure 4.5) can be used as an alternative to mapping the spatial distribution of residuals. Some drainage basins (e.g. 49 to 52: Northwest Yukon Territory) have a large number of glaciers with positive residuals, while others (e.g. 15: central Yukon Territory) accommodate glaciers with strongly negative residuals. By focussing on the glacial and environmental characteristics in these regions of 'outliers', it is possible to detect hitherto disregarded characteristics that distinguish surge-type glaciers from normal glaciers.

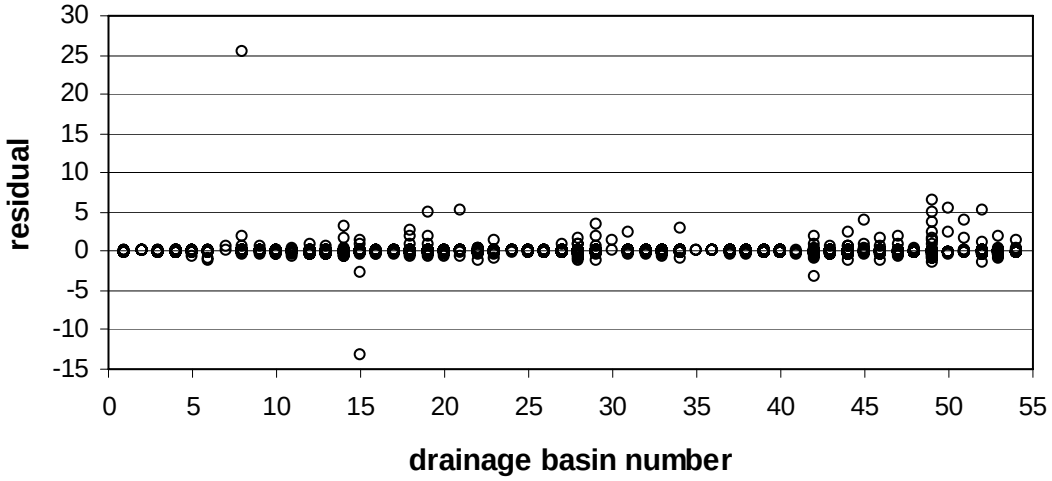

***Figure 4.5**: Residual plot of residual value vs drainage basin number.*

With the residual analysis it is also possible to focus on individual glaciers. For example, the glacier with the highest residual (+25) is clearly showing up in Figures 4.4 and 4.5. This glacier was classified as surge-type (S=1) but had a fitted value smaller than 0.01. On inspection this was a small tributary that had surged together with its main trunk in 1960. The main trunk had a fitted value of 0.7. It is possible that the tributary does not have its own surge regime but that its surge behaviour is associated to that of its trunk. Additionally, two glaciers (Kaskawulsh South and Maxwell Glacier) in drainage basin 15 were predicted to be of surge-type glacier with fitted

values above 0.85. Both glaciers have extensive wasted tongues. This feature was used to classify a number of surrounding glaciers as surge-type. It is possible that the two are of surge-type, but have not been identified as such from aerial photographs. If, however, the glaciers are not of surge-type then further inspection of these might hold clues to controls on surging.

4.7 Discussion of the logit models and comparison with other methods

Clarke (1991) used four geometric glacier parameters in his multiple regression analysis: glacier length, glacier width, glacier slope, and Fowler's index. Tests using traditional multiple regression statistics showed that the correlation between any variable and surging could be explained by the primary correlation between glacier length and surging, and that the remaining parameters had no additional explanatory power (Clarke, 1991). Using a logit model it was possible to show that Fowler's index has some influence on glacier surging, but the influence of this parameter varies with glacier length. Fowler's index is suggested to be smaller than the order of one for surge-type glaciers (Fowler, 1989: Section 2.5.8). The model findings agree with this prediction, as surging and Fowler's index are negatively correlated as shown by the negative sign of the parameter estimate in the multivariate model. Furthermore, surge-type glaciers in the Yukon Territory appear to have glacier margins at slightly higher altitudes than those of normal glaciers. Whereas the general trend of the model performance is positive (more surge-type glaciers than normal glaciers are predicted to be of surge-type by the model) the additional residual analysis indicated that a number of individual glaciers were not fitted well by the model. The reason of the poor fit of these glaciers might be disclosed by plotting the residuals against variables included in the model as well as variables that were not tested (see Figure 4.4 and 4.5). The spatial distribution of glaciers with high residuals might also give directions to further clues for glacier surging. As this case-study of Yukon glaciers is primarily used to demonstrate the use of logit models in glacier populations, the physical interpretation of model results will be left to Chapter 8 (Discussion)

There are concerns about how little the results from statistical modelling adds to the understanding of the workings in analysed systems (Kirkby, 1987). This is certainly true if variables were randomly tested. However, given the data analysis is based upon predetermined knowledge about physical relations between different elements in the glacier system, the technique of logit modelling can be utilised to test the validity of hypothesised instability criteria related to glacier surging (Chapter 2). Furthermore, the step-wise interactive facilities of the logit models enables the effects of physical parameters on the system to be tested. By using this approach, the results from the logit models can aid in our understanding of the process of glacier surging.

4.8 History and background of multi-model photogrammetry

The majority of glaciers are located in remote mountainous or polar areas and/or are surrounded by terrain that is difficult to penetrate. Surge-type glaciers offer additional difficulties as surges can disrupt a glacier surface to such an extent that the glacier becomes inaccessible. Given that most surges are only detected after the surge has started, it is often too late to install instrumentation in order to take field measurements. It is only possible to take valuable ground-based measurements on surge dynamics from glaciers that are expected to surge (e.g. Variegated Glacier) or where the surge has only a limited disruptive effect (e.g. Bakaninbreen, Svalbard and West Fork Glacier, Alaska) (Kamb *et al.*, 1985; Harrison *et al.*, 1994; Murray *et al.*, 1998). If the glacier proper is inaccessible, ice displacement measurements are sometimes taken using time-lapse cameras and terrestrial photogrammetry from para-glacial locations (Osipova *et al.*, 1990; Harrison *et al.*, 1994). In order to monitor changes in glaciers it is therefore often cheaper and easier to use aerial photography and remote-sensing techniques (e.g. Bauer, 1968; Post and LaChapelle, 1971; Wright Locke, 1981; Haeberli *et al.*, 1998). For glacier changes occurring on an annual or decade scale this offers an adequate solution. However, changes in surging glaciers are often too rapid to be picked up or tracked by conventional remote sensing techniques such as aerial photography, and only if special airborne surveys are carried out, often supported by terrestrial photogrammetry, the changes during surge can be registered (Osipova *et al.*, 1990; Knizhnikov *et al.*, 1997). Moreover, aerial photographs can suffer from other limitations such as a poor angle of view, shadows or clouds that obscure parts of a glacier, inconvenient scale and infrequent coverages. Satellites with high pass-over frequencies can improve the registration of surging glaciers, and satellite imagery has become an increasingly common tool for the identification and monitoring of glacier surges (e.g. Williams, 1983; Joughin *et al.*, 1996; Dowdeswell and Williams, 1997; Rolstad *et al.*, 1997; Engeset and Weydahl, 1998; Dowdeswell *et al.*, 1999). However, the scale of satellite images can be problematic for analysing small-scale features such as lakes and crevasse patterns and to adequately record vertical changes. Occasionally, airborne expeditions equipped with cameras are carried out during a surge to improve the detail and frequency of observations, but these only give a scattered coverage over the glacier providing a fragmented picture of the glacier in surge (e.g. Molnia, 1994).

A number of the above shortcomings can be overcome using the technique of multi-model photogrammetry (Pillmore *et al.*, 1981). This is a new computer-assisted technique that enables precise three-dimensional measurements from a series of overlapping small frame colour photographs or slides and conventional vertical aerial photographs (Dueholm, 1992). The technique was developed at the Institute of Surveying and Photogrammetry (ISP), Technical

University of Denmark and the U.S. Geological Survey in Denver (Pillmore *et al.*, 1981). For a full discussion about procedures relating to the setting up of new models into the multi-model and the mathematical background see Pillmore *et al.* (1981) and Dueholm (1992).

In order to survey and map the Tertiary basalt stratigraphy of the Blosseville Kyst region between Kangerdlugssuaq and Scoresby Sund (66ºN to 70ºN), the Danish Lithosphere Centre (DLC) carried out two airborne stereo-photography expeditions to the area during August 1994 and July 1995 (Pedersen *et al.*, 1995). Strips of overlapping photographs of geological sections of the mountain sides were taken from a Twin-Otter, providing stereographic coverage of long sections of terrain. These stereo photographs were subsequently set-up in the photogrammetric multi-model, where they are complementary to the 1981 vertical aerial photographs of the terrain (Larsen *et al.*, 1995; Pedersen *et al.*, 1997). Photographed geological sections were preferentially oriented perpendicular to the coast along the major glaciers (Larsen *et al.*, 1995). Besides the photographs containing a wealth of quantifiable information about the geological outcrops, they also reveal the lateral parts of glaciers along which the strips were collected. One of these glaciers, Sortebræ (68°45'N, 27°05'W), was observed to have very different surface characteristics from the surrounding glaciers (L.M. Larsen, pers. comm., 1996). On closer inspection of these images it was suggested that the glacier was actively surging (C.E. Bøggild, pers. comm., 1996). The glacier had already been identified as surge-type by A. Weidick from the 1981 aerial photographs (Weidick, 1988). By examining a selection of stereo photographs, the author discovered that it was possible to deduce quantifiable information on the glacier surge from analysing these photographs using the multi-model photogrammetric method.

4.9 Purpose of photogrammetric measurements

One of the basic applications of ‘glaciological’ photogrammetry is the construction of contour maps of glaciers. Over time the change in contours reflects the change in volume or redistribution of ice volume of a glacier. Because of the scale of glaciers, measurements of volume change are more accurately made from aerial photographs covering the entire glacier than from scattered ground-based point measurements (e.g. Hagen, 1987; 1988). It has been argued that a measurement of the change in mass is a much better indication of the glacier’s ‘state of health’ than the advance or retreat of its terminus (Paterson, 1994). This viewpoint can also be applied to the ‘state of health’ of surge-type glaciers as the redistribution of mass during a surge, like the switch in flow velocity, reflects the transition from one state of imbalance to another (Clarke, 1987a). Additionally, photogrammetry deals with structure. Structures in dynamic systems, such as glaciers, represent the distribution of stresses within the glacier, and reflects the kinematics taking place in the glacier system (Vaughan, 1993). The study of these

structural changes over time can provide information on the dynamics during glacier surges (e.g. Sharp *et al.*, 1988; Osipova and Tsvetkov, 1991; Lawson, 1997; Rolstad *et al.*, 1998: see also Section 1.4.2).

The purpose of the photogrammetric measurements on the surge of Sortebræ presented in Chapter 5 of this thesis is:

- To quantify the vertical and horizontal movements that have taken place during the surge.
- To quantify the redistribution and changes in ice volume that resulted from the surge.
- To quantify the surplus calving volume and estimate calving fluxes associated with the surge.
- To identify and examine changes in surface features associated with the surge.
- To study the distribution of crevasse patterns and derive surge kinematics.
- To identify changes in the glacier hypsometry resulting from the surge.

4.10 Theoretical aspects of multi-modelling photogrammetry

The multi-model method uses an analytical stereoplotter to measure and map compilations of stereographic photographs. An analytical stereoplotter can be envisaged as a computer-controlled stereoscopic instrument, in which the underlying stereoscopic network is mathematically steered by the computer system (Dueholm, 1992). After a stereoscopic network is set up for a specific geographical region (using control points taken from topographic maps, vertical photographs for which aerotriangulated control points are available, and preferably some ground control points (Dueholm, 1992), virtually all types of photographs from that region can be accommodated. The multi-model program then enables the simultaneous set-up of strips of small-frame stereo photographs as well as aerial photographs, jointly forming complimentary and overlapping sets of stereoscopic models (Dueholm, 1992). The operator of the stereographic plotter can then freely move around in the 'virtual' terrain and switch between aerial and small-frame models. As all coordinates in the terrain are set up in the computer system, it is possible to accurately measure points and lines. Additionally it is possible to plot terrain maps onto a range of common geologic projections (Dueholm, 1992). Furthermore, measured points, lines, contours, *etc.*, can be stored in the computer system and exported to different software packages (e.g. geological or statistical) from which further data analysis is possible (Humlum, 1992).

Stereo photographs are commonly assembled into strips of photographs and mounted onto stage plates (a frame-like construction that holds the photographs together) (Dueholm, 1992). Two stage plates are used to assemble pairs of stereo photographs: the left photograph and right

photograph in the photograph-pair are mounted on different stage plates. These two stage plates are then installed simultaneously into the Kern DSR15 photogrammetric plotter. Stage plates are structured such that two templates form stereo pairs of *n* photographs, visible in a continuous strip through eyepieces with stereoscopic optics. One of those strips thus consists of *(2n-1)* stereographic models. The 1994/95 stereo photographs of the Blosseville Kyst were mounted in strips of 20 photographs per template: two of these templates form 39 stereographic models. Each model is included in the Kern DSR15 system of multi-models and is mathematically transformed into the proper system of coordinates that ties all models together (Dueholm, 1992).

4.10.1 Measurement procedures

The multi-model photogrammetric model for the Blosseville Kyst region was set up for the Kern DSR15 analytical plotter at the Institute of Surveying and Photogrammetry (ISP) in Copenhagen. With the aid of A.K. Pedersen, the author took a number of measurements on Sortebræ's surge. For this purpose we used a combination of multi-models from 1981 vertical aerial photographs at scale 1:150000 and 1994/1995 airborne near-horizontal stereo small frame photographs at different scales. The majority of stereo photographs in the photogrammetric model were flown at a distance of about 500 m from the mountain sides and are at scale 1:10000. The remainder were taken from longer distances and are at smaller scales (e.g. 1:40000 from a distance of 1500 m) than the preceding ones (Pedersen, pers. comm., 1999). Besides, some objects on a photograph are in the background and are thus at a smaller scale than the overall scale of the photograph. The measurement procedure with the Kern DSR15 analytical plotter at ISP can be summarised as a three step procedure (Dueholm, 1992):

(1) Resetting of multi-blocks

After the stage plates with photographs have been installed in the Kern DSR15, four tickmarks used to set-up (orientated) the stage plates in the model have to be remeasured on each of the two templates in one model (Dueholm, 1992). This takes only a few minutes.

(2) Measuring

The operator measures points in the multi-model by means of guiding an illuminated floating mark over the images while viewing the images through eye-pieces with stereoscopic optics in the Kern DSR15. The analytical plotter monitors the x, y, and z coordinates of the floating mark and these coordinates are displayed on the computer screen and can be saved accordingly. From registration of these coordinates it is possible to compare subsequent coordinates and measure distances between them. The floating mark is adjustable in size and brightness and is thus visible on both dark (moraine/water) surfaces and light (ice) surfaces. Furthermore the Kern

DSR15 analytical plotter has zoom optics with 5 to 20 times enlargements, so that even the aerial photographs at scale 1:150000 can be viewed at a scale of 1:7500 (Dueholm, 1992)

The main features that could be measured for the purpose of glacier surging research were the vertical distances between strandlines of ice from the pre-surge glacier surface and the contemporary (1994/95) glacier surface. Comparing the z-coordinate of a point on the pre-surge ice surface to the z-coordinate of a point on the post-surge glacier surface (preferably lying in a vertical position directly under the first point) gives an elevation difference at that location. This distance is the down-draw resulting from mass removal during the surge. At other locations, elevation differences between the 1981 glacier surface (from the 1981 aerial photographs in the multi-model) and that of 1994/95 could be measured for the same x-y coordinates. When this height difference was positive, an uplift of the glacier surface had taken place, resulting from the additional ice volume storage in that part of the glacier. Furthermore, heights of the calving glacier front could be measured, as well as horizontal position of the glacier front and dimensions of surface features such as lakes and crevasses.

(3) Plotting and further analysis

Three-dimensional coordinates measured with the Kern DSR15 can be digitised into the computers' memory and later be imported into geological software such as GEOPROGRAM (Dueholm and Coe, 1989). Using this software the operator can use and manipulate three-dimensional data and calculate geological parameters (dip, strike, stratigraphic thickness of beds *etc.*). The program can subsequently be used to plot the selected optical features onto a range of plot projections (Dueholm, 1992). Due to the experimental nature of the use of multi-model photogrammetry in glaciology these plotting facilities were not used for the research presented in this thesis. There are however a range of possibilities for the use of the plotting facilities in glacier research. The elevation of the glacier surface along the glacier margins could be traced, as well as the strandline elevation of the pre-surge glacier surface. Given these surfaces are visible in an almost continuous line, a very accurate estimate of volume displacement can be made. Moreover, DEMs of the glacier surface could be constructed from digitising contours from the aerial photographs (see for example Hagen, 1987) or from digitising contours that connect points with similar elevations along the margins. Subsequently, profiles, contour maps and 3D images can be plotted or saved in a digital format. These digitised data can subsequently be imported in standard spreadsheets (e.g. Excel) and several parameters, such as mean altitudes and surface areas, can be calculated (Humlum, 1992).

4.10.2 Accuracy

The measurement accuracy using the Kern DSR15 photogrammetric plotter depends on (1) the photograph scale, (2) the quality of control points (triangulation), (3) the scale-limited error of the floating point and (4) on the precision of the person taking the measurements.

1) The absolute accuracy of measurements taken with the Kern DSR15 is better than 20 microns on the photograph scale (Dueholm, 1992). Thus, for the 1981 vertical aerial photographs used in this study (scale 1:150000) it is 3 m, and for the majority of the 1994/95 stereo photographs (scale 1:10000) it is 20 cm.
2) The control points error introduced in the multi-model programme depends on the aerotriangulation error, the error in the transfer of control points and on the accuracy and vicinity of groundcontrol points. The 1:150000 triangulation introduces an absolute standard error of 5 m in plane and 3 m in height (Pedersen and Dueholm, 1992). Because only height differences were considering and as this is a systematic error that is constant for all measurements and independent of the photograph scale in the multi-model, this error need not be included in the measurement error. The additional error from transferring the triangulation points from one scale photographs to another is within 20 microns of the photograph scale. Hence, for photographs at scale 1:150000 it is 3 m in plane and 2 m in height (Dueholm, 1992; Pedersen and Dueholm, 1992). Any additional field measurements (e.g. plane position, measured distances, compass directions, altimetric elevations) reduce these errors (Dueholm, 1992). Although the absolute control-points error can be large (up to 8 m in horizontal and 5 m in vertical), the ground control points are weighted during bundle block adjustment. Thus, the relative accuracy between the models remains equal to the photogrammetric accuracy as outlined above (Dueholm, 1992).
3) The scale-limited absolute error is dependent on the smallest distance that can be measured with the photogrammetric plotter. As the coordinates are measured up to three decimal places on the metric scale the accuracy is half the smallest distance on that scale, thus 0.5 mm (Squires, 1976). However, the absolute error of measuring with a floating point precision of 0.5 mm is dependent on the photograph scale and the magnification in photogrammetric plotter. The DSR15 has a magnification possibility of up to 20 times enlargement but magnifications of 10 times were commonly used in the measurements.
4) Finally, given that locating of the measurements is dependent on the skills and experience of the operator of the floating point, human error may also influence measurement precision. This measurement precision is primarily dependent on the photograph scale. Using a magnification of up to 10 times enlargement and a random error with a possibility of being 0.3 mm off-target, the human error is generally within 0.3 m for the 1:10000 stereo

photographs, within 1.2 m for the 1:40000 photographs and within 4.5 m for the vertical aerial photographs.

For combining these errors the scale-limited errors (1 and 3) were multiplied by 2/3 to approximate random errors and all four error terms were incorporated in following equation for cumulative errors (Squires, 1976):

$$\varepsilon_T^{\,2} = \left(\varepsilon_1^{\,2} + \varepsilon_2^{\,2} + \varepsilon_3^{\,2} + \varepsilon_4^{\,2}\right) + \varepsilon_1\left(\varepsilon_2 + \varepsilon_3 + \varepsilon_4\right) + \varepsilon_2\left(\varepsilon_1 + \varepsilon_3 + \varepsilon_4\right) + \varepsilon_3\left(\varepsilon_1 + \varepsilon_2 + \varepsilon_4\right) + \varepsilon_4\left(\varepsilon_1 + \varepsilon_2 + \varepsilon_3\right), \quad (4.6)$$

where ε_T is the total absolute error and ε_1, ε_2, ε_3, and ε_4 are the errors 1 to 4 above. The second term in this equation is the error in the interaction terms. Since the errors ε_1, to ε_4 are independent the average value of the interaction terms is zero (Squires, 1976). Therefore, the error calculation used only the first term in this equation. The errors for three different photograph scales in the multi-model and a magnification of 10 times are summarised in Table 4.4.

ABSOLUTE VERTICAL ERRORS [M] FOR 10 TIMES MAGNIFICATION			
Photograph scale	1:150000	1:40000	1:10000
Absolute instrument error*	2.00	0.53	0.13
Triangulation error (scale-dependent)	2.00	0.53	0.13
Floating point error of 0.5 mm*	5.00	1.33	0.33
Human error of 0.3 mm	4.50	1.20	0.30
Total absolute error [m] without interaction terms	**7.30**	**1.95**	**0.49**

Table 4.4: *Errors determining the accuracy of vertical measurements with the DSR15 photogrammetric plotter. Errors marked with * are scale-limited errors and have been multiplied by 2/3 to approximate random errors in order to calculate the cumulative error.*

I used the absolute vertical measurement errors corresponding to the three photograph scales to define three categories of errors: (1) ***0.49 metres*** for objects on photographs at distances between 500 and 1000 metres (approximate scale 1:10000 to 1:30000), (2) ***1.95 metres*** for objects at distances from 1000 to 3000 metres (approximate scale 1:30000 to 1:100000) and (3) ***7.30 metres*** for objects at a distance further than 3000 m (approximate scale 1:100000 to 1:150000) (see bold numbers in Table 4.4). These errors are a worst-case scenario and actual errors are likely to fall well within these error limits.

As distances between measurement points (down-draw or uplift of the glacier surface) are considered in this research, the error in distance ($\varepsilon_{\Delta H}$) was calculated by combining the errors of the measured points. For a vertical distance ΔH that is calculated from two measured points (H_1 and H_2) the absolute cumulative error ($\varepsilon_{\Delta H}$) is:

$$\varepsilon_{\Delta H} = \sqrt{\varepsilon_{H_1}^2 + \varepsilon_{H_2}^2}\,, \tag{4.7}$$

where ε_{H_1} is the absolute error in the first measurement point and ε_{H_2} the absolute error in the second measurement point (Squires, 1976). It is possible that the two points were measured on two different photograph scales, thus that the two errors are not equal (see Table 4.3).

4.10.3 Corrections

A number of measurements were corrected by remeasuring nearby points with known elevations. The magnitude of surface elevation correction is the difference between the measured elevation and the 'true' elevation of a point with known elevation. Six surface elevations in the vicinity of the frontal ice cliff were corrected by setting a nearby sea level measurement to 0 m asl and subsequently correct the measurement of the height of the ice cliff by adding the correction factor for sea level. These corrections improve the accuracy of the measurements at the glacier margin. No corrections were made for tidal movements as no tidal data was available. All sea-level measurements taken with a magnification factor of 10 or larger lay within the absolute error of 7.5 m (Table 4.4) from the 'true' sea level of 0 m asl. This indicates that the calculated accuracy categories agree with the measured errors. Theoretically, measurements taken further up-glacier can also be corrected from points with known elevations (e.g. mountain peaks), but there was no opportunity to do this.

4.11 Concluding remarks

The multivariate statistical method of logistic regresssion presented in this chapter undoubtedly has the potential to enhance our perception of the complex relationships between different elements in the glacier system and how these might relate to glacier surging. So far, the case study on Yukon glaciers (Section 4.6 and subsections) clearly demonstrated the strength of multivariate logit modelling as compared to other glacier population analysis techniques. The fact that continuous and categorical glacier and environmental data can be analysed simultaneously will be beneficial to the intended testing of hypothesis on glacier surging. An additional useful quality of logit models is that the model results can be verified on individual

glaciers, which can offer additional information on possible controls on glacier surging. However care should be taken to correctly interpret the model results, particularly in terms of the feasibility of physical processes.

The main benefit of the photogrammetric multi-model presented in this Sections 4.8 to 4.10 is that it provides the ability to accurately measure and analyse visual glacier attributes from a remote source. This can possibly enhance the quantitative aspect of analysing the dynamics of glacier surging from remote sources.

CHAPTER 5:
Svalbard Data Presentation and Univariate Logit Modelling Results

The multitude was surging hither and thither

1 Samuel 14

5.1 Introduction

This chapter consists of four parts following this introduction. Section 5.2 and subsections describe Svalbard and its glaciology and lists the data and data sources that were used in the analysis of surge-type glaciers in Svalbard. In Section 5.3 and subsections all individual variables are presented with the purpose of discovering general patterns in the data that possible distinguish surge-type glaciers from normal glaciers in Svalbard. Section 5.4 and subsections give the results of the univariate logit modelling, where each variable is fitted individually. This univariate analysis gives a first crude impression of which glacial and environmental characteristics could control surging in Svalbard. Statistically significant variables in these univariate models can then be incorporated into the multivariate models in Chapter 6 in order to disentangle which variables are primary and which variables are secondary characteristics of surge-type glaciers. Section 5.5 and subsections contain a discussion of the qualitative and quantitative results from Sections 5.3 and 5.4. Here initial ideas are presented about controls on surging on the basis of the general patterns that distinguish surge-type from normal glaciers and from the univariate logit analysis results. From these results, the combinations of variables that have yet to be disentangled can be identified. Parts of Sections 5.3 to 5.5 have been published in Jiskoot *et al.* (1998) and Jiskoot *et al.* (in review).

5.2 The Svalbard archipelago

The High Arctic archipelago of Svalbard (latitude 76-81ºN, longitude 9-33ºE) consists of six major islands (Spitsbergen, Nordaustlandet, Edgeøya, Barentsøya, Prins Karls Forland and Kvitøya) and a number of smaller island groups (Figure 5.1). The islands are bounded by the north Atlantic Ocean to the west, the Arctic Ocean to the North and the Barents Sea to the east. Svalbard's total land area is approximately 63000 km^2 of which about 60% is glaciated (Hagen and Liestøl, 1990). Although the islands Hopen and Bjørnøya are officially part of the Svalbard archipelago, they are not included in this study's maps and descriptions, because they are not glaciated and thus are not of interest in this research on the controls on glacier surging in the archipelago.

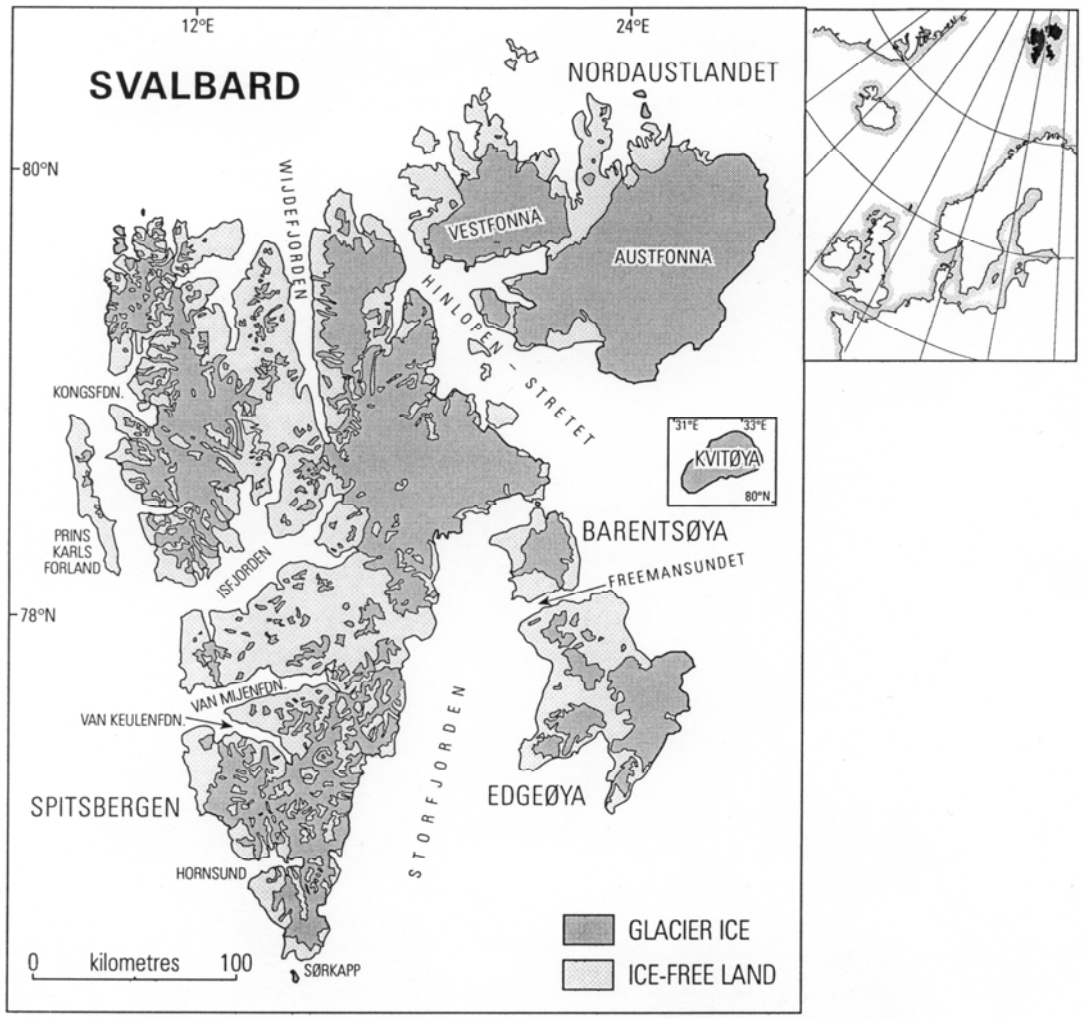

Figure 5.1: *The Svalbard Archipelago.*

5.2.1 Geology of Svalbard

The islands of Svalbard are the emerged parts of the Svalbard plateau, which is an extension of the Baltic continental shelf. The region has been greatly affected by crustal movement, which resulted in sinking and upthrusting of crustal blocks along north-south trending fault-lines (Hjelle, 1993). Identified seismically active regions include Heer Land, Prins Karls Forland and Oscar II Land, the western parts of Nordaustlandet, the inland of the Hornsund area, but the magnitude of earthquakes hardly ever exceeds 2 on the Richter scale (Górski, 1997). The largest island, Spitsbergen, has a generally alpine topography, intersected by broad valleys and fjords, often following structural weaknesses (e.g. Wijdefjorden, Figure 5.1). Svalbard's highest peak, Newtontoppen (1717 m asl), is located in the north-east of Spitsbergen. The other islands, which consist of generally weaker and less strongly folded geologies, are less peaked and topographically lower than Spitsbergen. Svalbard’s geology spans an almost complete stratigraphic succession from the Precambrian to the Cenozoic (see Figure 5.2).

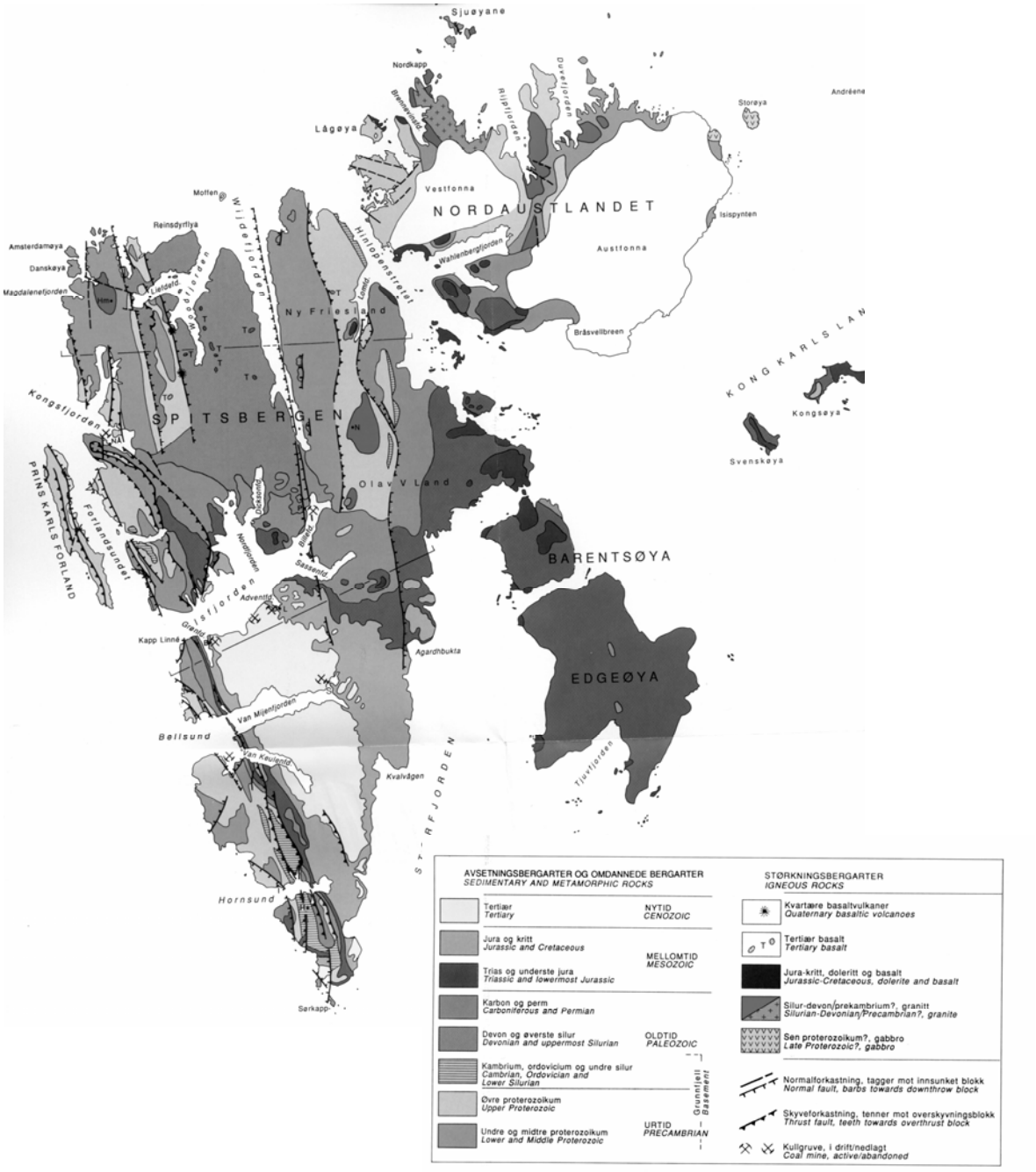

Figure 5.2: *Geology of Svalbard (From: Hjelle, 1993).*

The geological sequence can subdivided into three major divisions (Hjelle, 1993):

1) *The basement* (formerly Hecla Hoek series) consists of igneous and metamorphic rocks and tillites. These rocks were formed during Precambrian to Silurian times and have been metamorphosised and strongly folded in subsequent times. The basement is part of the Caledonian fold stretching from Scotland and Norway to East Greenland. Caledonian folds mostly trend north-south in Svalbard, which can also be inferred from the spatial pattern of basement outcrops: occurring along the west coast and in the north-east of Spitsbergen, in northern Nordaustlandet and on Kvitøya (Figure 5.2).

2) *Unaltered sedimentary rocks*, including sandstones, siltstones, limestones, shales, coal, and conglomerates, were formed during major periods of erosion in the Devonian period and Carboniferous to Tertiary times. The rocks form a trough-shaped structure radiating from central Spitsbergen, with the youngest rocks in the centre and older rocks along the edges (Hjelle, 1993: see also Figure 5.2). Apart from slight folding and local episodes of erosion, these rocks have mostly remained undisturbed and contain many well-preserved fossils. Eastern parts of Spitsbergen and most of the eastern islands have been subject to Jurassic-Cretaceous igneous instrusive activity, while Tertiary basalts emerge in north-west Spitsbergen.
3) *Unconsolidated deposits* are of Quaternary age and include glacial, glacio-fluvial, marine, talus and rock-floor deposits. These are predominantly found close to the erosional agents, ice and water, in the lower lying valleys and along the coastal zones. Quaternary deposits are particularly abundant on Edgeøya and Barentsøya. Well developed strandflats can be found in western and north-western Spitsbergen (Hjelle, 1993). Freeze-thaw action is a major cause of bedrock erosion, resulting in large talus slopes and blockfields. The soil cover of Svalbard is very thin and dominated by blockfloors and locally shaley or schistose mineral soils on the higher grounds and sands and clays in the valleys and coastal plains. Organic soils are almost completely absent (Hjelle, 1993). Due to a lack of vegetation cover, erosional surface processes are very effective and heavily braided rivers show a dominance of bedload transport (Repp, 1988).

5.2.2 Climate of Svalbard

Climatologically Svalbard is classified as arctic-maritime, with an average annual temperature of -6°C on the western coast and slightly colder inland (Hagen and Liestøl, 1990). These temperatures are on average 20°C warmer than those in continental regions at the same latitudes (e.g. North Greenland, Arctic Canada and northern Siberia) (Jania and Hagen, 1996). The precipitation on the west coast of Spitsbergen is about 400 mm a^{-1}, slightly higher along the coasts of the eastern islands, and only 200 mm a^{-1} in the northern inland areas of Spitsbergen (Liestøl, 1993: see also Figure 5.3). Due to orographic effects the precipitation is higher on glaciers, but seldom exceeds 2-4 m of snow per balance year (Hagen *et al.*, 1993). The greatest precipitation results from cyclones travelling eastwards, and give the eastern and higher parts of the archipelago the greater amount of precipitation (Baranovski, 1977). Both the temperature and precipitation gradients show a trend from the south-west to the north-east. These gradients are controlled by the local topography and the movement of air masses. The cyclonic Atlantic weather system, brings in mild air from lower latitudes to Svalbard from the south-west, whereas the anti-cyclonic Arctic/Siberian weather system brings in cold dry air from the north-

east (Hamilton, 1992). Svalbard is 'wedged' between these contrasting weather systems, which frequently shift to the north and south. This results in Svalbard's weather and temperature being highly variable; during winter and spring temperature variations of 20°C may occur within days, and heavy snow fall occurs occasionally in summer. (Hagen and Liestøl, 1990). The increase in proportion of melt layers in ice cores over the last 70-130 years suggest an overall warming trend in the High Arctic, which is confirmed for Svalbard by an overall increase in mean annual temperature since the beginning of this century (Dowdeswell, 1996).

Figure 5.3: *Precipitation in Svalbard in mm a^{-1} (From: Hagen et al., 1993).*

Sea-ice conditions are controlled by temperature, oceanic currents and storm activity. For Svalbard this means that cold polar waters transport pack-ice south along its northern coastlines, while the warmer Atlantic waters are transported to the western side of Spitsbergen with the northward flowing West Spitsbergen Current (Wadhams, 1981). Pack-ice encloses the entire archipelago between November and April, with minimum densities along the west-coast of Spitsbergen, but the ice often remains present throughout the year around the north-eastern parts of the archipelago. Pack ice and fast ice can stay on until late May/early June in the major fjords and close to the coastline (Dowdeswell, 1989).

5.2.3 Permafrost, springs, and periglacial processes in Svalbard

Ice-free areas of Svalbard are inferred to have continuous permafrost conditions (90-100% area cover) with estimated permafrost thicknesses between 100 and 500 m in the interior (Liestøl, 1977). The active layer has a maximal thickness of 1-1.5 m (Liestøl, 1977). Ground-ice content is mainly dependent on the type of terrain (alpine or lowland), and for Svalbard it is inferred that up to 20 % of the soil volume consists of ground-ice (Brown *et al.*, 1997). However, permafrost is absent beneath fjords, large lakes and the larger glaciers. As most glaciers have a subpolar thermal regime, the pressure melting of water beneath the warm parts of these glaciers will produce a downward groundwater flow, which Liestøl (1977) assumes to continue under the permafrost layer and towards the coast. This process sometimes results in the subsequent warming of the groundwater by geothermal heat and the formation of warm springs. Major springs found in the south Spitsbergen limestone karst regions produce water with temperatures of the order of 5-15°C which do not freeze in winter (Hjelle, 1993). Proper thermal springs with constant water temperatures of the order of 20-30°C occur in the Bockfjorden area, NW Spitsbergen (Liestøl, 1977). These springs are the remains of the once active Quaternary volcanoes in this region. Other springs mainly occur in the northern part of Edgeøya and on Spitsbergen in the western coastal and central drainage basins, around Woodfjorden, and Sørkapp Land (see Figure 5.1 for location names). Solifluction, frost-heave and frost-shattering are the most common periglacial processes in Svalbard. About 80 pingos, some up to 40 m in height, have been observed in Svalbard and patterned ground is widespread in the lower regions (Liestøl, 1977; Hjelle, 1993). Frost-shattered resistant rocks form talus slopes, while softer shales form mineral soils. The larger talus slopes sometimes develop into small rock glaciers (Hagen *et al.*, 1993).

5.2.4 Past glaciation in Svalbard

There is not much evidence preserved of Pre-Weichselian glaciation in Svalbard. Precambrian tillites have been found in north-eastern Spitsbergen, western Nordaustlandet and along the western coast of Spitsbergen. These tillites are the remains of a glacial period that occurred about 600 million years BP (Troitsky, 1981). As the tillite beds are the youngest Proterozoic strata, directly underlying the Cambrian, they form an important key horizon for dating the under- and overlying deposits (Hjelle, 1993). Not until the Quaternary, was the region glaciated again. At the beginning of the Quaternary, the area was at an elevation a few hundred metres above the present level, and the Barents Sea area was a continuous landmass connected to northern Scandinavia and north-western Russia. During the Elsterian and Saalian the glaciers were by some considered not larger than today's, but others suggest from geological evidence

that the most extensive glaciation occurred during the Saalian (Troitsky, 1981; Landvik *et al.*, 1988). From the sparse locations where the pre-Weichselian glacial deposits have been preserved from subsequent glacial erosion it is inferred that three major advances must have taken place prior to the last Ice Age (Hjelle, 1993).

De Geer (1900) was the first who inferred that an ice sheet might have existed on Svalbard during the last Ice Age (Weichselian). Evidence from glacial striae and erratics suggested that the centre of glaciation lay in the north-eastern part of Svalbard. Subsequent theories on the glacial history of Svalbard and the Barents Sea have not been uniform in the interpretation of ice extent, particularly of that during the last glacial maximum (18,000 BP). Major topics for debate include whether or not the Barents Sea was glaciated, and whether or nor extensive ice domes were present. Boulton (1979) argued, on the basis of a lack of geological evidence, that the ice only extended to the coasts of the islands, but it is now generally agreed that the northern and central Barents Sea region was covered with a Late Weichselian ice sheet (Ingólfsson *et al.*, 1995). Ice sheet models and glacial isostacy models agree with the geological evidence for the centre of the Weichselian ice sheet, south and east of Kong Karls Land, but the exact duration, extent and thickness still remain topics for debate (Lambeck, 1995; Siegert and Dowdeswell, 1995; Ingólfsson *et al.*, 1995).

Studies by Landvik *et al.* (1995) and Lambeck (1995) suggest that up to 15,000 BP an extensive ice sheet covered the Barents Sea, but that rapid deglaciation of large marine-based parts must have occurred before a period of rapid uplift between 10,000 and 9,000 BP. This explanation was based on relative sea-level curves from Edgeøya and Bjørnøya coasts combined with mathematical models of isostatic rebound. Salvigsen *et al.* (1995) looked at evidence for directions of ice movement and postulated that three distinct phases of Late Weichselian glaciation took place in the Svalbard and Barents Sea region. During the maximum phase the ice extended from a centre south-east of Kong Karls Land to southern Spitsbergen. Then a phase of Barents Sea deglaciation occurred in which ice caps centres were located on Nordaustlandet and Kong Karls Land. In the last phase only local ice caps remained on the major islands of the archipelago. The above evidence suggests that the period of extensive ice cover was shorter on Svalbard than in Scandinavia.

During the Holocene, Svalbard glaciers are inferred to have fluctuated with periods where the size and extent of glaciation was smaller than today (Landvik *et al.*, 1995). Glaciers were close to their late Holocene maximum at the end of the 19th century/beginning of the 20th century, an advance that resulted from the Little Ice Age cooling that occurred approximately between 1650-1850 (Hagen *et al.*, 1991). Expeditions at the end of the 19th century often reported very

advanced and active glacier margins, although some of these may have been due to surge advances (e.g. Conway, 1898). Evidence for glacio-isostatic rebound is perfectly preserved on the archipelago in the form of well-exposed raised beaches from which relative sea level curves can be reconstructed (e.g. Troitsky, 1981; Lambeck, 1995). The highest dated beaches are found at Gipsvika, Sassenfjorden, where the 75 m level is dated to 9,500 BP (Hjelle, 1993). According to the position relative to the centre of the former ice sheet(s), there are large spatial variations in the amount of uplift. The largest uplift of up to 85 m occur in the eastern parts of the archipelago and the smallest uplift of approximately 10 m in the south-west and north-west of Spitsbergen (Troitsky, 1981). It is suggested that the formation of flights of raised beaches is due to the Holocene transgression following the deglaciation of the Weichselian ice sheets, and that subsequent isostatic rebound has lifted the beaches above present sea level (Troitsky, 1981). The evidence in the raised beaches give only one suggestion of a eustatic sea level rise, occurring about 11,000 BP, which is preserved in the 60 m beaches, whereas the emergence of the beaches is thought to have been interrupted once by a mid-Holocene transgression (Landvik *et al.*, 1988).

5.2.5 Present-day glaciation in Svalbard

With a total glaciated area of 36598 km^2, Svalbard's present degree of glaciation is 60% (Hagen *et al.*, 1993). However, the glacial coverage varies between the drainage basins from 6% on Kong Karls Land to 99% on Kvitøya (see Figure 5.5). Hagen *et al.* (1993) counted the number of glaciers in the early 1980s and recorded a total of 2229 glaciers of various types, of which 1029 were larger than 1 km^2.

The main source of information on Svalbard glaciers is the *Glacier Atlas of Svalbard and Jan Mayen* (Hagen *et al.*, 1993). This atlas lists 1029 Svalbard glaciers larger than 1 km^2, classified according to the glacier-numbering system of the World Glacier Monitoring Service guidelines (IAHS(ICSI)/UNEP/UNESCO, 1989). Throughout this thesis glaciers are referred to by glacier name (if available), followed by a reference number in brackets. Glacier reference numbers consist of 5 digits: the first digit is for the region (1 = Spitsbergen, 2 = Nordaustlandet, 3 = Barentsøya and Edgeøya,4 = Kong Karls Land and 5 = Kvitøya), the second for the major drainage basin in that region, the third is for the secondary drainage basins and the fourth and fifth digits give the glacier number (Hagen *et al.*, 1993). For example: 'Kongsvegen (155 10)' means: the tenth glacier counted clockwise in drainage basin 155, which is the drainage basin draining into Kongsfjorden, NW Spitsbergen. Figure 5.4 shows the complete numbering of all drainage basins, hence of the first three digits of any glacier reference number. Maps with individual numbering of glaciers can be found in Hagen *et al.* (1993).

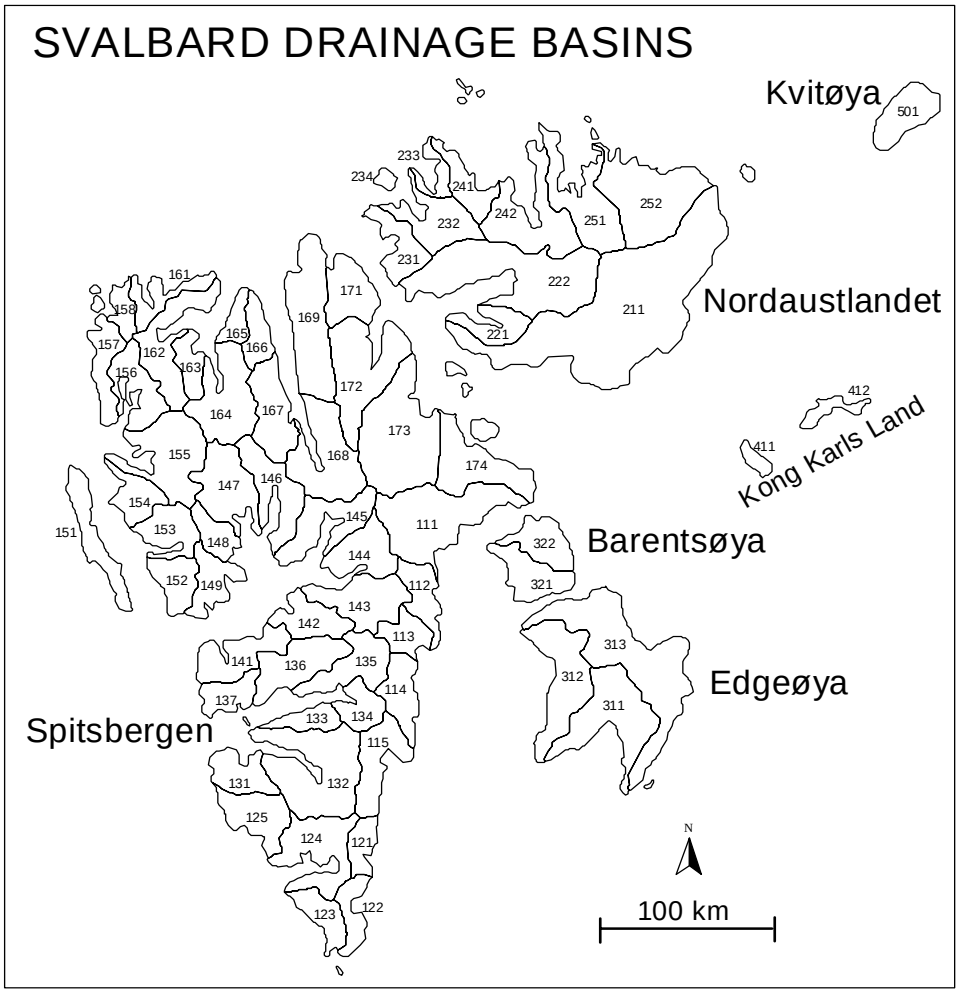

Figure 5.4: *Drainage basin numbering in Svalbard (After: Hagen et al., 1993).*

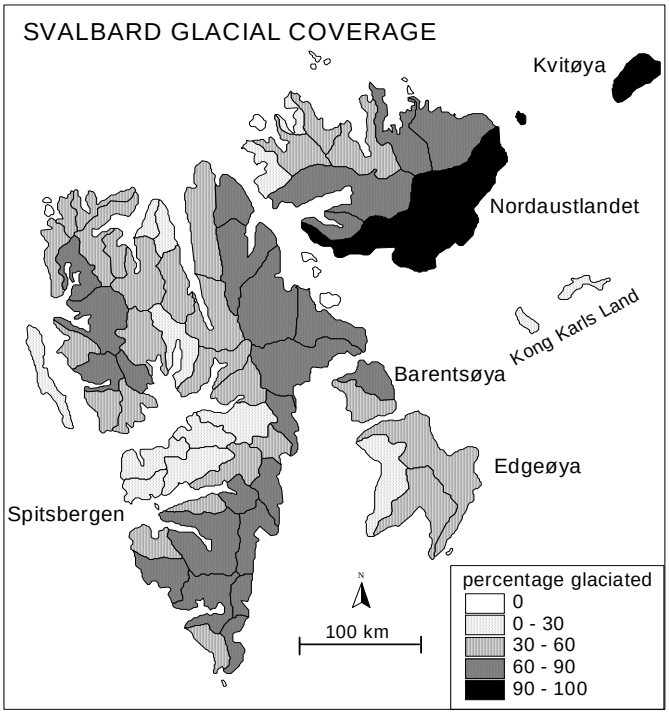

Figure 5.5: *Glaciation in percentages in Svalbard (Data from Hagen et al., 1993).*

The southern and western regions of Spitsbergen are dominated by valley glaciers, with a few larger outlet and tidewater glaciers draining from the plateaux. Tidewater glaciers dominate the east coast of Spitsbergen, and local ice caps can be found in the higher elevated flatter northern parts of Spitsbergen as well as on Nordaustlandet and the eastern islands. In total almost 20% of Svalbard's coastline is composed of ice cliffs and major calving episodes have been reported, often associated with glacier surge (Dowdeswell, 1989). Since the 1930s an overall retreat of glaciers has been observed (Hagen *et al.*, 1993). This retreat has been intermitted with brief advances of surge-type glaciers. Presently, the majority of Svalbard glaciers are thought to be subpolar (Hagen *et al.*, 1993). A large number of glaciers are characterised by warm 'wet' ice underlying cold 'dry' ice in the inner zones, while in the outer zones the ice is often cold throughout the profile (Schytt, 1969; Kotlyakov and Macheret, 1987; Ødegard *et al.*, 1997). This polythermal regime restricts the free runoff through subglacial streams and instead, the water drains as groundwater and emerges proglacially where it often refreezes as icings, shaping specific structure in the forefield (Baranovski, 1977). The occurrence of icings is thus indicative for a polythermal regime. However, Liestøl (1969) argues that if small, cold glaciers surge then the surge-generated meltwater could produce icings as well. Thus, icings could also be indicative for glacier surging. Furthermore, thermal regime of Svalbard glaciers is inferred to play a role in the anomalously high sediment content of Svalbard glaciers, even though glacier dynamics, especially surging, is probably the main control on the process of subglacial debris incorporation (Clapperton, 1975; Porter *et al.*, 1997). Other common features of Svalbard glaciers include well-developed supraglacial drainage systems and frequently occurring but short-lived supraglacial lakes. Surface meltwater apparently cannot easily penetrate the cold ice and due to the lack of crevasses and moulins it runs-off supraglacially (Hodgkins, 1997). Some of the supraglacial lakes in Svalbard could be related to surging: the undulating surface associated with surge-type glaciers causes water to pond until a supraglacial or englacial water drainage is established (Liestøl *et al.*, 1980).

Because direct measurements of thermal regime are only available for very few Svalbard glaciers, radio-echo sounding (RES) data have been used to indirectly determine the thermal regime of many glaciers (Macheret and Zhuravlev, 1982; Dowdeswell *et al.*, 1984a; Bamber, 1987; Kotlyakov and Macheret, 1987; Macheret, 1990). There have been two major RES campaigns in Svalbard; by Russian scientists between 1974 and 1979 and 1984 (Macheret and Zhuravlev, 1982; Macheret, 1990) and by an Anglo-Norwegian collaboration of SPRI and the Norsk Polarinstitutt in 1980 and 1983 (Dowdeswell *et al.*, 1984a). These RES datasets regularly reveal single continuous internal reflection horizons (IRHs) at a depth between 70-190 m below the glacier surface (Macheret and Zhuravlev, 1982; Dowdeswell *et al.*, 1984a; Bamber, 1987). IRHs are thought to be caused by differences in the dielectric constant and/or in loss tangent of

ice with different densities, structure, impurity content and water content from other ice layers (Macheret and Zhuravlev, 1982). Borehole investigations on Svalbard glaciers suggest that specific continuous IRHs in this region are caused by the internal pressure melting point isotherm (Ødegard *et al.*, 1997). The position of these continuous IRHs could thus reflect the difference in water content between an upper non-temperate zone and lower temperate zone (Bamber, 1987; Kotlyakov and Macheret, 1987), and are thus an indication for a polythermal regime. For about 200 glaciers and ice masses the results of RES measurements are published and glaciers with IRHs exclusively occur on Spitsbergen (Macheret, 1981; Macheret and Zhuravlev, 1982; Dowdeswell et al., 1984a; Kotlyakov and Macheret, 1987; Bamber, 1987, 1988 and 1989; Macheret, 1990). The reason for the geographical distribution of glaciers with IRHs is unclear. Some suggest it to be related to the distribution of surge-type glaciers (Hamilton and Dowdeswell, 1996), others to climate factors (Bamber, 1987), and yet others to glacier thickness, which decreases towards the north and west of Spitsbergen (Macheret, 1981).

RES data has further been used to reconstruct bed profiles and subglacial relief and thus hold information on glacier depth and volume. Macheret and Zhuravlev (1982) suggested that the ice thickness in western Spitsbergen decreases from south to north and westward in northern areas. However, Dowdeswell *et al.* (1984) question the accuracy of these measurements as for the same glacier, Penckbreen (132 05), the Russians suggested a maximum thickness of 140 m (Macheret, 1981; Macheret and Zhuravlev, 1982) whereas the SPRI/NPI measurements suggests a thickness of up to 240 m. This inaccuracy is thought to result from a lack of penetration due to the higher frequency of the Russian system (440 and 620 MHz systems as opposed to 60 MHz for the SPRI system), which can be problematic for glaciers with relatively high temperatures and glaciers which have large surface and internal inhomogeneities (Dowdeswell *et al.*, 1984b).

Svalbard glaciers are predominantly nourished through snowfall, but as in other subpolar regions the formation of superimposed ice also contributes to the net balance (Hagen *et al.*, 1993; Dowdeswell and Nuttall, 1996; Woodward *et al.*, 1997). Like thermal regime measurements, mass balance measurements of Svalbard glaciers are scarce. The Norsk Polarinstitutt started bi-annual systematic mass balance studies in 1950 on Finsterwalderbreen (132 02) and these continued until 1968 (Hagen and Liestøl, 1990). Austre Brøggerbreen (155 04) and Midre Lóvenbreen (155 06) followed in 1966 and 1967 and these measurements are continued until today. After White glacier in the Canadian High Arctic, these constitute the longest running mass balance records in the High Arctic (Liestøl, 1984; Lefauconnier and Hagen, 1990; Hagen *et al.*, 1991). The yearly balance series of these glaciers show an average negative but stable net balance of -0.25 m water equivalent per year. Only two years of positive net balance (1987 and 1991) occurred on Austre Brøggerbreen and three years (1987, 1991 and

1996) on Midre Lóvenbreen (Hagen *et al.*, 1991; Hagen *et al.*, 1993; IAHS(ICSI)/UNEP/UNESCO, 1999). For Austre Brøggerbreen this means a loss of approximately 35 m of ice over 80 years (Lefauconnier and Hagen, 1990). From extrapolation of climate data (precipitation and temperatures) it is inferred that the net balance for small glaciers in the Kongsfjorden area has been negative since 1918 (Lefauconnier and Hagen, 1990). Steady-state would only be attained if either winter precipitation increased by about 50% or if the average summer temperature was lowered by approximately 1°C (Hagen and Liestøl, 1990). In contract, the Austfonna ice cap, Nordaustlandet, is inferred to be in balance (Dowdeswell and Drewry, 1989). Other Svalbard glaciers with mass balance records include Vöringbreen (141 05) since 1966, two glaciers in central-west and one in east Spitsbergen between 1973 and 1976, Hansbreen (124 20) since 1988 and Kongsvegen since 1987 (Kotlyakov, 1985; Hagen *et al.*, 1993; Jania and Hagen 1996; Melvold and Hagen, 1998). The overall observation is that although small glaciers experience negative net balances, the larger glaciers, with higher accumulation areas, are closer to steady-state (Hagen *et al.*, 1993). There are no indications for increasingly negative net balances in Svalbard, which corresponds with findings for the entire Arctic region (Dowdeswell *et al.*, 1998).

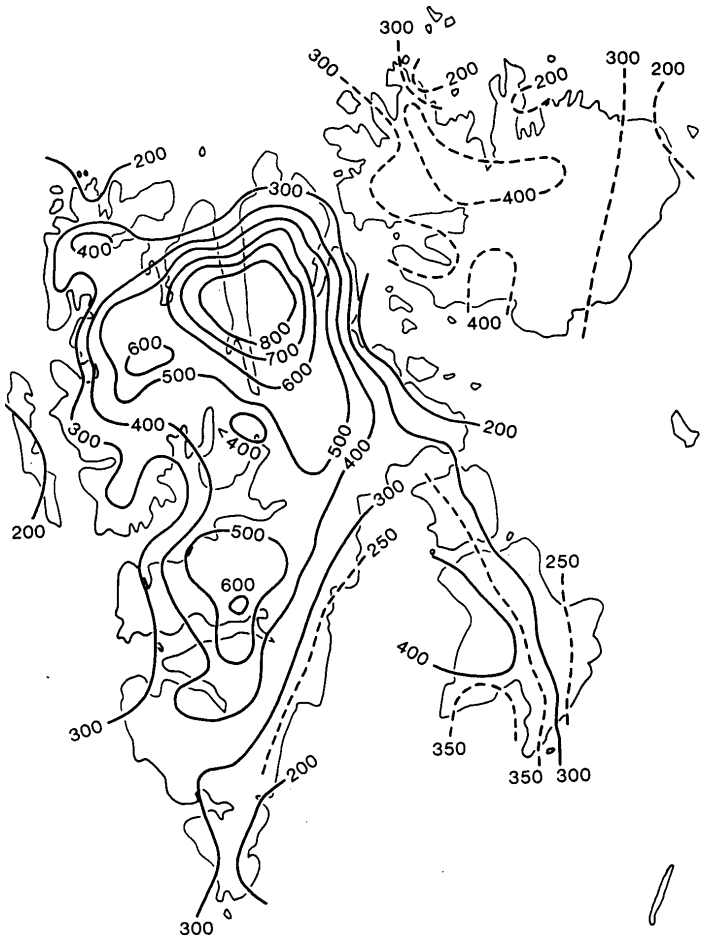

Figure 5.6: *Distribution of the equilibrium line altitude over Svalbard after Liestøl and Roland (From: Lefauconnier and Hagen, 1990).*

The distribution of equilibrium line altitude (*ela*) corresponding to zero net balance conditions is given in Figure 5.6. The distribution of the *ela* over the archipelago is believed to be fairly accurate, but the actual *ela* is probably at a higher elevation (+100 m) as the glaciers experience a negative net balance in most years (Hagen *et al.*, 1993). Svalbard glaciers are believed to have a net balance of zero or higher when the median elevation is at least 50 to 100 m higher than the actual *ela* (Lefauconnier and Hagen, 1990). The asymmetric snowline distribution, clearly visible on Edgeøya, Barentsøya, and Nordaustlandet, probably reflects a higher amount of precipitation on the eastern side of these islands (Dowdeswell and Bamber, 1995).

5.2.6 Surge-type glaciers and glacier surging in Svalbard

From the distribution of surge-type glaciers world-wide it becomes clear that Svalbard has a higher than average concentration of surge-type glaciers (see Table 1.1). As surging is a 'common' phenomenon in Svalbard and occurs in a variety of glacier types it makes it an excellent region to study glacier surges (e.g. Liestøl, 1969; Schytt, 1969; Hagen, 1987; Jania, 1988; Dowdeswell *et al.*, 1991; Lefauconnier and Hagen, 1990; Hamilton, 1992; Dowdeswell and Nuttall, 1996; Porter, 1997; Rolstad *et al.*, 1997; Murray *et al.*, 1998; Murray *et al.*, in review).

The earliest information about extreme glacier advances in Svalbard, by some interpreted as surges, are known from expeditions in the mid 1800s (Liestøl. 1984). The first proper observation of glacier surge in Spitsbergen was from De Geer (1910), reporting that Sefströmbreen (147 16) had advanced 6 km between 1882 and 1886, and retreated more than 2 km between 1886 and 1908. De Geer suggested that this behaviour was no exception for Svalbard glaciers. First estimates of numbers of surge-type glaciers indicated that their concentration on Svalbard was higher than average found for cluster regions of surge-type glaciers (Liestøl, 1969; Schytt, 1969). Svalbard surges can cause exceptional frontal advances: the largest ever recorded surge advance is ascribed to the 1937-38 surge of Bråsvellbreen (211 10), advancing approximately 21 km over a 15 km wide front and covering 600 km^2 of previously unglaciated area. Hagen (1988) studied surge behaviour of different surge-type glaciers and suggested that there are two contrasting types of surge behaviour in Svalbard. The larger outlet and tidewater glaciers surge with relatively low velocities and over a long period, while the smaller valley glaciers have a shorter surge phase and rapid block-like movement. Whereas glaciers terminating in the sea have high, intensively crevassed calving fronts, land-based surges result in markedly convex glacier fronts.

In Svalbard, a number of individual surge-type glaciers, either in surge or in quiescence, have been well studied. Studies on the 1978-1985 surge of Usherbreen (112 04) revealed that an ice volume of 0.82 km^3 was transported downglacier, which is about 20% of the total ice volume. The surge advance was only 1.5 km over a 3 km wide front, but ice velocities were as high as 1 m/d (Hagen, 1987). A series of concentric moraines formed during the surge advance. Similar morainic ridges had previously been observed on Iceland (Sharp, 1985) and multiple terminal moraine complexes were subsequently used as a diagnostic feature of glacier surging by Croot (1988). According to Hagen (1987), the conditions necessary for the formation of these types of moraines include proglacial permafrost, the presence of old moraine ridges and a sudden (surge) advance. In contrast, slower climatologically controlled advances would build a large single moraine crest. The high surge velocities and availability of deformable sediments led to the conclusion that part of the movement during the surge might have been contributed to bed deformation (Hamilton, 1992). Bodleybreen (222 06), Aldousbreen (222 08), Fraserbreen (222 09) and Idunbreen (222 10), all outlet glaciers from Vestfonna, Nordaustlandet, probably have surge behaviour superimposed on already fast flow conditions and the same is true for certain drainage basins of Austfonna (Dowdeswell and Collin, 1990; Dowdeswell *et al.*, 1999). Furthermore, for Bodleybreen, bed deformation is inferred to play a major role in the support of fast flow as the glacier has overridden unlithified marine sediments and large turbid water plumes appear from the terminus.

The initiation of an EC funded project on glacier surging has contributed greatly to the understanding of glaciers surging and surge behaviour in Svalbard (Dowdeswell and Nuttall, 1996). The results proved so valuable that a number of participants have continued and expanded the research (e.g. Murray *et al.*, in review). Research was mainly focussed on two glaciers: Finsterwalderbreen, in quiescence, and Bakaninbreen, in surge. Major conclusions from this research were that Finsterwalderbreen is building up towards a new surge (the glacier surged last around 1900), and that the actual velocity is approximately 60% lower than the balance velocity (Nuttall *et al.*, 1997). Bakaninbreen started surging in 1984/85 and was in the late surge phase in 1994. The surge phase estimated to have lasted for 5 to 15 years, but it is difficult to distinguish between the full surge conditions and the slowdown phase (Murray *et al.*, 1998). Although a 60 m steep surge bulge propagated rapidly downglacier, the surge terminated before the bulge reached the terminus and subsequently the surge did not result in an advance of the terminus. An estimated volume of 0.67 km^3 was transported from the upper to the lower basin during the surge. Remarkable characteristics of Bakaninbreen's surge include the low surge velocities, 1.1 km a^{-1} maximum, and an indistinct termination, contrasting to the termination within days of some Alaskan glaciers (Kamb *et al.*1985; Harrison *et al.*, 1994; Fleisher *et al.*, 1995). Studies on the tectonic evolution of a number of Svalbard surge-type

glaciers revealed that the rate of terminus advance in surging tidewater glaciers is dependent on position of the compressive surge front relative to the low effective pressure zone close to the margin. Two types of surging can be identified: a relatively steady *push* prior to the surge front arriving at the low pressure zone, and a more rapid *rush* afterwards (Sharp *et al.*, 1988; Hodgkins and Dowdeswell, 1994: see also Section 1.3.3). Further, the structural evolution of a number of surge-type glaciers suggests that particular processes for the incorporation of subglacial sediment are associated with surges (Sharp *et al.*, 1988; Hambrey and Huddart, 1995; Hambrey *et al.*, 1996).

As for other areas, it is unclear in Svalbard what the trigger(s) and cause(s) of surge instabilities are, and thus what controls surging. An extensive discussion of the possible surge mechanisms and controls on surging is given in Chapter 2 of this thesis. From the analysis of characteristics of surge-type glaciers and surge behaviour in Svalbard, a number of possible surge controls have emerged, of which some are specific to the region. From the intensive geophysical studies on Bakaninbreen the role of bed deformation and thermal regime in glacier surging has been elucidated (Porter, 1997; Murray *et al.*, 1998; Murray et al., in review) From satellite image analysis it was postulated that the profiles of Nordaustlandet drainage basins are intrinsically unstable: the profiles are shallower and have higher surface roughness than calculated balance profiles (Dowdeswell, 1986; Dowdeswell and McIntyre, 1987). Further, Drewry and Liestøl (1985) give a possible mechanism for the surge of Bråsvellbreen, due to a marked fall in bedrock (from 200 m asl to 100-500 m bsl) at the margin of the icecap. The icecap extends beyond this fall, and sliding or even surging becomes possible over easily deformable water-saturated sediments. This extended icefront becomes unstable because the net accumulation inland is too small to maintain the mass flow to the lower parts. As a result the margin becomes starved and sliding stops. Advance will therefore alternate with retreat to a more stable position close to the topographic step. It has also been suggested that changing mass balance controls surging and surge frequency in Svalbard. The end of the Little Ice Age (LIA) was marked by a sudden increase in mean annual temperature of up to 5°C (Dowdeswell *et al.*, 1995). It is assumed that most Svalbard glaciers had a cold thermal regime during the LIA. The subsequent climate warming penetrated into the ice as a warm wave, causing increased deformation and lowering of fiction at the bed, which could have increased the overall movement of the glacier (Baranovski, 1977). Further, after the LIA, the glaciers had to adjust their profiles to a new mass budget because of the changing climate. This combination of changing rheology and changing mass budget might have triggered a number of surges at the end of the LIA (Lefauconnier and Hagen, 1990). However, as most glaciers were at their maximum extent at the end of the LIA, it can be difficult to discriminate surge advances from maximum extent in response of climate deterioration (Hagen and Liestøl, 1990).

A number of studies have been focussed on the duration of the surge phase and the quiescent phase of Svalbard surge-type glaciers in contrast to other regions. Statistical analysis on a small number of glaciers with recorded durations of surge and quiescent phases suggests that Svalbard surge-type glaciers have longer and more 'sluggish' surges and considerably longer quiescent phases than surge-type glaciers in other regions (Dowdeswell *et al.*, 1991; Dowdeswell *et al.*, 1995). In Svalbard, the return period for surges is assumed to exceed 50 years, with upper limits of 500 years for the larger Nordaustlandet surge-type drainage basins. In Alaska, the Yukon Territory, the Pamir, and West Greenland glaciers have been observed to surge every 20-40 years (Dolgoushin and Osipova, 1975; Weidick, 1988; Kamb *et al.*, 1985; Blake, 1992; Muller and Fleisher, 1998). This difference in return period of surges is ascribed to the slower rate at which mass builds up in Svalbard as compared to the other regions. Further, it has been suggested that the surge related down-draw in the upper part of the glacier is larger in Svalbard than elsewhere (Dowdeswell *et al.*, 1991). However, a lack of accurate data on down-draw rates makes this hypothesis difficult to justify. Furthermore, Dowdeswell *et al.* (1995) observed a steady decline in the surge frequency between 1936 and 1990: the numbers of glaciers in surge on aerial photographs from 1936/38, 1969/70/71 and 1990 decreased from 18 to 10 to 5. This trend was associated with a change in mass balance over the same period, and the resulting negative net balances (Dowdeswell *et al.*, 1995). However, since 1990 at least five more glaciers have been observed to surge: Monacobreen (162 11), Fridtjovbreen (137 08), Unnamed (164 26): Mühlbacherbreen (124 117) and Mittag-Lefflerbreen (pers. comm. G. Hamilton to T. Murray, 1995; pers. comm. J.O. Hagen, 1998), creating some reservations about the validity of the inferences of Dowdeswell *et al.* (1995). Stronger evidence exists on the surge duration of Svalbard glaciers. Bakaninbreen's surge duration is estimated between 10-15 years (Murray *et al.*, 1998), Bodleybreen is thought to have surged for 7 years, Usherbreen for 8, but Osbornebreen for only 2-3 years (Rolstad *et al.*, 1997). Further, a number of smaller glaciers had surge durations ranging from 4-10 years. Surge duration in other regions is 3 years maximum (e.g. Dolgoushin and Osipova, 1978; Kamb *et al.*, 1985; Weidick, 1988). As during surge the internal processes dominate the glacier dynamics, whereas during quiescence the climatic conditions prevail (Robin and Weertman, 1973), the reason for a longer surge duration for Svalbard glaciers has to originate in the surge mechanism. The principal theories developed to explain surges in Svalbard emphasise the role of deformable substrate and thermal regime in controlling subglacial drainage and associated water pressure (Hamilton, 1992; Porter, 1997; Murray *et al.*, 1998; Murray *et al.*, in review). However, as the surge behaviour of Svalbard glaciers is so unlike that in other regions, the surge mechanism(s) in Svalbard could be different from the surge mechanism(s) in other areas and subsequently the controls on surging in Svalbard may not hold for other regions.

5.3 Data base compilation of Svalbard glaciers

As explained in Section 5.2.5, an inventory of 1029 Svalbard glaciers is published in Hagen *et et al.*, 1993. A complete dataset covering geometry, orientation, elevation, glacier-type, frontal characteristics and activity were available for only 504 of these 1029 glaciers. These tended to be the larger glaciers covering circa 93% of the total glaciated area of Svalbard (Jiskoot *et al.*, 1998). The retained 504 glaciers form the core of the Svalbard database and additional variables were collected for this dataset. A full list of variables collected for the Svalbard database is presented in Table 5.1. While the primary data was directly available from Hagen *et al.* (1993), additional variables were assigned by the author using other sources. Secondary data (average slope, elevation span, Fowler's index, AAR and hypsometry) were directly calculated from the primary data (see Section 5.4 and subsections). Geological data was collected using geology maps, publications and aerial photographs from the Norsk Polarinstitutt. The geological classification specific to the glaciers was developed by the author (see Section 5.4.12). Datasets on internal reflection horizons (IRHs) and thermal properties were compiled from publications only.

CONTINUOUS VARIABLES	CATEGORICAL VARIABLES	
Latitude[1]	Orientation of accumulation area[1]	(8*)
Longitude[1]	Orientation of ablation area[1]	(8*)
Glacier length[1]	Glacier type[1]	(6*)
Glacier area[1]	Glacier form[1]	(10*)
Glacier volume[1]	Type of glacier front[1]	(6)
Maximum altitude[1]	Petrological category[3]	(3)
Median altitude[1]	Geological age[3]	(8*)
Minimum altitude[1]	Lithology type[3]	(25*)
Equilibrium line altitude[1]	Lithological boundary type[3]	(9*)
Average surface slope[2]	Lithological boundary number[3]	(4)
Mean glacier width[2]	Lithological boundary direction[3]	(4)
Elevation span[2]	Internal reflection horizon[3]	(3)
Fowler's index[2]	Fowler's index[2]	(3)
Hypsometry[2]	Hypsometry[2]	(3)
AAR[2]	AAR[2]	(3)

Table 5.1: *List of variables used in the analysis of surge-type glaciers in Svalbard. The numbers in brackets indicate the number of classes in the categorical data. The asterisked numbers indicate that for modelling purpose the data of this categorical variable were reclassified into fewer, larger classes.* [1]*'Primary' data from Hagen et al. (1993),* [2]*Secondary data calculated by the author from the primary data,* [3]*Data collected from maps and publications by the author. Fowler's index, hypsometry and AAR have both been assigned as continuous and categorical variables (see Section 5.4.8 and 5.4.11).*

Aerial photograph interpretation of primary evidence of surging as well as the most of the geological data collection was performed during visits of the author to the Norsk Polarinstitutt archives in the period 1996-1998. The majority of Svalbard glaciers are covered over a period of about 60 years by at least 3 stereo-sets of aerial photographs from the coverage years 1936, 1938, 1948, 1956, 1961, 1966, 1969, 1970, 1971, 1977, 1990, and 1995. TM Landsat images for the entire archipelago were only available for 1980, while partial coverages were available at the Norsk Polarinstitutt for other years (pers. comm. Jostein Amlien, 1998).

5.3.1 Timing, accuracy and reliability of glacier data

In general, the timing and accuracy of data measurements can affect this data analysis. As most of the glacier data was collected during the compilation of the glacier inventory (1980-81; Hagen *et al.*, 1993), the data used in our analysis corresponds to glaciers in different stages in their surge cycle. For some glaciers this might have been at a time just after a surge. For these glaciers, the overall slope and geometry might be unfavourable for a surge in the near future or a surge within a few decades. Provided that the mass balance conditions remain positive, these glaciers might be building up to a new surge. As explained in Section 5.2.5, an overall trend of glacier retreat has been observed in Svalbard since the 1930s. Because the most recent information on length, area and volume of the glaciers was collected from 1980 Satellite images, these data are thought to be an overestimation of the glacier extent at the present time (Hagen *et al.*, 1993). However, as it is assumed that surge-type glacier form a separate class, and as the majority of glacier data were collected in the same period, comparison between glaciers is possible. The only data that is collected over a timespan longer than 10 years are geological data and RES data, but it is assumed that major changes in these variables only take place over a period longer than decades.

Data accuracy for the primary data is given in Hagen *et al.* (1993). Accuracy for equilibrium line altitude and median elevation are on average within 25-100 metres, while area is generally within 10-15% (Hagen *et al.*, 1993). The author of this thesis is aware that errors and inaccuracies in these first order variables propagate while calculating second order variables. Data accuracy for the geological variables is explained under Section 5.4.12.

5.3.2 Classification of surge-type glaciers in Svalbard

The definition ‘surge-type’ means that either one or multiple surges have been recorded in a glacier, or that the morphological characteristics of a glacier show strong enough evidence to infer that a surge has occurred in the past and might occur again (Meier and Post, 1969; see

Section 1.3). Publications listing surge-type glaciers are not always transparent in the type of primary evidence used for the classification of surge-type glaciers. Therefore, additional examination of glaciers proved necessary for the surge classification of Svalbard glaciers. This examination involved the collection of direct and indirect surge evidence from aerial photographs, satellite images and maps (see Section 1.4).

The initial surge classification was based on publications on glacier surging (e.g. Croot, 1988; Hagen, 1988; Hagen *et al.*, 1993; Lefauconnier and Hagen, 1990; Liestøl, 1993). In some cases this documentation on glacier surges was ambiguous (e.g. Liestøl, 1990), while other glaciers were listed as surge-type on the basis of disputable morphological evidence for surging. Croot (1988), for instance, classified a number of glaciers as surge-type on the basis of terminal moraine complexes. The maximum extent of some of these glaciers is probably not due to a surge advance, but rather reflects the maximum extent during the Little Ice Age, which occurred about 1900 in Svalbard (Lefauconnier and Hagen, 1990; Jiskoot *et al.*, 1998). The author therefore initially classified the 504 Svalbard glaciers according to a three digit surge index (see Section 3.2.2 for surge indices), with S = 0 for glaciers without surge evidence, S = 1 for glaciers with possible morphological surge evidence and S = 2 for definite evidence of surge behaviour (*i.e.* a recorded surge or diagnostic morphological surge evidence: see Section 1.4.4). All glaciers with a surge index S = 1 and all glaciers without a recorded surge but classified as S = 2, were double-checked by the author, as well as a number of random other glaciers. In total 129 glaciers were inspected: these glaciers are indicated as checked in a column of the Svalbard database (Appendix V). For these glaciers the surge evidence was verified by means of aerial photograph interpretation of (primary) morphological evidence of surging as well as on additional evidence from maps and publications (see Section 1.4). The result of this examination was the discovery that a number of glaciers were probably mis-classified as surge-type in earlier reports (e.g. Croot, 1988). Eventually the glaciers were classified according to a two digit (dichotomous) system, with S = 0 for normal glaciers with no evidence or unambiguous evidence for surging, and S = 1 for surge-type glaciers with convincing morphological evidence or recorded surges. Thus, some of the initial S = 1 glaciers were ultimately assigned to S = 0 category, while other, for which strong enough evidence for surging was found, were assigned to the new S = 1 category.

Of the 504 glaciers used in this analysis, 132 (26%) were classified as surge-type and 372 as normal (74%). This is the majority of the total of 136 (13%) glaciers larger than 1 km^2 (1029) that were classified as surge-type. Although the vast majority of excluded glaciers from the database are smaller than 4 km^2 and of 'normal' type, the limited information available for these glaciers may make the estimate of 13% surge-type glaciers in the archipelago unreliable (Jiskoot

et al., 1998). It is certainly very small as compared to estimates of 36-90% made by others (Lefauconnier and Hagen, 1990; Hamilton and Dowdeswell, 1995). The glaciated area covered by surge-type glaciers was also calculated; the percentage was expected to be higher, because surge-type glaciers are generally larger than normal glaciers (Clarke *et al.*, 1986; Hamilton, 1992). Of the total glaciated area (36598 km^2) (Hagen *et al.*, 1993), 47% is occupied by surge-type glaciers, whereas for the sample of 504 glaciers (34195 km^2), 48% of the area is so occupied. However, there are large variations in the percentage of surge-type glaciers between the different drainage basins (Figure 5.7).

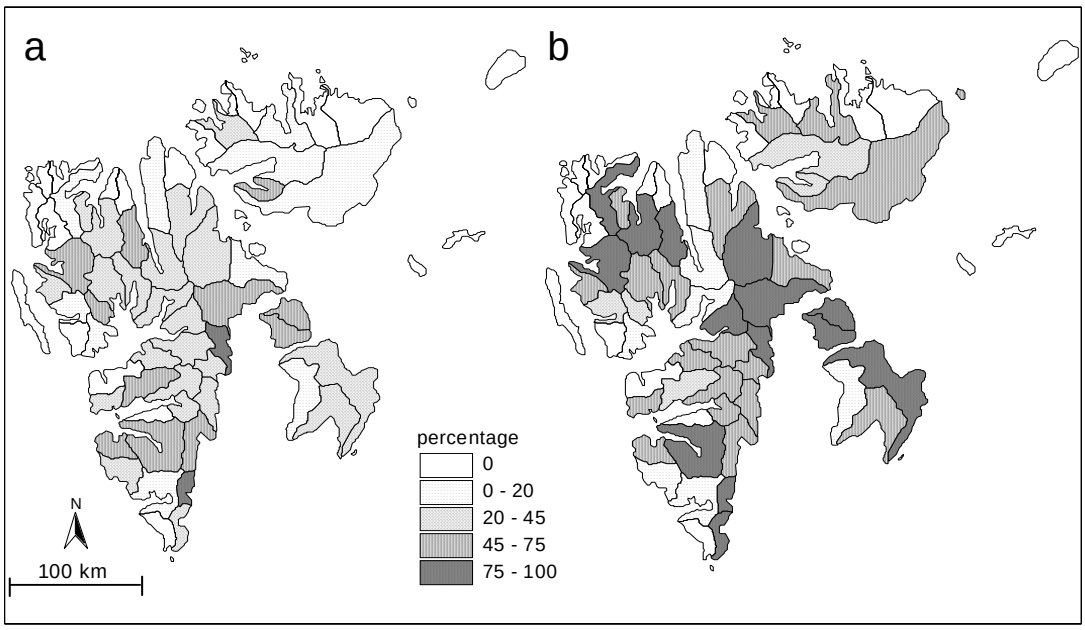

Figure 5.7. *Spatial variation of surge-type glaciers between Svalbard drainage basins. (a) percentage of surge-type glaciers, (b) percentage of glaciated area covered by surge-type glaciers (After: Jiskoot et al., 1998).*

The calculated percentages of surge-type glaciers compare poorly with the frequently quoted estimation that 90% of the glaciers in Svalbard are surge-type (Lefauconnier and Hagen, 1990). This estimate of 90% is believed to be an overestimation unless typical quiescent phases are significantly longer than the length of observation in the archipelago, and towards the upper end of the range 50-500 years suggested by Dowdeswell *et al.* (1991). If this is the case it would be possible that this study has failed to detect glaciers as 'surge-type'. The period of observation of unusual glacier advances started locally around the mid- to late 1800s and glaciers with quiescent phases longer than 100-200 years might not be identified as surge-type because the morphological evidence of a surge becomes less clear with time. Furthermore, it is suggested that some glaciers may have discontinued to be of surge-type through changing mass balance conditions (Dowdeswell *et al.*, 1995). Yet, in order to approximate the estimate of 90% the author would have failed to identify almost 800 glaciers as being of surge-type. As lists of

surge-type glaciers by others only add a small number, maximal 10, of possible surge-type glacier to the total of 132, it is very unlikely that the estimated 90% is a realistic estimate for the present situation (pers. comm. Bernard Lefauconnier, 1997; pers. comm. Jaçek Jania, 1998).

5.4 Qualitative data analysis: Data description and visual data interpretation

Simple data visualisation (plotting data in histograms, scatter plots, etc.) can reveal patterns in the data that can be helpful in the detection of variables distinguishing surge-type from normal glaciers (Jiskoot *et al.*, 1998). Initial ideas about these patterns can be tested using simple statistical methods such as chi-square tests and correlation statistics (e.g. Davis, 1986). This exploratory data analysis also aids the decision about how to reduce the number of categories of each categorical variable in the logit analysis (see Section 5.5). Dataplots can also reveal outliers and mistakes in the data, which, in some cases could be rectified before the actual logit data analysis was initiated.

Whereas for normally distributed samples, the mean and standard deviation are a good measure to represent the central tendency, these statistics cannot be used for data that are not normally distributed. If the frequency histograms of a variable did not show a typical bell shaped normal distribution around the mean, then normality tests were performed (see Davis, 1986). Whenever these tests confirmed that a variable was not normally distributed the 'median value' was used to quantify the central tendency (Jiskoot *et al.*, 1998). The majority of continuous variables used in this analysis were log-normally distributed. After log-transformation these can be treated as normally distributed data. For example, length and slope data in the histograms 5.12 and 5.15 are plotted on a log-normal scale in order to show that, after transformation, the data distribution is approximately normal. When log-transformed data provided significantly better results in the logit analysis than the non-transformed data, the log-transformed version of the variable was retained. Below, the variables are introduced one-by-one and general patterns of surge-type glaciers and normal glaciers are presented.

5.4.1 Latitude and longitude

Latitude and longitude of the Svalbard glaciers are the coordinates of the mid-glacier locations of the equilibrium line (Hagen *et al.*, 1993). These approximate central locations of the glacier units were given in degrees, minutes and tenths of seconds, but were for modelling purposes converted into degrees and tenth of degrees (in order to obtain linearly increasing variables). The distribution of these central points is shown in Figure 5.8. Although latitude and longitude proper have no physical meaning, they are clearly related to the geographical distribution of

glaciers, mainly because the climatic zonation is distributed over the globe according to latitude and continentality. Particularly temperature, precipitation and solar radiation are directly related to geographical position and have much influence of the distribution of glaciers. At local scales it is however more difficult to isolate the latitudinal influence as other variables have much influence at this scale (Sugden and John, 1976). For Svalbard, latitude and longitude locations can be used as approximations of geographically distributed environmental factors. Local variations in accumulation rate, temperature, permafrost conditions, topography, continentality, insolation and seismicity are strongly dependent on location and often display a non-random geographical distribution. This is also true for the regional distribution of the limit of glaciation and equilibrium line altitude (Sugden and John, 1976; Haeberli, 1980; Lefauconnier and Hagen, 1990).

At first sight the distribution of surge-type glaciers does not appear to show a particular pattern, and it follows neither the distribution of the precipitation over the archipelago (Figure 5.3) nor that of permafrost or hot springs.

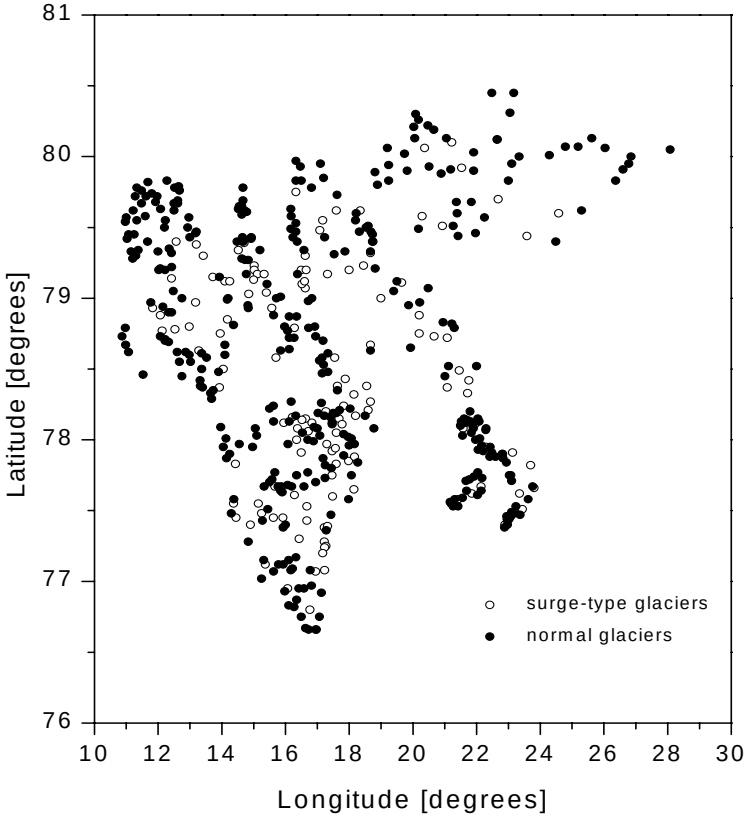

Figure 5.8: *Location of surge-type glaciers and normal glaciers.*

5.4.2 Glacier type, glacier form and type of glacier front

The morphological classification of glaciers according to glacier type, form and frontal activity in glacier inventories is a means to categorise glaciers according to physical properties and

climatic characteristics (Ahlmann, 1948; Kotlyakov, 1980; Ommanney, 1980; IAHS(ICSI)/UNEP/UNESCO, 1989). Moreover, the classification into frontal types is directly related to glacier dynamics. It is common knowledge that surging occurs in most glacier types (Meier and Post, 1969). Figure 5.9 shows that glacier surging in Svalbard has been observed in four of the six common glacier types of the archipelago, but surge-type glaciers are predominantly of the valley and the outlet types. In terms of glacier form (Figure 5.10) it seems that surge-type glacier have predominantly more that one composite firn area, whereas more than half of the normal glaciers have a single firn area. Glaciers with a single firn area have one flow unit, glaciers with a composite firn area are formed by two nearly equal flow units, each having its own accummulation area and glaciers with multiple composite firn areas are formed by more than two nearly equal flow units, each having its own accummulation area (Kotlyakov, 1980).

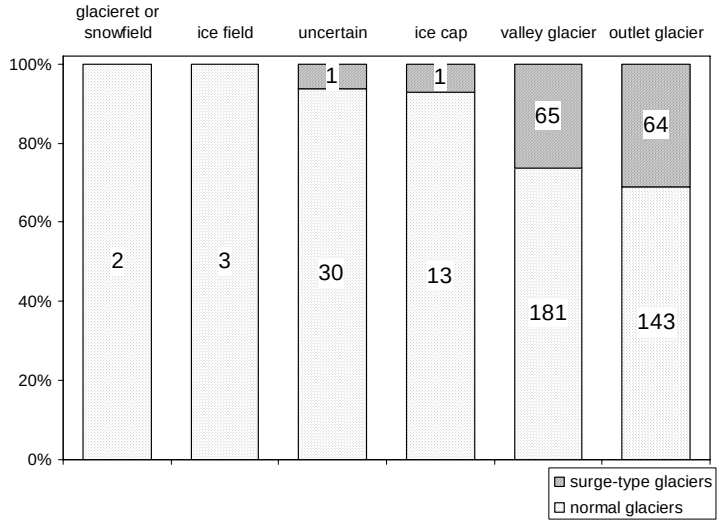

Figure 5.9: *Histograms of glacier types. The numbers in the bars are the counts of normal or surge-type glaciers of that glacier type.*

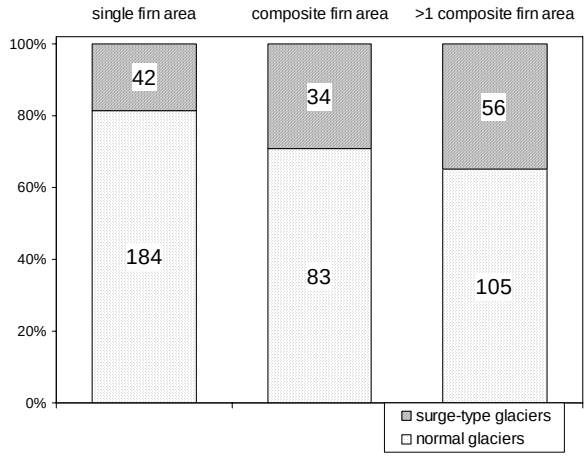

Figure 5.10: *Histograms of glacier forms. The numbers in the bars are the counts of normal or surge-type glaciers of that glacier form. The proportional division in the bars is chosen as to show the proportion of surge-type and normal glaciers in each glacier type.*

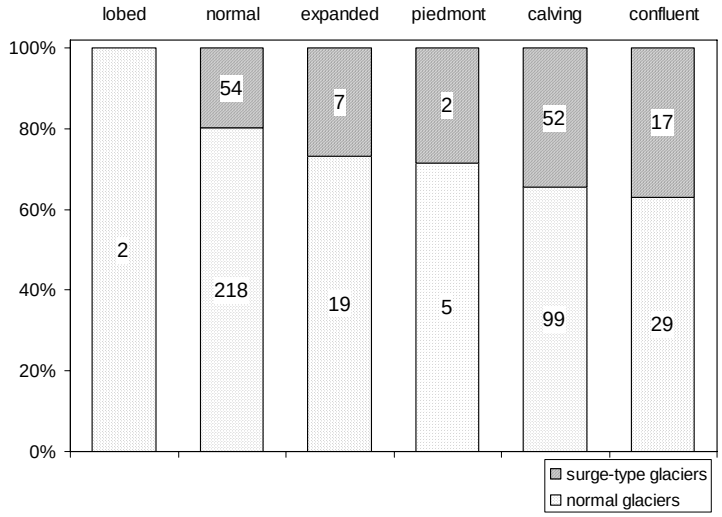

Figure 5.11: *Histograms of glacier front types. The numbers in the bars are the counts of normal or surge-type glaciers of that glacier form.*

The majority (59%) of non-surge-type glaciers have normal/valley type fronts, whereas for surge-type glaciers, calving fronts (39%) and normal fronts (41%) are almost equally present (see Figure 5.11). Moreover, the percentage of confluent front types in the surge-type glacier population (13%) is almost double that for normal glaciers (7.5%). Thus, one third of the confluent glaciers and over one third of the calving glaciers and expanded glaciers are of surge-type. These glacier types thus appear to have a higher likelihood of surging than other glacier types.

5.4.3 Glacier length

Glacier length is the length in kilometres along the centre line of a glacier (Hagen *et al.*, 1993). Glacier length in the dataset of 504 glaciers ranges from a minimum of 1.5 km to a maximum of 68.4 km, with a range of 1.5 to 47 km for normal glaciers, and 2.0 to 68.4 km for surge-type glaciers. From the observed frequency curves length was expected to be log-normally distributed, and normality tests confirmed this observation. The median length of surge-type glaciers is 13.1 km and the median length of normal glaciers is 6.5 km. Histograms of the length of normal and surge-type glaciers show that surge-type glaciers tend to be longer than normal glaciers. Research in other cluster regions of surge-type glaciers also suggested that glacier length is strongly related to glacier surging (Glazyrin 1978; Clarke *et al.*, 1986; Clarke, 1991; Hamilton and Dowdeswell, 1995: see Chapter 3).

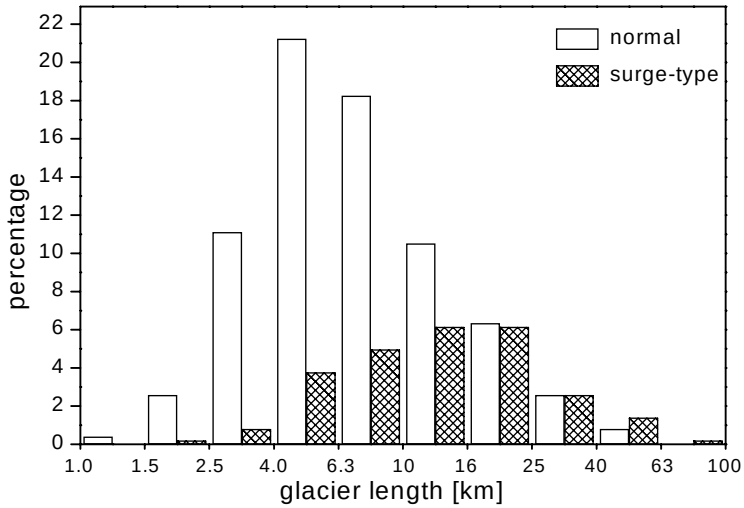

Figure 5.12: *Length of surge-type and normal glaciers. Length is plotted on a logarithmic scale.*

5.4.4 Glacier Area

Glacier area is the planar glacier surface area in km^2 (Hagen *et al.*, 1993). Glacier area ranges from 1.8 to 1270 km^2 for surge-type glaciers and from 1.8 to 720 km^2 for normal glaciers. The median area for surge-type glaciers is 49 km^2 and for normal glaciers 14 km^2. The four largest glaciers in the database with an area of more than 1000 km^2 are all of surge-type. As glacier area is directly linked to glacier length (r^2 = 0.79) the relation between glacier area and surging is similar to that of glacier length and surging: surge-type glaciers tend to have larger areas than normal glaciers. This relationship is significant using χ^2 tests at 95% significance level.

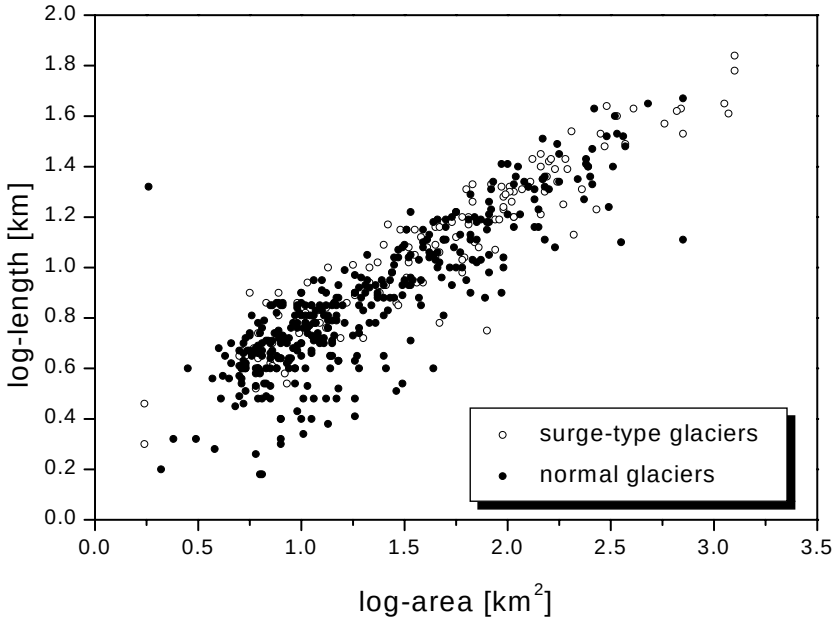

Figure 5.13: *Scatterdiagram of length vs. area. The normal glacier diverging from the positive linear trend is possibly an incorrect value for area from Hagen et al. (1993).*

5.4.5 Mean glacier width

Mean glacier width (km) was calculated by dividing glacier area by glacier length. Hence, the relation to surge-type glaciers is likely to be similar to those found for these primary data. Mean glacier width ranges from 0.7 to 54 km for normal glaciers and from 0.6 to 29 km for surge-type glaciers. Mean glacier width is unlikely to be a valid parameter in determining ice flow, unless the glacier geometry is simply rectangular. However, for very narrow widths in respect to length, both shape factor and valley wall friction can play an important role in the overall flow dynamics (Paterson, 1994).

5.4.6 Glacier Volume

Glacier volume could theoretically be a useful parameter in this analysis as it can be used as a proxy for mean glacier depth as well as for valley shape. However, only for very few Svalbard glaciers is volume measured. Hagen *et al.* (1993) calculated glacier volume for all glaciers in the glacier inventory on the basis of extrapolation of radio-echo sounding and direct glacier depth measurements of about 100 glaciers. Depending on glacier type and size, one of three empirical formulae were used to calculate glacier depth for the individual glaciers. However, in studies of glacier response to climate change, Oerlemans (1996) argued that reliable relations between glacier volume and area do not exist. Furthermore, Hagen *et al.* (1993) did not take into consideration whether a glacier was of surge-type or not: glacier volume formulae for surge-type glaciers are the same as for normal glaciers. It is therefore very unlikely that this 'theoretical' measure for glacier volume can differentiate between surge-type and normal glaciers in the dataset.

5.4.7 Average surface slope

The average surface slope was calculated from the overall length of the glaciers and the elevation span according to the following equation:

$$\alpha = \tan^{-1}\left(\frac{max - min}{L}\right), \tag{5.1}$$

with α average surface slope (rads), *max* maximum glacier elevation (m asl), *min* lowest elevation of the terminus (m asl), and *L* is glacier length (m) (Hamilton, 1992). Throughout this thesis surface slope is expressed in degrees, except where stated specifically. The surface slope of glaciers in the dataset varies between 0.7º and 18.4º and is log-normally distributed. Although

about 50 percent of the glaciers have slopes larger than 5º, very few have slopes steeper than 9º (see Figure 5.14). The range for normal glaciers lies between 0.8 and 18.4º and for surge-type glaciers between 0.7 and 14.0º. The median surface slope for surge-type glaciers is 3.1º and for normal glaciers it is 5.1º. Qualitatively, the distribution of surface slopes suggests that surge-type glaciers have low surface slopes. However, scatter plots between glacier length and surface slope indicate that there is a strong inverse relation between these two parameters (Figure 5.15). Clarke (1991) states that for glaciers in the Yukon Territory "slope has no explanatory value not accounted for by the correlation between length and surge tendency". Similar results were found for Spitsbergen glaciers, essentially a subset of the Svalbard glaciers in this study (Hamilton, 1992; Hamilton and Dowdeswell, 1996). Thus univariate plots for length and slope do not reveal which of the two variables is primarily related to glacier surging and which is secondary.

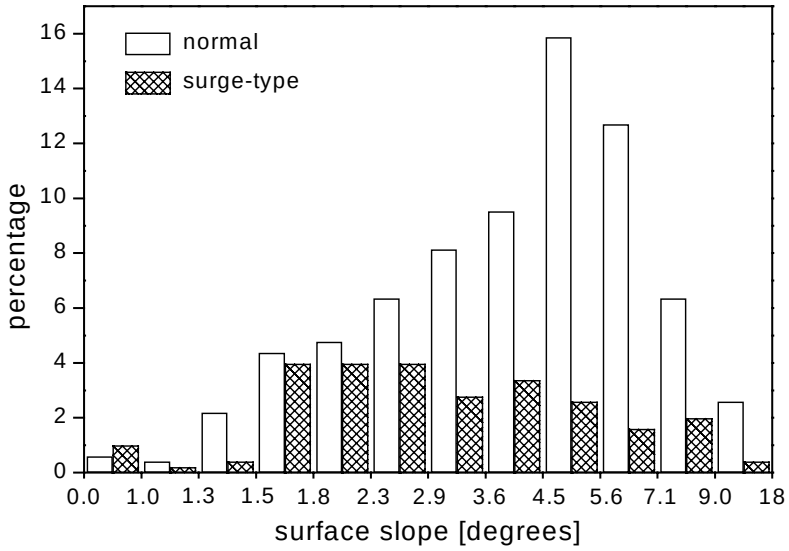

Figure 5.14: *Slope of for surge-type and normal glaciers. The axis for slope is on a logarithmic scale.*

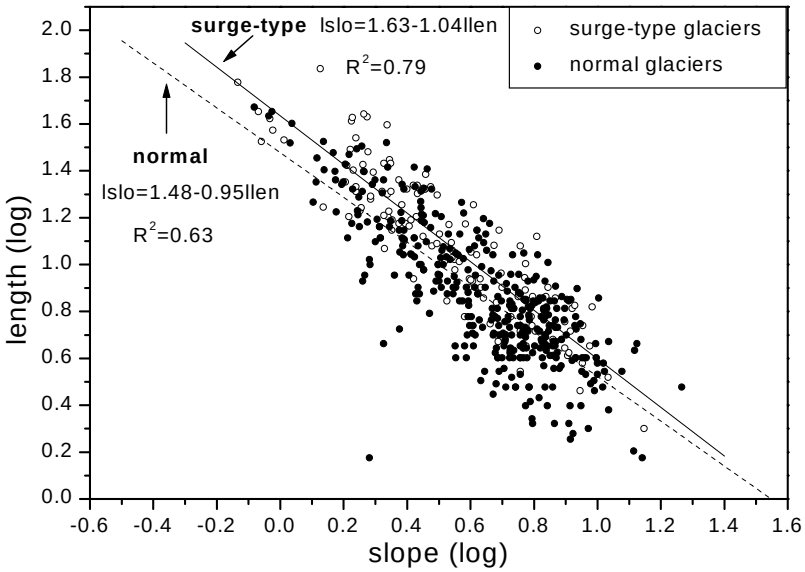

Figure 5.15: *Scatterdiagram of length vs. slope. The regression line of surge-type glaciers appears to be steeper which is confirmed by the regression parameter (-0.95 vs. –1.04). In the regression equations 'llen' is log-transformed length and 'lslo' is log-transformed surface slope.*

5.4.8 Fowler's index

Fowler's index (see Section 2.4.8) was calculated by multiplying average surface slope (in radians) by mean glacier width squared. Fowler (1989) postulated that this index would be smaller than the order of one for surge-type glaciers. However, for surge-type glaciers in Svalbard, Fowler's index ranges from 0.04 to 24.2, while for normal glaciers the range is from 0.0003 to 83.7. The index is log-normally distributed and the median value for surge-type glaciers is 0.9 and for normal glaciers it is 0.5. Fowler's index was subsequently divided into three categories to separate those glaciers with indices smaller than the order or one from glaciers with indices of the order of one and larger. Table 5.2 shows that, qualitatively, Fowler's postulate does not hold for Svalbard glaciers.

FOWLER'S INDEX			
	$\tilde{\tilde{F}}$ **<0.5**	**0.5** $\leq \tilde{\tilde{F}} \leq$ **2**	$\tilde{\tilde{F}}$ **>2**
Normal glaciers	184 (83%)	129 (65%)	59 (69%)
Surge-type glaciers	38 (17%)	68 (35%)	26 (31%)

Table 5.2: *Fowler's index* $\left(\tilde{\tilde{F}}\right)$*. Surge-type glaciers should have indices smaller than the order of one (Fowler, 1989), which would correspond with the left column in this table.*

5.4.9 Glacier elevation

The glacier elevation measures for Svalbard include: maximum (*max*), minimum (*min*), median (*med*) elevation, elevation span and equilibrium line altitude (*ela*). These measures are related to glaciation level and mass balance conditions of individual glaciers and are determined by local climate conditions and glacier type (IAHS(ICSI)/UNEP/UNESCO, 1989). Figure 5.16 shows that the *max* (altitude of the highest point of the glacier) for surge-type glaciers ranges from about 400 to 1700 m above sea level (asl) and for normal glaciers between about 200 to 1350 m asl. The *min* (altitude of the lowest point of the terminus) for surge-type glaciers varies between 0 and 400 m asl and for normal glaciers the range is between 0 and 500 m asl. The *med* (altitude in m asl of the contour line that divides the glacier surface area in half) for both glacier types varies between about 150 and 1050 m asl and *ela* ranges between 100 and 800 m asl. Some argue *med* is a more reliable measure for mass balance than *ela*, as the latter is highly variable from year to year (Braithwaite and Müller, 1980). It should be noted that the distribution of the *ela* across the archipelago varies according to latitude and distance from the ocean (see Figure 5.6). The lowest values are found in the southern and western areas of Spitsbergen and the highest values appear in the central northern part of Spitsbergen. It is difficult to differentiate between surge-type and normal glaciers using elevation data as the altitude ranges overlap

considerably (see Figure 5.16). However, the elevation span of surge-type glaciers is larger as they are found up to 350 m higher than normal glaciers whereas the minimum altitude for both is at sea level.

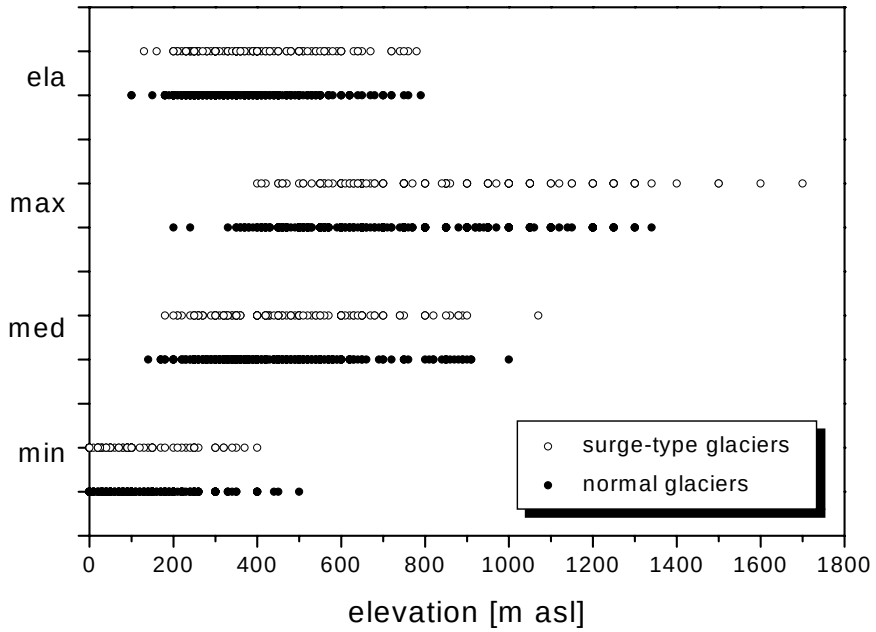

Figure 5.16: *Glacier elevation ranges of surge-type glacier and normal glaciers in the Svalbard dataset. ela = equilibrium line elevation, max = maximum elevation, med = medium elevation and min = mimimum elevation. Data from Hagen et al. (1993).*

Clearly, glacier length elevation span and surface slope are correlated, not the least because average surface slope is directly calculated from elevation span and length (see Section 5.4.7). Figure 5.17 shows that whereas the relation between length and elevation span is clearly positive and log-linear, the relation between surface slope and elevation span is not so obvious. This is probably the result of the tangent in equation 5.1. The glaciological implication of a larger elevation span with increasing length is encripted in the non-linear feedback loops between mass balance and glacier response. For example, the sensitivity of glacier length to changes in the equilibrium line altitude is inversely proportional to the average bed slope (Oerlemans, 1989). This implies that glaciers resting on a shallow bed are more sensitive to climate change, therefore glaciers with a smaller elevation span for the same length would have an increased sensitivity to climate change. On the other hand, surging glaciers would change their elevation span on a shorter time scale than that or normal glaciers, as surges can result in marked frontal advance, whilst during quiescence the glacier retreats over approximately the same distance. For glaciers with relative steep slopes in the lower reaches this horizontal fluctuation has a considerable effect on the overall shape of the mass balance curve, quite unlike the simple up and down moving mas balance curve of glaciers that deplete over their entire surface (Haeberli and Hoelzle, 1995). However, for a full understanding of elevation-glacier

length correlations, the effect of glacier geometry and therefore glacier hypsometry (see Section 5.4.11) cannot be ignored (Furbish and Andrews, 1984).

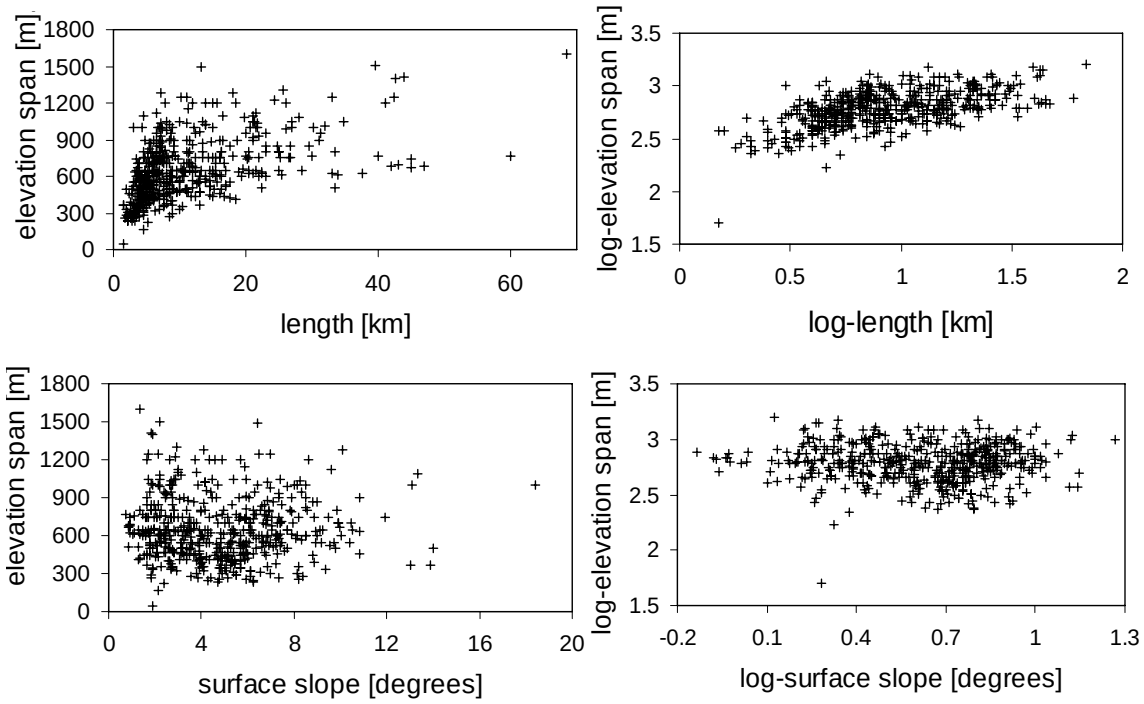

Figure 5.17: *Plots of length vs. elevation span and surface slope vs. elevation span.*

5.4.10 Glacier orientation

Orientation or aspect of a glacier holds information about orographic effect on snow distribution, insolation, topographic shading or local wind patterns, all accounting for mass and energy balance of the glacier. Furthermore, combination of orientations of upper and lower reaches of glaciers can be used as a measure for curvature in the direction of ice flow. Glaciers with strong channel curvatures might be subject to restricted outflow (see Section 2.4.12). Orientation of accumulation area and ablation area of the glaciers in the dataset is expressed in octants (Figure 5.18). The diagrams show that 51% of the surge-type glaciers have their accumulation area facing in easterly directions (NE, E, SE), whereas only about 36% of the normal glaciers do. For the ablation area the percentages are 49% and 37% respectively. This would suggest that surge-type glaciers have a higher probability of facing in easterly directions than normal glaciers. However, many of the east orientated surge-type glaciers in Svalbard are located in south-east Spitsbergen and also have calving fronts (Lefauconnier and Hagen, 1990).

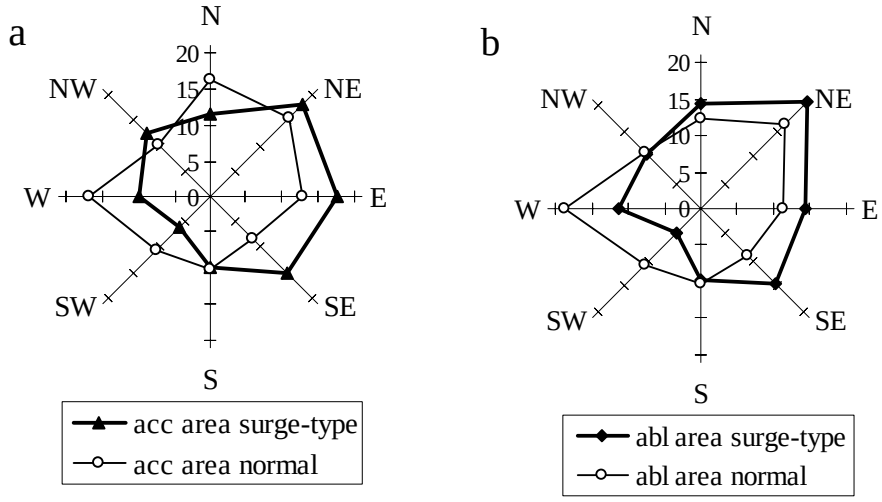

Figure 5.18: *Glacier orientation expressed in octants* ***a)*** *orientation of the accumulation area,* ***b)*** *orientation of the ablation area (After: Jiskoot et al., 1998).*

Furthermore, glaciers in the northern hemisphere descending from north facing slopes tend to be longer than glaciers with south facing orientations (Kasser, 1980). To disentangle possible relationships between glacier surging, orientation and type of glacier front a multivariate analysis is necessary.

5.4.11 Glacier hypsometry and accumulation area ratio

Hypsometry is the area-elevation distribution of a glacier defined as the hypsometric curve of a glacier's planometric area in relation to elevation (Furbish and Andrews, 1984). For the description of hypsometry, non-dimensional elevation and area parameters are used and the hypsometric curve is a function of these parameters. Glacier hypsometry is dependent upon valley shape, topographic relief and glacier depth (Furbish and Andrews, 1984; Wilbur, 1988). Accumulation area ratio (AAR) is the ratio of the accumulation area to the total glacier area, usually given as a fraction or percentage. The AAR can be expressed as:

$$\int_{\max}^{ela} \frac{dA}{dz} dz \Big/ \int_{\max}^{\min} \frac{dA}{dz} dz \,, \tag{5.2}$$

where A is glacier area [m^2] and z is the vertical distance. Generally, an accumulation area ratio (AAR) of 0.7 is representative for a temperate valley glacier with a net zero balance (Paterson, 1994). For Svalbard and other High Arctic regions, balance AARs are assumed to be lower: AAR values between 0.5 and 0.6 would correspond to a zero net balance in these regions (IAHS(ICSI)/UNEP/UNESCO, 1996). Lefauconnier and Hagen (1990) define Svalbard glaciers

with an equilibrium line altitude (*ela*) 50-100 m lower than their median elevation (*med*) as having a net balance of zero or positive, thus to be in steady-state. In the database, about 60% (291) of the glaciers have the *ela* 50 m or more below the *med* and 156 of these have their *ela* 100 m or more below the *med*. However, the majority of small glaciers in Svalbard have negative net balance conditions (Dowdeswell et al., 1998). Kongsvegen (155 10), on the contrary, has a positive net balance, but its *ela* is only 30 m below the *med*. A shortcoming of the AAR and *ela-med* methods describing glacier health is that no account is taken of the influence of glacier hypsometry. Because changes in *ela* and mass balance are associated with glacier geometry, hypsometry is closely interlinked with mass balance distribution, long term stability and response to climate (Ahlmann, 1948; Furbish and Andrews, 1984; Oerlemans, 1989). For this analysis only *ela* and *med* were available from Hagen *et al.* (1993) as measures for glacier health. To improve the analysis of the relationship between mass balance and glacier surging two additional mass balance related variables were therefore introduced. For all glaciers in the database a measure was defined for glacier hypsometry and derived the AAR.

Data for glacier hypsometry are ideally derived from detailed elevation maps. For the 504 glaciers in the database this process would be very time consuming and moreover, the contour lines of some of the glaciers are inaccurate or not surveyed. Whereas (synthetic) non-linear functions have been developed for the calculation of terrain hypsometry (e.g. Marshall and Clarke, 1999), these are not applicable to the calculation of glacier hypsometry. The author therefore developed a method to calculate proxies for hypsometry and AAR from the available elevation and area data (Hagen *et al.*, 1993). The Svalbard glacier inventory data used to calculate proxies for net mass balance are maximum elevation (*max*); median elevation (*med*); minimum elevation (*min*); equilibrium line elevation (*ela*) and glacier area (*A*).

Information about glacier area only exists for three elevations: at $max \Rightarrow A = 0$, at $med \Rightarrow A = 0.5$, and at $min \Rightarrow A = 1$. Glacier area is assumed to increases linearly from zero to 0.5 between *max* and *med*, and similarly from 0.5 to 1.0 between *med* and *min*. For glaciers other than equi-dimensional, the slopes of area increase are different above and below the median elevation (see Figure 5.19). Basically I assume that glacier area above the median has a rectangular shape and the glacier area below the median has a rectangular shape. These are crude assumptions, but as the exact shape of the glacier areas is unknown, it is preferable to start with the simplest assumption than to experiment with non-linear functions. Glacier hypsometries can be approximated by plotting maximum (Area = 0), median (Area = 0.5) and minimum (Area = 1) elevation as a hypsometric curve and linearly interpolate between these three points (Figure 5.19). Although the calculations for hypsometric curves are based on the hypsometry definition by Furbish and Andrews (1984) the curves are represented in a different way: the elevation is on

the y-axis and area on the x-axis, with increasing values going up and right (Figure 5.19). This representation was chosen because it is easier to envisage the hypsometric distribution with the elevation going up.

Dimensionless parameters for elevation and area were calculated by normalising the glacier elevation and area. Normalised elevation (Z^*), for instance, can be expressed as:

$$Z^* = \frac{Z_x - Z_{\min}}{Z_{\max} - Z_{\min}}, \tag{5.3}$$

so that at Z_{max}, $Z^* = 1$ and Z_{min}, $Z^* = 1$. Z_x is here the actual elevation of the glacier at a certain point, Z_{max} is the highest elevation and Z_{min} the lowest elevation.

As numerical values for glacier hypsometry are more useful for modelling purposes than the obtained hypsometric curves, the hypsometric curves were transformed into hypsometry indexes (HI). The HI equals the elevation range above the median elevation divided by the elevation range below the median elevation. The HI is comparable to altitude skewness (Etzelmüller and Sollid, 1997). This relative distribution of area in a glacier provides a measure of grouping glaciers into different hypsometric curve shapes (Wilbur, 1988). A HI larger than 1 indicates 'surplus' area in the upper regions and a HI lower than 1 indicates a 'surplus' area in the lower regions. A piedmont glacier would have a HI greater than 1 and a keyhole-shaped valley glacier would have a HI less than 1. The HI for the Svalbard glaciers ranges between 0.06 and 4.88 with 90% of the glaciers having indices between 0.25 and 1.75. Because these hypsometry measures were relatively crude they were converted into a categorical variable. Hypsometry index values were divided into three categories: (1) equi-dimensional ($0.9 \leq \mathrm{HI} \leq 1.1$), (2) bottom-heavy (HI > 1.1) and (3) top-heavy (HI < 0.9) (following Furbish and Andrews, 1984; Wilbur, 1988; Ødegard *et al.*, 1998). The counts of normal and surge-type glaciers in each of these categories are shown in Table 5.3. There appears to be no predominance of surge-type or normal glaciers in either hypsometry type.

GLACIER HYPSOMETRY			
	top-heavy	***equi-dimensional***	***bottom-heavy***
Normal glaciers	104 (71%)	52 (68%)	216 (77%)
Surge-type glaciers	42 (29%)	24 (32%)	66 (23%)

Table 5.3: *Glacier hypsometry. The classes are calculated from hypsometry indices.*

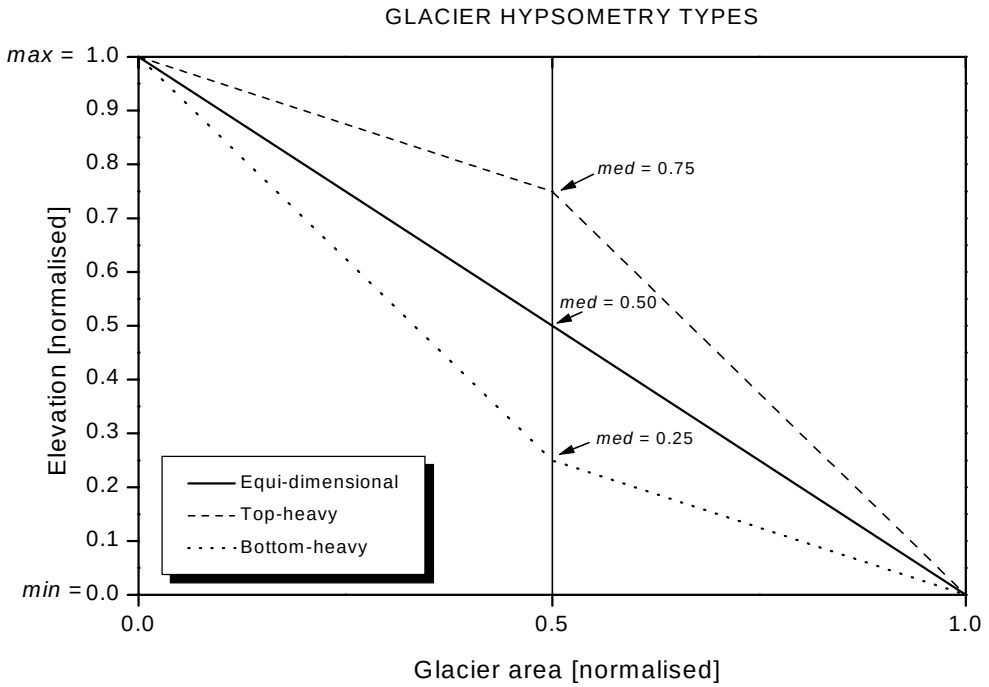

Figure 5.19: *Glacier hypsometry types according to the position of the median elevation (med). From this graph can also be inferred that for an ela at a normalised elevation of 0.5 the AAR of the equi-dimensional glacier equals 0.5, the AAR for the bottom-heavy glacier equals 0.67 and the AAR for the top-heavy glacier equals 0.33.*

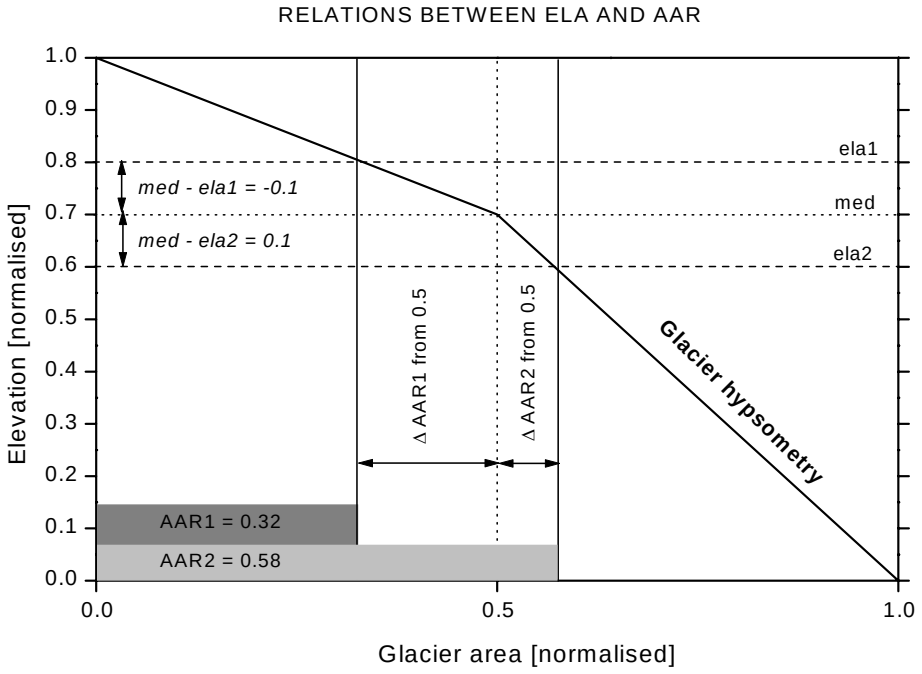

Figure 5.20: *The relation of hypsometry to AAR showing the effect of the elevation difference between the median elevation (med) and the equilibrium line altitude (ela) on the AAR. Two situations are shown for a similar bottom-heavy glacier hypsometry. When the ela is at a higher elevation than the med, the AAR is smaller than 0.5 (ela1 = 0.8, AAR = 0.32) and when the ela is at a lower elevation than the med, the AAR is larger than 0.5. (ela2 = 0.6, and AAR2 = 0.58). The relation of Δela to ΔAAR is non-linear as the shape of the hypsometric curve is non-linear.*

Plotting equilibrium line altitudes on the hypsometry profile gives a crude measure for the AAR of each glacier (see Figure 5.20). For the Svalbard glaciers it is given that the median elevation is the elevation of the contour line at which 50% of the glacier area lies above and 50% below this contour, the vertical position of the equilibrium line relatively to the median elevation is an indication for the AAR. There are three possible situations:

Case 1) The *ela* is at the same elevation as *med* then the AAR = 0.5,

Case 2) The *ela* is at a lower elevation than *med* thus AAR > 0.5,

Case 3) The *ela* is at a higher elevation than *med* thus AAR < 0.5.

The AAR for cases 2 and 3 can then be quantified as 0.5 plus the accumulation area that lies below the *med*, or minus the ablation area that lies above the *med*. The elevation difference between the *med* and *ela* can be calculated as a fraction of the elevation difference between *med* and *min* or between *max* and *med*. This fraction has to be added to or subtracted from the 50% area that coincides with the median elevation. However, as AAR is relative to the total glacier area, the fraction should be taken from 100% and not from the 50% area above or below the median elevation, and thus has to be divided by 2.

Case 2 can be mathematically expressed as:

$$0.5 + \frac{(med - ela)/(med - min)}{2}, \tag{5.4}$$

where *med-ela* is a proxy for the 'area between *med* and *ela*'. As for case 2 (*med-ela*) > 0, this results in an AAR > 0.5.

Case 3 can be mathematically expressed as:

$$0.5 + \frac{(med - ela)/(max\text{-}med)}{2}. \tag{5.5}$$

These expressions result in a dimensionless fraction and as (*med* - *ela*) < 0 for case 3, this results in an AAR < 0.5. For case 1 (*ela* and *med* coincide) either equation (5.4 or 5.5) can be applied as (*med* - *ela*) = 0, which makes the whole term on the right-hand side zero and gives an AAR of 0.5 in all cases. Equations 5.4 and 5.5 can be problematic if the *ela* is at a higher elevation than the *max* or at a lower elevation than the *min* or equal to the *max* or *min*. In the first case the AAR should be set to zero and in the second case to one. However, these situations do not occur in the Svalbard glacier data. Multiplying the fractional AAR as calculated in equations 5.4 and 5.5 with the total area further quantifies the AAR. This gives a measure for the absolute size of the accumulation area in km^2.

The AAR measures calculated from equations 5.4 and 5.5 give a range from 0.03 to 0.89 with 90% of the glaciers having AARs between 0.4 and 0.75. Comparing these AAR measures with published Svalbard AAR data shows that the error in the calculated AAR is within 5% (Lefauconnier and Hagen, 1991; Hagen *et al.*, 1993; IAHS(ICSI)/UNEP/UNESCO, 1996). In order to differentiate between groups of glaciers on the basis of mass balance conditions, categorical values for AAR were assigned. Class boundaries for AAR were based on calculated AAR values for a zero net balance. This 'balance AAR' lies between 0.55 and 0.6 for Svalbard glaciers (IAHS(ICSI)/UNEP/UNESCO, 1996). The continuous AAR values were consequently grouped into 3 classes: (1) AAR < 0.55, (2) 0.55 ≤ AAR ≤ 0.6 and (3) AAR > 0.6, roughly representing a negative net balance, a zero net balance and a positive net balance (Jiskoot *et al.*, in review). The numbers of surge-type and normal glaciers in each of AAR classes are listed in Table 5.4.

ACCUMULATION AREA RATIO			
	AAR < 0.55	***0.55 ≤ AAR ≤ 0.6***	***AAR > 0.6***
Normal glaciers	129 (68%)	71 (66%)	172 (76%)
Surge-type glaciers	41 (32%)	36 (34%)	55 (24%)

Table 5.4: *Accumulation area ratio (AAR). The three classes divide the glaciers into those with a negative mass balance, those in equilibrium and those with a positive mass balance.*

No apparent difference between normal and surge-type glaciers could be detected from the dataplots of hypsometry and AAR. However, Figure 5.21 shows that the range in AAR is larger for short glaciers than for long glaciers. The AAR might thus be related to the size of a glacier and should be analysed in conjunction with other glacier variables as well. This also applies for hypsometry. When plotting the hypsometry index against equilibrium line elevation it appears that with increasing *ela* glaciers tend to become more top-heavy (Figure 5.22). When plotting the hypsometry index and AAR against latitude and longitude it was noticed that the variability in the data is larger in an east west direction than in a north south direction. Hypsometry index shows a decreasing trend in eastward direction, with the majority of glaciers east of 20ºE being top-heavy glaciers. This trend is possibly a simple reflection of the distribution of glacier types over the archipelago.

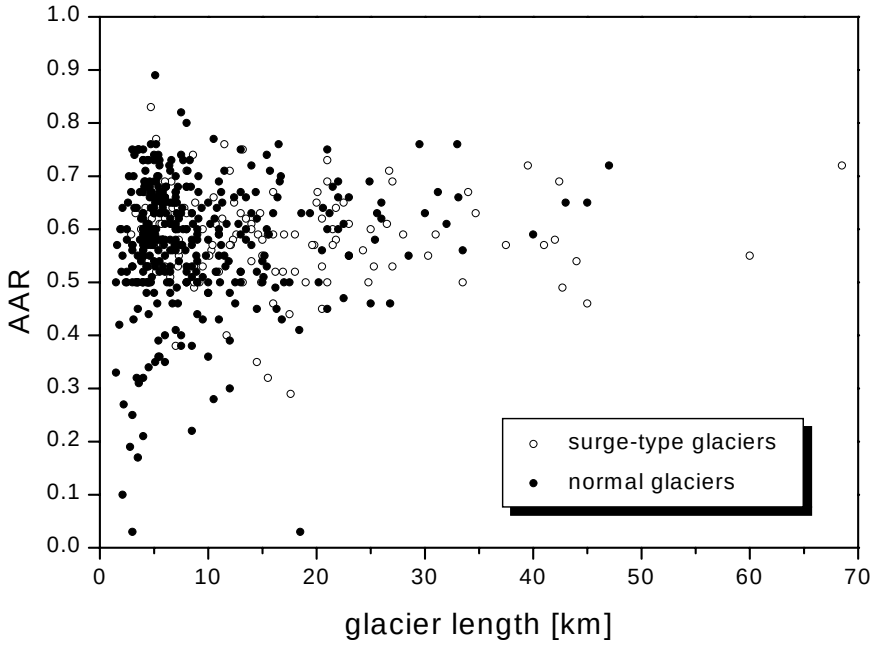

Figure 5.21: *Relation between glacier length and accumulation area ratio (AAR).*

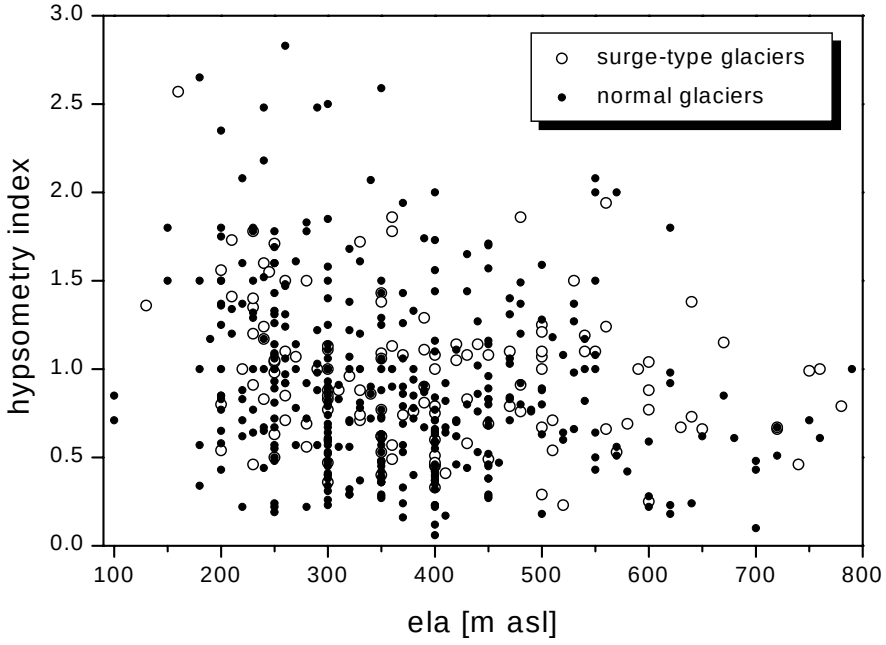

Figure 5.22: *Relation between equilibrium line altitude (ela) and hypsometry index. The stripes over overlapping dots to the nearest 50 ms result from the ela assignment procedure to the nearest 50 m by Hagen et al. (1993).*

5.4.12 Geology: petrographical category, lithology type and geological age

Bedrock geology in combination with geological age can be used as proxies for erodibility, type of substrate, bed roughness, bed permeability, geothermal heat, seismic activity, geologic activity, terrain topography, etc. (see Section 2.4.11). The basic geology and distribution of bedrock types over the archipelago are explained in Section 5.2.1 and Figure 5.2. Geological data for individual glaciers were collected from maps and literature available from the Norsk Polarinstitutt. For the initial lithological classification a five digit geological index was assigned indicative of the 'dominant' lithology of each glacier (Table 5.5). A 'dominant' lithology is the bedrock type beneath more than 50% of the glacier base. In cases where multiple lithologies were present, the bedrock underlying the majority of the lower region of the glacier was assigned (Jiskoot *et al.*, 1998). This full classification proved too complicated for modelling purpose and the 3rd and 4th digit (prefix and layers or inclusions) were later abandoned.

LITHOLOGY CLASSIFICATION						
1 *Petrological category*		**2** *Lithology*	**3** *Prefix*	**4** *Layers or inclusions*		**5** *Age*
1 igneous	0	undefined	undefined	Undefined	1	Pre/Cambrian
	1	granite	granitic	Granite	2	Devonian
	2	basalt	with basalt	Basalt	3	Carboniferous
	3	gabbro	carbonate/dolomite	Gabbro	4	Permian
	4	intrusive		Intrusive	5	Triassic
	5	diorite		Diorite	6	Jurassic
	6	porphyric			7	Cretaceous
	7				8	Tertiary
	8				9	Quaternary
2 metamorphic	0	undefined	undefined	undefined		
	1	quartzite	quartzitic	quartzite		
	2	schist/phyllite	schist (phyllitic)	schist (phyllitic)		
	3	amphibolite	amphibolitic	amphibolite		
	4	migmatite	migmatite	migmatite		
	5	diamictite	diamictite	diamictite		
	6	gneiss	gneiss	gneiss		
	7	marble	marble	marble		
	8			metamorphic mixed		
3 sedimentary	0	undefined	undefined	undefined		
	1	sandstone	coarse/shelly/sandy	sandstone/quarzite		
	2	siltstone	silty	siltstone		
	3	shale/mudstone	muddy/shaly	shale		
	4	limestone/carbonate/dolomite	carbonate-rich	limestone/carbonate		
	5	conglomerate	conglomerate	conglomerate		
	6	coal	coaly	coal		
	7	chert		coal+shales		
	8	tillite		siltstone+shales		
	9	marine		sand-+siltstone		

Table 5.5: *Full geological classification. For example, a glacier with digits 31263 would overlie a silty sandstone with coal layers of Carboniferous age.*

From the glacier count on each bedrock type (Table 5.6) it can be seen that some categories hold very few glaciers and some hold only normal or only surge-type glaciers. The lithologies were therefore combined into a smaller number of categories. After experimenting in the logit models (see Section 5.5) the optimal and geologically most sensible classification was into four groups: (1) Igneous lithologies, (2) Metamorphic lithologies, (3) Shale and mudstones, and (4) Sandstone and the remaining sedimentary lithologies. In the dataset 74.6% of all glaciers predominantly overlie sedimentary bedrock (13.5% shale/mudstone, 60.1% other sedimentary), 18.6% overlie metamorphic bedrock and only 6.8% overlie igneous bedrock. However, 30% of the surge-type glaciers overlie shale/mudstone lithologies, which is significantly higher than the average (Figure 5.23). This suggests that glacier surging is more likely to occur on shale or mudstone than on other lithologies.

GLACIER COUNTS PER LITHOLOGY TYPE			
Petrological category	*Lithology*	*Normal glaciers*	*Surge-type glaciers*
igneous	undefined	6	0
	granite	14	1
	gabbro	1	0
	intrusive	9	2
	porphyric	1	0
metamorphic	undefined	0	1
	quartzite	15	0
	schist/phyllite	26	3
	amphibolite	0	3
	migmatite	22	0
	diamictite	2	1
	gneiss	9	8
	marble	2	2
sedimentary	undefined	1	0
	sandstone	177	61
	siltstone	4	4
	shale/mudstone	29	39
	limestone/carbonate/dolomite	42	2
	conglomerate	4	0
	chert	2	0
	tillite	5	5
	marine	1	0

Table 5.6: *Total number of surge-type glacier and normal glaciers per lithology type.*

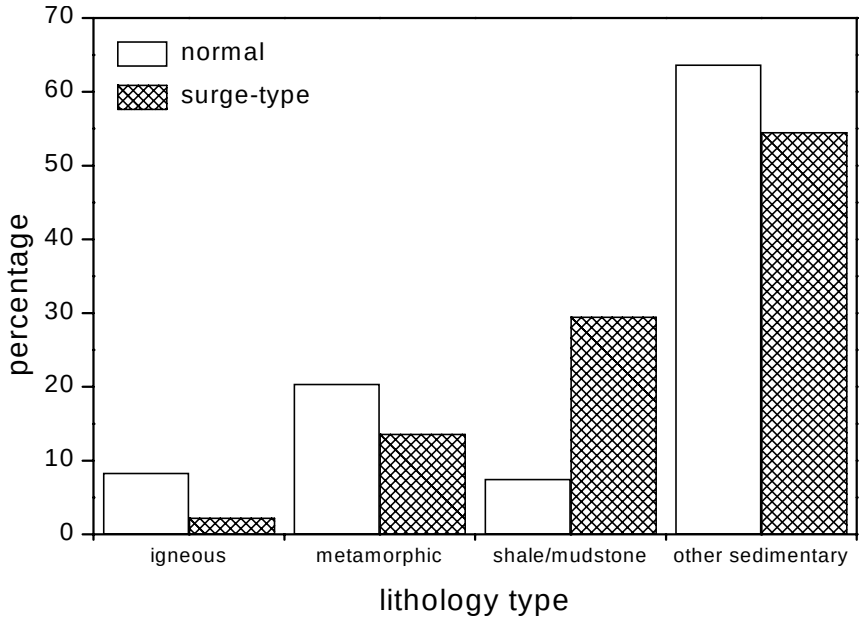

Figure 5.23: *Lithology histogram (From: Jiskoot et al., 1998).*

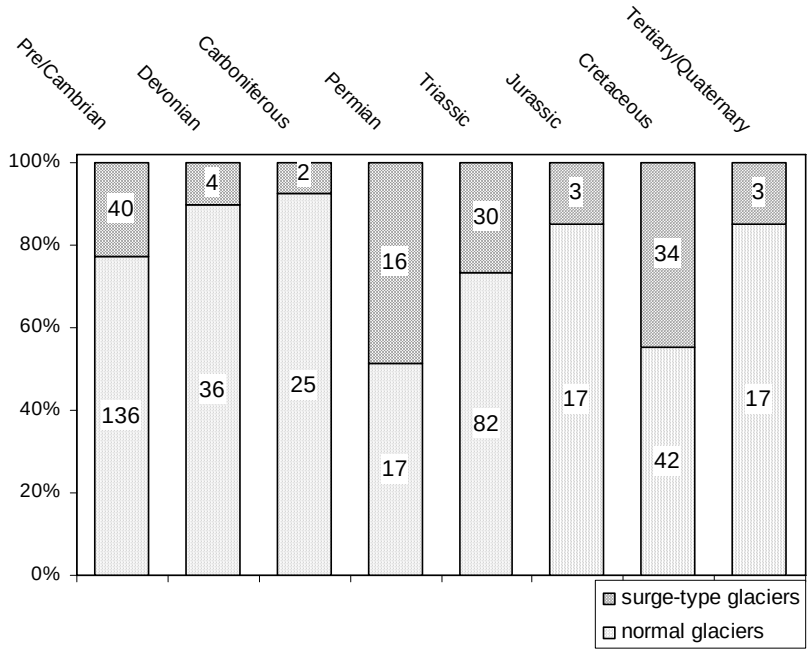

Figure 5.24: *Geological age histogram.*

The percentage of surge-type glaciers overlying Cretaceous (26%) and Permian (12%) aged lithologies is significantly higher than the percentage of normal glaciers in these categories (11% and 5%), whereas the percentage of normal glaciers overlying Precambrian (37%), Devonian (10%) and Carboniferous (8%) is significantly higher than that of surge-type glaciers (30%, 3% and 5%). The percentages of surge-type and normal glaciers overlying Triassic, Jurassic and Tertiary bedrock are almost equal. From these raw data it appears that bedrock older than Permian is not favourable for surging and that surge-type glaciers are more likely to overlie lithologies of Permian and Tetiary age (Figure 5.24). Because of the small number of

surge-type glaciers in some of the periods (Figure 5.24) geological age was combined for modelling purposes into fewer classes with larger counts: (1) The Precambrian, (2) Devonian (Middle Palaeozoic), (3) Carboniferous and Permian (Upper Palaeozoic), (4) Triassic, Jurassic and Cretaceous (Mesozoic), (5) Tertiary and Quaternary (Cenozoic).

5.4.13 Geological boundaries: type, number and direction

Geological transitions could imply changes in bed roughness, permeability, erodibility, pore water pressure, geothermal heat flux, groundwater and permafrost conditions (Post, 1969; Boulton, 1971, 1979; Alley, 1989; Bamber, 1989; Clarke, 1991). Not only the type of boundary is important for these changes, but also the alignment in respect to the ice flow. Besides which, rock is more homogenous parallel to bedding than transverse to bedding leading to differentiation in erosion rate, groundwater flow and subglacial drainage continuity (Walder and Hallet, 1972; Boulton and Hindmarsh, 1987). Furthermore, the availability of a variety of source material for the development of a till bed, could result in tills with different rheology than tills from a single geological source (Dreimanis and Vagnes, 1972; Clarke, 1987). Moreover, the direction of geological boundaries can be related to geological fault systems and tectonically active regions (Post, 1969). It should however be noted that the abrupt transitional effects at geological boundaries could have a limited effect on transitions in the subglacial conditions of glaciers overlying thick sequences of unconsolidated (soft) beds.

Almost all glaciers in the database appear to flow across different lithologies and it might well be the case that certain geological transitions induce flow instabilities that lead to surge behaviour. With the aim of incorporating both measures for specific subglacial physical transitions as well as for overall geological complexity, three types of geological boundary variables were assigned. (1) *type of boundary*: nine possible transitions between sedimentary, metamorphic and igneous lithologies (2) *direction of boundary:* perpendicular, parallel or oblique, (3) *number of boundaries*: none, one or more (Table 5.7). The majority of normal and surge-type glaciers (294 of the 504) cross geological boundaries of the type sedimentary-sedimentary. Fifty percent of the igneous-sedimentary and sedimentary-igneous boundaries are overlain by surge-type glaciers, whereas for sedimentary-sedimentary and metamorphic-metamorphic type boundaries about half is so. Other boundary types are found under only few glaciers. These figures suggest that surging could possibly be enhanced by certain physical conditions associated with transitions from igneous to sedimentary bedrock or from sedimentary to igneous bedrock.

GEOLOGICAL BOUNDARIES		
Boundary type	***surge-type glaciers***	***normal glaciers***
none	2	4
igneous-igneous	0	6
igneous-metamorphic	0	13
igneous-sedimentary	9	13
metamorphic-metamorphic	12	37
metamorphic-igneous	1	13
metamorphic-sedimentary	18	42
sedimentary-sedimentary	80	214
sedimentary-igneous	7	12
sedimentary-metamorphic	3	18
Boundary direction		
none/unknown	16	50
perpendicular	90	264
parallel	17	37
oblique	9	21
Number of boundaries		
zero/unknown	16	49
one	94	240
more than one	22	83

Table 5.7: *Classification of geological boundaries and numbers of normal and surge-type glaciers in each class. The order of lithology in the boundary type indicated a transition from lithology A to lithology B in the direction of glacier flow (From: Jiskoot et al., in review).*

5.4.14 Internal reflection horizon as proxy for thermal regime

For a large number of Svalbard glaciers, radio echo-sounding (RES) measurements have been published (e.g. Macheret, 1981, 1990; Macheret and Zhuravlev, 1982; Dowdeswell *et al.*, 1984a; Drewry and Liestøl, 1985; Kotlyakov and Macheret, 1987; Bamber, 1987, 1988; Glazovsky *et al.*, 1991; Björnsson *et al.*, 1995; Murray *et al.*, 1998), few of these have direct measurements of thermal regime (e.g. Hansbreen and Finsterwalderbreen) (e.g. Jania *et al.*, 1996; Ødegard *et al.*, 1997). Data on thermal regime for glaciers in the database was collected from these publications, using the presence of an IRH as an indication of a polythermal regime (see Section 5.2.5). RES data were available for 137 of the 504 glaciers in the database. Thermal regime for the remaining glaciers was treated as unknown and the author therefore only analysed and modelled 'thermal regime' for glaciers with RES measurements. Of the 137 glaciers with RES measurements, 50 have a continuous IRH (Figure 5.25 and Table 5.8). This is 36% of the sample, which is consistent with Macheret's figure of 33% (Macheret, 1990). For glaciers that have just gone through a surge (e.g. Tunabreen, Bogebreen, Hessbreen) the IRH and bed return might not show up as these reflections can be obscured by scattering from the crevassed surface (Dowdeswell *et al.*, 1984b), but there is not much we can do about this problem. The data in Table 5.8 shows that an IRH is more frequently observed in surge-type

glaciers than in normal glaciers and this hypothesis is confirmed by Chi-square tests at the 95% significance level (χ^2 = 22.1 for 1 d.f.). This suggests that, in Svalbard, a polythermal regime might be related to glaciers surging.

RADIO ECHO SOUNDING AND INTERNAL REFLECTION HORIZONS			
	no RES data	no IRH	IRH
Normal glaciers	285 (78%)	68 (68%)	19 (38%)
Surge-type glaciers	82 (22%)	19 (22%)	31 (63%)

Table 5.8: *Radio-echo sounding data for normal and surge-type glaciers.*

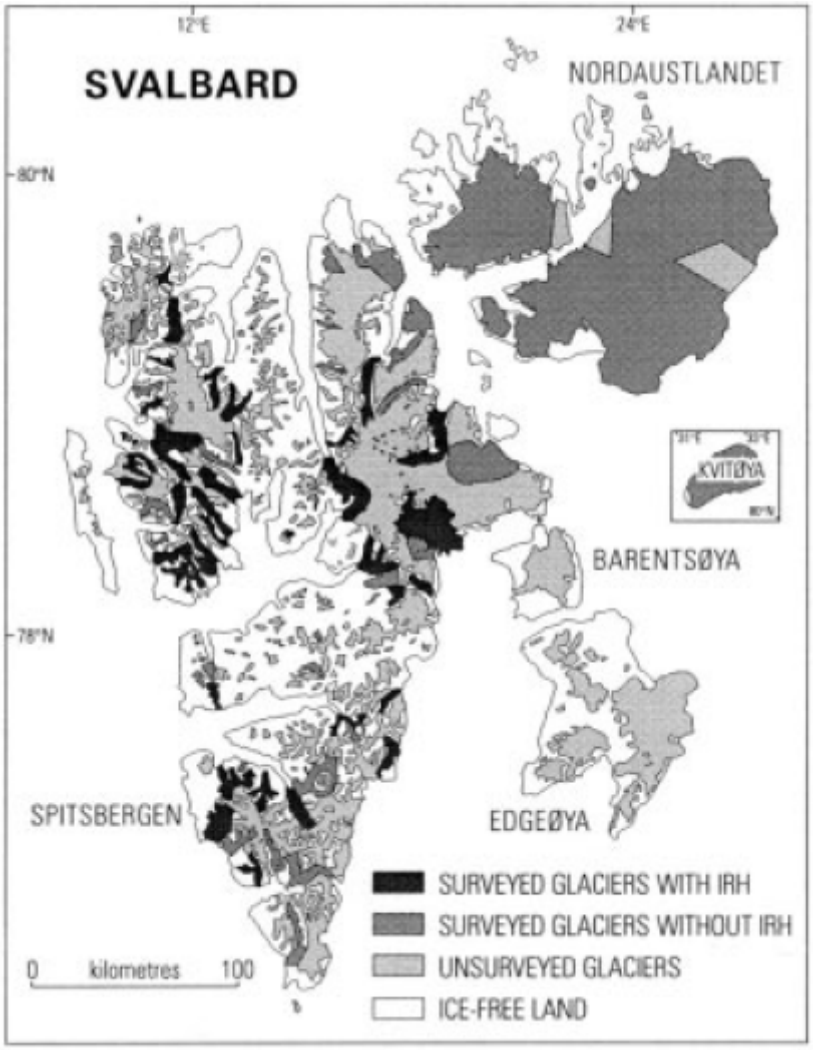

Figure 5.25: *Map of the distribution of 50 glaciers with a continuous internal reflection horizon (IRH) in dark shading. Primary data sources are 137 glaciers with radio echo-sounding data from Macheret and Zhuravlev (1982), Macheret (1990), Dowdeswell et al. (1984a), Kotlyakov and Macheret (1987) and Bamber (1987, 1988, and 1989). Although radio echo-sounding data is available for east Svalbard regions such as Nordaustlandet, glaciers with IRHs tend to be clustered in the western parts of Spitsbergen (From: Jiskoot et al., in review).*

5.5 Univariate logit modelling results

The results of the univariate logit modelling of surge-type glaciers in Svalbard are presented in the sections below. Methodology and procedures of the logit modelling technique can be found in Chapter 4. The individual variables that are included in the univariate models have been introduced earlier in this chapter (Section 5.4 and subsections). Model results for individual variables should always be compared to the model characteristics of the null model: this is the first model in all result tables (Tables 5.9 to 5.13). The null model for the full dataset (504 glaciers) gives a model deviance of 579 for 504 degrees of freedom (d.f.). The null model for the reduced dataset (137 glaciers) used to fit the IRH variable to surge-type glaciers (Section 5.12) and for all model fits to IRH (Section 5.13) gives a model deviance of 179 for 136 degrees of freedom (d.f.). A model is only significant if the reduction in model deviance, caused by the inclusion of a variable, is larger than the critical chi-square value for the associated reduction in degrees of freedom. Continuous variables take one d.f. when fitted in univariate models. For a loss of one d.f. the critical χ^2 value at a significance level of 95 percent is 3.84, hence univariate continuous models are significant when the model reduction is larger than 3.84. For categorical variables the reduction in deviance is equal to the number of classes minus one. As explained in Section 4.3.2, categorical variables are fitted in GLIM as 'factors'. The parameter for the first level of each factor is used as a baseline and the parameters for subsequent levels of the factor are expressed as differences from this base. Significant parameter estimates were converted into probabilities (see Section 4.3.3). For categorical variables the probability, as compared to the probability of the base category, gives a quantitative measure of how much the likelihood of being a surge-type glacier is increased by this class of the variable. Tables with model results include model deviance, degrees of freedom, parameter estimates and standard errors. Estimate probabilities are mentioned in the test, while discussing the model results.

5.5.1 Model fits to surge-type glaciers

Model results for continuous variables (Table 5.9).

Of the continuous variables, logtransformed glacier length caused the largest reduction in the deviance (63) from the null model. The parameter estimate (+1.186) shows that the probability of being surge-type increases with length. Including log-length in the model increases the probability of fitting surge-type glaciers with 0.79. Glacier area reduced the null model deviance by 46, and the parameter estimate was smaller (0.532) despite the relationship between area and length. Log-area only increases the probability with 0.58. Surface slope is, with a reduction in model deviance of 29 and an estimate of -0.958, significantly and negatively related to surging; univariate models suggest that glaciers with shallow slopes are more likely to surge. All four

groups of glacier altitude data are significantly related to surging. Of these, maximum altitude, with a model deviance reduction of 25, is most significant but the parameter estimate of 0.002 is very small. The large (negative) value for the intercept of the log-transformed value suggests that the log-transformed variable gives problematic values or patterns which disturb the logit regression. However, maximum altitude, just as all other altitude variables, is a log-normally distributed variable and thus log-transformation is a legitimate operations. It is beyond the scope of this research to detect the exact nature of the problem. Hence, log-transformed maximum altitude should be disregarded as a valid parameter to include in the logit models. Fowler's index is only significant when included in the log-transformed form; the estimate of 0.28 suggests that the probability of surging is raised by 0.29 when including Fowler's index in the logit model. Model results for log-transformed hypsometry index indicate that this variable is only marginally significant: bottom-heavy glaciers would have a slightly higher likelihood to be of surge-type. Finally, the estimate for latitude is negative (-0.33) and significant, suggesting that surge-type glaciers would be less likely to occur in the northern zones of the archipelago. However, the extremely large values for the intercept estimate (24.6) and standard error (8.9) indicate that this variable is erroneously fitted in the model. The accompanying model results should therefore be treated with extreme caution. To evade this problem, the variable was normalised but this only results in a partial solution. The nature of the problem with latitude and longitude data is probably hidden in the structure of logit models, but locating the exact nature of the problem is beyond the scope of this research. Therefore, latitude and longitude have to be treated as uncertain variables when assessing the model results.

Table 5.9 (overleaf): *Univariate logit modelling results for continuous variables. For each variable (left column), two models are given: one for the untransformed variable and one for the log-transformed or normalised variable. Continuous variables are significantly related to surge-type glaciers if the reduction in model deviance is more than 3.84.*

UNIVARIATE LOGIT MODELLING RESULTS: CONTINUOUS VARIABLES

Variable	Subgroup	Estimate	s.e.	Deviance	d.f.
null model	intercept	-1.036	0.101	579.64	503
latitude	intercept	24.620	8.924	571.23	502
	latitude	-0.327	0.113		
	intercept	-0.422	0.231	571.26	502
	normalised latitude	-1.236	0.431		
longitude	intercept	-1.072	0.486	579.63	502
	longitude	0.002	0.027		
	intercept	-1.051	0.205	579.63	502
	normalised longitude	0.050	0.587		
glacier length	intercept	-1.976	0.182	527.63	502
	length	0.080	0.012		
	intercept	-3.695	0.391	516.74	502
	log length	1.186	0.160		
glacier area	intercept	-1.350	0.310	549.15	502
	area	0.004	0.001		
	intercept	-2.850	0.310	533.03	502
	log area	0.532	0.081		
glacier width	intercept	-1.415	0.152	565.85	502
	width	0.088	0.025		
	intercept	-1.777	0.203	558.66	502
	log width	0.265	0.140		
glacier volume	intercept	-1.283	0.117	551.98	502
	volume	0.018	0.004		
	intercept	-1.624	0.149	533.44	502
	log volume	0.427	0.066		
surface slope	intercept	-0.043	0.223	554.61	502
	slope	-0.222	0.047		
	intercept	0.256	0.256	550.30	502
	log slope	-0.958	0.182		
maximum altitude	intercept	-2.566	0.337	554.61	502
	max altitude	0.002	0.0004		
	intercept	-11.46	2.158	554.35	502
	log max altitude	1.581	0.325		
median altitude	intercept	-1.773	0.293	572.20	502
	median altitude	0.0016	0.0006		
	intercept	-5.373	1.749	573.25	502
	log median altitude	0.718	0.288		
minimum altitude	intercept	-0.810	0.133	573.22	502
	min altitude	-0.003	0.001		
	intercept	-0.679	0.155	571.22	502
	log min altitude	-0.124	0.043		
equilibrium line altitude	intercept	-1.786	0.314	573.09	502
	ela	0.002	0.001		
	intercept	-5.079	1.783	574.36	502
	log ela	0.688	0.302		
elevation span	intercept	-2.767	0.320	541.60	502
	elevation span	0.0026	0.0004		
	intercept	-13.29	2.031	536.63	502
	log elevation span	1.896	0.311		
Fowler's index	intercept	-1.059	0.106	579.15	502
	Fowler's index	0.014	0.020		
	intercept	-0.946	0.105	569.55	502
	log Fowler's index	0.277	0.088		
AAR	base	1.360	0.553	579.28	502
	AAR	0.558	0.935		
	base	-0.751	0.264	578.10	502
	log AAR	0.504	0.437		
Hypsometry	base	1.144	0.206	579.27	502
	hypsometry	0.115	0.189		
	base	-0.964	0.106	575.32	502
	log hypsometry	0.373	0.182		

Model results for categorical variables (Tables 5.10 and 5.11).

Among the categorical variables, lithology causes the largest reduction in the null model deviance (39.77), for the loss of only three d.f.. The highest positive parameter estimates for shale/mudstone (2.63) and other sedimentary lithologies (1.15) show that the odds of surging are highest for glaciers overlying these types of bedrock. The odds are lowest for glaciers overlying igneous lithologies, with a parameter estimate of -2.34. The parameter estimate for metamorphic lithologies is not significantly different from the base category of igneous rocks, as its value is less than twice its standard error. These lithology results indicate that bed conditions associated with sedimentary beds could be favourable to surging behaviour. These results are partially consistent with Hamilton's findings for Spitsbergen, who also argued that sedimentary beds are favourable to surging, but who found the highest surge prevalence in glaciers overlying limestone lithologies (Hamilton, 1992; Hamilton and Dowdeswell, 1995). The results for geological age show that only that geology of the Triassic/Jurassic/Cretaceous age has a significantly different effect to the Precambrian base category: the probability of surging is increased with 0.39 when glaciers overly bedrock of Mesozoic age.

Univariate models of boundary type gave extremely high standard errors in each class, indicating that the class sizes were too small to be significant. The geological boundary types were therefore collapsed into larger coarser categories and subsequently two new variables were created, each consisting of four classes. The first variable describes boundary transitions from a particular geology to any other type, so from igneous, metamorphic, or sedimentary to any other type. The second variable describes transitions from any geology to a particular geology, so from any type to igneous, metamorphic, or sedimentary. In addition a class for 'unknown or absent' transitions in these variables was specified. However, none of the univariate models were significant. These results indicate that, for Svalbard, the significance of glacier length in the distribution of surge-type glaciers is not an alias for geological boundaries as was suggested by Post (1969) and Clarke (1991).

Of glacier type, only outlet and valley glaciers appear to be related to surge-type glaciers, with estimates of 1.9 and 1.7 respectively (Table 5.10). Of glacier form, surge-type glaciers seem to be more likely to have composite and multiple composite firn areas. Moreover, from the glacier form histogram (Figure 5.24) it is clear that a mere one third of all surge-type glaciers occur in glaciers with a single firm area. The type of glacier front reduced the null deviance by 14.8, which is significant for the loss of five d.f., but small compared to the other categorical variables. The positive and significant parameter estimates for confluent (0.86) and calving glaciers (0.75) indicate an increased likelihood of surging compared to the normal glacier fronts. However, glacier type, form and type of glacier front may be associated with glaciers of

particular dimensions or direction (many tide-water glaciers flow from the eastern drainage basins of Svalbard in easterly directions Lefauconnier and Hagen, 1990). It is therefore necessary to analyse these variables in a multivariate model where the significance to the likelihood of surging can be assessed while controlling for confounding effects of other variables.

Models for the fully subdivided variables for orientation of the ablation and accumulation area are significant, but only one or two of the octants have significant parameter estimates (see Table 5.10). Glacier orientation was therefore reclassified on the basis of the general patterns emerging from the diagrams of these variables (Figure 5.18). The new classification includes one class with orientations in a broad arc clockwise from north-east to south-west and one class including orientations in a broad arc from the south-west to the north-east. The reduction in the null model deviance for the reclassified orientation of the ablation area (8.6) is larger than for the orientation of the accumulation area (6.0). The positive parameter estimates for both ablation and accumulation area for the north-west to south-east orientations demonstrate that the odds of surging are significantly higher in these directions.

None of the univariate models including hypsometry or AAR variables gave significant reductions in model deviance compared to the null model. This implies that, in combination with the marginally significant model results for the *ela*, mass balance related factors are not strongly related to surge-type glaciers as is suggested by Budd (1975: see Section 2.4.6).

The categorical variable for Fowler's index gives a model deviance reduction of 18 for the loss of 2 d.f. and is thus highly significant. However, the hypothesis (Fowler, 1989) of glaciers having an index smaller than the order of one does not clearly penetrate from the parameter estimates in the model. Comparing the probability of the base category, which is defined as Fowler's index smaller than one, with that of Fowler's index larger than the order of one suggests that the probability of obtaining a surge-type glacier is only 0.01 higher for the former than for the latter. This would suggest that Fowler's index, alone, would not separate surge-type from normal glaciers as suggested by Fowler (1989).

UNIVARIATE LOGIT MODELLING RESULTS: CATEGORICAL VARIABLES					
variable	**subgroup**	**estimate**	**s.e.**	**deviance**	**d.f.**
null model	intercept	-1.036	0.101	579.64	503
orientation accumulation area	S	-1.386	0.289	566.05	496
	SW	0.521	0.416		
	W	-0.176	0.420		
	NW	-0.198	0.484		
	N	0.313	0.432		
	NE	0.948	0.407		
	E	0.672	0.385		
	SE	0.521	0.377		
orientation ablation area	S	-0.884	0.273	562.94	496
	SW	-0.190	0.412		
	W	-0.656	0.394		
	NW	-1.013	0.515		
	N	-0.188	0.421		
	NE	0.302	0.395		
	E	0.442	0.368		
	SE	-0.282	0.378		
orientation accumulation area	S, SW, W	-1.408	0.191	573.63	502
	NW, N, NE, E, SE	0.542	0.226		
orientation ablation area	S, SW, W	-1.471	0.190	571.03	502
	NW, N, NE, E, SE	0.644	0.225		
glacier type	uncertain	-2.708	0.730	562.31	498
	ice field	-3.856	9.371		
	ice cap	0.143	1.269		
	outlet glacier	1.904	0.746		
	valley glacier	1.684	0.745		
	glacieret or snowfield	-3.856	11.460		
glacier form	single firn area	-1.477	0.171	566.09	501
	composite firn area	0.585	0.266		
	>1 composite firn area	0.849	0.238		
type of glacier front (I)	normal	-1.396	0.152	564.84	498
	piedmont	0.479	0.850		
	expanded	0.397	0.468		
	lobed	-4.160	6.951		
	calving	0.752	0.229		
	confluent	0.861	0.341		
type of glacier front (II)	normal and others	-1.354	0.141	566.69	501
	calving	0.710	0.222		
	confluent	0.820	0.337		
AAR (categorical)	0.00-0.55 (negative mb)	-1.146	0.179	575.88	501
	0.55-0.60 (equilibrium mb)	0.467	0.272		
	0.60-1.00 (positive mb)	0.006	0.237		
Hypsometry (categorical)	<0.9 (top-heavy)	-0.412	0.284	576.89	501
	0.9-1.1 (equi-dimensional)	-0.773	0.247		
	>1.1 (bottom-heavy)	0.134	0.307		
Fowler's index (categorical)	<0.5 (smaller than O(1))	-0.758	0.295	561.81	501
	0.5-2.0 (approximately O(1))	0.179	0.279		
	>2 (larger than O(1))	-0.819	0.235		

Table 5.10: *Univariate logit modelling results for categorical variables. For 'orientation' both model results for the full classification and the reclassified (collapsed) version are presented. For other variables only the model results of the optimal (re-)classification is given. Categorical variables that are most likely to be related to glacier surging are those that give the highest reduction in model deviance for the associated loss in d.f. Variables are only significantly related to glacier surging if the reduction in model deviance exceeds the critical chi-square value for the associated loss in d.f..*

UNIVARIATE LOGIT MODELLING RESULTS: GEOLOGICAL VARIABLES					
variable	**subgroup**	**estimate**	**s.e.**	**deviance**	**d.f.**
null model	intercept	-1.036	0.101	579.64	503
lithology	igneous	-2.335	0.595	539.87	500
	metamorphic	0.894	0.650		
	shale/mudstone	2.631	0.610		
	other sedimentary	1.148	0.606		
geological age	Precambrian	-1.224	0.118	566.31	499
	Devonian	-0.973	0.552		
	Carboniferous/Permian	0.377	0.334		
	Triassic /Jurassic/Cretaceous	0.480	0.233		
	Tertiary	-0.511	0.651		
geological boundaries: number	zero	-1.328	0.240	577.34	501
	one	0.391	0.269		
	more than one	0.209	0.374		
geological boundaries: direction	no	-1.076	0.122	578.43	500
	perpendicular	0.298	0.317		
	parallel	0.229	0.416		
	oblique	-0.063	0.312		
geological boundaries: type I	none or unknown	-7.565	10.890	558.9	494
	igneous-igneous	0.000	13.160		
	igneous-metamorphic	7.198	10.890		
	igneous-sedimentary	6.439	10.890		
	metamorphic-metamorphic	5.000	10.940		
	metamorphic-igneous	6.718	10.890		
	metamorphic-sedimentary	6.581	10.890		
	sedimentary-sedimentary	7.026	10.900		
	sedimentary-igneous	5.773	10.900		
	sedimentary-metamorphic	6.872	10.920		
geological boundaries: type II	unknown and other-igneous	-1.253	0.358	574.21	500
	other-metamorphic	-0.259	0.458		
	other-sedimentary	0.541	0.428		
	sedimentary-sedimentary	0.269	0.382		

Table 5.11: *Univariate logit modelling results for geological variables (all categorical). Type II geological boundaries are the reclassified type I boundaries: the original classes have been combined to form fewer, larger classes Variables are only significantly related to glacier surging if the reduction in model deviance exceeds the critical chi-square value for the associated loss in d.f..*

Model results for internal reflection horizons (Table 5.12).

A separate model was created to test the hypothesis that a polythermal regime (substituted by the presence of an internal reflection horizon) is related to glacier surging (Table 5.12). As RES data were available for only 137 glaciers only these were included in the model, as for the remainder of the glaciers the thermal regime has to be treated as unknown (see Section 5.4.14). The null model for this reduced dataset gives a model deviance of 179.80 for 136 d.f. Including the dichotomous variable for thermal regime causes a significant reduction in model deviance (22 for 1 d.f.). The estimate for presence of an internal reflection horizon is 1.77 and is significant. The probability that a glacier is of surge-type glacier is increased with 0.64 for glaciers with IRH as compared to glaciers without IRH. Thus, polythermal glaciers would have a higher probability of being of surge-type than glaciers with a cold thermal regime in Svalbard (there are no completely temperate glaciers in the archipelago).

UNIVARIATE LOGIT MODELLING RESULTS: INTERNAL REFLECTION HORIZON 137 glaciers					
variable	**subgroup**	**estimate**	**s.e.**	**deviance**	**d.f.**
null model		-0.554	0.177	179.80	136
internal reflection horizon	absent	-1.275	0.259	157.73	135
	present	1.765	0.390		

Table 5.12: *Univariate logit modelling results for internal reflection horizon. This model only contains 137 glaciers with measured IRH.*

5.5.2 Model fits to internal reflection horizons

The conditional relationship between glacier surging and a polythermal regime is not clear: it is possible that thermal regime is a cause of glacier surging but it could also be an effect of glacier surging (Clarke and Jarvis, 1976; Hamilton and Dowdeswell, 1996). To detect which attributes are most strongly correlated with the presence of an IRH a new set of logit models was created. Instead of the dichotomous surge index as response variable (see Chapter 5) a dichotomous IRH index with IRH = 1 for 'presence' and IRH = 0 for 'absence' of IRH was assigned. The presence of an IRH would indicate that the glacier is polythermal and where an IRH is absent the glacier is either cold throughout or is temperate. The IRH logit models include 137 glaciers (those with measured RES: see Section 5.4.14), with 50 glaciers in the category IRH = 1 and 87 glaciers in the category IRH = 0. Significant univariate models are presented in Table 5.13.

SIGNIFICANT UNIVARIATE LOGIT MODELLING RESULTS FOR IRH 137 glaciers					
Variable	**Subgroup**	**Estimate**	**s.e.**	**Deviance**	**d.f.**
null model	intercept	-0.554	0.177	179.80	136
glacier form	single firn area	-4.060	0.171	113.08	134
	composite firn area	4.586	1.055		
	>1 composite firn area	4.583	1.044		
surge index	normal glaciers	-1.275	0.259	157.73	135
	surge-type glaciers	1.765	0.290		
latitude	intercept	65.420	16.520	161.86	
	latitude	-0.837	0.210		
longitude	intercept	6.273	1.274	134.46	135
	longitude	-0.407	0.078		
glacier length	intercept	-2.806	0.848	171.15	135
	log length	0.804	0.290		
maximum altitude	intercept	-23.420	4.823	149.81	135
	log maximum altitude	3.449	0.724		
median altitude	intercept	-9.424	3.465	172.21	135
	log median altitude	1.473	0.573		
elevation span	intercept	-23.29	4.610	146.04	135
	log elevation span	3.454	0.696		
hypsometry	base	-1.588	0.438	172.24	135
	hypsometry	1.104	0.421		
geological boundaries	unknown and other-igneous	-1.705	0.544	168.32	133
	other-metamorphic	0.655	0.699		
	other-sedimentary	1.830	0.649		
	sedimentary-sedimentary	1.395	0.612		

Table 5.13: *Significant univariate logit models to fit internal reflection horizons.*

Variables that appear to be strongest related to a polythermal regime are: glacier form (reduction in model deviance of 66 for a loss of 2 d.f); longitude (45 for 1 d.f.); elevation span (33 for 1 d.f.); maximum altitude (30 for 1 d.f.) and; surge index (12 for 1 d.f.) (Table 5.13). The supremacy of a polythermal regime (glaciers with IRH) in glaciers with one or more than one composite firn area is illustrated in Figure 5.26. Only one of the fifty glaciers with IRH has a single firn area. This is Antoniabreen (131 17) just south of Van Keulenfjorden (Figure 5.1), and has a rather artificially defined drainage basin boundary, which could easily be redefined as sharing part of the firn area with Recherchebreen (131 16) (see Hagen *et al.*, 1993). The strong correlation between longitude and polythermal regime (the negative estimate for longitude indicates that glaciers with an IRH are more likely to occur in the more western regions of Svalbard). This is not surprising as no glaciers with an IRH are found outside Spitsbergen, where they have been predominantly detected in the north-west (see Figure 5.25). Results for maximum altitude and elevation span could be related to the location of the glacier and the type of glacier form. However, models for maximum altitude, latitude and elevation span have extremely high values for the intercepts and the validity of these models should be questioned (see under univariate models for continuous variables). The results for surge index (Table 5.13) are exactly the reverse of the surge model with IRH as independent variable (Table 5.12), which is to be expected. The likelihood of a glacier having a polythermal regime is increased with a probability of 0.35 as compared to normal glaciers. However, from these univariate models no statements can be made about cause-and-effect relation of glacier surging and polythermal regime.

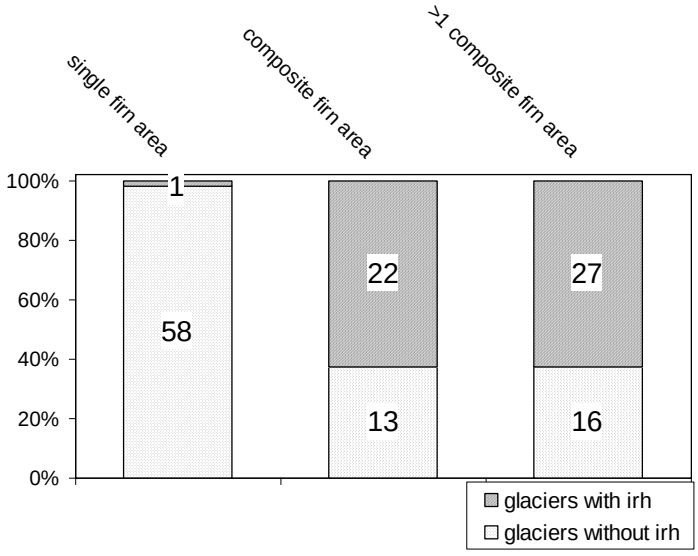

Figure 5.26: *Histograms of firn area types for glaciers with and without IRH. The numbers in the bars are the number of glaciers with or without IRH of that type of firn area.*

The fact that than the model with glacier length only gives a marginally reduction in deviance as compared to the other significant variables suggests that glacier length is only marginally related

to a polythermal regime. Moreover, nor area nor volume being significant indicated that an internal reflection horizon is not directly related to glacier size as suggested by Hamilton and Dowdeswell (1996). However, volume is not a 'real' variable and it is still possible that (measured!) glacier depth is related to the presence of and IRH. Alternatively, the distribution of IRHs could be controlled by the regular decrease in glacier thickness on Spitsbergen going north and westward (Macheret, 1981). Because glacier depth (average glacier thickness) is missing from our dataset it has not been possible to directly validate this hypothesis.

5.6 Implications from univariate data analysis

From the data presentation and univariate logit modelling results the following can be derived:

1. A large number of variables, both continuous and categorical, are strongly correlated to glacier surging, but scatterplots show that many of these are also related to each other.
2. The detailed classification of the variables lithology, orientation, geological boundary, glacier type and type of glacier front resulted in some of the classes containing too small numbers of glaciers to be statistically significant in the logit models. These models were therefore reclassified to form fewer, larger classes for modelling purpose and statistical inference. Groups were only combined if doing so resulted in sensible and physically meaningful new classes.
3. A number of variables or transformed variables appeared to give numerical problems in the logit models, emerging in extreme values for the base or intercept estimate: inferences from these models should be taken with extreme caution, and subsequently these variables will not be included in the multivariate models.
4. The variables length, area, volume, surface slope, glacier orientation, elevation span, glacier form, lithology, geological age and the presence of an internal reflection horizon emerge as most likely related to glacier surging from the univariate logit models.
5. None of the lithological boundary variables is significantly related to glacier surging nor is AAR nor hypsometry. These variables will not be included in the multivariate models in Chapter 6.
6. The variables glacier form, glacier surging and longitudinal location emerge as most likely related to the presence of an IRH from the univariate logit models.

CHAPTER 6:
Multivariate Logit Modelling Results and Residual Analysis

Tu ne prévois les événements que lorsqu'ils sont déjà arrivés

Eugène Ionesco (Le Rhinocéros, Acte 3).

6.1 Introduction

In this chapter, optimal multivariate logit models for glacier surging and for polythermal regime are presented. Thereafter follows an assessment of the model performance for individual glaciers through a residual analysis, in which the focus is on those glaciers that are classified as surge-type fitted as normal and *vice versa*. Surge evidence of these glaciers is verified through aerial photograph interpretation and it is investigated whether reclassification of these glaciers is necessary. The logit modelling methodology and residual analysis used in this chapter have been introduced in Sections 4.3 and 4.4. Parts of this chapter have been published in Jiskoot *et al.* (1998) or are under review in Jiskoot *et al.* (in review).

6.2 Confounding effects

Results from the univariate logit analysis can be biased through confounding effects between the explanatory variables, due to these variables not being independent of each other. Bivariate plots of continuous glacier data in Chapter 5 have already indicated that the environmental and glacial variables used in the analysis are indeed not independent. Correlations between log-transformed continuous glacier variables are summarised in the Pearsonian correlation matrix in Table 6.1. It can clearly be seen that many variables are strongly correlated to glacier length, either directly (e.g. accumulation area with an r^2 value of +0.90) or inversely (e.g. slope with an r^2 value of -0.83). Furthermore, strong correlations between categorical variables and continuous variables are also to be expected, for example: glacier type with glacier size. Evidently, some of the variables giving significant univariate model results are possibly not the primary controls on glacier surging, but, through strong correlation with variables that are primary controls, reflect a hidden influence on glacier surging.

Correlations in glacier systems have been analysed in context of local interactions in the glacier system (e.g. Smolyarova, 1987; Glebova *et al.* 1991) or have been used in scaling studies to mass balance and glacier characteristics world-wide (e.g. Meier and Bahr, 1996; Dyurgerov and Bahr, 1999). Other correlations can be due to conditions specific to Svalbard, for example, a large number of large calving glaciers can be found along the east coast drainage basins of Spitsbergen and locally predominantly eastward orientated (Lefauconnier and Hagen, 1991).

CORRELATION MATRIX OF CONTINUOUS GLACIER DATA														
	length	ac.area	area	volume	width	span	max	fowler	med	hypso	AAR	ela	min	slope
length	1.00													
ac.area	0.90	1.00												
area	0.89	0.98	1.00											
volume	0.89	0.97	1.00	1.00										
width	0.61	0.86	0.90	0.90	1.00									
span	0.58	0.44	0.37	0.37	0.10	1.00								
max	0.38	0.23	0.16	0.16	-0.08	0.89	1.00							
fowler	0.37	0.70	0.73	0.73	0.93	0.11	-0.04	1.00						
med	0.15	0.06	-0.01	-0.01	-0.16	0.52	0.76	-0.12	1.00					
hypso	0.10	0.00	0.02	0.02	-0.06	0.31	0.29	-0.04	-0.31	1.00				
AAR	0.09	0.19	-0.02	-0.02	-0.13	0.36	0.36	-0.10	0.35	-0.08	1.00			
ela	0.06	-0.07	-0.06	-0.06	-0.16	0.33	0.61	-0.13	0.84	-0.22	-0.07	1.00		
min	-0.55	-0.59	-0.60	-0.59	-0.54	-0.27	0.10	-0.44	0.41	-0.13	0.00	0.52	1.00	
slope	-0.83	-0.80	-0.84	-0.84	-0.69	-0.03	0.14	-0.38	0.17	0.09	0.13	0.15	0.49	1.00

Table 6.1: *Correlation coefficients of log-transformed continuous glacier data. The data are ordered on decreasing correlation with glacier length. Correlation values range from –1, for a perfect inverse correlation, to 1, for a perfect direct correlation, while 0 means no correlation. Correlation coefficients for minimum elevation are not statistically sound as this variable is not normally distributed due to the zero m asl cut-off value (glaciers do not extend to elevations beneath sea level).*

Furthermore, certain interactions in the glacier system cannot directly be confirmed through statistics but have been suggested through observations and mathematical modelling. For example, the response of glaciers is related to glacier size (e.g. Jóhannesson *et al.*, 1989), whilst research in the European Alps indicated that glacier size appears to be controlled by topographical orientation (Kasser, 1980). Therefore, we have to control for the effect of orientation on glacier size, while analysing the relation to glacier surging. Furthermore, certain ranges of variables are restricted to certain values for other variables and therefore not all combinations are physically possible. For example, by comparing different glacier types with intrinsically different geometries and typical AARs may obscure modelling of the AAR and hypsometry. To resolve this, specific examination to the interaction terms of hypsometry and AAR variables with glacier type is needed. If interaction terms show a strong correlation to surging but the single variables do not, then the likelihood of surging is confined to specific combinations of variables.

Therefore, in order to discover which variables are primary controls on surging and which are secondary we have to correct for all possible confounding effects. As is explained in Section 4.3, the multivariate logit analysis allows the combined analysis of continuous and categorical explanatory variables and the identification of the independent effects of variables whilst

controlling for the confounding effects of other variables. Provided the data are appropriate the method will identify the primary factors related to the probability of surging.

6.3 Optimal model for glacier surging

The optimal multivariate model for surge-type glaciers in Svalbard is presented in Table 6.2. All of the variables listed in Table 5.1 (Section 5.3) were tested in the multivariate models; variables that are not discussed below made no significant improvement to the model results. The optimal model includes the variables length, slope, orientation of the ablation area, lithology and geological age (Table 6.2) and causes a reduction in model deviance of 154 for a loss of 10 d.f. (χ^2_{crit}=18.3). The model is adequate, as its model deviance is less than its degrees of freedom (Francis *et al.*, 1993). Parameters with the highest estimates compared to their standard errors are those which effect the likelihood of surging most (see Section 4.3.3).

The estimate for log-length (3.224) is significantly greater that zero and the probability (0.98) significantly greater than 0.5, thus according to this model for glacier surging in Svalbard, the likelihood that a glacier is of surge-type increases with increasing glacier length. Log-transformed average surface slope gives also a large estimate (2.268) and probability (0.91) and indicated that, in combination with all other variables in the model, steep slopes increase the likelihood of surging (see also Section 6.3.1). Further, the ablation zones of surge-type glaciers tend to be orientated in a broad arc, clockwise from the north-west to the south-east although the parameter estimate is not very large (0.6911) as compared to that of length and slope. However, the probability increase of fitting a surge-type glacier is 0.67, and therefore the surging probability is increased in glaciers with orientations in this arc. However, as suggested in the qualitative description, there was a need to test whether this association results from a relationship between surging and calving glaciers, which are locally predominantly eastward orientated (Lefauconnier and Hagen, 1991). A possible length-orientation-glacier type association might confuse the results for glacier surging with one of these variables: e.g. any correlation between surge potential and orientation that is indicated in the univariate models could be resulting from a possible correlation between surging and calving glaciers. By removing calving glaciers from the analysis a decrease in the parameter significance of the relationship between orientation of the ablation zone and surging could be observed. Even so, orientation towards easterly directions gave significantly high probabilities of fitting surge-type glaciers and inclusion of this variable did result in a significant reduction in the model deviance. Hence, ‘orientation of the ablation area’ was retained in the final multivariate model.

As in the univariate model, the multivariate model shows that glaciers predominantly overlying shale/mudstone have a high positive parameter estimate (3.034), followed by other sedimentary rock types, with an estimate of 1.338. However, the estimate for sedimentary lithologies is only 1.97 times larger than its standard error, and as the rule of the thumb requires an estimate-standard error ratio of at least two, the sedimentary lithology type is (marginally) insignificant. The estimate for metamorphic rock types was not significantly different to the base category as its standard error exceeds its parameter estimate. Geological age is the last variable retained in the final multivariate model and bedrock of Devonian age has a significant negative estimate (value -1.411). The probability of 0.2 implies that with inclusion of Devonian age bedrock the likelihood of surging decreases significantly.

OPTIMAL MULTIVARIATE LOGIT FOR SURGE-TYPE GLACIERS						
Variable	**Subgroup**	**Estimate**	**s.e.**	**Probability**	**Deviance**	**d.f.**
null model	intercept	-1.036	0.101	0.26	579.64	503
intercept		-13.42	1.799	0.00	425.23	493
glacier length	log length	**3.224**	**0.456**	**0.96**		
surface slope	log slope	**2.268**	**0.495**	**0.91**		
aspect	NW, N, NE, E, SE	**0.691**	**0.264**	**0.67**		
lithology	metamorphic	0.463	0.718	0.61		
	shale/mudstone	**3.034**	**0.738**	**0.95**		
	other sedimentary	1.338	0.679	0.79		
geological age	Devonian	**-1.411**	**0.655**	**0.20**		
	Permian/Carboniferous	0.317	0.461	0.58		
	Triassic/Jurassic/Cretaceous	0.515	0.400	0.63		
	Tertiary	-0.883	0.775	0.29		

Table 6.2: *Optimal multivariate logit model for glacier surging. The figures in bold indicate the model results for variables that are significantly related to surge-type glaciers.*

6.3.1 Reversal of slope effects on surging

Many of the findings from the univariate analysis are confirmed by the multivariate analysis. However, the dependency between slope and length affects the relationships in the multivariate analysis. As can be seen in Table 5.9 (Section 5.5.1), glacier slope is inversely related to surging when fitted in a univariate model. However, when glacier length is added to the model the relation between slope and surging becomes significantly positive (Table 6.2). This indicates that with increasing length and increasing slope the probability of surging increases. The multivariate analysis therefore revealed that, once length is accounted for, the relationship between slope and surging is reversed. This reversal is a rare occurrence in logit models and is known as Simpson's paradox (Simpson, 1951). Simpson's paradox only occurs if the two variables have a strong reverse correlation, as is the case for glacier length and glacier slope (see Table 6.1).

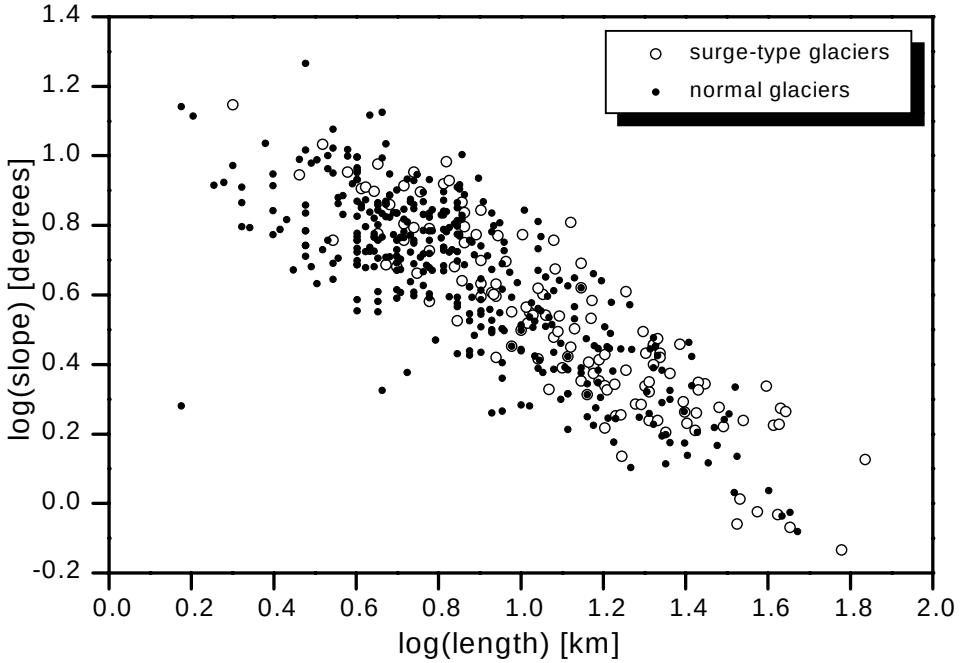

Figure 6.1: *The relation between log-transformed length and log-transformed slope for surge-type and normal glaciers: R^2=69.5%. Both the axis are logarithmic.*

The combination of length and slope in the optimal multivariate model indicate that long glaciers with steep slopes are conducive to surging. But, interpretation of 'steep' is not straightforward and depends on the length of a glacier. As the overall log-transformed surface slope decreases linearly with log-transformed glacier length, the slope of the regression line determines average length-steepness relationship (Figure 6.1). For glaciers of 7 km length the median surface slope is 4.5º, for 10 km length it is 3.5º and for 25 km length it is 1.8º. A steep glacier is therefore defined as having a slope greater than the median for glaciers of that length.

6.3.2 Evaluation of 'critical' thresholds for length and slope

Clarke *et al.* (1986) and Hamilton and Dowdeswell (1995) found a monotonic increase in surge probability with increasing glacier length (see Figure 3.1). Instead of drawing a graph where length is averaged over certain length intervals (bins), a full plot of all individual observations over the complete range of lengths can possibly reveal more detailed patterns. Although the optimal logit model generates fitted values, which are not equivalent to actual (surge) probabilities (see Francis *et al.*, 1993), this value could be seen as a likelihood that a glacier is of surge-type. Therefore plots of glacier or environmental attributes versus fitted values are an approximation of the effect of these attributes on the surge probability. The plot of length versus fitted value (Figure 6.2) reveals that the pattern is more complicated than suggested by Clarke *et al.* (1986) and Hamilton and Dowdeswell (1995). Over the whole range of lengths high and low fitted values (thus high and low surge probabilities) occur. However, the pattern for log-

transformed length suggests that only from a length of approximately 3 km (0.5 on the logarithmic scale), the fitted values are above 0.6, hence glaciers are predicted to be of surge-type. Nevertheless, Figure 6.2 does not reveal critical lengths for surge-type glaciers, nor for fitted values, nor when plotting glacier length against surge index. Moreover, Figure 6.2c and 6.2d show no clear difference in length distribution between normal and surge-type glaciers. Moreover, the patterns in these plots give no justification for the existence of two or more distinct groups of surge-type glaciers, neither do other diagrams of attributes versus fitted values. This result could however be resulting from the nature of logit models because these can not describe non-linear relations between attributed and glacier surging (see Section 4.3).

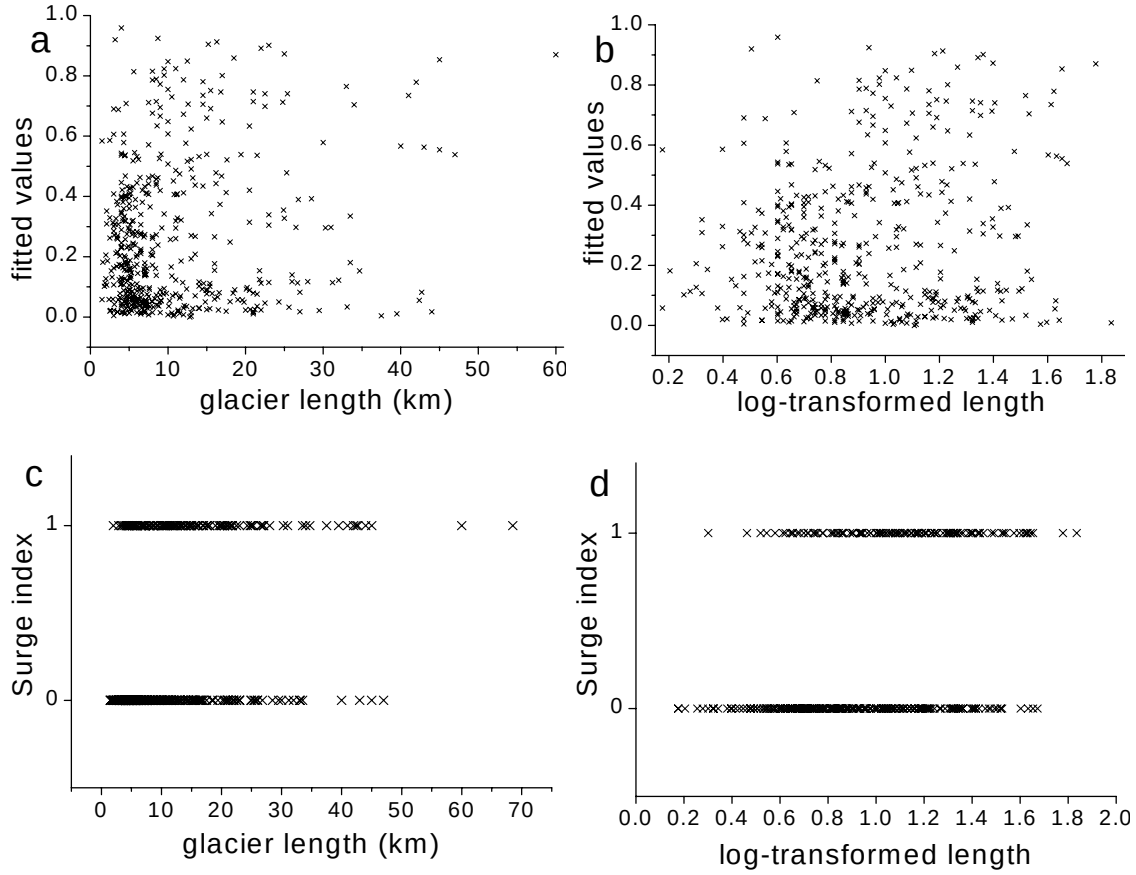

Figure 6.2: *Glacier length and fitted values.* ***a)*** *Length in km, and* ***b)*** *Length in km on a log-transformed scale. Glacier length and surge index (S=1 is surge-type glaciers, S=0 is normal glaciers)* ***c)*** *S vs. length in km, and* ***d)*** *S vs. length in km on a logarithmic scale.*

To test the hypothesis that critical geometries and critical dimensions exist for which surge instability would take place (e.g. Raymond, 1987; Clarke, 1991), a test was developed to investigate to what extent changing values for glacier length and average surface slope would change the fitted value for a glacier. By selecting one of the normal (S=0) glaciers in the database, Reidbreen (132 24), and changing its length and slope values, whilst keeping other parameters fixed, the effect of these changes on the fitted value of this glacier can be analysed

on the occurrence of critical thresholds. Critical thresholds would occur when a fitted values of a glacier changes from significantly low (0.33) to significantly high (0.66), marking the transition from a low likelihood to a high likelihood of being of surge-type.

As no experiments of this kind are known to have been performed with logit models (pers. comm. P. Boyle, 1998), the statistical significance of such experiments has not been analysed. However, because a sample set of 504 glaciers is large enough to generate a robust model (Francis *et al.*, 1993), input data changes of one unit (Reidbreen) will not affect the overall model performance. In order to verify the robustness of the model, fitted values of the remaining 503 glaciers in each of the Reidbreen models were compared to their initial fitted values. As no change occurred in any of these fitted values it can be concluded that the obtained results for Reidbreen are adequate reflections of the overall effects of length and slope on the likelihood of glacier surging as prescribed in the model.

Results of the experiments with length and slope for Reidbreen are shown in Table 6.3 and Figure 6.3. These can be summarised as four separate experiments:

1) Δ*Length*: here length is adjusted but slope is held constant at 9º (its original value),
2) Δ*Slope with length at 12 km*: here slope is varied, while length is fixed at 12 km,
3) Δ*Slope with length at 20 km*: here slope is varied, while length is fixed at 20 km,
4) Δ*Length+Slope*: here length and slope are both adjusted to generate a more physically realistic combination of glacier length and slope.

Initially, Reidbreen has a length of 4 km and a slope of 9º, and is with a fitted value of 0.11 not predicted to be of surge-type. By increasing the length with intervals of 4 to 10 km and decreasing the slope so that it approximately matches the median slope for glaciers of corresponding length, a large range of fitted values was generated. At 12 km length, the fitted value is 0.76 and the glacier is predicted to be of surge-type. To verify the effect of changing slope at this 'threshold' length, the slope was varied while keeping the length fixed. Already for a slope of 4.5º, which is steeper than the median slope of 3° for glaciers with lengths of 12 km, the fitted value is below 0.5 and the glacier is not predicted to be of surge-type. For a longer glacier (20 km), the threshold slope below which the glacier is not predicted to be of surge-type is about 2º. For the combination of length and median slope, the fitted value, thus likelihood of being of surge-type, is steadily increasing. However, none of these combinations give fitted values above 0.5, not even at a length of 20 km. This simple experiment confirms the multivariate model results for length and slope (see Section 6.3). Further it demonstrates that specific combinations of elements in the glacier system are much more critical to the likelihood of surging than controlling factors individually, even though glacier length is by far the strongest control on surging detected yet.

FITTED VALUES OF REIDBREEN TESTS					
Input data		**Model results (Fitted values)**			
Length (km)	*Slope (deg)*	ΔLength Slope is 9º	ΔSlope Length is 12 km	ΔSlope Length is 20 km	Δlength+Slope
4	***9.0***	**0.11**	0.76	0.92	**0.11**
8	*4.5*	0.51	0.44	0.79	0.19
12	*3.0*	0.76	0.25	0.63	0.25
16	*2.3*	0.87	0.15	0.48	0.31
20	*1.8*	0.92	0.09	0.36	0.36
30	*1.2*	0.97	0.04	0.17	0.43
40	*0.9*	0.99	0.02	0.10	0.50

Table 6.3*: Length and slope experiments for Reidbreen. Values in bold are the measured (actual) length and slope of the glacier and the corresponding fitted value. See also Figure 6.3.*

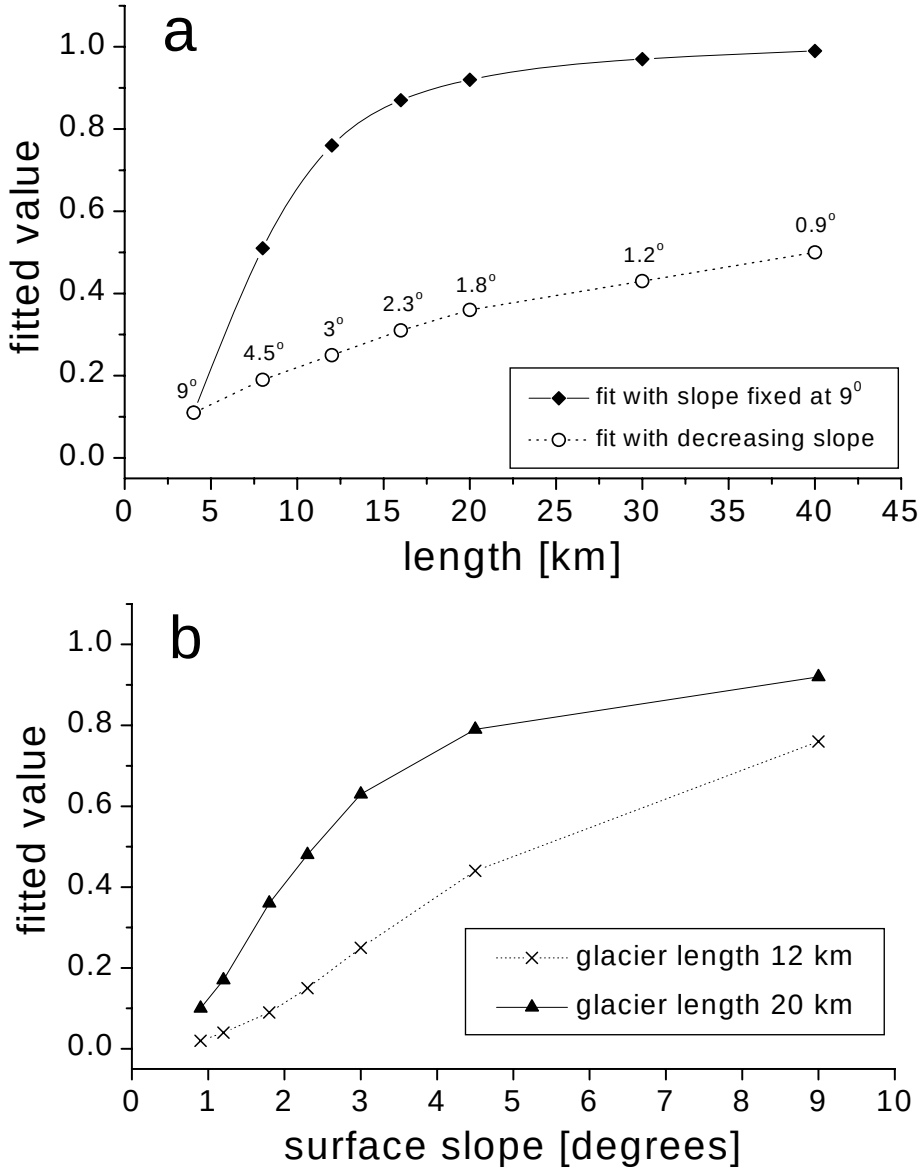

Figure 6.3*: **a)** Reidbreen experiments with increasing length and effect of changing slope, **b)** Experiments with increasing slope and length fixed at 12 and 20 km respectively.*

6.3.3 Optimal model for glacier surging with thermal regime

Conforming to the inclusion of a term for thermal regime in the univariate models (Section 5.5.1) only the 137 glaciers for which RES measurements are available can be included in multivariate models for testing of the effect of a polythermal regime on glacier surging. The optimal multivariate model for these 137 glaciers gives a significant reduction in model deviance of 54.2 for 5 d.f. (χ^2_{crit}=11.1) (Table 6.4). This optimal model includes the variables lithology, IRH and glacier length. Glaciers with a continuous internal reflection horizon, thus those inferred to have a polythermal regime, give a higher probability (0.82) of fitting a surge-type glacier than glacier length with a probability of 0.75. For this reduced dataset, the number of glaciers overlying shales or mudstones is too small (8) for this lithology class to be significant. Instead, sedimentary lithologies have the only significant estimates (1.756) and, given the probability of 0.85 are inferred to be most strongly related to surge-type glaciers. Therefore, the parameter estimates indicate that, in this subset, long polythermal glaciers underlain by sedimentary lithologies are most likely to be of surge-type. However, the full optimal model (Table 6.2) is likely to reflect the characteristics of surge-type glaciers better than the model including 137 glaciers (Table 6.4), simply because it includes 367 glaciers more than the model for glaciers with RES measurements. The results for lithology in Table 6.3 are therefore not considered as factors primarily related to glacier surging. Nonetheless, the probability results for polythermal regime indicate that this factor is probably one of the strongest influences on the distribution of surge-type glaciers, because its estimate probability is higher than that for glacier length, which is the strongest primary control of glacier surging according to the full optimal logit model.

OPTIMAL MULTIVARIATE LOGIT MODEL FOR GLACIER SURGING WITH RES

137 glaciers

Variable	Subgroup	Estimate	s.e.	Probability	Deviance	d.f.
null model	Intercept	-0.554	0.177	0.36	179.80	136
	Intercept	-5.850	1.363	0.00	125.57	131
Length	log-length	**1.125**	**0.385**	**0.75**		
thermal regime	Polythermal	**1.495**	**0.448**	**0.82**		
Lithology	Metamorphic	0.664	0.898	0.66		
	Sedimentary	**1.756**	**0.811**	**0.85**		
	shales or mudstones	10.860	14.130	1.00		

Table 6.4*: Optimal multivariate logit model for glacier surging for glaciers with available RES data. The figures in bold indicate significant model parameters.*

6.4 Optimal model for glaciers with internal reflection horizons

Following the procedures explained in Section 5.5.2 an optimal multivariate logit model was fitted for glaciers with a continuous internal reflection horizon (IRH). This model, with presence or absence of an IRH as response variable, is presented in Table 6.4. This multivariate IRH model includes 137 glaciers (those with measured RES), with 57 glaciers in the category IRH=1 and 80 glaciers in the category IRH=0. The purpose of fitting this model is to detect which attributes are most strongly correlated with the presence of an IRH, and to detect to what extent surge-type glaciers and glaciers with an IRH are mutually correlated. The optimal model for IRH causes a deviance reduction of 78.4 for a loss of 3 d.f. (χ^2_{crit}=7.81). Glacier form is most strongly and positively related to glaciers with an IRH, followed by surge-type glaciers, length and longitude (Table 6.5). The distribution of glaciers with an IRH therefore appears to be related to the distribution of long surge-type glaciers and internal reflection horizons are less likely to occur in the eastern parts of the archipelago, although glacier length is only marginally related to polythermal regime as the estimate is exactly twice as large as its standard error. Moreover, glaciers with composite firn areas increase the likelihood that a glacier is polythermal with a probability higher than 0.95.

OPTIMAL MULTIVARIATE LOGIT MODEL FOR IRH
137 glaciers

Variable	Subgroup	Estimate	s.e.	Probability	Deviance	d.f.
null model	Intercept	-0.554	0.177	0.36	179.80	136
	Intercept	-0.891	2.464	0.29	89.71	131
Longitude	Longitude	**-0.338**	**0.128**	**0.42**		
surge index	surge-type glacier	**1.685**	**0.573**	**0.84**		
glacier length	log length	**0.996**	**0.486**	**0.73**		
glacier form	Composite firn area	**3.220**	**1.172**	**0.96**		
	>1 composite firn area	**2.979**	**1.140**	**0.95**		

Table 6.5*: Optimal multivariate logit model for a polythermal regime. The figures in bold indicate the significant model parameters.*

Although the locational variable 'longitude' has no physical meaning by itself, it suggests that other spatially distributed variables could be controlling the distribution of polythermal glaciers. The distribution of glaciers with a continuous IRH could thus be related to the spatial distribution of temperature or precipitation (Bamber, 1987). Given the indication that glaciers with polythermal regime are less likely to occur in the eastern parts of the archipelago is not specific enough to correlate this finding to for example the more complicated distribution of precipitation over the archipelago. However, as the parameters for *ela*, hypsometry and AAR do not significantly improve the multivariate model, it is uncertain if a polythermal regime is directly related to climate factors. Macheret (1981) suggested that the regular decrease in glacier

thickness on Spitsbergen going north and westward might control the distribution of glaciers with IRH. Ideally tests should be performed to the interaction between glacier depth and the presence of an IRH, but no data was available for glacier depth. As explained in Chapter 5 (Section 5.4.6), glacier volume was calculated from area using three empirical formulae, hence does not allow for the differentiation of various glacier types such as glaciers with IRH and without IRH, or surge-type glaciers and normal glaciers. Therefore, volume cannot be used as a proxy for glacier depth. Furthermore, glacier length is only marginally significant in the IRH logit model: inclusion reduced the model deviance with 4.53 while the χ^2_{crit} is 3.84 and gives lower probabilities of fitting a polythermal glacier than other parameters included in the model (see Table 6.5). Although this suggests that no strong relation between glacier depth and a polythermal regime exists, not until measured glacier thickness data are available the exact relation between polythermal regime and ice thickness can be verified.

Because the effect of surge behaviour on the presence of a polythermal regime is almost the reverse of the effect of the presence of a polythermal regime on surge behaviour, the dilemma of cause and effect concerning thermal regime and glacier surging is still an ongoing debate (e.g. Clarke and Jarvis, 1976; Hamilton and Dowdeswell, 1996).

6.5 Evaluation of model performance through residual analysis

The optimal multivariate model for 504 glaciers was evaluated through generation of fitted values and residuals for each individual glacier. In this way 'unusual' glaciers can be identified: these are surge-type or normal glaciers that have different characteristics from the characteristics of majority of surge-type or normal glaciers in the dataset.

The model performance (Figure 6.4) can be expressed by the match between the initial surge classification (S) and the fitted values ($\hat{S}$). The general trend of the model performance is positive. The fit for the majority (86%) of the normal glaciers was good with estimated fits between 0.0 and 0.4. Of the surge-type glaciers 35% were predicted with fits larger than 0.6. The ten surge-type glacier with the highest fitted values ($\hat{S}$>0.85) in the logit model were, in decreasing order of goodness of fit: Hinlopenbreen (173 10), Strongbreen (115 02), Penckbreen (132 05), Chydeniusbreen (173 07), Monacobreen (162 11), Negribreen (111 05), Besselbreen (322 02), Stonebreen (313 18), Finsterwalderbreen (132 02) and Liestølbreen (132 17). All these glaciers have strong evidence for surging or have a recorded surge. These 10 glaciers are all overlying sedimentary lithologies, most of these are of tide-water type and all glaciers except Finsterwalderbreen (11 km) are longer than 20 km. Of the 317 normal glaciers with low fitted values the 10 lowest fitted values ($\hat{S}$<0.01) have length ranges between 5-29 km. Most of these

glaciers are of the icecap type, but the two glaciers with the lowest fit ($\hat{S}$<0.001) are the only two glacierets (numbers 251 03 and 171 03) in entire Svalbard dataset. Glacierets are by definition not of surge-type. Four of the lowest fit glaciers are overlying sedimentary-, three metamorphic- and three igneous lithologies.

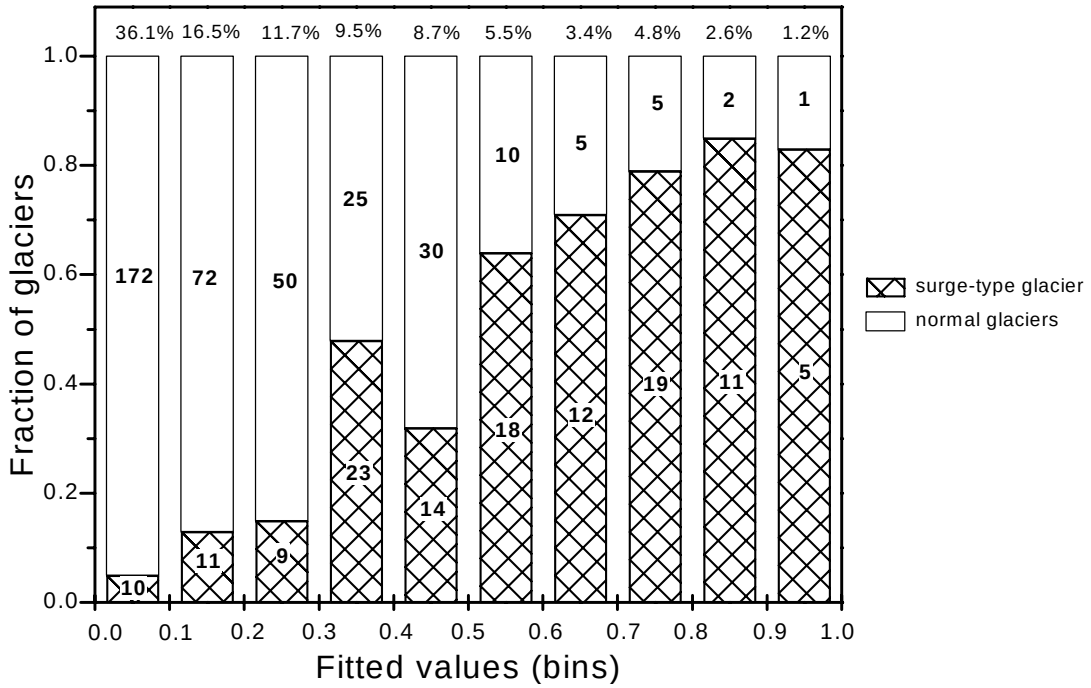

Figure 6.4: *The model performance shown as fraction of glaciers predicted in each of the 10 bins of fitted values (0.0<$\hat{S}$<0.1, 0.1<$\hat{S}$<0.2, etc.). Glaciers with high fitted values ($\hat{S}$>0.6) are predicted to be of surge-type while glaciers with low fitted values ($\hat{S}$<0.4) are predicted to be non-surge-type. The percentages on top of the bars indicate the percentage of glaciers in each bin and the numbers in the bars are the numbers of normal and surge-type glaciers in each bin. The figure shows a direct relationship between increasing fit and fraction of surge-type glaciers.*

The distribution of average fitted values for each drainage basin of the archipelago can be seen in Figure 6.5. It is notable that the higher fitted values occur along in the eastern drainage basins of Spitsbergen and on Barentsøya. Comparing this distribution to that of the actual distribution of surge-type glaciers over the archipelago (Figure 5.7), shows that the pattern created with the logit model defined characteristics of surge-type glaciers is oversimplified and regions such as eastern Nordaustlandet and east and north-eastern Spitsbergen are not identified as cluster regions for surge-type glaciers. This implies that many glaciers in these regions have not been fitted well in the model: these glaciers give large residuals. Residuals above one are glaciers classified as surge-type glaciers but have very low fits in the model ($\hat{S}$<0.35), while residuals smaller than -0.8 are normal glaciers with high fitted values in the model ($\hat{S}$>0.65). Visual interpretation of residual plots with pronounced patterning can then help to understand what is distinctive of these glaciers. If a systematic pattern occurs, for example high or low residuals only occurring on certain lithologies, it will transpire whether the model 'overpredicts' or

'underpredicts' surging on that lithology (Wrigley, 1985). Furthermore, examination of residual patterns could suggests introduction of a new explanatory variable that might control the distribution of surge-type glaciers.

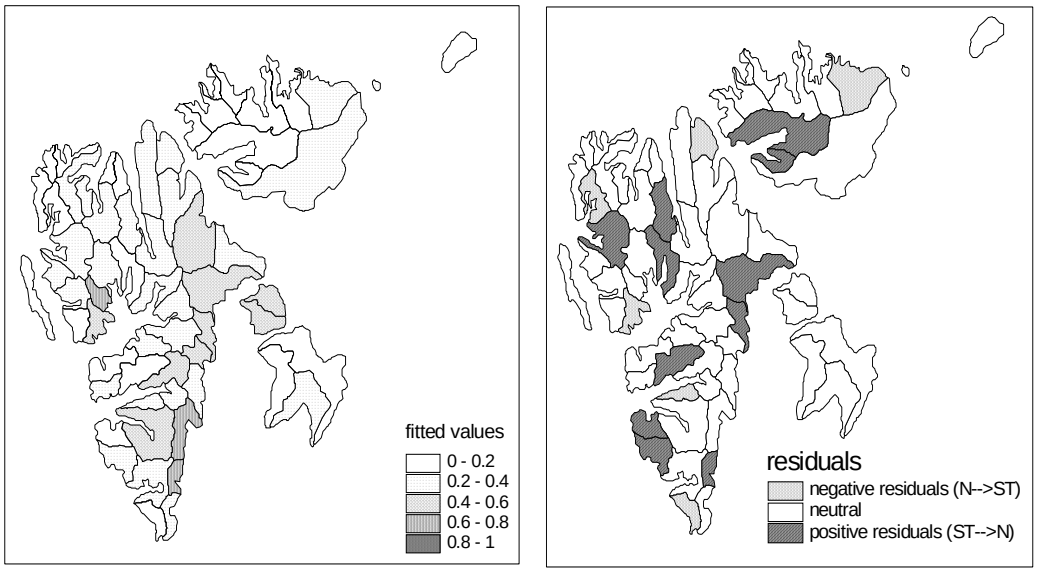

Figure 6.5: a) *Average fitted values for glaciers in each drainage basin.* ***b)*** *Average residual values for each drainage basin. Some drainage basins accommodate few glaciers (<5) and for these the average values are not statistically sound. N→ST indicates that negative residuals are glaciers classified as normal (S=0) but predicted by the model to be of surge-type, and ST→N indicates that positive residuals are glaciers classified as surge-type (S=1) but predicted by the model to be normal.*

The glaciers with large (absolute) residuals were divided into two classes. Class A includes glaciers listed in the inventory as normal but having high fitted values ($\hat{S}$>0.6) in the model. Class B includes glaciers listed as surge-type but have low fitted values in the logit model ($\hat{S}$<0.4). The general distribution of class A and class B glaciers is presented in Figure 6.5b. The spatial pattern in this figure represents the discrepancy between the actual distribution of surge-type glaciers over the archipelago (Figure 5.7) and the modelled distribution (Figure 6.5a).

Class A contains 13 glaciers (3.5% of the normal glaciers) of which 8 have fitted values larger than 0.7. The characteristics of these glaciers suggest that they are of surge-type according to the optimal model. The author re-examined aerial photographs of these 13 glaciers predicted to be of surge-type. Morphological evidence (e.g. Figure 6.6) showed that seven of these should be re-classified as surge-type (see Table 6.6). The length and slope characteristics of these seven glaciers are shown in Figure 6.6 as comparison to ten glaciers of Class B having low model fits. A clear trend can be seen of increasing fit with glacier length as well as with decreasing glacier slope. For the glaciers with an intermediate length range of 8-13 km (log-transformed length 0.9-1.1), glaciers with steeper slopes (numbers 3 and 8) are predicted to be of surge-type, whereas glaciers with low slopes (e and b) are predicted to be non-surge-type.

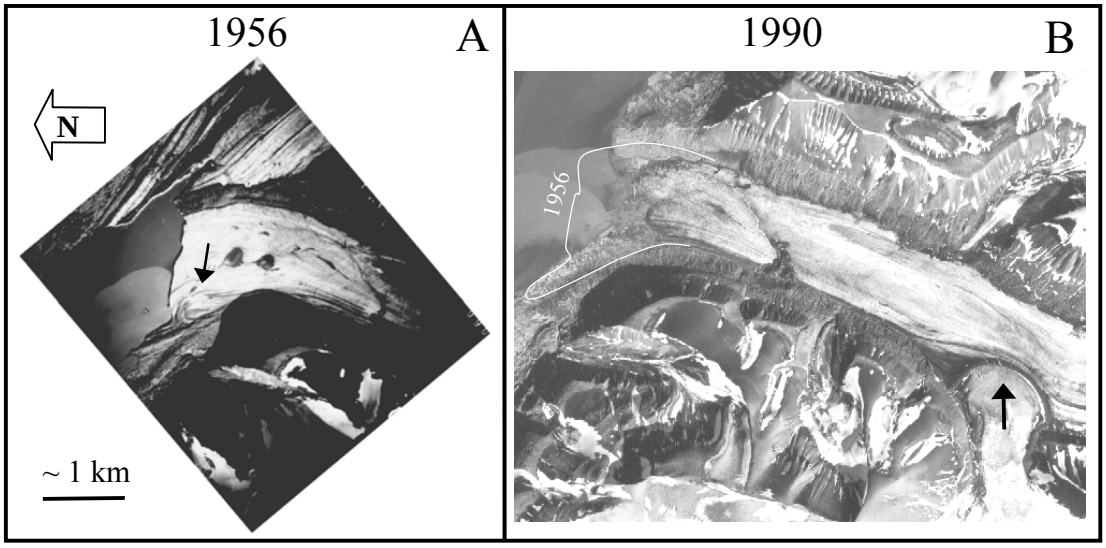

Figure 6.6: *Surge evidence of Scheelebreen.* ***(a)*** *Part of 1956 aerial photograph (S56 6060, © Norsk Polarinstitutt) showing the confluent tide-water margins of Scheelebreen, Paulabreen and Bakaninbreen at the head of van Mijenfjorden, SW Spitsbergen. The lower 5 km of Scheelebreen is visible including an elongated moraine loop (see arrow). This loop originates at a western tributary (Luntebreen) 6 km from the margin (just off this photo, but visible on b).* ***(b)*** *Part of 1990 aerial photograph (S90 3270, © Norsk Polarinstitutt) showing the lower 7 km of Scheelebreen. Since 1956 Scheelebreen has retreated 1.5 km and has become landbased. The elongated moraine loop has disappeared, but Luntebreen is forming a new loop while protruding onto the glacier surface (see arrow). At a next surge this loop will be elongated along with the trunk of Scheelebreen. Both photographs are approximately at the same scale.*

EVIDENCE FOR SURGE BEHAVIOUR				
Glacier	**Type**	**Fit**	**Morphological Evidence**	**Interpretation**
Zawadskibreen	tide-water	0.93	Elongated moraine loops (1961) Block-like flow	surge-type
Nordsysselbreen	Confluent	0.86	Looped medial and terminal moraines (1936) Convex cross-section	surge-type
Helsingborgbreen	Valley	0.82	Tributary loop elongated to terminus (1961) Rapidly depleting glacier Compound frontal moraine complex	surge-type
Sveabreen	tide-water	0.79	S-tributary has contorted moraine (1936) Chaotic crevasse-patterns	surge-type
Petermannbreen	tide-water	0.75	Convex cross section Undulating surface	?
Nordenskioldbreen	tide-water	0.74	Elongated moraine loops stand above depleted surface (1936 and 1948) Crevassed surface	surge-type
Kantbreen	tide-water	0.73	Looped moraine stands above surface (1936) Elongated moraine loops (1966)	surge-type
Scheelebreen	was tide-water	0.72	Moraine loop elongated to terminus (1956) Depleted surface	surge-type

Table 6.6: *Glaciers listed as normal in the glacier inventory (Hagen et al., 1993) but predicted as surge-type in the optimal logit model with model fits larger than 0.7. Morphological evidence for surge behaviour was derived from aerial photographs; the years in this column indicate the photo year(s) with the strongest morphological evidence.*

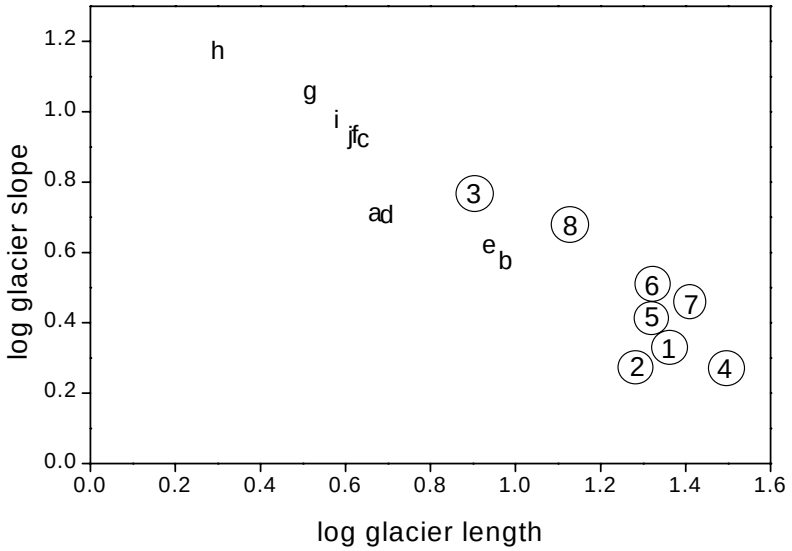

Figure 6.7: *Length and slope characteristics of eight normal glaciers predicted to be of surge-type with model fits higher than 0.7 (numbers 1-8) and ten surge-type glaciers predicted not to be of surge-type with model fits smaller than 0.1 (letters a-j). The numbered (normal) glaciers correspond to: 1=Zawadskibreen, 2=Nordsysselbreen, 3=Helsingborgbreen, 4=Sveabreen, 5=Petermannbreen, 6=Kantbreen, 7=Nordenskioldbreen, 8=Scheelebreen. Aerial photograph interpretation led to the reclassification of some of these as surge-type (Tables 6.6 and 6.7). The lettered (surge-type) glaciers correspond to: a=Wandbreen, b=Werenskiolbreen, c=Scottbreen, d=Martinbreen, e=Pedasjenkobreen, f=S-Crammerbreen, g=Livbreen, h=Arebreen, i=Plogbreen, j=Fyrisbreen.*

Of concern is that there may be other glaciers that are coded as non-surge-type which have no high residuals in the model but have nonetheless (previously undetermined) surge characteristics. To check whether any detailed aerial photograph interpretation would reveal a considerable number of 'new' surge-type glaciers, a detailed aerial photograph interpretation on a control set of 30 random selected glaciers was undertaken. These glaciers are a mixture of surge-type and normal glaciers with a large range of fitted values and distributed randomly over the archipelago (see Appendix I). Aerial photograph interpretation of this control set of glaciers only disclosed clear evidence for surging on Svalbreen (124 10) and probable evidence on north-east Buchananisen (151 08). Possible, but no convincing surge features were found on ten further glaciers. The probability of reclassification from a random survey is thus between 7 and 20% whereas the probability of reclassification using the model results is more than 50%.

Class B contains 55 glaciers with fitted values between 0.0 and 0.4. The length and slope characteristics of the ten surge-type glaciers with fits lower than 0.1 are shown in Figure 6.7 as comparison to the seven glaciers of Class A with high model fits and surge characteristics. In total 41% of the surge-type glaciers were predicted not to be of surge-type with values lower than 0.4. It is possible that some of these glaciers have stopped surging as a result of present mass balance conditions (Dowdeswell *et al.*, 1995). These glaciers may have lapsed out of the

population of surge-type glaciers and, at present, have characteristics that are not favourable to surging. Also, some of the glaciers that have low fitted values might not be of surge-type after all, but the observed advance might have been the Little Ice Age maximum, which occurred around 1900 in Svalbard (Lefauconnier and Hagen, 1991). In total 12 glaciers in class B had surges inferred in the period between 1850 and 1936. I double checked these glaciers on surge evidence in literature and on aerial photographs and concluded that two of these (Austre Brøggerbreen (155 04) and Midre Lovénbreen (155 06)) did not have strong enough evidence to classify them as surge-type. Consequently, these glaciers were reclassified as normal glaciers (see Table 6.7). The primary surge evidence for these glaciers was originally derived from expedition material and photographs of Hamberg in 1895, who reported the glacier fronts as very much advanced, steep and crevassed (Liestøl, 1990). Since this advanced position coincides with the glacier maximum at the end of the Little Ice Age, it is not completely clear if these advances were indeed the result of a surge. At present, both glaciers are very much depleted and retreated from the terminal moraine complex, while the medial moraines stand as prominent ridges above the terminus and continue into the proglacial area.

Glaciers in class B can be grouped according to 'conditions unfavourable for surging', which can be derived from the spatial distribution of these glaciers over the archipelago (see Figure 6.5). A cluster of surge-type glaciers with high residuals occurs in the north-west of Spitsbergen. All these surge-type glaciers are relatively small, and hence, have low fitted values in the model. A second cluster of poorly fitting surge-type glaciers can be found in eastern central Spitsbergen and Nordaustlandet: most surge-type glaciers in these areas are very large but have extremely low slopes. These findings agree with the observation that the ice surface profiles of most Nordaustlandet surge-type glaciers lie below their theoretical profiles (Dowdeswell, 1986). As data collection at the compilation of the glacier inventory (1980-81; Hagen *et al.*, 1993) might have been within a few decades after a surge or just prior to a surge, the overall slope and geometry of a glacier could be unfavourable for surging. For example, Palanderbreen (221 02) and Bodleybreen (222 06) surged in 1969 and between 1970 and 1980 respectively (Lefauconnier and Hagen, 1991). These glaciers might be building up to a new surge in the future, providing the outflow is restricted and consequent steepening of the overall profile takes place. Thirdly most of the poorly fitting surge-type glaciers in drainage basins south-west and north Spitsbergen overlie bedrock that is not favourable to surging such as the Precambrian metamorphic Hekla Hoek lithologies. However, plotting residuals against variables in the model did not reveal obvious overprediction or underprediction of specific variables, neither could additional controlling factors be revealed through the spatial analysis of residuals.

6.6 Model results with a new surge classification

Results from the aerial photograph interpretation and model results of the optimal logit model led to the reclassification of 25 glaciers in the database. Nineteen glaciers were added to the class of surge-type glaciers. Six glaciers were removed from that class as, after reconsideration, it was decided that the evidence for surge behaviour was not strong enough to state that there had been surges in the past nor could evidence be found for future surge behaviour (see Table 6.7). From the 504 glaciers a total of 145 are now classified as surge-type (S=1) and 359 as normal (S=0). This means that according to the data presented in Chapers 5 and 6 of this thesis, 14% of the glaciers larger than 1km^2 in Svalbard are of surge-type. The location of these 145 surge-type glaciers is given in Figure 6.8, which is an updated map from previously published material (Dowdeswell *et al.*, 1991).

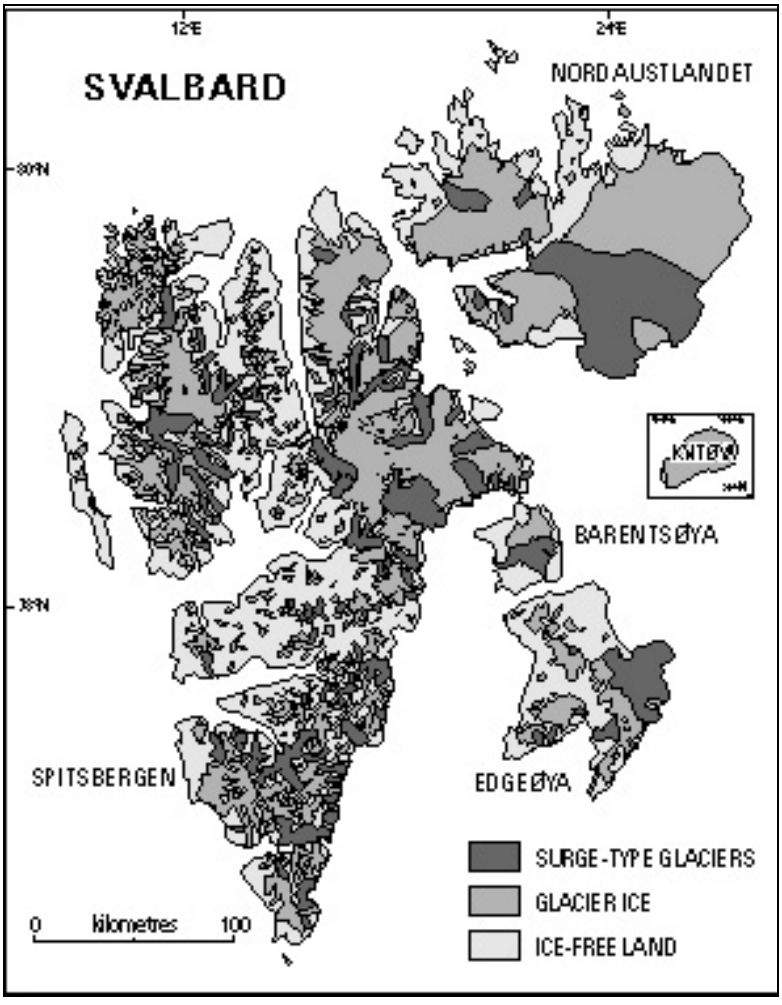

Figure 6.8: *Map of Svalbard with the updated distribution of surge-type glaciers in dark shading. These 145 surge-type glaciers include glaciers with an observed surge and those with clear morphological evidence of surge activity. This distribution of surge-type glaciers represents the reclassified glacier data (S_{NEW}). This map is an update of Fig. 1 from Dowdeswell et al. (1991). (From: Jiskoot et al., in review).*

RECLASSIFIED GLACIERS	
***ADDED* to surge-type list**	***REMOVED* from surge-type list**
Beresnikovbreen*	Austre Brøggerbreen[1]
Bergmesterbreen	Comfortlessbreen[3]
Borebreen	Deltabreen[3]
Hannbreen	Körberbreen[3]
Helge Backlundbreen*	Midre Lovénbreen[1]
Helsingborgbreen	Wandbreen[2]
Hornbreen	
Kantbreen*	
Mittag-Lefflerbreen	
Nordenskiöldbreen	
Nordsysselbreen	
North-east Buchananisen	
Orsabreen	
Samarinbreen	
Scheelebreen	
Storbreen	
Svalbreen	
Sveabreen	
Zawadskibreen	

Table 6.7: *Reclassified glaciers based on logit model results and verification by aerial photograph interpretation. In the new surge classification (S_{NEW}) 19 glaciers were added to the original list of surge-type glaciers and 6 removed from it. The glaciers removed from the list were originally interpreted as surge-type by [1]Liestøl (1993), [2]Lefauconnier and Hagen (1991) or [3]Croot (1988). Glaciers marked * in the 'added' list were already suggested to be of surge-type by Lefauconnier and Hagen (1991). Other glaciers in this column were not recognised as surge-type previously (After: Jiskoot et al., in review).*

A new optimal logit model was fitted with the corrected classification (S_{NEW}) as the changed values for the response variable might give different results in terms of surge controls. Large changes were neither expected nor observed as less than 5% of the glacier data were reclassified. The overall pattern of the optimal model for S_{NEW} (Table 6.8) is similar to the optimal model for S (Table 6.2): the parameter estimates only changed slightly. The only notable change is that now not only shale and mudstone but also other coarse-grained sedimentary bedrock is conducive to surging, although to a lesser extent than the fine-grained sediments. But, fitting elevation span (Table 6.9) instead of average surface slope improved the model slightly by reducing its model deviance by 0.51 for the same degrees of freedom. In this model the effect of glacier length on surging is being reduced from a probability of 0.99 to 0.8, while parameter estimates for other variables remain the same. Although the correlation (see Table 6.1) between glacier length and elevation span is not very strong (0.58), and that between slope and elevation span virtually non-existent (0.03) there are apparently confounding effects between these variables that obscure which controls on surging are primary and which are secondary (see Section 5.4.9 for discussion). Although glacier length is still a primary control in this optimal model, the effect of surface slope on surging is completely replaced by that between elevation span and surging. This suggests that interpretation of glacier slope in terms of controls on glacier surging is more complicated than initially suggested (Section 6.3). Hence, critical

analysis of this term in terms of physical significance is needed and furthermore, elevation span could imply a hitherto disregarded climate related control on surging.

OPTIMAL MODEL WITH S_{NEW} ……. INCLUDING SLOPE						
Variable	**Subgroup**	**Estimate**	**s.e.**	**Probability**	**Deviance**	**d.f.**
null model	Intercept	0.926	0.098	**0.72**	601.21	503
intercept		-18.190	2.125	0.00	386.62	493
glacier length	Log length	4.542	0.543	**0.99**		
surface slope	Log slope	3.178	0.552	**0.96**		
aspect	NW, N, NE, E, SE	0.821	0.278	**0.69**		
lithology	Metamorphic	0.566	0.756	0.64		
	Shale/mudstone	3.293	0.769	**0.96**		
	Other sedimentary	1.468	0.704	**0.81**		
geological age	Devonian	-1.126	0.673	0.24		
	Permian/Carboniferous	0.464	0.503	0.61		
	Triassic/Jurassic/Cretaceous	1.291	0.430	**0.78**		
	Tertiary	0.612	0.703	0.65		

Table 6.8: *Optimal multivariate model for the distribution of surge-type glaciers based on the reclassified surge index (S_{NEW}). This model contains 504 glaciers and the reduction in model deviance is 218 for a loss of 10 d.f (χ^2_{crit}=18.3). The figures in bold indicate the significant model parameters.*

OPTIMAL MODEL WITH S_{NEW}……. INCLUDING ELEVATION SPAN						
Variable	**Subgroup**	**Estimate**	**s.e.**	**Probability**	**Deviance**	**d.f.**
null model	intercept	0.926	0.098	**0.72**	601.21	503
intercept		-27.400	3.601	0.00	386.09	493
glacier length	log length	1.369	0.2332	**0.80**		
elevation span	log span	3.194	0.5513	**0.96**		
aspect	NW, N, NE, E, SE	0.8128	0.2785	**0.69**		
lithology	metamorphic	0.5579	0.7596	0.64		
	other sedimentary	1.467	0.7077	**0.81**		
	shale/mudstone	3.299	0.7721	**0.96**		
geological age	Devonian	-1.125	0.6728	0.25		
	Permian/Carboniferous	0.4698	0.5035	0.62		
	Triassic/Jurassic/Cretaceous	1.293	0.4298	**0.78**		
	Tertiary	0.5971	0.7018	0.64		

Table 6.9: *Optimal multivariate model for the distribution of surge-type glaciers based on the reclassified surge index (S_{NEW}). This model contains 504 glaciers and the reduction in model deviance is 218 for a loss of 10 d.f (χ^2_{crit}=18.3). The figures in bold indicate the significant model parameters.*

Another model with the S_{NEW} classification was fitted for the 137 glaciers with a known thermal regime. Fifteen glaciers (11%) in this subset changed class. The main difference between this model (Table 6.10) and the initial IRH model (Table 6.4) is that now the mass balance related variables (AAR and elevation span) are included, although the model reduction and parameter estimates for these variables are only marginally significant. However, this indicates that the model is very sensitive to changing the response variable for a relatively small number of glaciers as the total number of glaciers in the model is limited to 137.

OPTIMAL MULTIVARIATE LOGIT MODEL WITH S_{NEW} FOR IRH 137 glaciers						
Variable	**Subgroup**	**Estimate**	**s.e.**	**Probability**	**Deviance**	**d.f.**
null model	intercept	-0.339	0.173	**0.42**	186.04	136
	intercept	-20.890	6.836	0.00	103.70	128
length	log-length	1.398	0.503	**0.80**		
thermal regime	polythermal	1.120	0.547	**0.75**		
elevation span	log-span	2.163	1.123	**0.90**		
lithology	metamorphic	0.488	1.050	0.62		
	sedimentary	2.097	0.950	**0.89**		
	shales or mudstones	11.080	13.870	1.00		
AAR	AAR<0.55	-0.213	0.564	0.45		
	0.55<AAR<0.60	1.475	0.688	**0.81**		

Table 6.10: *Optimal multivariate model for the distribution of surge-type glaciers using glaciers with measured RES and the corrected surge classification (S_{NEW}). The model includes 137 glaciers and the reduction in model deviance is 83 for a loss of 8 d.f. (χ^2_{crit}=15.5).*

6.7 Implications from the multivariate data analysis

The specific combinations of parameters and explanatory variables in the optimal multivariate model for the full dataset indicate that, in Svalbard, long glaciers with relatively steep slopes overlying relatively young fine-grained sedimentary lithologies, with orientations in the arc NE to SW are most likely to be of surge-type. The observation that long glaciers are more likely to be of surge-type is in accordance with previous studies (Clarke *et al.*, 1986; Hamilton, 1992). However, the positive and significant results for glacier slope (Table 6.2) do not match the conclusions of previous research, where no significant positive relationship between surging and surface slope was detected while controlling for glacier length (Clarke, 1991; Hamilton, 1992). Furthermore, the significant increase of fitting surge-type glaciers correctly when a measure for thermal regime (RES) is included suggests that, in Svalbard, polythermal regime is related to glacier surging. Although composite firn areas were found to control polythermal regime, this attribute did not affect the models for surge-type glaciers. The significance of the polythermal regime in models fitting surge-type glaciers together with the significance of surge-type glaciers in models fitting polythermal glaciers suggest that surging and polythermal regime are mutually related. However, the models were unable to disclose the cause and effect dilemma of surging and thermal regime. Finally, inspection of glaciers with large residuals led to the reclassification of 25 of these: 19 glaciers were added to the list of surge-type glaciers and 6 were removed from this list. Hence, the optimal logit model can be used as a predictive tool in glacier surging. Optimising a new multivariate logit model for glacier surging, including the 25 reclassified glaciers, suggests that the interpretation of average glacier slope in discriminating between surge-type and normal glaciers is possibly not as straightforward as was derived from the initial optimal logit model results, because surface slope can be substituted by elevation span. This result implies that climate related factors could after all control surge behaviour.

CHAPTER 7:
Characteristics and Surge Behaviour of Sortebræ

The ice was here, the ice was there
The ice was all around
It cracked and growled, and roared and howled
Like noises in a swound

ST Coleridge (Ancient Mariner)

7.1 Introduction

The behaviour of Greenland's surge-type glaciers is inadequately documented (e.g. Rutishauser, 1971; Colvill, 1984; Weidick, 1988) and quantitative data are particularly sparse for this region (e.g. Reeh *et al.*, 1994; Joughin *et al.*, 1996; Mohr *et al.*, 1998). Six surges have been documented for West Greenland and only four in East Greenland (Weidick, 1988). With the documentation and quantitative description of the surge behaviour of Sortebræ it is hoped to fill a gap in the knowledge about glacier surging in Greenland. A secondary purpose of this chapter is to connect environmental setting and glacier morphology to specific behaviour and development of surging glaciers. Furthermore, the data presented on Sortebræ's surge will provide information on specific discharge properties of surging tidewater glaciers in Greenland.

During the compilation of a surge-type glacier inventory of East Greenland at the Geological Survey of Greenland and Denmark (GEUS), Sortebræ (Figure 7.1) was identified from 1981 aerial photographs as a surge-type glacier. Surge evidence includes characteristic elongated moraine loops of tributaries, surface pitting and the bulging protrusion of tributaries onto the trunk. Stereo photographs taken during the 1994 and 1995 geological expeditions of the Danish Lithosphere Centre (DLC) to East Greenland (Larsen *et al.*, 1995) revealed an active surge: Sortebræ was completely crevassed, the upper basin had lowered dramatically and the glacier had advanced into the fjord. Because of the wealth information available at GEUS and DLC it was decided to undertake a detailed study of the surge history and the 1990s surge of Sortebræ.

7.2 Location and dimensions of Sortebræ

Sortebræ (68°45′N, 27°05′W) is a surge-type tidewater glacier in central East Greenland draining from the Geikie Plateau into a Blosseville Kyst fjord bordered by Kap Savary to the south and Kap Daussy to the north (Figure 7.1). Sortebræ is Danish for *Black glacier*, a name that is probably based on the black appearance of the glacier surface and calving ice cliff, caused by an abundance of dark moraine ridges. All other names used to describe the different components of Sortebræ in this chapter (see Figure 7.1) are unofficial names assigned by the author of this thesis.

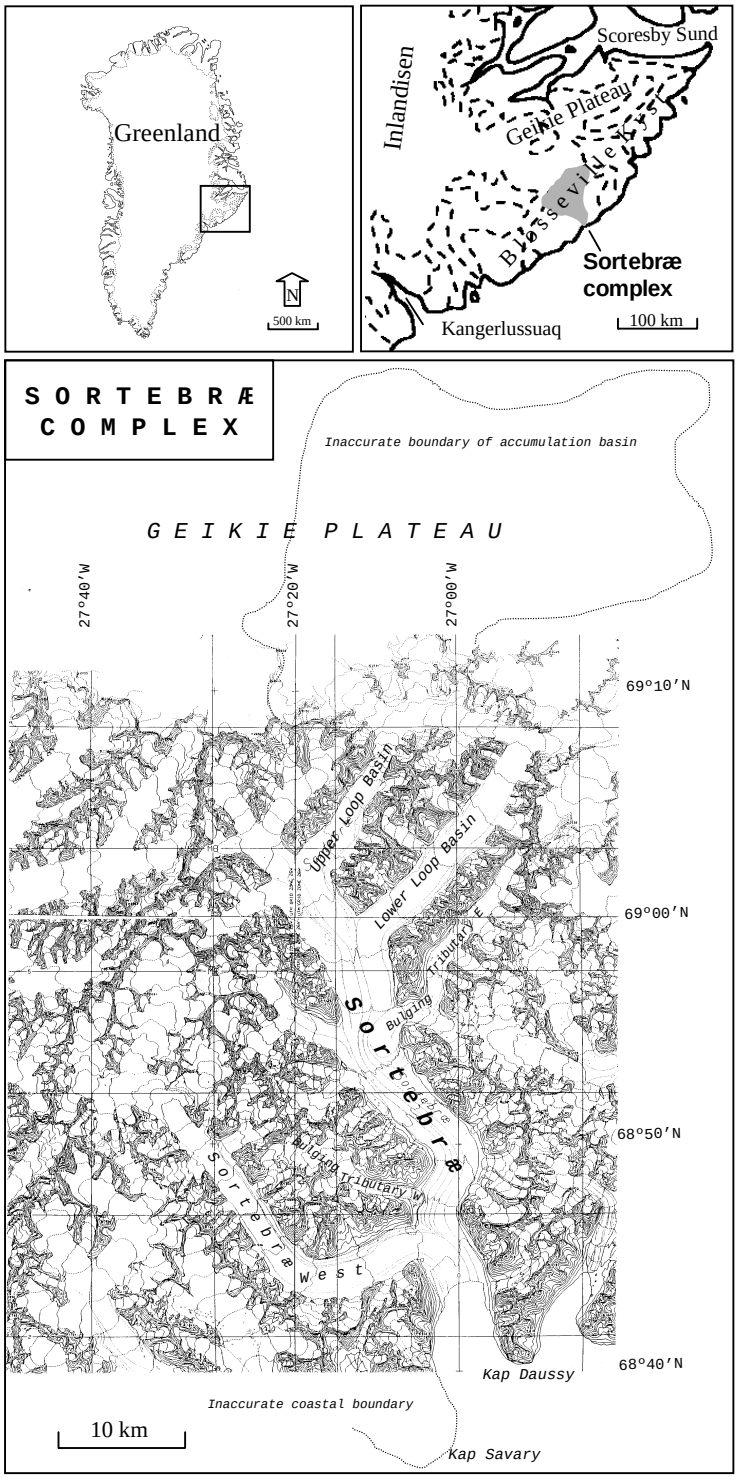

Figure 7.1: *Location map of the Sortebræ complex, based on the 1:100000 topographic maps of the pre-surge geometry GEUS, 1996). For areas south of 68º40'N no topographic maps were available at this scale, while for large parts of the Geikie Plateau the contours are inaccurate or missing. Contour interval is 100 m.*

Sortebræ is glaciologically complex and consists of two confluent valley glaciers: Sortebræ and Sortebræ West. Sortebræ is the main branch and has a compound accumulation area. The glacier primarily drains southwards from the Geikie plateau (2650 m asl) through two narrow valleys (*Upper* and *Lower Loop Basin*). From the northwest Sortebræ is fed through a number of cirque-like accumulation basins with maximum elevations of 2000 m asl. A large number of tributaries join Sortebræ's south-southeast flowing trunk.

Pre-surge glacier geometry was measured from topographic maps (GEUS, 1996; 1997), based on 1981 aerial photographs (Kort & Matrikelstyrelsen, 1981) of Sortebræ. Stereopairs of these aerial photographs were also used to trace the extent of the accumulation area of Sortebræ.The overall pre-surge length of the glacier is 77 km with an average slope of 2°. The minimum slope (less than 1°) is measured on the plateau and the maximum slope (9°) at the head of the Upper Loop Basin. The calving front of Sortebræ is about 4 km long and between 20 and 65 m high. Sortebræ's total glaciated area is 675 km^2, of which approximately 280 km^2 occur on the plateau. This area excludes *Sortebræ West* (*circa* 250 km^2) and *Bulging Tributary East* (E) and *West* (W) (together *circa* 60 km^2) as these are inferred to have separate flow regimes from Sortebræ (Figure 7.1). Nuttall (pers. comm. 1997), using Landsat images, estimated the area of the entire Sortebræ complex as 855 km^2. The difference (70 km^2) between these area estimates comes from a discrepancy in the delineation of the drainage basin boundary on the Geikie Plateau.

At about 18 km inland from Kap Savary Sortebræ is confluent with *Sortebræ West*, which joins Sortebræ at an almost straight angle (Figure 7.1). Sortebræ West is 44 km long and has an area of about 250 km^2. Its accumulation basin consists of a number of cirque-like basins at a maximum elevation of about 2000 m asl. Sortebræ West descends to an elevation of about 50 m asl at confluence region with Sortebræ and its average surface slope is 2.5°. The flow direction of Sortebræ West is southeast for the upper 33 km, northeast until it joins Sortebræ and then the glacier bends sharply to the south-southeast following the fjord orientation.

7.3 Environmental setting of Sortebræ

About 57% of Sortebræ's drainage basin is ice covered, compared to an average of 69% for the region inland of Blosseville Kyst (pers. comm. Nuttall, 1997). The glaciers surrounding Sortebræ are a variation of small cirque glaciers to large size dendritic outlet and valley glaciers, many of which drain from the Geikie Plateau. In central East Greenland about 26 glaciers (including Sortebræ) show morphological evidence of surge behaviour (Weidick, 1988).

Sortebræ is situated in the transition zone between continuous and discontinuous permafrost, which coincides with the annual mean temperature isoline of -4° to -5°C (Thomsen and Weidick, 1992). Both precipitation and temperature gradients are steep and decrease inland as functions of altitude and topography (Ohmura, 1987; Ohmura and Reeh, 1991). Mean annual precipitation rates decrease from about 600 mm a^{-1} on the coast to 300 mm a^{-1} on the Geikie Plateau (extrapolated from Aputetiq and Scoresby Sund Met. Stations: Ohmura and Reeh, 1991). Furthermore, the region is subject to violent katabatic winds flowing from the inland to the coast (Brooks, 1975; Ohmura and Reeh, 1991). These local climate factors influence the distribution of ice-free terrain as well as the glacier mass balance regimes.

The geology between Scoresby Sund and Kangerdlugssuaq (Figure 7.1) consist of a large continuous Tertiary Basalt Plateau up to 5.5 km in thickness, overlying Precambrian granites. The basalts in the Sortebræ region consist predominantly of subaerial lava flows and have been affected by substantial post-volcanic tectonism (Pedersen *et al.*, 1997). The lower 30 km of Sortebræ overlies 12° south-eastwards dipping basalts of the coastal flexure zone, whereas the basalts on the Geikie Plateau dip 4-7° north. At the confluence of Lower Loop Basin with Sortebræ's trunk the basalts are fragmented and all dip away from a common point due to a local point-source uplift (Pedersen *et al*., 1997). The general topography is that of a steep headland divided by deeply incised fjords, often following fault zones (Brooks, 1979). The ruggedness of the terrain is dependent on the rock type and the intensity of intrusive dykes: mountain slopes vary between 45° for unmetamorphosed basalts and 60° for metamorphosed basalts and concentrations of dykes.

The Geikie Plateau ice cap consists of a relatively thin ice resting on an almost horizontal surface of Tertiary basalts (Brooks, 1979). From similar geologic provinces 200 km West of the Geikie Plateau no debris was found to appear from under the ice, suggesting hard-bedded glaciers on the Plateau (Brooks, 1979). The outlet valley glaciers draining from the Geikie Plateau are deeply incised into the plateau basalts. The presence of numerous medial moraines on Sortebræ suggests that substantial subaerial erosion or weathering of the geological outcrops takes place.

7.4 The surge history and behaviour of the Sortebræ complex

The ice covered Geikie Plateau was first explored in the early 1930s by the 7th Thule Expedition under the leadership of Knud Rasmussen (Gabel-Jørgensen, 1940). As the hinterland is extremely inaccessible most exploration was done from ships and from airborne surveys. The majority of the research inland of the Blosseville Kyst has been focussed on geological mapping and exploration. No glaciological studies have been carried out in the region north of Kangerdlugssuaq and south of Scoresby Sund and few groundbased observations are available on the glacier behaviour in this area (Brooks, 1979; Weidick, 1988). The surge history and behaviour of Sortebræ is therefore reconstructed from a variety of published and unpublished remote visual material collected between 1933 and 1995 (Table 7.1).

IMAGERY OF SORTEBRÆ				
Date	**Material**	**Coverage**	**Scale**	**Source**
1933	Oblique aerial photographs	Lower and middle basin Sortebræ		Gabel-Jørgensen (1940)
1943	Oblique and vertical aerial photographs	Lower basin and fragments of middle basin	1:40 000	KMS
5/9/1980	Landsat MSS row 5 path 11 246	Complete		Print in GEUS archives
14/81981	Vertical stereographic aerial photographs	Complete	1:150 000	KMS
8/8/1987	Vertical stereographic aerial photographs	Lower basin	1:150 000	KMS
20/9/1988	Landsat image Path/Row: 227/012	Complete		A.-M. Nuttall (pers. comm., 1997)
13/8/1989	Oblique photo from aircraft	Lower and middle basins of Sortebræ		H. Röthlisberger print in GEUS archives
9/4/1991	Landsat image Path/Row: 288/011	Complete		T. Tukiainen, (pers. comm., 1997)
July-August 1994	Detailed stereo small film images from aircraft	Almost complete coverage of Sortebræ	1:10000 Variable	(A K Pedersen, Danish Lithosphere Centre)
July-August 1995	Detailed stereo small film images from aircraft	Almost complete coverage of Sortebræ	1:10000 Variable	(A K Pedersen, Danish Lithosphere Centre)

Table 7.1: *Remote material on the Sortebræ complex used in this study. Complete coverage means that both Sortebræ and Sortebræ West are covered.*

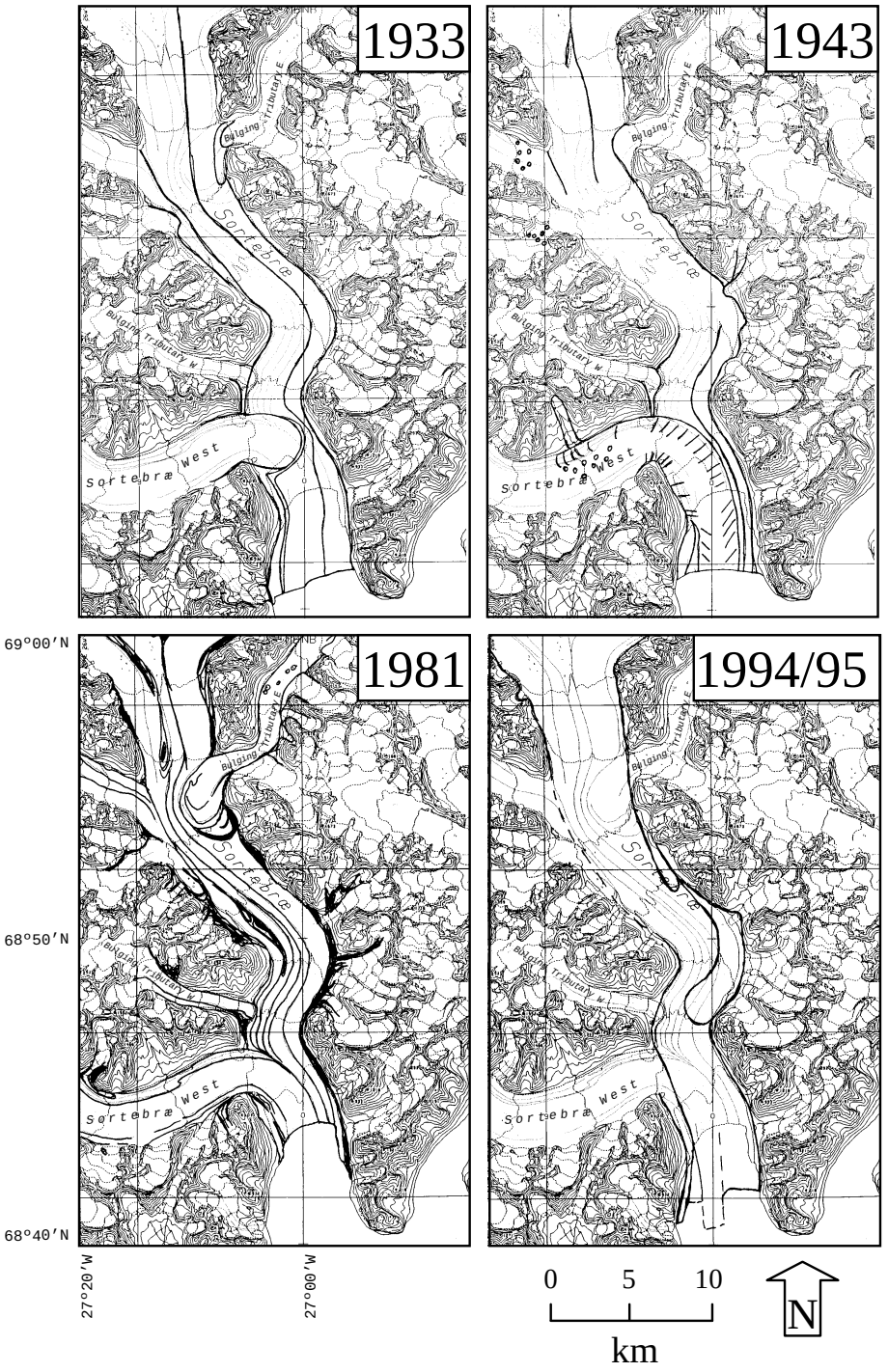

Figure 7.2: *The configuration of surface markers (moraines and crevasses) in the lower regions of Sortebræ and Sortebræ West in 1933, 1943, 1981 and 1994/95 (see Table 7.1 for source material). Basemap topography is from the 1:100000 topographic maps (©GEUS, 1996).*

On the two 1933 aerial photographs covering the lower and middle basins of Sortebræ the ice surface is not crevassed and the glacier seems not to be very active. A number of elongated moraine loops are visible in the middle basin. Sortebræ West is protruding as a large moraine loop into Sortebræ, reaching to about two-thirds of the width of Sortebræ. Only a narrow flow unit of Sortebræ West reaches the fjord and makes up the western kilometre of the calving front,

while the remaining 3.5 km is from the Sortebræ flow unit. The calving front appears regular and straight and the marginal position is at about 1 km inland from Kap Daussy. From the character of the elongated moraines and the straight calving front it is assumed that Sortebræ went through a surge some time before 1933. Sortebræ's position and surface features in 1933 are shown in Figure 7.2.

In 1943 the upper basin of Sortebræ is partly snow covered while the glacier surface is smooth with occasional pitting. This pitting is a common characteristic of surge-type glaciers in Greenland (Rucklidge, 1966; Weidick, 1988). All major tributaries form protruding moraine loops onto the trunk of Sortebræ. Most medial and lateral moraines stand as prominent ridges above the glacier surface indicating depletion of the glacier surface. No surface water or runoff can be detected. The appearance of Sortebræ's upper basin is in strong contrast to the appearances of Sortebræ West and Sortebræ's lower basin. Sortebræ West went through a surge between 1993 and 1943: in 1943 the glacier is completely crevassed (as far up as the photo coverage) and has advanced into the fjord. The main basin of Sortebræ did not join in the surge of Sortebræ West: only the lower 9 km are crevassed and sheared along with Sortebræ West. The flow unit of Sortebræ West obstructs the lower 9 km of Sortebræ and the latter has been pushed to the northern edge of the fjord. Only about 1 km of the width of the calving front comprises of the Sortebræ flow unit, whereas Sortebræ West covers the southern 4.5 km of the calving cliff. Although Sortebræ West has advanced more than 5 km into the fjord, the position of the calving front of the Sortebræ complex has retreated over 1.5 km since 1933. The tidewater margin is actively calving and the central region has probably retreated some distance since the maximum surge extent. The duration of this surge of Sortebræ West is estimated between 1 and 8 years: the onset of the surge cannot be detected from the 1933 photos, while on the 1943 photos the crevasses appear to be closing and are filled with at least one winter's snow. From the 1943 photos it clearly emerges that Sortebræ and Sortebræ West have separate flow regimes and that Sortebræ West has a distinct surge behaviour. The position and surface features of the Sortebræ complex in 1943 are shown in Figure 7.2.

On the 1980 Landsat image it can be seen that Sortebræ has retreated over a distance of about 5 km since 1943. The flow unit of Sortebræ now takes up about one third of the calving front. Sortebræ produces many small icebergs in comparison to icebergs discharging from the surrounding glaciers of the Blosseville Kyst. Bulging Tributary E has protruded over a distance of 2.5 km to about halfway the width of the Sortebræ. Its moraine loop is slightly bent downglacier with the trunk, indicating that Sortebræ is not completely stagnant. It is possible that Bulging Tributary E surged between 1943 and 1980. The surge must have terminated long

before 1980 as the surface of Bulging Tributary E appears inactive and very pitted on the 1981 aerial photographs.

The position of the Sortebræ's glacier margin on the 1981 aerial photographs is similar to that in 1980. The fjord-water adjacent to the calving margin appears turbid. The crevasses on Sortebræ West are closing and some form the characteristically pitted surface of a surge-type glacier in quiescence. Likewise, Sortebræ is pitted in its upper reaches and its larger tributaries as well. These tributaries protrude onto the trunk with prominent concentric moraine ridges. Transverse crevasses are visible at head of Upper Loop Basin at an elevation range of 1200-1700 m asl. These crevasses are probably topographically controlled by the steep surface gradient: a 500 m elevation difference over only 3 km. Some crevassing is also visible in the upper reaches of Bulging Tributary W. Most striking on the 1981 aerial photographs are the clearly elongated and contorted moraine loops in the Upper and Lower Loop Basins (Figure 7.1), indicating a former surge. Sortebræ's position and surface features in 1981 are shown in Figure 7.2.

The position and surface characteristics of Sortebræ in 1987, 1989 and 1991 are similar to those in 1981. However, on the 1987 aerial photographs Bulging Tributary W has protruded with a loop onto the trunk of Sortebræ and while a small tributary opposite Bulging Tributary W appears crevassed. Possibly these two tributaries have surged at some point between 1981 and 1987.

On the airborne stereophotos taken in 1994 and 1995, Sortebræ appears completely crevassed, the moraine loops in both Loop Basins have been elongated, a dramatic down-draw of the glacier surface took place in the upper reaches of the glacier and the glacier complex has advance into the fjord. Between 1991 and 1994-95 the lower 50 km of Sortebræ apparently went through a major surge. A detailed account of this surge including quantitative measurements is presented in Section 7.5. Sortebræ's position and surface features in 1981 are shown in Figure 7.2.

7.5 Quantitative and qualitative results of the 1990s surge of Sortebræ

Quantitative measurements on the 1990s surge of Sortebræ were made using the multi-model photogrammetric equipment (Kern DSR15) at the Institute of Surveying and Photogrammetry (ISP) of the Technical University of Denmark (see Sections 4.8 to 4.10). Measurements of surface depression and uplift are presented in Section 7.5.3. From these measurements the total volume displacement as a result of the surge was calculated (Section 7.5.4). Further, a detailed account of the morphological changes during the surge is given as well as descriptions of

surface features, frontal position, quiescence and surge velocities and calving characteristics. Additionally hypsometric curves were reconstructed from the pre- and post-surge area elevation distributions and subsequent changes in mass balance conditions were investigated using equilibrium line elevation estimates. For a complete description of the multi-model photogrammetry technique, measurement procedures and error calculations see Section 4.8 and onwards.

7.5.1 Surge duration

The 1990s surge of Sortebræ is inferred to have started after 1991, as no evidence of a surge onset can be detected on the 1991 Landsat images. By 1994/95 more than 50 km of Sortebræ is affected by the surge and the margin has advanced 4-5 km compared to the pre-surge position. In 1995 the crevasses in the Upper Loop Basins already seem to be closing and are filled with probably one winter's snow. As the middle and lower basins of Sortebræ are still completely crevassed in 1995 and no winter snow can be seen in the crevasses it is inferred that Sortebræ has not yet terminated its surge in 1995. However, as a major volume displacement has taken place by 1994/95 and the surge has reached Sortebræ's margin it is likely that the surge has terminated not long after 1995. Evidence supporting this hypothesis is the state of disintegration of the calving front, suggesting the major advance has ceased (Figure 7.5). The surge duration of the 1990s Sortebræ surge can thus be estimated in the range of 2-4+ years, but probably not much longer than 5 years.

The length of Sortebræ's quiescent phase is at least 60 years as the 1994 photos are the first evidence of a surge from a set of images covering the glacier over the period 1933-1995.

7.5.2 Frontal position

During the 1990s surge the front of Sortebræ advanced over 5 km along the southern margin and 4 km along the northern margin (see Figures 7.2 and 7.4). The total surge advance added a minimum area of 26 ± 1.56 km^2 to the glacier. Because of the state of disintegration of the terminus in 1995 it is assumed that the glacier is already in retreat since its maximum extent. The position of 1994/95 is similar to that of 1933 and 1943.

7.5.3 Depression and uplift of the glacier surface

A glacier surge transports a surplus ice volume from a reservoir area to a receiving area (see Section 1.3). This results in an upglacier thinning and a downglacier thickening and potentially

frontal advance. The lower (pre-surge) 53 km of Sortebræ was affected by the surge, covering an area of 335 km^2, about half of Sortebræ's basin size (Figure 7.4b). Along the margins of the upper and middle basin of Sortebræ a down-draw of the glacier surface was observed from the remains of ice ('strandlines') hanging on the valley walls. This down-draw was quantified by measuring the elevation difference between the former (strandlines) and present (1994/95) glacier surface using the 1994/95 photogrammetric model in the Kern DSR15. Surface uplift was quantified in the Kern DSR15 by measuring surface elevations at the same locations in 1981 and in 1994/95, which produced a difference in surface elevation corresponding to the thickening of the glacier. In total 52 measurements were taken with the photogrammetric plotter. The locations of the measurements are indicated in Figure 7.4 and local details are given in Figure 7.5. In the region between Bulging Tributary E and Sortebræ West only few measurements could be taken. This gap in the geographical coverage is a consequence of a shortage of 1994/95 airborne photographs in this region.

The vertical measurements of down-draw and uplift are summarised in Table 7.2. Where possible the measurements have been corrected using nearby sea level observations (see Section 4.10.3). Depression of the glacier surface varies between 11 and 219 metres, with the maximum occurring in the Loop Basins. The lowering of the glacier surface generally decreases downglacier to a zero-point (estimated just upstream of Bulging Tributary W) below which the glacier thickens (Figure 7.3). Thickening of the lower glacier varies between 24 and 74 metres. The height of the calving cliff varies between 25 and 60 metres, which is not much different from the cliff height before the surge.

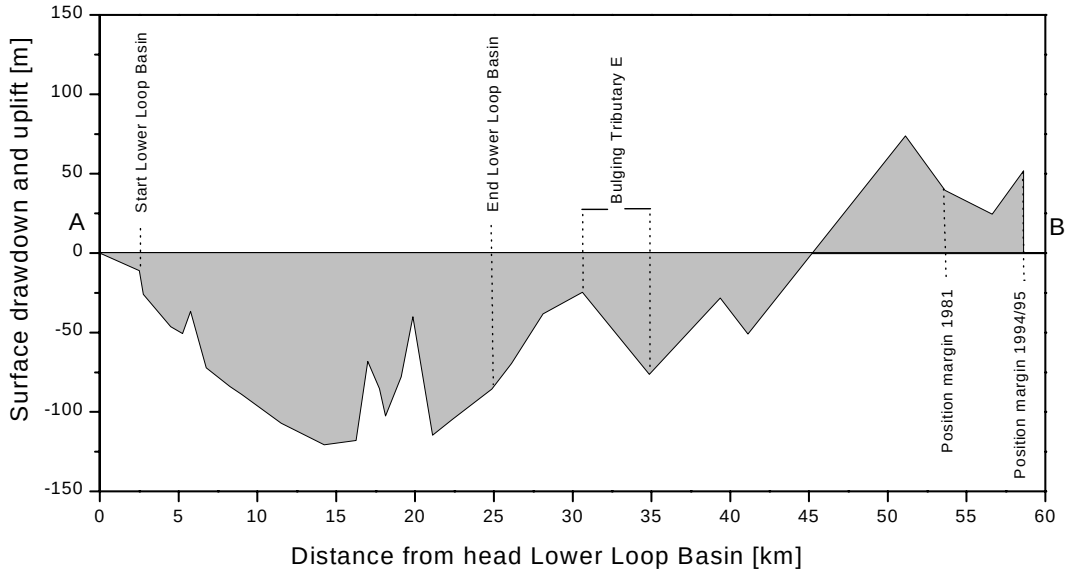

Figure 7.3: *Transect of surface down-draw and uplift as a result of the surge. Location of transect A-B is shown in Figure 7.4.*

7.5.4 Volume displacement and calving surplus

Displacement of ice volume was measured by dividing the glacier into 35 zones of different areas (A) and calculating an average down-draw or uplift (ΔH_A) for each zone by taking the average ΔH values of measured locations within that zone. Zone and measurement locations are given in Figure 7.4, measurements and errors in Tables 7.2 and 7.3.

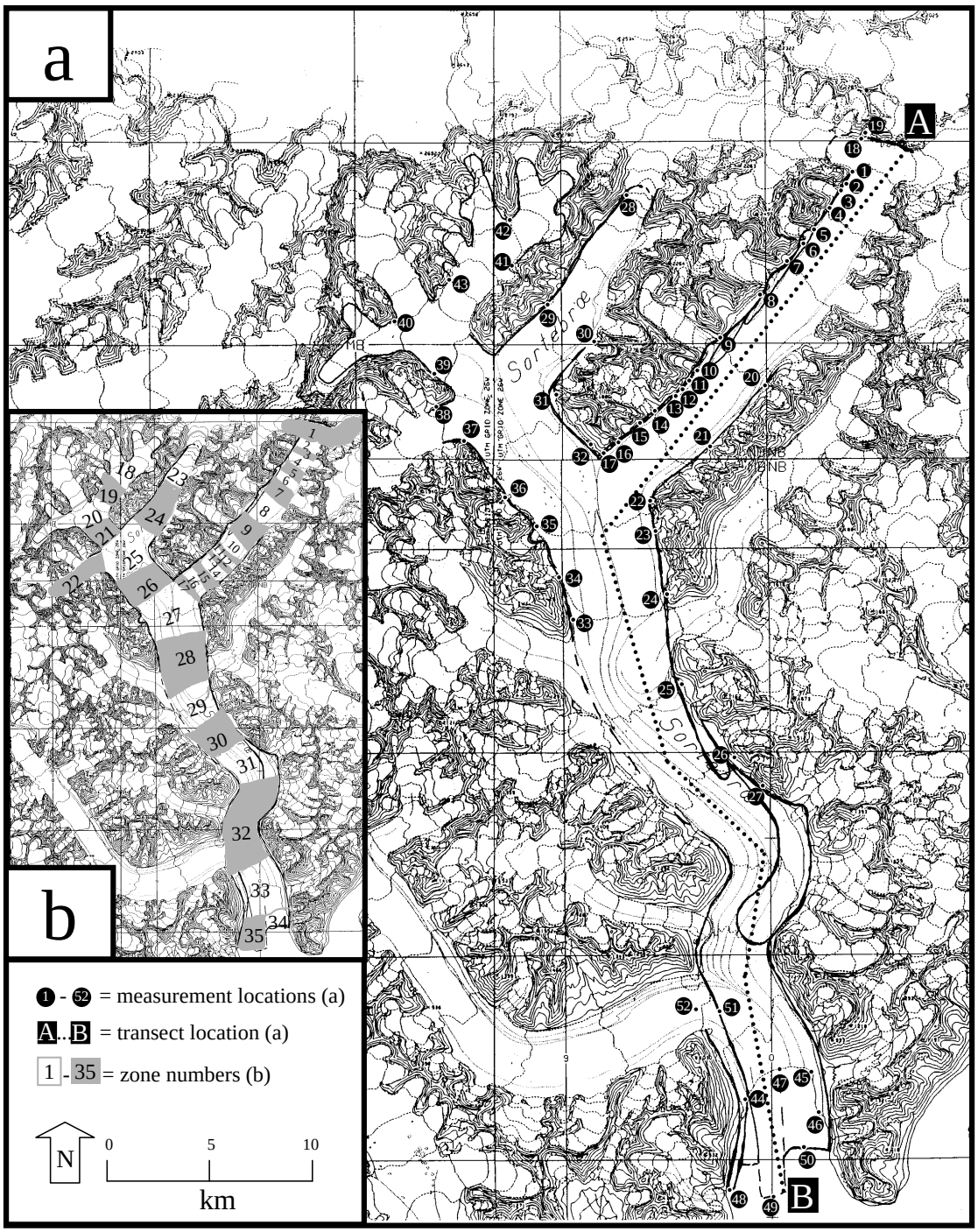

Figure 7.4: *(a) Location map of 52 surface down-draw and uplift measurements (Table 7.2) and approximate position of the longitudinal transect of down-draw and uplift (Figure 7.3). (b) Location map of zones of down-draw and uplift (Table 7.2)*

Error calculation was realised through a three-step procedure, using general theories on error estimation (Squires, 1976):

Step 1: Calculating measurement errors in down-draw/uplift and area for each zone

Error calculations were based on absolute height errors ($\varepsilon_{\Delta H_A}$) in each zone and relative area errors (ε_A) expressed as percentages. The absolute error in the down-draw and uplift ($\varepsilon_{\Delta H}$) was calculated for each measurement point as explained in Section 4.10.2. If more than one measurement was used to calculate the average zone downdraw, the cumulative error (see equation 4.6) of the measurement points was used. The measurement error in zone area (ε_A) was estimated as a percentage of that area. After experimenting with a 1%, 2%, 5% and 10% error in area, I decided to use a 5% error in area for further calculations.

Step 2: Calculating precisions of volume change for each zone

As zone volume is the multiplication of average zone height and zone area, the error of zone volume is calculated from the cumulative precisions of zone height and zone area (Squires, 1976). Precision for volume loss or gain in a zone (p_V) can be calculated from:

$$p_V = \sqrt{{p_{\Delta H_A}}^2 + {p_A}^2}\,. \tag{7.1}$$

Here $p_{\Delta H_A}$ is the dimensionless zone height precision and p_A the zone area precision defined as:

$$p_{\Delta H_A} = \left(\frac{\varepsilon_{\Delta H_A}}{2\Delta H_A}\right) \times 100 \tag{7.2}$$

and

$$p_A = \left(\frac{\varepsilon_A A}{2A}\right) \times 100\,, \tag{7.3}$$

where $\varepsilon_{\Delta H_A}$ is the measurement error of zone height, ε_A is the measurement error of zone area (ε_A = 0.1 for a 10% error) (see Step 1), ΔH_A is the average zone down-draw or uplift (m) and A is the area (km^2) of a zone (see Table 7.2).

Step 3: Calculating the absolute error in calving volume

Having obtained the volume precision (p_V) from Step 2, the absolute error (ε_V) in calculated volume (V) for each zone was calculated from:

$$\varepsilon_V = 2V \frac{p_V}{100}, \tag{7.4}$$

where ε_V is the volume error in km^3 for each zone (Table 7.2). The total error in calving volume is the cumulative error of the ice volume removed from the reservoir zone and the ice volume stored in the receiving zone. The error in volume removed from the reservoir zone (ε_{Vr}) is the cumulative error of the 31 zones with volume loss, and the error in volume stored in the receiving zone (ε_{Vs}). is the cumulative error of the 4 zones with volume gain (see Table 7.2). The total error in calving volume ε_{VT} was subsequently calculated from:

$$\varepsilon_{VT} = \sqrt{\varepsilon_{Vr}^2 + \varepsilon_{Vs}^2}\ . \tag{7.5}$$

Errors in volume removed from the reservoir zone are within 5% of the estimated ice volume, while errors in volume stored in the receiving zone are within 20% of the estimated volume (see Table 7.3). This variation reflects the difference in coverage of measurement points in the two zones: the receiving zone had fewer measurements per area unit and also fewer measurements from stereophotos taken within 1000 m distance (see Figure 7.4). The overall error in calving volume lies within 15% of the estimated calving volume indicating that these measurements are very accurate compared to other ice volume displacement and calving volume estimates (*e.g.* Hagen, 1987; Harrison *et al.*, 1987; Murray *et al.*, 1993; Reeh *et al.*, 1994). The inaccuracy of other volume estimates is mostly caused by a lack of accurate measurements in the upper basins.

No.	Pre-surge elevation *(m asl)*	Post-surge elevation *(m asl)*	Down-draw – Uplift + *(m)*	Error ΔH *(m)*	***Zone***	Area *(km^2)*	Volume loss *(km^3)*	Volume gain **B (–10)* *(km^3)*	Volume gain **B (-300)* *(km^3)*	Volume error *(km^3)*
1	1227	1181	-46	0.69	*1*	18.8	-0.26			0.03
2	1166	1115	-51	0.69	*2*	1.3	-0.06			0.00
3	1100	1064	-37	0.69	*3*	1.3	-0.05			0.00
4	1125	1053	-72	0.69	*4*	3.1	-0.23			0.01
5	1073	989	-84	0.69	*5*	2.5	-0.21			0.01
6	1023	934	-89	0.69	*6*	2.5	-0.22			0.01
7	994	887	-107	0.69	*7*	3.8	-0.40			0.02
8	928	807	-121	0.69	*8*	7.5	-0.90			0.05
9	881	763	-118	0.69	*9*	7.5	-1.00			0.09
10	851	782	-68	0.69	*10*	3.8	-0.26			0.01
11	855	770	-85	0.69	*11*	2.3	-0.19			0.01
12	828	725	-103	0.69	*12*	1.5	-0.15			0.01
13	809	731	-78	0.69	*13*	2.3	-0.15			0.01
14	796	756	-40	0.69	*14*	3.0	-0.12			0.01
15	757	642	-115	0.69	*15*	3.0	-0.34			0.02
16	752	648	-105	0.69	*16*	2.3	-0.24			0.01
17	706	644	-62	0.69	*17*	2.3	-0.17			0.01
18	1202	1191	-11	0.69	*18*	14.1	-0.95			0.16
19	1210	1184	-26	0.69	*19*	4.4	-0.19			0.02
20	896	749	-147	10.32	*20*	9.4	-0.69			0.04
21	833	777	-56	2.76	*21*	6.3	-0.35			0.02
22	729	637	-92	0.69	*22*	10.9	-0.71			0.05
23	645	600	-45	2.76	*23*	12.0	-0.78			0.13
24	586	569	-17	0.69	*24*	12.5	-2.56			0.22
25	496	420	-76	0.69	*25*	18.8	-1.56			0.10
26	428	400	-28	2.76	*26*	12.5	-0.91			0.07
27	377	326	-51	0.69	*27*	26.6	-1.43			0.15
28	1149	1019	-130	10.32	*28*	20.0	-0.49			0.03
29	959	740	-219	10.32	*29*	15.8	-0.60			0.03
30	923	732	-191	10.32	*30*	16.9	-0.48			0.05
31	799	739	-60	0.69	*31*	9.4	-0.24			0.01
32	719	610	-109	0.69	*32*	42.5		+3.14	+3.14	0.47
33	588	555	-32	0.69	*33*	23.8		+1.00	+1.00	0.35
34	674	643	-31	2.76	*34*	1.6		+0.05	+0.51	0.03
35	665	619	-47	2.76	*35*	8.6		+0.53	+3.01	0.17
36	767	705	-62	2.76						
37	855	726	-129	2.76		total	-16.90	+4.72	+7.66	0.72
38	888	758	-130	2.76						
39	934	879	-55	2.76						
40	1015	941	-74	2.76						
41	1285	1129	-157	10.32						
42	1308	1194	-115	2.76						
43	1125	1082	-43	2.76						
44	44	88	+44	10.32						
45	49									
46	19									
47	65	105	+39	10.32						
48		45	+45	7.30						
49		59	+59	7.30						
50		24	+24	7.30						
51		121	+74	10.32						
52	48									

Table 7.2: *Depression and uplift of Sortebræ's glacier surface during the 1990s surge, with corresponding zones of volume loss and volume gain. *B(-10) is with a subglacial bathymetry of –10 m bsl and *B(-300) with a subglacial bathymetry of –300 m bsl. The volume error is for scenario *B(-300), but these errors are only marginally different from those of other scenarios. Location of measurement points and the delineation of zones are given in Figure 7.4. Shaded 'number' cells correspond to locations on the photos in Figure 7.5. For error estimation procedures see Section 4.10.2 and 7.5.4.*

VOLUME DISPLACEMENT AND CALVING SURPLUS					
	No crevassing		**Crevassing**		
	Grounded -10	Grounded –300	Grounded –300		
			5% porosity	*10% porosity*	*20% porosity*
Volume loss reservoir zone	16.90	16.90	17.75	**18.59**	20.28
Volume storage receiving zone	4.72	7.66	-7.27	**6.89**	-6.12
Calving surplus	12.19	9.24	10.48	**11.71**	14.16
ERROR CALCULATIONS					
	Grounded -300				
	1% area error	*2% area error*	*5% area error*	*10% area error*	
Error volume	± 0.33	± 0.33	± **0.39**	± 0.53	
Error volume storage	± 0.57	± 0.57	± **0.61**	± 0.72	
Total error calving surplus	± 0.66	± 0.66	± **0.72**	± 0.90	

Table 7.3: *Volume displacement and calving surplus for scenarios of a grounded margin with a subglacial bathymetry of –10 m bsl, a grounded margin with a subglacial bathymetry of –300 m bsl and a grounded margin with a subglacial bathymetry of –300 m bsl with different intensities of crevassing. Error calculations are based on absolute height errors (Table 7.2) and relative area errors expressed as percentages in this table. These errors are a worse case scenario. Figures in bold reflect the calculated values for the best estimate.*

By adding the volumes of the zones with volume loss it was estimated that an ice volume of 16.90±0.39 km^3 was removed from the reservoir zone (Table 7.2 and 7.3). This volume was transported downglacier and partly stored in the receiving area of the glacier. By adding the volumes of the zones with volume gain it was estimated that an ice volume of 4.72±0.61 km^3 was stored in the receiving area. The remainder volume (12.19±0.72 km^3) must have been discharged into the fjord as calving surplus (or as meltwater). For this estimate of calving surplus it is assumed that zones 34 and 35 (see Figure 7.3) are grounded and that the average zone thickening in these zones equals the average zone uplift plus 10 metres. For this scenario a bathymetry of 10 m deep water is assumed: the terminus thickness is then the average height of the cliff plus 10 m below the sea level.

There are a number of uncertainties in the above method of calculation of ice volume redistribution.

- From the appearance of the calving front it is assumed that zones 34 and 35 are grounded deeper below sea level than the above proposed 10 m and are perhaps even floating (see Figure 7.5). For these scenarios the storage of ice in zones 24 and 35 would be underestimated as a large thickening of ice under water would be disregarded. Extrapolation

of bathymetric measurements along Blosseville Kyst (Brooks, 1979; 1:250000 geology maps (GEUS, 1988)) suggests that the fjord depth adjacent to Sortebræ is between 100 and 300 m deep, although Sortebræ could have eroded a slightly deeper channel during former glacial extent (Brooks, 1979). These data imply that Sortebræ cannot be free floating as the water depth under the ice is less than 9 times the average height above the ice: for free floating conditions with an average ice density of 900 kg m^{-3} about 10 per cent of the ice would above sea level (Paterson, 1994). It is therefore assumed that the ice in the marginal region of Sortebræ is grounded at approximately 100-300 m below sea level. The ice thickness in this region is then estimated as the average height of zones 34 and 35 plus the depth of the fjord. With this hypothesis two new calving volumes were calculated: (1) For the 100 m depth scenario an extra volume of 0.91 km^3 would be stored in the glacier resulting in a calving surplus of 11.28 ± 0.72 km^3. (2) For the 300 m depth scenario an extra volume of 2.93 km^3 would be stored in the glacier resulting in a calving surplus of 9.24 ± 0.72 km^3. These scenarios thus lead to a reduction in calving surplus of respectively 0.91 and 2.74 km^3 compared to the calving surplus for the shallow grounded margin (Table 7.3). For further calculations the outcome for the 300 m depth scenario is used (see Table 7.3).

- During the surge numerous crevasses developed throughout the surging basin (see Section 7.5.8). Disregarding the volume taken up by the opening up of crevasses results in an underestimation of the ice volume removed from the reservoir area and an overestimation of the ice volume stored in the reservoir zone. Assuming the crevasse spacing corresponds to an average increase in ice porosity of 10%, the surplus calving volume would increase by 2.59 km^3 to a total of 11.71 ± 0.72 km^3. See Table 7.3 for estimates of 5% and 20% increase in ice porosity. Inclusion of a term for crevassing clearly has a significant effect on the estimated calving surplus. It is believed that the calving surplus estimate including crevassing is more realistic than the estimate without. In most other studies the volume taken up by crevassing is ignored in the estimates of redistribution of volume (e.g. Murray *et al.*, 1998).
- For the ice volume calculations I assume that rectangular blocks of ice were removed from or stored in the reservoir or receiving zones. In reality, the pre-surge surface cross-section is convex with the maximum surface elevation at the centre flowline. Assuming rectangles would thus underestimate the volume removed from the reservoir zone and overestimate the volume stored in the reservoir zone. Furthermore, glacier sides narrow with depth, at a rate depending on a shape factor (Paterson, 1994). Working with vertical sides of a rectangle leand to an overestimation of the volume removed from the reservoir zone and an underestimation of the volume stored in the receiving zone. However, as these two 'shape errors' have opposite effects they could balance each other out in the calculation of calving

surplus. Taking this into account and because of the unknown shapes of the cross-sections, corrections for rectangle errors have not been considered feasible.

- By using combined measurements of 1994 and 1995 to reconstruct one (post-surge) glacier profile, any ice volume distribution occurring in the period 1994-95 has been ignored. Error estimates for this dynamic behaviour would be pure speculation and there is no alternative but to work with the available data.
- Release of subglacially stored water or closing of subglacial cavities could result in a down-draw of the glacier surface (Kamb *et al.*, 1985). If either of these processes take place the removal of ice from the reservoir zone is overestimated. However, it is unlikely that the space between glacier and bed is more than the order of one metre (Lliboutry, 1969; Kamb, 1987). The resulting error in the total volume removed from the reservoir zone would thus be less than 0.26 km^3 and is negligible.
- In a surge it is possible that surface down-draw in the reservoir zone is preceded by a surface uplift as a result of the passage of the surge front (Meier and Post, 1969; Dolgoushin and Osipova, 1975; Murray *et al.*, 1998). If this were the case for Sortebræ its surface depression would have been overestimated; leading to an overestimation of the volume loss from the reservoir area. Comparison of the pre-surge glacier surface elevation measured from 1981 topographic maps (GEUS, 1996) with the surface elevation measured from the 1994/95 photographs did not reveal a systematic rise of the 1994/95 surface. Both positive and negative differences between the surface elevations were measured in a range of 4-58 $\pm$ 10 metres. Yet, the pre-surge glacier surface of 1994/95 is on average 8 $\pm$ 10 m higher than in 1981. If this were the result of the passage of a surge front the ice volume removal from the reservoir zone would have been overestimated by 2.1 km^3 at the most (= 0.008 km x 257.8 km^2). As very little is known about a possible surge bulge for Sortebræ, and as a very crude (visual) method of comparison of the 1981 and 1994/95 surfaces was used, reservations about this estimate are in place.

After consideration of the above mentioned errors and uncertainties, a best estimate scenario was chosen. For the 'best estimate' scenario of calving surplus a terminus grounded at 300 m below sea level, crevassing resulting in a 10% increase in ice porosity and a maximum 5% error in the zone area calculation were chosen. Summarising, 18.59 $\pm$ 0.39 km^3 of ice was discharged from the reservoir zone of which 6.89 $\pm$ 0.61 km^3 was stored in the receiving zone and the most realistic value for calving surplus is therefore 11.71 $\pm$ 0.72 km^3 (see bold figures in Table 7.3). Annual calving flux is then estimated as 2.3 $\pm$ 0.1 to 5.9 $\pm$ 0.4 km^3 a^{-1} for a surge duration of 5 and 2 years respectively. This is about one fourth of that of Greenland's most productive calving glacier, Jacobshavn Isbræ, more than all North Greenland glaciers together, and about half of that of Storstrømmen in surge (Higgins, 1990; Reeh *et al.*, 1994; Weidick, 1995). For the right

perception of this calving rate we need to compare it to the 'background' calving rate. Background- or non-surge-calving can be calculated from quiescence velocity (Section 7.5.5), the 1981 calving front width (4 km) and height (50-200 m), giving an estimated annual calving rate of 0.02-0.16 km^3 a^{-1}. Hence, the 1990s surge of Sortebræ increased its calving rate 15 to 100 times.

The quantity of dirty icebergs and the irregular profile of the Sortebræ's calving margin in 1995 (Figure 7.5) clearly suggest that the terminus is disintegrating. This process could possibly result in a rapid post-surge retreat. Furthermore, the average size of the icebergs appears to be larger than observed on the pre-surge 1981 and 1987 aerial photographs.

***Figure 7.5**: (overleaf: (abcd) on page 204 and (efgh) on page 205): Photographs of the surge of Sortebræ in 1994/1995 (© Danish Lithosphere Centre). Numbers on the photos indicate approximate locations of measurements with the Kern DSR15 (see also Table 7.2 and Figure 7.3). On close-up photos the height difference between the strandline of the pre-surge surface and the post-surge surface is indicated with a vertical arrow. **a)** North-western crevassed accumulation basins **b)** Marginal turbid lake of circa 600x200 m. **c)** Waves on the post-surge surface of Lower Loop Basin **d)** Surface depression, elongated moraine loops and sheared tributary in Lower Loop Basin. **e)** Shear zone between Sortebræ West (inactive, looking upglacier) and Sortebræ (active, ice flow from right to left) **f)** Marginal shear zone (g) Crevassing and rifting middle basin **h)** Advanced calving margin of Sortebræ, looking upglacier. Largest tabular iceberg is circa 200 m across.*

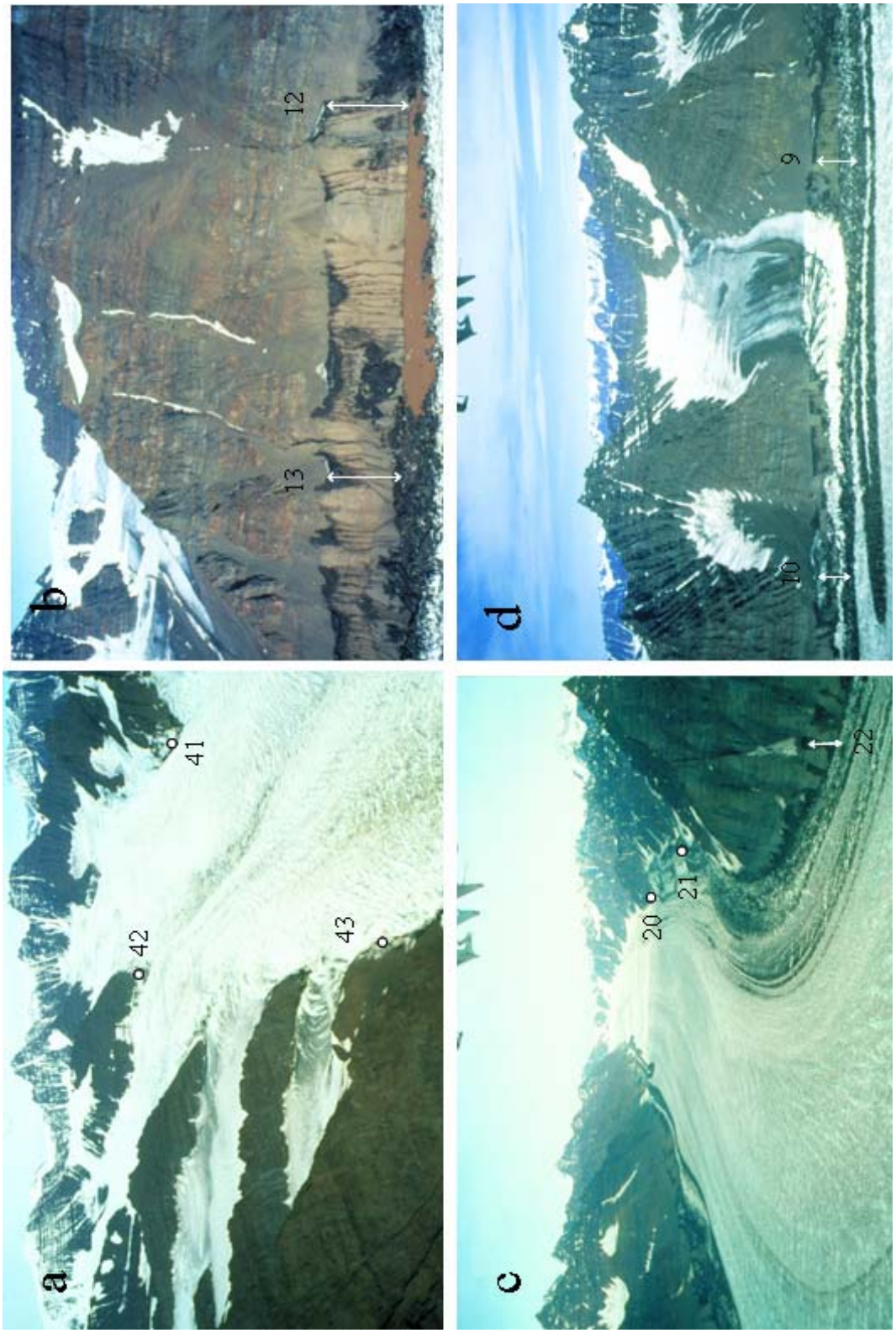
a
41
42
43
b
12
13
c
20
21
22
d
9
10

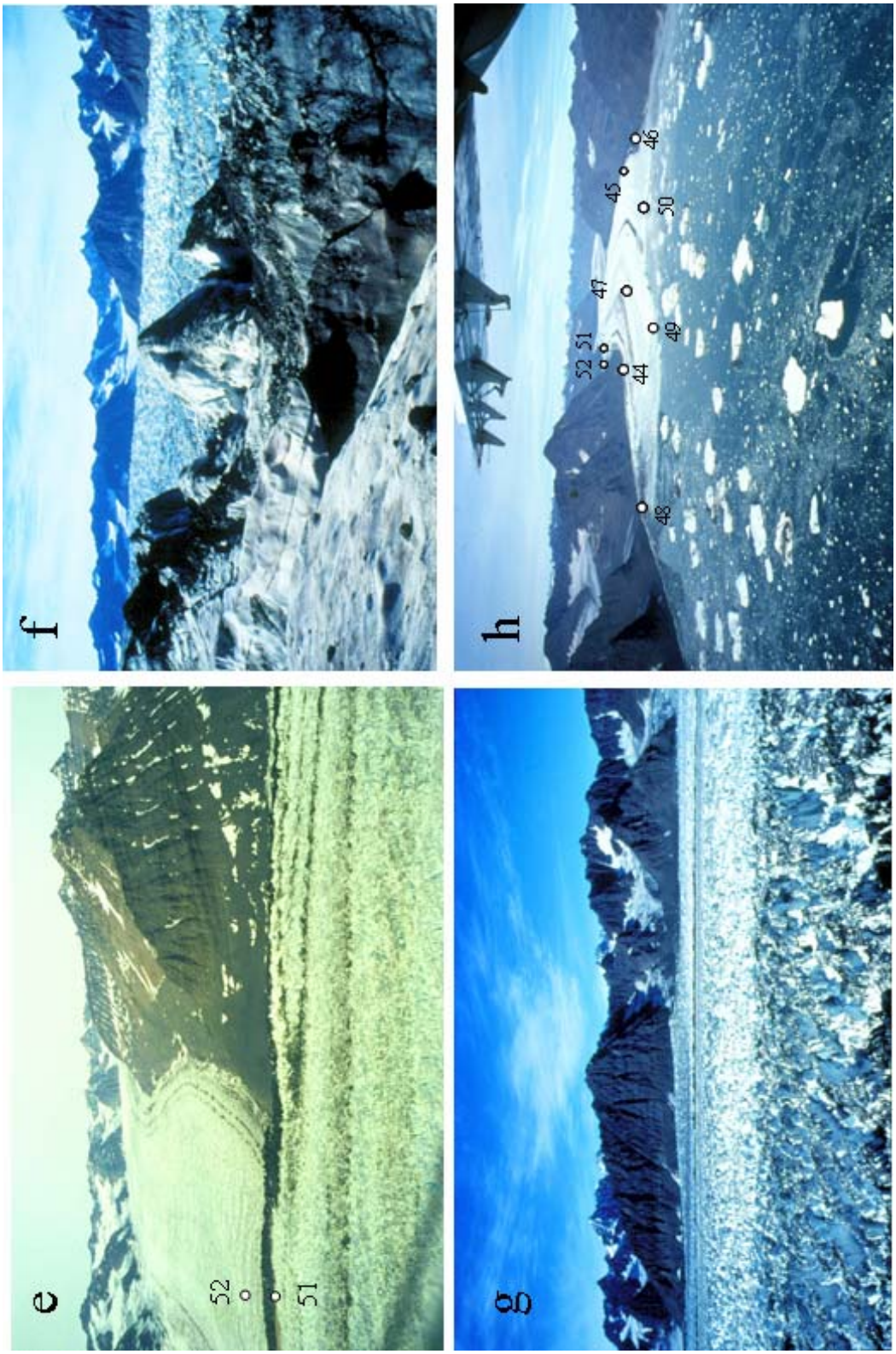
f
h
52
51
46
45
50
47
49
52 51
44
48

7.5.5 Observed velocities

The main characteristic of a surge is the marked increase in ice flow velocity over a short time (see Section 1.3). Although a limited number of surface markers could be traced over subsequent photo coverages, it was possible to derive estimates for quiescent and surge velocities for Sortebræ. Between 1933 and 1943 a moraine fragment in the centre unit of Sortebræ's middle basin was displaced over 2 km and between 1981 and 1987 the moraine loop of Bulging Tributary W was elongated by 450 m. Consequently, the estimated quiescent phase flow velocities vary between 75 and 200 ± 50 m a^{-1}. These values are in the range found for other (possibly surge-type) tidewater glaciers in East Greenland (Dwyer, 1993; pers. comm Nuttall, 1997) but are ten times lower than those measured on tidewater outlets at the head of Nordvestfjord, Scoresby Sund (Olesen and Reeh, 1969, 1973). The measured surge velocities of Sortebræ are considerably higher than the quiescent velocities. Elongation of moraine loops during the surge varies between 2.5 km in the Upper Loop Basin to 5-10 km for the tributary loop of Bulging Tributary E. The glacier advanced 4-5 km over a period of less than 2 years. Therefore, surge-velocities are estimated to be in the range of 625-2500 m a^{-1} in the upper basin and 1700-10000 m a^{-1} in the middle and lower basins of Sortebræ. These measurements imply a minimum 3-fold and a maximum 50-fold increase of flow velocity from quiescence to surge. For further calculations a surge velocity of 2500 m a^{-1} was used.

The propagation velocity of a surge front can be calculated from horizontal surge velocities and thickness differences between active and passive parts of a surge-type glacier by assuming volume conservation (Raymond *et al.*, 1987). This is particularly important for the estimates on the surge duration and for comparison of surge characteristics worldwide. The propagation velocity of a surge front, *w*, is calculated from:

$$w = \frac{u_2 h_2}{h_2 - h_1}, \tag{7.6}$$

where u_2 is the horizontal surge velocity and h_2 and h_1 the average post surge and pre-surge thickness of the glacier respectively (Raymond *et al.*, 1987). For an estimated centre line ice thickness of approximately 1/4 to 1/8 times the cross-sectional glacier width (for a shape factor of 0.7-0.8: Paterson, 1994) the propagation of the surge front can be calculated at locations where velocity estimates are taken and where surface uplifts are measured. For the zone starting at the confluence of Sortebræ and Sortebræ West the height difference between the surging part and the stagnant part was calculated to be in the order of 53 ± 17.9 m (see Table 7.2 for average uplift of measurement numbers 44, 47 and 51/52). For a 4 km wide cross-section and a surge

velocity of 2500 m a^{-1} the surge front propagation is estimated to be 65-140 m d^{-1} dependent if a pre-surge glacier thickness of 500 m or 1000 m is chosen. It would thus approximately take between 1 and 2½ years for the surge front to travel over a distance of 53 km (length of the surge affected basin) before reaching the terminus. The proposed 2-5 years surge duration is thus a reasonable estimate (see above). However, the exact position of the surge nucleus is not known and the surge could have started lower down the glacier than at the head of the surge affected basin (see Section 7.5.8). If this were the case the time until the surge front reaches the terminus would be reduced: for every 10 km shorter the duration will be reduced with approximately 2 to 6 months. Given the calculation of surge front propagation is very sensitive to changes in the assumption of ice thickness, varying 15 m d^{-1} for a 100 m difference in ice thickness, there are large uncertainties attached to the above calculated values for surge front propagation.

7.5.6 Hypsometry

Glacier hypsometry is the distribution of glacier area over elevation (see also Section 5.4.11). It is determined by valley shape, topographic relief and ice volume (Wilbur, 1988). Hypsometry is important to long term glacier response through its link with mass balance elevation distribution (Furbish and Andrews, 1984; see also Section 7.5.7). Research by Wilbur (1988) suggests that once a glacier becomes bottom-heavy, surge behaviour is favoured (see Section 3.3.8). Furthermore, a glacier surge would not result in a significant change in the shape of the hypsometry curve, unless the surge results in a proportionally large change in ice volume proportions (Wilbur, 1988). Although some surge-type glaciers can have a large redistribution of ice volume, changes in hypsometry shape can only take place when either a substantial advance or a substantial melting of the terminus area takes place. This is more often the case for surges of small surge-type glaciers (<10 km^2) than of large surge-type glaciers (Wilbur, 1988; see also Section 3.3.8).

Hypsometric curves for before and after the 1990s surge of Sortebræ are shown in Figure 7.6. The pre-surge hypsometry is measured from topographic maps at scale 1:100000 which are based on 1981 aerial photographs (GEUS, 1996). The post-surge hypsometry is reconstructed from interpolating measurements of the post-surge surface with the DSR-15 photogrammetric plotter (Figure 7.4 and Table 7.2). Errors in surface area measurements for hypsometry are believed to be within 5%. Elevation errors are generally within 10 m, but at elevation ranges 700-1200 m asl and 0-100 m asl they can be up to 50 m. However, it is assumed that the general shape of the hypsometry curves is not significantly affected by these errors.

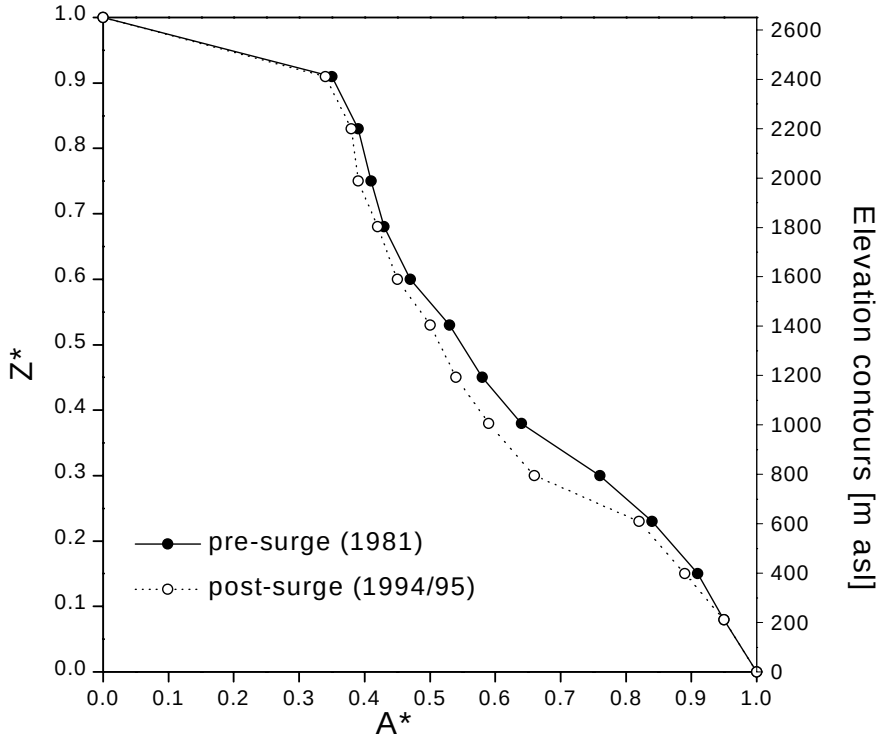

Figure 7.6: *Pre-surge and post-surge hypsometries of Sortebræ. A* and Z* are dimensionless units for area and elevation (Furbish and Andrews, 1984). A* is the cumulative area above a certain elevation. At the terminus of the glacier Z*=0 and at the head of the glacier Z*=1. On the top axis the elevation is given in metres above sea level in order to facilitate interpretation of the curves.*

Figure 7.6 shows that the general shapes of the 1981 and 1994/95 hypsometric curves are similar. According to hypsometry classifications they would fall into a combined 'ice-cap' and 'alpine-valley' type (Wilbur, 1988). The shape of the upper part of the curve (approximately between 2000 and 2650 m asl) is convex and resembles that of an 'ice-cap' type, while below an elevation of about 2000 metres the curve resembles more those of the 'valley-alpine' types (Wilbur, 1988). Sortebræ's hypsometry is top-heavy: the areal distribution function (steepness of the curve) is largest between 2400 and 2650 m asl, while it is smallest at a lower elevation between 1800 and 2000 m asl. This observation disputes the suggestion that surge-type glaciers are commonly bottom-heavy (Wilbur, 1988). However, if the higher (ice cap like) glacier elevations on Geikie Plateau are disregarded, the hypsometry curves tend to be bottom-heavy, as the function Z*(A*) is largest where the area increase is large for a small change in elevation (Wilbur, 1988).

Even though a considerable surge advance took place, the surge of Sortebræ has clearly not affected the general shape of the hypsometry curve. This finding agrees with Wilbur's hypothesis for surges of large glaciers (Wilbur, 1988). The only notable difference between the 1981 and 1994/95 hypsometries is that the post-surge hypsometry is slightly pronounced

bottom-heavy than before the surge, which is to be expected from a surge advance of a glacier with a low average surface slope in the region of advance.

7.5.7 Equilibrium line altitude and accumulation area ratio

Very little is known about mass balance conditions of glaciers in central East Greenland. The nearest glaciers to Sortebræ for which mass balance data are available are Fröyagletscher (74º24'N, 20º50'W) and Midtluagkat Glacier (65°41'N, 37°54'W), both small valley glaciers at a distance of about 1000 km from Sortebræ (Ahlmann, 1948; Weidick, 1995). Even the most basic observations on Sortebræ (snowline position and approximate length of melt season) could help to establish the fundamentals of mass balance of the larger glaciers in East Greenland.

Assuming no superimposed ice is formed on a glacier, the transient snowline late in the melt season can be used as a proxy for the equilibrium line altitude (*ela*) of a glacier (Paterson, 1994). On a number of aerial photographs and on the 1994/95 stereophotos the position of the snow line was observed. In 1933 the position of the snowline is above 1000 m asl, but due to the nature of these photos it is not possible to be more specific. In 1943 fresh snowfall covered the entire glacier and obscured the late Summer snowline. On August 8th 1981 the snowline was at an elevation of 1100 m asl, whilst on September 4th 1981 fresh snowfall had lowered the snowline to below 400 m asl. In July 1994 a snowline occurred at an elevation of 800 m asl on a tributary in the lower section of Sortebræ. The validity of this observation in terms of Sortebræ's mass balance is questionable. In July 1995 the snowline occurs again at 1100 m asl in the Upper Loop Basin. Additionally, the 1:10000 topographic maps (GEUS, 1996) reveal a transition from convex to concave elevation contours between 1100 and 1200 m asl, which can be indicative for the position of the *ela* (Sugden and John. 1976).

From the above data it is suggested that the end of the melt season on Sortebræ occurs between early August and early September. Combining the transient snowlines for the period 1933-1995 gives an *ela* in the range of 1100-1200 m asl. Using this *ela* range and the pre- and post-surge hypsometries for Sortebræ (Figure 7.6) it is possible to calculate AARs for Sortebræ. For the 1981 pre-surge hypsometry the AAR is approximately $0.58\text{-}0.61 \pm 0.05$ and for the 1994/95 post-surge hypsometry the AAR is approximately $0.54\text{-}0.57 \pm 0.05$. This decrease in AAR reflects a normal trend for glaciers that have recently surged: these glaciers change from a state of positive imbalance before the surge to one of a negative imbalance after the surge (Budd, 1975). However, it is likely that the mass balance conditions have changed as a result of a change in surface conditions after the surge. The natural response of a glacier to a reduced post-surge AAR is the melting back and retreat of the glacier in quiescence. These very basic data

would suggest a balance AAR of 0.56-0.59 ± 0.05 for Sortebræ. Nonetheless, the balance AAR for Sortebræ is in agreement with the range of values found for balance AARs for glaciers in subpolar regions (IAHS(ICSI)/UNEP/UNESCO, 1996; 1999; Dyurgerov and Meier, 1997; Dowdeswell *et al.*, 1998).

7.5.8 Surface features: crevasses, lakes and sediments

Crevasse formation reflects the stress distribution over a glacier (Vaughan, 1993). Generally, longitudinal crevasses occur as a result of compressive forces and transverse crevasses as a result of extensional forces (Paterson, 1994). Moreover, crevasse pattern distribution over a glacier basin can inform us where a surge initiated (nucleus), how the surge front propagated, and about the characteristics of the transverse velocity distribution (Hodgkins and Dowdeswell, 1994; Lawson, 1996). Above the surge nucleus forces are mainly extending and crevassing is predominantly transverse, while below the surge front a combination of compression and extension takes place and crevassing is a combination of longitudinal and transverse types often resulting in chaotic crevasse patterns (Lawson, 1996). Examples of crevasse distribution patterns typical for surge-type glaciers are given in Section 1.4.2.

Although the 1994/95 photo coverage of the marginal zones of Sortebræ is almost complete, the region of the central flowline is only occasionally visible. Observations on the 1994/95 crevasse distribution of Sortebræ are thus incomplete. Yet, from the observations along the margins it can be seen that surface crevassing affected the entire surge basin (335 km^2). Crevasse types include transverse crevasses in the far upper basins and at the tributaries; concentric, transverse and longitudinal crevasses in the upper and middle basins; conjugate crevasses at the shear margins and at the boundaries between flow units in the middle and lower basins; and chaotic crevassing in the lower basin (Figure 7.5). Crevasse width in the middle and lower basin is approximately up to tens of metres, while the ice in Sortebræ's lower basin is broken up into 'wavy' rifts with individual heights of tens of metres. These rifts were observed up to 15 km from the advanced terminus. These crevasse pattern types are very similar to those observed during surges of large calving glaciers such as on Bering Glacier, Osbornebreen and Bodleybreen (Hodgkins and Dowdeswell, 1994; Molnia, 1994; Rolstad *et al.*, 1997; see Section 1.4.2).

Longitudinal and chaotic crevasse patterns on Sortebræ first start to appear halfway the Lower Loop Basin. Upstream of the junction of Lower Loop basin with the trunk (Upper Loop Basin and the cirque-like accumulation basins) only transverse crevassing has been observed. This would suggest that the surge initiated halfway the Lower Loop Basin, migrating both up- and downglacier. In the lower half of the Lower Loop Basin the post-surge surface appears wavy

with a wavelength of about 2 km and an amplitude of about 25 m (Figure 7.3 and 7.5). The waves become more pronounced in a downglacier direction. Dynamic waves with a similar frequency but double the amplitude have been observed to travel downglacier during the 1963 surge of Medvezhiy (Dolgoushin *et al.*, 1963). The waves on Sortebræ could thus possibly indicate the passage of kinematic waves or a surge bulge, although the available material is insufficient to make strong statements on either of these.

Shearing occurs along the entire margin of the surge basin. Although the tributaries proper remain unaffected by the surge, the lower sections of most tributaries are sheared off and transported downglacier with Sortebræ, leaving tributaries in the reservoir zone hanging and those in the receiving zone blocked (Figure 7.5). Sortebræ West and Bulging Tributary W have been cut off by the surging trunk and their surfaces appear at an elevation of about 50-70 below that of Sortebræ. The combination of marginal shear zones with a relatively flat surface in transverse cross-section suggests that the ice velocity profile is that of block motion, which is common for surging glaciers (Kamb *et al.*, 1985; Reeh *et al.*, 1994; see also Section 1.3).

At all shear zones large amounts of sediments emerge. What are interpreted as thrust planes and upthrusted dirt cones up to 3 m in height were observed in 1995 at the northern margin of Sortebræ (pers. comm., A.K. Pedersen, 1997: Figure 7.5). This process has transformed many of the former concentric moraine loops into elongated tear-shaped moraine loops (Figure 7.5). Turbid lakes with a high suspended sediment content developed in conjunction with the surge. These lakes mainly occur in the shear margins of the Loop Basins and at the shear zone between Sortebræ and Sortebræ West. They have rectangular shapes with maximum dimensions of approximately 200x600 m with the longest axis in the direction of ice flow (Figure 7.5). No surface water could be detected on any of the pre-surge images and the lakes form the first evidence of supraglacial water on Sortebræ. Further, the lake water must have been subglacially derived because of its high sediment content. The appearance of supraglacial lakes are a common phenomenon on surge-type glaciers, although they are mostly clear and sediment free (Liestøl *et al.*, 1980; Lingle *et al.*, 1994; Reeh *et al.*, 1994). Turbid shear zone lakes have only been observed before on Bering Glacier, although turbid water was found in crevasses of Variegated glacier (Kamb *et al.*, 1985; Molnia, 1994).

7.6 Comparing Sortebræ to other surge-type glaciers

Variations in surge behaviour such as differences in surge period, velocity development during a surge, and morphological adjustment during a surge, are particularly important in understanding flow dynamics. In order to comprehend glacier surging, and thus to understand the physics

behind surge mechanisms it is important to search for systematic differences in surge behaviour, and attempt to relate these differences to for example environmental conditions and/or glacier morphology (e.g. Dowdeswell *et al.*, 1991). Differences in surge duration and velocity development are suggested to result from differences in glacier size, glacier type, thermal and substrate conditions and geographical location (Meier and Post, 1969; Clarke *et al.*, 1986; Dowdeswell *et al.*, 1991; 1995; Hewitt, 1998; Murray *et al.*, 1998). Below follows a systematic comparison of the surge of Sortebræ with other surges in Greenland as well as in other regions. For this study a small selection of example data on active glacier surging world-wide was used (see Table 7.4).

SURGE CHARACTERISTICS											
Glacier	Length *km*	Surge advance *km*	ΔH upper *m*	ΔH lower *m*	Volume displ. km^3	Calving rate $km^3\ a^{-1}$	Quiescent Velocity $m\ a^{-1}$	Surge velocity $m\ a^{-1}$	Surge front propagation $m\ a^{-1}$	Surge duration *yr*	Quiesc. Duration *yr*
Finsterwalder[1]	12	1.5	-50	+100			13				
Usherbreen[1]	12	1.5	-40	+120	0.82			550-1570	>365	8	
Fridtjovbreen[1]	13	2.5						1250		>3	130
Bodley[1]	16	2-3.5	-15	+60			197	510	2372	7+	
Bakaninbreen[1]	17	0	-15	+40	0.67*	-	1-5	88-1100	1000-1800	5-15	>60
Osbornebreen[1]	20	2	-100	+100				440-2190	2190-2555	3+	
Hinlopen[1]	68	3				2 km a^{-1}		5100-5800		4+	
Medveziy[2]	13	1.6	-100	+150	0.06	-	0.5-550	25000-38000	29000	0.4-1	10-15
Chiring[3]	15.5	2.5	-150	+130	1-1.5					3	110
Variegated[4]	20	2-5	-50	+100			75	5000-18000	5500-29000	2	20
Black Rapids[4]	43	6.4	+45	-125			50-70			1	
Steele[4]	50	12	-70	+100				6000			
Muldrow[4]	63	6.6	-60	+60				6600		2-4	50
Bering[4]	200	9.7	-50				365	4015-12000	32850	2-3	20-30
West Fork[4]	40		-60	+123	3.7		60	4380	8395	<1	50
Løberen[5]	22	7.5				-		>1000		7-15	150-200
Bjørnbo Gl.[5]	35	10?		+160		-				5-6	>100
Roslin Gl.[5]	38	10	-?	+?		-	4-10				
Sortebræ[5]	**77**	**4-5**	**-200**	**+75**	**18**	**2.6-5.3**	**75-200**	**1700-10000**	**23500-51000**	**2-5**	**>65**
Storstrømmen[5]	120	10	-80		50	10.8	130-300	1500-2000		5-6	70

Table 7.4: *Comparison of surge characteristics of Sortebræ with other surging glaciers. Glaciers are sorted per geographic region on increasing length.* [1]*Svalbard glaciers (Hagen, 1987; 1988; Hodgkins and Dowdeswell, 1994; Glasser et al., 1998; Murray et al., 1998; Nuttall et al., 1997; Rolstad et al., 1997);* [2]*Pamir glaciers (Dolgoushin and Osipova, 1975);* [3]*Karakoram glaciers (Hewitt, 1998);* [4]*Alaska glaciers (Meier and Post, 1969; Stanley, 1969; Kamb et al., 1985; Harrison et al., 1994; Lingle et al. 1994; Molnia, 1994; Fleisher et al., 1995; Heinrichs et al., 1995);* [5]*Greenland glaciers (Colvill, 1984; Reeh et al., 1994; Rutishauser, 1969; Weidick, 1988). *Volume displacement for Bakaninbreen is estimated for the first two years of the surge (pers. comm., Tavi Murray, 1999).*

With an estimated ice volume redistribution of 18.6 ± 1.35 km^3 and a frontal advance of 5 km Sortebræ can compete with large scale surges of calving glaciers such as Storstrømmen, NE Greenland, and Bering Glacier, Alaska (Reeh *et al.*, 1994; Sauber *et al.*, 1995). The surface down-draw with maxima around 200 m is large compared to most other observation and not many glaciers have average down-draws exceeding the uplifts (see Table 7.4). This anomaly

could have been balanced by simultaneous thickening of Sortebræ below sea level (see Section 7.5.4). The ratio of advance over total length of Sortebræ is on the lower end of the limits of 5-25%. In general, tidewater glaciers appear to have lower advance ratios than valley glaciers (Table 7.4). Although the difference between Sortebræ's quiescent and surge velocities are of the same order as for most tidewater glaciers, the surge velocities proper are of an order magnitude lower than those for the typical surging valley glacier such as Variegated and Medveziy. However, the values found for the propagation of the surge front are amongst the fastest found for surge-type glaciers. Some reservation on this value is necessary due to the crude method used to calculate this quantity.

According to Dowdeswell *et al.* (1991, 1995) Svalbard surge-type glaciers are unique for the long duration of their surges (3-10 years), the long quiescent phases (50-500 years) and the low surge velocities. These characteristics have been accredited to specific substrate and thermal conditions, mass balance and rate of down-draw (Dowdeswell *et al.*, 1991; 1995; Murray *et al.*, 1998). Data on 4 glaciers in East Greenland (including Sortebræ) suggest a surge duration of 2 to >10 years (commonly 4+) and quiescent phase duration of 60 to 150 years. These figures imply that surges in East Greenland are intermediate between the fast and short period surges glaciers of Alaska and the Pamir, and the slow long period surges common for Svalbard. Recently, Hewitt (1998) also recorded that for Karakoram surge-type glaciers the surge and quiescent phases were longer than for the usual figures of 2-3 years for a surge and 20-30 years for quiescence (Meier and Post, 1969). West Greenland surging glaciers have surges of 1-2 years and quiescent phases of 30-50 years (Weidick, 1988). These glaciers overlie basalts similar to those in the Blosseville Kyst region, thus it seems unlikely that lithology is a primary control on the duration of surges or quiescent phases. Moreover, Svalbard glaciers overly a range of different lithologies (see Section 5.4.13). Statistical analysis by Dowdeswell *et al.* (1991) indicated that glacier size is not significantly related to the duration of the active surging phase. However, thermal regime, in combination with substrate, seems to play an important role in surge propagation (Murray *et al.*, in review). Many surge-type glaciers in Svalbard have polythermal structures (Macheret and Zhuravlev, 1982; Dowdeswell *et al.*, 1984; Bamber, 1989). The only measurements on the thermal regime of central East Greenland glaciers are from boreholes drilled in Schuchert Gletscher, Stauninger Alps, and from RES measurements on Roslin Glacier, Stauninger Alps, suggesting that both glaciers are polythermal (Kirchner, 1963; Davis *et al.*, 1973). Other valley glaciers in the Stauninger Alps are described as subpolar (Mercer, 1975). It is plausible that the larger central East Greenland are polythermal, because aerial photograph interpretation reveals hardly any surface water on the Blosseville Kyst glaciers and because the annual mean temperatures around Sortebræ are -4° to -5°C, whilst the maximum Summer temperature is below 10ºC (Colvill, 1984; Thomsen and Weidick, 1992)

7.7 Implications of the surges in the Sortebræ complex

1) Calving properties

The 1990s surge of Sortebræ resulted in a surplus calving rate of 2.3 ± 0.1 to 5.9 ± 0.4 km^3 a^{-1}. For comparison, non-surging outlet glaciers draining from the Inland Ice into the innermost part of Scoresby Sund have calving rates between 0.2 and 10 km^3 a^{-1} (calving front lengths around 2-6 km), while in North Greenland calving rates are only in the order of 0.1-0.7 km^3 a^{-1} (Olesen and Reeh, 1969; 1973; Higgins, 1990).

Sortebræ's calving rate has not only increased during its surge, but the glacier also produces larger icebergs than during quiescence (Section 7.5.4). This is in contrast to observations on the calving of Svalbard surge-type glaciers, where surges result in a reduction of the size of icebergs (Dowdeswell, 1989). The size of icebergs could be determined by a combination of transverse crevasse spacing and the degree of chaotic crevassing at the terminus. Crevasse spacing on surging Nordaustlandet glaciers is less than 30-50 m apart (Dowdeswell, 1989). This is probably similar for Sortebræ (see Section 7.5.8). Further, tidewater termini in Svalbard are thin and probably all grounded (Dowdeswell, 1989). In contrast, Sortebræ's terminus ice thickness is probably greater than in Svalbard and could exceed the crevasse depth to such an extent that for Sortebræ crevasse spacing is possibly not a primary control of iceberg dimensions.

Sortebræ's calving surplus and the nature of its icebergs during the surge could have a periodic effect on the iceberg distribution in the Atlantic shipping routes. The iceberg volume calculated for Sortebræ might be indicative for other large surging tidewater glaciers in East Greenland (see Weidick, 1988). Major iceberg calf events are known to take place at Scoresby Sund and south of Kangerdlugssuaq (Thomsen and Weidick, 1992). Few other surge related calving events have been reported from East Greenland. A certain event is associated with the surge of Storstrømmen, and a possible event was inferred from the rapid disintegration of Kangerdlugssuaq's terminus in 1936 (Field, 1975; Reeh *et al.*, 1994). Although Reeh *et al.* (1994) reported an increase in iceberg production associated with Storstrømmen's surge it was not cited if any changes in berg size took place.

2) Interacting glacier systems

Sortebræ, Sortebræ West and both Bulging Tributaries are inferred to have separate flow regimes. Although the glaciers surge independently it appears that the surges may have influenced the flow regimes of one another suggesting that the tributaries and trunks are interacting systems. Tributaries joining a surge-type glacier are often observed to form a bulge or moraine loop on the surface of the trunk (Meier and Post, 1969). A surge of such a tributary

could block the flow of the trunk at the point of confluence and create conditions necessary for the build-up of the trunk to a new surge. This process could have taken place in the early 1940s surge of Sortebræ West that blocked the outflow of Sortebræ. Similar situations have been observed at Roslin glacier, East Greenland, Black Rapids Glacier, Alaska, and Chiring Glacier, the Karakoram (Colvill, 1984; Heinrichs *et al.*, 1996; Hewitt, 1998). The opposite process is also possible: a surging trunk can restrict the outflow from a tributary. This process probably occurred for Sortebræ West, which was blocked by the raised surface of Sortebræ after the 1990s surge of the latter (Figure 7.5). Comparable observations exist for Steele Glacier, Alaska, where one of the tributaries started surging a year after the trunk had blocked its outflow (Stanley, 1969). However, observations from Fridtjovbreen, Svalbard, suggest that tributary surface can act as a décollement surface over which the trunk ice flows (Glasser *et al.*, 1998). Although the images from Sortebræ suggest shearing action, no conclusive statement on this issue is possible without field observations from Sortebræ. Nevertheless, observations on Sortebræ exemplify that the location at which a tributary joins a trunk is crucial for the type of interaction between the glacier systems. A tributary blocking its trunk should delineate the lower reaches of the trunk's reservoir zone, whereas a tributary being blocked by its surging trunk has to join the trunk in the receiving zone, thus lower down in the trunk's basin.

3) Subglacial conditions

The formation of turbid lakes in the shear zones implies that a considerable amount of free water must have been trapped sub- or englacially before the surge. In the Stauninger Alps, about 500 km north of Sortebræ, pressurised water observed in boreholes on the surge-type Schuchert Gletscher was connected to a potential surge instability (Kirchner, 1963). Presence of (pressurised) water may play an important role in the surge process and disruption of the subglacial drainage system has been suggested as a potential surge mechanism (Weertman, 1969; Kamb, 1987; see also Section 2.4.5). It is therefore to be expected that subglacial pressurised water plays a role in the surge mechanism of Sortebræ.

Although no subglacial observations are available on the nature of the substrate, the presence of fine-grained material in the glacier system is suggested by a number of observations on the 1990s surge of Sortebræ. These include: the turbidity of the marginal lakes, turbid meltwater plumes in the proglacial fjord waters, the observation of fine-grained material at the shear margins and in the icebergs (pers. comm. A.K. Pedersen, 1997). Moreover, the Tertiary basalts dominating Sortebræ's drainage basin, being extrusive igneous rocks, produce fine-grained end materials (Pedersen *et al.*, 1997). Furthermore, Sortebræ's termination in a fjord system suggests the presence of marine clays in the lower regions of the glacier (Gabel-Jørgensen, 1940). It is therefore not unlikely that Sortebræ is overlying a potentially deformable bed, at

least in its lower reaches. In addition, dense basalt can have a very low permeability and act as an aquitard (Freeze and Cherry, 1979). This could be important for hypotheses on a surge mechanism for Sortebræ: type of substrate could affect the nature of the surge mechanism and control the propagation and termination of a surge (Boulton and Jones, 1979; Dowdeswell *et al.*, 1991; Murray *et al.*, 1998). The occurrence of fine sediments overlying an aquitard is suggested to be particularly favourable for unstable bed deformation (Boulton, 1979, see Section 2.4.10).

7.8 Concluding remarks

The surge history of the Sortebræ complex described in this chapter suggests that two major surges took place in the glacier system: the first occurred between 1933 and 1943 in Sortebræ West and the second occurred between 1992 and 1995 in Sortebræ. Apart from (temporarily) blocking the outflow from the other glacier the surges of neither glacier had instantaneous effect on the flow regime of the other.

Measurement and detailed observations on the 1990s surge of Sortebræ reveal that:

1. The surge activated the lower 335 km^2 of Sortebræ's basin, just over half the glacier area, redistributed 18.6±0.4 km^3 of ice over the glacier, and resulted in a frontal advance of at least 4-5 km and a surplus calving rate of 2.3-5.9 $km^3\ a^{-1}$.
2. Measured surge velocities are in the range of 1070-10000 m a^{-1} while quiescence phase velocities are only 75-200 m a^{-1}.
3. The estimated duration of the surge phase (2-5 years) and quiescent phase (>60 years) conforms to values found for other surge-type glaciers in East Greenland and is closer to the long periods found on Svalbard surge-type glaciers than to the 'normal' surge periods (1-2 years) and quiescent periods (20-30 years) found elsewhere.
4. Crevasse patterns and surface features are similar to those found on other surging glaciers, but an unexplained phenomenon of the 1990s Sortebræ surge are the waves on the post-surge surface in Lower Loop Basin.

Further research on East Greenland surge-type glaciers could be essential for elucidating the causes of diversities in surge behaviour and for understanding the mechanisms of glacier surging.

CHAPTER 8:
Discussion

A new life is beginning for us, for the ice it is ever the same

Fridtjov Nansen's Farthest North

8.1 Introduction

Which proposed controls in glacier surging can be confirmed and which can be refuted through the presence or absence of characteristics that distinguish surge-type glaciers from normal glaciers? Which factors control the distribution of surge-type glaciers in Svalbard and what are the implications for possible surge mechanisms in this region? Are there distinct classes of surge-type glaciers and surge behaviour? In essence, we are asking if the results from the univariate and multivariate logit analysis of surge-type glaciers in Svalbard (Chapters 5 and 6) can be used to verify the hypothesised controls on glacier surging as presented in Chapter 2. Moreover, can these results, in combination with the findings of Chapter 7, be used to argue for or against the existence of groups of surge-type glaciers or surge behaviour?

8.2 Controls on glacier surging

In the optimal multivariate model for 504 Svalbard glaciers (Section 6.3), relatively high parameter estimates for glacier length, surface slope, lithology and orientation indicate that long glaciers with steeper slopes, overlying shale or mudstone with orientations in a broad arc from NW to SE have the highest probability of being surge-type. Geological age is marginally significant in this model and the negative parameter estimates for Devonian and Precambrian lithologies suggest that surge-type glaciers are less likely to overlie geologies older than approximately 360 Ma. However, in Section 6.6 it became apparent that surface slope can be substituted by elevation span, implying that slope is possibly not a primary control on glacier surging. For a 'reduced' model, including 137 Svalbard glaciers with available radio-echo sounding data, a polythermal regime emerged as most strongly related to glacier surging in Svalbard; the probability of fitting surge-type glaciers is highest for the attribute thermal regime and the significance even exceeds that of the attribute length in the model (Section 6.3.3). Model results for the Yukon Territory (Section 4.6 and subsections) suggest that Fowler's index also has some effect on the likelihood of surging as does elevation of the terminus, though Fowler's index only effects the surge probability of smaller glaciers. Therefore, attributes that distinguish between surge-type glaciers and normal glaciers include glacier length, glacier slope, thermal regime, lithology, geological age, aspect, elevation span, and to a lesser extent, minimum altitude and Fowler's index.

Tests using traditional multiple regression statistics showed that the correlation between any variable and surging could be explained by the primary correlation between glacier length and surging, and that the remaining parameters had no additional explanatory power (Clarke, 1991). However, all optimal multivariate logit models in this thesis include additional variables to glacier length, and therefore indicate that glacier surging is controlled by a combination of variables, including length, as was suggested by Clarke *et al.* (1986) and Hamilton and Dowdeswell (1995). According to Raymond (1987), critical thresholds in glacier geometry would exist at which surges would initiate and terminate. Whereas the nature of the analysis in this thesis was not designed to analyse dynamic changes in glacier systems, no threshold values of length or slope could distinguish surge-type from normal glaciers (Section 6.3.2). Keeping all other variables constant, surge probability increases with increases most strongly with a combination of increasing length and increasing slope.

Revisiting the discussion on the proposed implications of increasing surge probability with presence or absence of certain characteristics (Section 3.5), the main findings of the research presented in the Chapters 5, 6 and 7 are discussed in respect to the implications on flow instabilities and surge mechanisms.

The Svalbard model results for length, slope, elevation span, and direction of flow, and the results for the Yukon Territory for length and terminus elevation imply a relation between mass balance and the distribution of surge-type glaciers as for example suggested by Budd (1975). The specific combination of glacier orientation, length, slope and lithology could possibly be a proxy for orographic effect on snow distribution, variations of insolation with aspect, topographic shading or local wind patterns, all accounting for mass input and energy balance of the glacier (e.g. Meier, 1965). Studies on correlations between mass balance properties and other glacier attributes in 80 glaciers world-wide show that mass balance measurements at the glacier head and terminus are, for valley glaciers, best correlated to glacier length, but correlations with length are weaker for large compound glaciers (Dyurgerov and Bahr, 1999). Furthermore, mass balance has strong connections to all glacier elevation measures, including elevation span. To test the hypothesis of a mass balance control on surge potential continuous and categorical hypsometry and AAR variables as well as equilibrium line altitude were introduced into the univariate logit models (see Table 5.10). The model results revealed that none of these mass balance related variables were significant and the proposed mass balance control on surging is consequently not supported. It could have been possible that comparing different glacier types with intrinsically different geometries and typical AARs obscure modelling of the AAR and hypsometry. To resolve this, a detailed analysis of the interaction terms of hypsometry and AAR variables with glacier type was undertaken, but no relationships

could be confirmed. Therefore, the hypothesis that the specific combination of length, slope and aspect that increases the likelihood of surging in the multivariate models is in reality a substitute for a mass balance control, is rejected, because none of the available mass balance related variables improved the models for glacier surging. It is plausible that this null finding of a correlation between the mass balance related attributes (hypsometry, AAR and *ela*) is a product of the crude measurements of these attributes and that more detailed measurements of mass balance may reveal hitherto undetermined relations between mass balance and surge behaviour. No indication of this kind could be determined from qualitative comparison of the distribution of for example equilibrium line altitude, precipitation, glacier power, mass balance trends and that of surge-type glaciers (e.g. Andrews, 1972; Lefauconnier and Hagen, 1991; Hagen *et al.*, 1993; Dowdeswell *et al.*, 1997).

Clarke *et al.* (1986) postulated that longer glaciers would be more likely to cross geological boundaries and hence have a tendency to develop instabilities in the subglacial drainage system. Harrison *et al.* (1994) also state that ‘‘a complex bed cannot be eliminated as a necessary (though not sufficient) condition for surging’’, where surging would occur in a complex geological setting in which erosion rates are high, and no surging would occur on more competent bedrock. For example, the fault generated geometry and weak bedrock type along the tectonically active Denali fault zone, Alaska, is associated with the large number of surging glaciers in this region (Post, 1969; Echelmeyer *et al.*, 1987). Several physical processes at the ice-bed interface could relate geological boundaries and complex geologies to flow instabilities. For instance, the piezometric surface in glaciers, hence water pressure, is dependent on the hydraulic properties of the substrate. Beds of low hydraulic conductivity, e.g. fine-grained tills and lithologies of low porosity, require a steep hydraulic potential gradient (steepness of the piezometric surface) to obtain a water flux, whereas beds of high hydraulic conductivity, coarse-grained tills and lithologies of high porosity, require less steep hydraulic potential gradient to obtain similar water fluxes through the substrate (Boulton and Paul, 1976). Therefore, substrate of low conductivity can act as a dam, increasing the level of the piezometric surface at all upglacier points (Boulton and Paul, 1976). Geological boundaries perpendicular to the direction of ice flow could therefore affect the equilibrium piezometric surface, creating step changes in gradient and height of the piezometric surface. This process also indicates that effective pressure does not necessarily increase with increasing glacier thickness, but is primarily dependent on substrate conditions (Boulton and Paul, 1976). During events of high meltwater input, transitions from high to low conductivity substrate could raise the piezometric surface to such extent that the water pressure becomes very close to overburden pressure, possibly generating floating conditions and thus flow instabilities. Furthermore, a glacier overlying different lithologies in the direction of ice flow would have a layered structure of basally regelation

derived debris affecting the rheological properties of the basal ice layer (Boulton, 1970). Lateral variations in basal ice properties could cause differential drag conditions (sticky spots), which could be conducive to surging (e.g. McMeeking and Johnson, 1986; Alley, 1993). Deforming beds that create their own microstructure would represent a mechanism for enhanced basal friction: e.g. drumlins are more viscous (stiffer) than the surrounding till (Fowler, 1997). Because original inhomogeneities determine the relative strain of different parts of the substrate, inhomogeneous tills would be more conducive for drumlin-like bedform formation (Boulton, 1987). Till homogeneity is controlled by thermal regime, subglacial hydrology, source material, and transport distance (e.g. Dreimanis and Vagnes, 1972; Boulton and Paul, 1976; Clarke, 1987b; Mooers, 1990). Glaciers overlying different lithology types are thus likely to have a more inhomogeneous till as the source material is of a mixed composition.

To test the hypothesis that length is a substitute for geological boundaries, three attributes representing geological boundaries were introduced in the Svalbard models (Chapters 5 and 6). The results of these tests reject this hypothesis, because neither type nor direction nor number of geological boundaries is significantly related to the distribution of surge-type glaciers in Svalbard. Hence, glacier length is a primary control on surging, unless it is a substitute for other untested variables being possibly related to glacier surging such as, for example, glacier thickness.

A possible explanation of raised likelihood of surging in long glaciers with a large elevation span can be found in conjunction with the findings for lithology: glaciers overlying fine-grained sedimentary lithologies have higher surge probabilities than glaciers overlying different types of bedrock. This relationship suggests that surging may be related to the availability, erodibility, deformability and permeability of the substrate. The distribution of fine and coarse-grained tills is a function of source material and transport distance (Dreimanis and Vagnes, 1972). Compact sedimentary lithologies, for example shales and mudstones, tend to produce fine-grained sediments and the rocks themselves are relatively impermeable (Freeze and Cherry, 1979). Therefore, glaciers overlying these lithologies are more likely to be underlain by unconsolidated sedimentary beds. Furthermore, a till matrix becomes progressively rich in fines with increasing transport distance (Dreimanis and Vagnes, 1972), hence long glaciers are more likely to overly fine-grained tills. The occurrence of fine sediments overlying an aquitard has been suggested to be particularly favourable for unstable deformation of basal sediments (Boulton, 1979). Under conditions of low effective pressure, tills with a clayey matrix deform more rapidly than clays with a sandy matrix. Moreover, deformation of fine-grained substrate initiates at a smaller thickness of the till layer (Boulton, 1996). Recent investigations on relation between textural and granulometric properties of till underlying Ice Stream B and ice flow behaviour suggest that

fine-grained tills are likely to have ice-bed interface strength lower than the till strength, which involves a condition where sliding with ploughing is mechanically more advantageous that pervasive deformation of the underlying till (Tulaczyk, 1999). Hence, keeping other factors fixed, flow speeds would generally be higher in glaciers overlying fine-grained saturated substrate. In Svalbard, the lowest bedrock permeabilities (1×10^{-20} to 1×10^{-16} m^2) have been measured in Triassic shales and siltstones (Booij *et al.*, 1998). According to the model results in this theses, these lithologies are conducive to surge behaviour. Limestone, which is not favourable to surging in Svalbard according to the model results, can be much more permeable (0.001-0.05 m^2), thus preventing the build-up of high basal water pressures (Freeze and Cherry, 1979; Booij *et al.*, 1998). Moreover, in many regions in Svalbard, karstification has increased the secondary permeability of the limestones (Booij *et al.*, 1998). Igneous and metamorphic bedrock are generally of lower permeability than sedimentary bedrock, because they have fewer interconnected pore spaces, and would therefore be favourable to the building up of high basal water pressures. However, they are also more resistant to erosion than sedimentary rocks and hence produce thinner sediment layers beneath the glacier (Boulton, 1979). Besides, crystalline igneous and metamorphic rocks produce larger terminal grain sizes than non-crystalline rocks (Dreimanis and Vagnes, 1972).

There is a discrepancy between the distribution of surge-type glaciers and normal glaciers on different lithologies between Spitsbergen and the other islands of the Svalbard archipelago. In the regions of Spitsbergen investigated by Hamilton (1992), surge-type glaciers mainly overlie limestone. However, in the additional regions included in this thesis the majority of surge-type glaciers overlie shale/mudstone, and a relatively large number of normal glaciers overlie limestone/carbonate. The size and location of a regional study may restrict the environmental setting and it is therefore necessary to take into account the scale of the research before making statements about the relationship between surging and geology. In contrast to Svalbard, surge-type glaciers occur on igneous bedrock in, for example, Greenland and Iceland (Clapperton, 1975; Weidick, 1988; Björnsson, 1998). Another major cluster region of Greenland surge-type glaciers, the Stauninger Alps, is in terrain of mixed metamorphic lithologies (Rutishauser, 1971). Cluster regions of surge-type glaciers in Greenland and Iceland are however mainly in the basalt provinces: the grainsize of these igneous rocks is smaller than that of crystalline igneous rocks. The hydraulic conductivity and porosity of basalt is very anisostropic, but the smallest conductivities are generally found perpendicular to the direction of the basalt flows (Freeze and Cherry, 1979). Indeed, glaciers in the Tertiary basalt province of East Greenland tend to flow perpendicular to the strata (Larsen *et al.*, 1995). In conclusion, there appears to be no prevalence of surge-type glaciers on specific types of bedrock, but geology is certainly a controlling environmental factor in the distribution of hard and soft beds, hence of the

occurrence of possible hard and soft bed surge mechanisms. For Svalbard, the increased surge likelihood of long glaciers overlying fine-grained lithologies as indicated by the model results in this thesis suggests that surge-type glaciers overlie relatively thick fine-grained potentially deformable substrate. Hence, bed failure and rapid bed deformation, rather than bed separation on a hard bed, are suggested to play a role in the surge mechanism of Svalbard glaciers.

In most cluster regions of surge-type glaciers, and in general in glaciated regions, measurements of geothermal heat are sparse or even absent (e.g. Pollack *et al.*, 1993). Instead, lithology, in combination with geological age, has been used to estimate geothermal heat flow beneath glaciers (e.g. Sugden and John, 1976; Paterson, 1994). The results in this thesis imply a weak negative relationship between geological age and glacier surging; surge-type glaciers preferentially overlie young rocks. A possible explanation for the relation between surge potential and geological age is the overall higher geothermal heat flux in younger rocks (Sclater *et al.*, 1980). The average (continental) geothermal heat gradient is 57 ± 11 mW m^{-2} but varies with geologic age and rock type (Sugden and John, 1976; Sclater *et al.*, 1980). Variations in the radiogenic heat production mainly depend on orogenesis, erosion, metamorphosis and the distribution of heat generating elements (U, Th and K), while local variations in heat flow can be ascribed to groundwater flow (Sclater *et al.*, 1980). Apart from mean heat flow, geologic factors such as water circulation, orogenesis and related uplift and erosion rates are suggested to vary with geologic age of the crust (Sclater *et al.*, 1980; Stacey, 1992), and may relate to variations in subglacial conditions favourable to surging. The heat budget at the ice-bed interface is however extremely complex and it is uncertain what the exact contribution of geothermal heat to the total heat budget is (e.g. Clarke *et al.*, 1984). Other implications of glacier surging occurring predominantly in regions of relatively young geologies is the availability of erodible material (e.g. Post, 1969; Harrison *et al.*, 1994).

Which other explanations could there be given for a length control on surge potential? There are essentially two separate types of flow instability: floating (decoupling) and bed failure. Decoupling, thus a high sliding velocity, is determined by water supply (effective pressure), bed geometry and basal shear stress (Alley, 1989). Bed deformation is controlled by effective pressure, basal shear stress, till thickness and rheology, where rheology depends on texture and structure, homogeneity, deformation history, saturation and temperature conditions (e.g. Clarke, 1987b; Boulton and Dobbie, 1993; Murray, 1987; Tulaczyk *et al.*, 1998). As explained in Section 2.4.6, finite water layer thickness, calculated as a function of melt rate at the glacier bed, inverse water pressure and glacier length, show that the longer the glacier the greater the thickness of the water film that can develop (Weertman, 1969). Longer glaciers would therefore have higher probabilities of being surge-type, because a thick water film would inundate those

obstacles that give most resistance to basal motion. Weertman (1969) found that the highest probabilities of glaciers being surge-type are found in glaciers over 30 km in length with a 'smooth bed' with controlling obstacle size of about 1-2 mm. However, Walder (1982) proved that a continuous water film could is unstable and with increasing water pressure conduits would develop. Consequently, Weertman's hypothesis for glacier surging is rejected. On soft beds, given no obstacles (clasts or geomorphic forms such as drumlins) larger than the order of 1 mm occur in the top layer of the substrate, a distributed water film could however be stable beneath a glacier, hence could 'float' a glacier (Alley, 1989). Furthermore, Alley (1989) argues that, in the absence of a subglacial conduit drainage system, porous flow through substrate is optimised on thick aquifers where flowpaths are short. Small glaciers overlying soft beds would therefore have more effective drainage than larger glaciers. Boulton and Dobbie (1993) found a direct relation between the length of the flowline and the till thickness required to avoid instabilities. Hence, longer glaciers overlying relatively thin till beds would have a higher likelihood of flow instabilities.

Another possible explanation of the increased surge probability of long glaciers could be the distance-related attenuation of longitudinal stress (Kamb and Echelmeyer, 1987). Strain rate measurements on mini-surges and interpretation of tectonics of the 1982-83 surge of Variegated indicated that flow in surge-type glaciers is governed by longitudinal stresses rather than by basal strear stress alone (e.g. Raymond, 1980; Raymond *et al.*, 1986). Spatial variations in glacier movement are smoothed by longitudinal stress gradient coupling related to glacier thickness in the form of a 'longitudinal coupling length', which magnitude is being estimated between 1 and 3 times the glacier thickness for temperate valley glaciers (Kamb and Echelmeyer, 1987). Sinusoidal perturbations larger than 20 times the longitudinal coupling length appear to be least attenuated. Since glacier length increases non-linearly with increasing glacier thickness (for a parabolic glacier profile length increases with the square increase in thickness), longer glaciers could be more sensitive to longitudinal variations in movement between the upper and lower part of the glacier. These variations can be due to push-and-pull effects related to different throughput times of water in the accumulation and ablation areas (Fountain and Walder, 1998) or to the differential movement of the upper (increasingly active) and lower regions (increasingly stagnant) in the quiescent phase (Robin and Weertman, 1973). The larger stress gradients in longer glaciers could for example lead to a damming effect and the development of a trigger zone for surging (Robin and Weertman, 1973), or could facilitate conditions of raised drag, which causes a restriction in outflow or a stress singularity leading to unstable flow (McMeeking and Johnson, 1986). Furthermore, a downstream increase in drainage effectiveness and subsequent reduction of hydrostatic pressure towards the terminus can generate a downstream increase in sliding resistance (Clarke *et al.*, 1984). This last process

implies that the longer a (temperate) glacier is, the more likely it is to experience downstream resistance to sliding.

The apparent correlation between surge-type glaciers and steep slopes can be explained in a number of ways. Firstly, steep surface slopes could be not a control, but a result of glacier surging. This can be the result of a downstream restriction in outflow causing an upstream steepening, but also of the fact that retreating glaciers without a sliding component have steeper surface profiles than glaciers where sliding takes place (Schwitter and Raymond, 1993). Surge-type glaciers in quiescence are virtually stagnant and the contribution of basal sliding is negligible, thus develop relatively steep surface profiles. However, glaciers for which bed deformation contributes to the forward motion generally have lower equilibrium profiles than glaciers on inactive beds (Boulton and Jones, 1979). Secondly, for unstable flow over both rigid and deformable bed a steep slope could therefore be a necessity. Bed separation on hard beds occurs more rapidly when surface slopes are steep (Iken, 1981; Bindschadler, 1983). It was however found that, in the optimal multivariate model for glacier surging the effect of surface slope on surging could be substituted by an effect of elevation span on surging, and it is therefore ambiguous whether surface slope is a primary control of surging. No firm conclusion can be drawn from these model results on primary controls of either slope or elevation span, because, as explained in Section 5.4.9, length, slope and elevation span are intrinsically related.

The analysis in this thesis further suggests that a polythermal regime significantly increases the likelihood than a glacier is of surge-type. This finding agrees with Hamilton's (1992) findings on the Spitsbergen dataset, though his results were statistically controversial. Thermal regime being a diagnostic criterion for distinguishing between surge-type and normal glaciers implies that glacier surging in Svalbard is potentially thermally controlled. This thermal control is likely to operate at the glacier bed at the boundary between warm and cold ice, where raised basal water pressures could trigger a surge (e.g. Clarke *et al.*, 1984; Mooers, 1990). Furthermore, there are large differences in permeability between types of substrate in their frozen and unfrozen states. Although at unfrozen conditions the conductivity is virtually independent of temperature, at the transition from unfrozen to frozen conditions a sharp drop in hydraulic conductivity takes place: for a temperature decrease from 0 to -0.5ºC the hydraulic conductivity decreases up to a factor 4 (Freeze and Cherry, 1979). Polythermal glaciers could have a boundary zone where the top layer of the substrate is at the transition from an unfrozen to a frozen state, and therefore at high pressure. Furthermore, reflecting upon factors controlling till homogeneity, polythermal glaciers overlying geological boundaries would have a higher degree of inhomogeneity and are therefore more likely to experience differential basal drag (sticky spots) than temperate or cold glaciers overlying one type of bedrock. Measurements during in

the late surge phase of Bakaninbreen, suggest that during surge, the top layer of the substrate underlying 'warm' ice, is actively deforming and possibly above the melting point (Murray *et al.*, in review). Water generated in this zone is unable drain effectively through the frozen substrate down-glacier and high basal water pressures can be maintained.

A potential problem of interpreting the results for thermal regime presented in this thesis is the cause and effect dilemma between surge behaviour and polythermal regime: thermal regime is the effect of glacier dynamics and climate and it is thus possible that a surge affects a glacier's thermal regime (e.g. Krass *et al.*, 1991). It is however also clear that thermal regime can directly affect glacier response (Hutter, 1993). Although thermal regime has been measured for a number of surge-type glaciers in different settings (e.g. Bindschadler *et al.*, 1976; Clarke *et al.*, 1984; Clarke and Blake, 1991; Björnsson *et al.*, 1995; Murray *et al.*, in review) no comparative measurements of before and after surge exist. Consequently, the direct effect of a surge on the thermal regime remains obscure.

It has been suggested that a causal relationship exists between surge potential and a high subglacially derived debris content (e.g. Clapperton, 1975). Debris-rich basal ice can be less plastic than cleaner ice and could become stagnant when it is blocked by bedrock obstructions (e.g. Boulton, 1971; Sharp *et al.*, 1994). Souchez and Lorrain (1991) suggested that increasing content of solid impurities in the basal ice reduced the creep rate exponentially. Glaciers with a sediment content of more than 50% in their basal ice layers exhibit sandpaper friction at the bed for which basal sliding is only possible in the meltseason under conditions of high subglacial water storage (Schweizer and Iken, 1992). Glaciers with a small debris concentrate can slide throughout the year, with a relationship between sliding and subglacial water pressure as found by Iken and Bindschadler (1986). Cold based and polythermal glaciers appear to have a greater amount of subglacially derived debris than temperate glaciers (e.g. Boulton, 1970; Clapperton, 1975; Knight, 1997). Boulton (1970) argued that temperature is a controlling factor in debris incorporation into the ice, as only those glaciers in which basal freezing is important show large have debris rich basal ice. However, Andrews (1972) and Clapperton (1975) have questioned this hypothesis, arguing that glacier dynamics and duration of glaciation are primary controls of erosion rate. Yet, some thermal control on subglacial debris incorporation governing flow dynamics is conceivable. For example, thrusting could be one of the principal mechanisms of incorporating debris subglacially and in polythermal glaciers this process is concentrated in the transition zone of unfrozen to frozen bed (Mooers, 1990; Hambrey *et al.*, 1996; Hambrey *et al.*, 1999). These regions are therefore suggested to have different sliding properties than up-glacier regions and might therefore act as a zone of restricted outflow. Furthermore, the thickness of a basal ice layer increases from the glacier head to the margin, mainly through compressive

foliation close to the margin (Sharp *et al.*, 1994; Knight, 1997). Long polythermal glaciers overlying unconsolidated sedimentary beds could thus have thicker basal ice layers with a higher debris concentration than shorter ones and therefore be more likely to experience flow instabilities. In addition, deformation rate of ice is temperature dependent (see Section 2.3), thus polythermal glaciers could exhibit stress discontinuities at the boundary of warm and cold ice. Furthermore, instabilities occur in zones of compression rather than of extension, and the initiation of the zone of compression (the surge bulge) is temperature related (see Section2.4.3).

Whereas the role of tributaries and confluence of glaciers in the Svalbard database has not been analysed beyond the classification of glacier fronts, the behaviour of the surges in the Sortebræ complex suggest that neither surges of tributaries nor of trunks trigger surges in other flow units (see Section 7.7). In contrast, on West Fork Glacier, Alaska, it was found that some tributaries contribute to the surge of the trunk, while others do not (Harrison *et al.*, 1994). Sortebræ's behaviour of interacting flow units rather suggest that tributaries and confluent flow units might obstruct the outflow of other flow units, as has been previously been suggested for other surge-type glaciers in Alaska, Greenland and the Karakoram (e.g. Stanley, 1969; Colvill, 1984; Heinrichs *et al.*, 1996; Hewitt, 1998). Clearly, more research is necessary into the interaction of confluent flow units.

8.3 Synthesis of surge controls and surge theories

Recapitulating Table 2.1 with an overview of surge controls versus surge theories and instability mechanisms (see Chapter 2: Section 2.5), a new table (Table 8.1) can be constructed for the model results for controls of surging in Svalbard as presented in this thesis and discussed in the previous section. In Table 8.1, the Svalbard surge controls are contrasted with possible surge mechanisms. The presence of the specific combination of surge controls in Svalbard and the null findings for other tested attributed leads to the following hypothesis of surge mechanisms operating in Svalbard.

The observation that glaciers with relatively steep slopes are more likely to be of surge-type lends no support to Kamb's (1987) theory of linked cavity mechanism of surging on a hard bed. This conclusion is even stronger than that of Clarke (1991), who found for the Yukon Territory "slope has no explanatory value not accounted for by the correlation between length and surge tendency". Hamilton (1992) found similar results for Spitsbergen. Yet, both these studies show a slight but not statistically significant positive correlation between slope and surging. In contrast, our study, which uses multivariate models, shows a significant and positive correlation between surging and surface slope. Other evidence that can be used to argue against a linked-

cavity surge mechanism operating in Svalbard is the model results for Fowler's index. The hypothesis that surge-type glacier should have values for Fowler's index smaller than the order of one for (Fowler, 1989) is proven valid for small glaciers in the Yukon Territory, but no significant effect of Fowler's index on glacier surging could be established for longer glaciers in this region. Moreover, Fowler's index was not found to be significantly related to the surge probability of Svalbard glaciers. Hence, Fowler's hypothesis is not supported throughout the population of surge-type glaciers and appears too rigid to be a primary control of surging. These findings however suggest that more than one surge mechanism could hold for glaciers, with small glaciers having separate surge controls from large glaciers.

No mass balance control on glacier surging could be confirmed. Consequently, Budd's theory (Budd, 1975) of a critical balance flux for surge-type glaciers is not supported. Yet, the finding of steep slopes characteristic for surge-type glaciers lend some support to Budd's lubrication mechanism, in which the lubrication factor is directly related to surface slope (Budd, 1975).

Combining the results for lithology with the results for polythermal regime in the Svalbard archipelago suggest some support for a thermally controlled surge mechanism on a soft-bed rather than hard-bed. However, as the research into the incidence of glacier surging presented in this thesis is a regionally based study and because the glaciers in Svalbard are low altitude glaciers and often overlie thick sequences of fjord sediments this support for a soft bed surge mechanism may not hold in other regions.

SVALBARD SURGE CONTROLS AND POSSIBLE SURGE MECHANISMS												
Surge theories and instability indices →		Stress instability	Thermal instability	Lubrication instability *Weertman*	Lubrication instability *Budd*	Linked-cavity-system *Kamb*	Linked-cavity-system *Fowler's index*	Bed separation index *Iken*	Bed separation index *Bindschadler*	Bed deformation *B-H rheology*	Bed deformation *Haeberli's index*	Blocking or restricting
Svalbard surge controls ↓		2.5.2	2.5.3	2.5.6	2.5.6	2.5.8	2.5.8	2.5.8	2.5.8	2.5.10	2.5.10	2.5.12
Glacier length	long		+	+		+				+		+
Glacier slope	high	+			+			+	+			
Elevation range	large									+	+	
Glacier aspect	NW-SE											
Lithology	young		+				+			+		
	fine grained			+						+		
	impermeable			+	+							
Polythermal regime			+									

Table 8.1: *Controls on surging in Svalbard contrasted with surge theories and flow instability mechanisms.*

8.4 Classes of surge-type glaciers and surge behaviour

Interregional comparison of surge behaviour and characteristics of surge-type glaciers has indicated that a large variety of surge behaviour exists and that surging occurs in different environments across a range of glacier types (e.g. Meier and Post, 1969; Hagen, 1987; Weidick, 1988; Dowdeswell *et al.*, 1991; Hewitt, 1998). The analysis of the surge history and behaviour of Sortebræ, East Greenland, (Chapter 7) has been an attempt to contribute surge data for a region that is deficient in observations of active surges and quiescent periods. Surge and quiescence data of this glacier and of a number surge-type glaciers in Greenland and other regions imply that different types of surge behaviour exist, but that these cannot simply be regionally grouped as was postulated by Dowdeswell *et al.* (1991). Furthermore, the Svalbard and Yukon glacier population analysis results gives some support to the hypothesis that the combination of attributes controlling surging might not be similar for all types of surge-type glaciers and across all regions.

Despite the small number of recorded 'observed' surges, 6 in West and 7 in East Greenland, there appears to be a clear contrast in surge behaviour between the two regions. Weidick (1988) ascribed this contrast to glacier size. In the Disko-Nugssuaq area (69-71°N), West Greenland, small surge-type glaciers generally have surge durations in the order of 2-4 years and the quiescent phase is estimated to be 30 to 50 years, while the frontal advance during these surges is limited to maximal 1-2.5 km (Weidick, 1988). Larger surge-type glaciers in the Stauninger Alps and inland of the Blosseville Kyst (69-71°N), East Greenland, are inferred to have surge phases of 5 to 15 years and surge intervals of approximately 70-100 years. The displacement of surface features, such as moraine loops and crevasses, and frontal advance during East Greenland surges is in the order of 10 km (e.g. Hendriksen and Watt, 1968; Rutishauser, 1971; Colvill, 1984; Weidick, 1988; Reeh *et al.*, 1994). Due to a lack of precise surge onset and termination dates for Sortebræ, we can only infer that the surge started after August 1991 but before 1994 and terminated probably not long after August 1995. Therefore, the estimated surge duration of Sortebræ is between 2 and 4+ years. Hagen (1988) reported that small landbased glaciers in Svalbard had much shorter surge duration, 2-3 years, than found for longer surge-type glaciers (4-10 years). However, Dowdeswell *et al.* (1991) suggest that the long duration of the active phase in Svalbard typifies surges of high polar ice masses in general, and found it was not directly related to glacier size. The measurements on Sortebræ suggest that the surge character conforms with other surges in East Greenland, although the surge duration and frontal advance of 4-5 km suggest that intermediate types of surge duration and advance exist. Sortebræ is situated about 300 km further south than the major cluster of observed surges in the Stauninger Alps area, and is for East Greenland the most southerly reported surge. Although the

glacier is situated at a similar latitude (about 69º-70ºN) as the major surge cluster in the Disco-Nugssuaq peninsula region, the climate is markedly milder in West Greenland (Ohmura and Reeh, 1991). The abundance of moraine material on Sortebræ and the termination in a fjord implies that the glacier is potentially overlying a deformable bed. Many other surge-type glaciers in East Greenland also have tidewater termini or terminate in valleys with an abundance of unconsolidated sediments (e.g. Rutishauser, 1972; Weidick, 1988). Like Svalbard glaciers, East Greenland glaciers have been inferred to have polythermal regimes. Therefore, longer surge phases could be related to a thermally regulated surge propagation, similar to that suggested for Bakaninbreen, Svalbard (Murray *et al.*, in review). However, none of the Greenland surges have recorded surge initiation and termination, and it is therefore unclear if these transitions from slow to fast flow and *vice versa* are abrupt or gradual.

Since 1933, Sortebræ West has surged once (between 1933 and 1943) and so did Sortebræ (in the 1990s). Therefore, these glaciers have quiescent phases of 60+ years, which is longer than some Alaskan and Pamir glaciers, but of the same order as suggested for other surge-type glaciers in East Greenland and a number of surge-type glaciers in Svalbard (Rutishauser, 1969; Reeh *et al.*, 1994; Dowdeswell *et al.*, 1995; Muller and Fleisher, 1995; Lawson, 1996). However, many surge-type glaciers in Svalbard have inferred quiescent phases of the order of 50-500 years (Dowdeswell *et al.*, 1995). Although Meier and Post (1969) state that quiescent phases ‘‘commonly last 20-30 years’’, the majority of glaciers world-wide appear to have (estimated) quiescent phases of 50+ years, and those with short periods are thus rather an exception than the norm. It is therefore interesting that in a region such as Alaska, surge phases of glaciers vary between 20 years (e.g. Variegated Glacier and Bering Glacier) and >50 years (e.g. West Fork Glacier) (Kamb *et al.*, 1985; Harrison *et al.*, 1994; Muller and Fleisher, 1995), and that in other regions, such as East Greenland and Svalbard, longer quiescent phases prevail. If the recovery time of a surge-type glacier would mainly depend on the accumulation rate, the duration of quiescence would be primarily climatically controlled (e.g. Dyurgerov *et al.*, 1985; Dowdeswell *et al.*, 1995: see also Section 2.5). Indeed, the 20-year cycle of Variegated Glacier could be related to the heavy precipitation on the south side of the St. Elias Range. For Bering Glacier, west of this region, it has even been suggested that its 20 years cycle of is triggered by several years of above-normal snow accumulation (Tangborn, 1999). In contrast, the 50-60 year cycle of West Fork Glacier is in a region of moderate precipitation (Harrison *et al.*, 1994). However, the actual time it takes for the glacier to build up to its pre-surge geometry (the geometry at the surge initiation) not only depends on the initial ice volume displacement (depletion of the upper region) and accumulation rate, but also on the flux imbalance (this difference between balance flux and actual flux is controlled by the degree of restriction in outflow). If this were the case, it could be that all glaciers world-wide were potentially of surge-

type on the condition that they were substantially restricted in their outflow over a considerable period of time. Perhaps focussing the research to the controls on glacier surging on what causes the restriction of outflow (e.g. Clarke *et al.*, 1984; Alley, 1993; Fischer *et al.*, 1999) in conjunction with research into causes of flow instabilities would contribute to the further understanding of the causes of surges and surge mechanisms.

8.5 Methodology critique

Logit models can be used to explore relationships between different types of variables and the results from a well designed can elucidate the complexity of processes that are encountered in glaciers. Although logit modelling would appear to be a powerful quantitative technique in glaciology, there are a number of drawbacks to the method. Firstly, logit models are designed to explore linear relations between a set of explanatory variables and a response variable, and as such cannot be used to explore non-linear relationships. Secondly, the method is essentially an exploratory technique: models are developed interactively which requires an experienced user with a background knowledge of the data (Atkinson *et al.*, 1998). Limitations of statistical population analysis techniques in general are that they cannot deal with spatial and temporal variations in surge behaviour, cannot model time series, and cannot grasp spatial patterning of individual glaciers.

The residual analysis presented in Chapter 6 does not conform to the usual methods of prediction in statistical analysis (e.g. Davis, 1986). Normal procedures of using statistical regression analysis as a predictive tool involves the setting up of a statistical model with a training set and predicting units, independent of the training set, through the model obtained using the training set. Using the procedure of logit modelling, where the optimal model is obtained by using the complete dataset, thus including the glaciers that are to be 'predicted'. However, the purpose of logit models is to obtain the most accurate information on controls on glacier surging and this is optimised by using an as large as possible sample size. As can be seen from the development of optimal models for the reduced dataset of 137 glaciers with RES measurements, the sample size indeed affects the significance of the different components in the models and different pictures of surge controls emanate from different models. However, obtained logit regression equations can be used to fit surge probabilities for glaciers that have not been included in the models.

There are also number of problems related to the assignment of attributes to glaciers. Firstly, assigning a dichotomous surge index to glaciers (S=0 for normal glaciers and S=1 for surge-type glaciers) is not representative for the surge probability of individual glaciers. In reality the

response variable in the logit models would be continuous, with range 0-1, and its value corresponds to the predicted probability that the glacier is of surge-type (e.g. Clarke *et al.*, 1986). But, for the purpose of finding distinctive characteristics of surge-type glaciers, the crude dichotomous surge index proved effective. Further, the crude method of assigning the variables *ela*, AAR and hypsometry oversimplifies real mass balance data, hence can obscure the possible climate signal in surge-type glaciers. An additional comment is that detailed classification of categorical variables, such as lithology, orientation, geological boundary, glacier type and type of glacier front, resulted in some of the classes containing too small numbers of glaciers to return statistically significant results in the logit models. The only solution to this problem in logit modelling was to reduce the number of classes in these variables and constructing new models with the reclassified schemes. The disadvantage of this procedure is that possibly vital physical information is lost.

Additionally, this study raises a number of issues in relation to general research into interactions of glacier properties and the use of glacier inventory data (e.g. Smolyarov, 1987; Haeberli and Hoelzle, 1995; Haeberli *et al.*, 1998; Dyurgerov and Bahr, 1999). In these studies one has to have reservations about the validity of commonly used attribute data from glacier inventories in terms of their direct relation to glacier dynamics or mass balance, and it is necessary to correctly establish relationships between these. For example, does a measure for average glacier slope indeed give information on glacier dynamics or is this measure too crude to be of any value? What is the effect of increasing glacier length on glacier dynamics? As overall glacier length emerges from all studies as a primary control of surging, it could be useful to collect not only overall length of a glacier but also length data of segments of the glaciers (for example, length of tributaries, separate flow units and length of accumulation and ablation area). These length data could, in conjunction with mass balance and hypsometry data, elucidate relations of length and flow dynamics.

Finally, although statistical techniques, such as correlation and regression, can reveal interesting patterns and can suggest new relationships between glacial or environmental parameters and surging, it does not provide physical solutions for the controls on surging. It may however help focus further research into the appropriate surge mechanisms.

CHAPTER 9:
Summary and Conclusions

He asked if there were any other Poles such as a Bear of Little Brain might discover

A.A. Milne (Winnie-the-Pooh)

9.1 Summary and conclusions

The research in this thesis was an attempt to explore and quantify the relations between surge-type glaciers and glacial and environmental variables by isolating factors that discriminate surge-type glaciers from normal glaciers. This approach allows resolving of the complex processes of glacier surging into simpler components, through which conceived mechanisms of surging can be verified. Theories on surge mechanisms, surge triggers and flow instabilities enclose a series of possible controls on surging. Through analysing which of these proposed controls correspond to the common characteristics of surge-type glaciers in a glacier population, it is possible to verify which surge mechanisms may be in force in the analysed regions. The analysis in this thesis involved the development of logit regression models of glacier populations in order to identify which combination of attributes distinguishes surge-type glaciers from normal glaciers in the glacier population. Further, this thesis evaluates, through comparing characteristics and surge behaviour of surge-type glaciers within and between regions, if there is a rationale for identifying different groups of surge-type glaciers or surge behaviour.

For 1726 glaciers in the Yukon Territory, a multivariate logit regression model was generated in order to analyse which combination of glacial attributes distinguishes surge-type glaciers from normal glaciers in this region. The model results indicate that long glaciers with termini at higher than average elevation and small values for Fowler's index are more likely to be of surge-type. It however appears that the effect of Fowler's index on surge probability is only valid for short glaciers.

For 504 glaciers in Svalbard a dichotomous surge index was assigned to differentiate surge-type glaciers from normal glaciers. For all 504 glaciers data were collected on glacial, geological and mass balance characteristics. For the full set of attributes, univariate logit regression models were generated, in order to detect which variables appear to be strongest related to glacier surging when analysed separately and which variables have no influence on the incidence of glacier surging. The variables length, area, volume, surface slope, glacier orientation, elevation span, glacier form, lithology, geological age and the presence of an internal reflection horizon emerge as most likely related to glacier surging from the univariate logit models. In contrast,

geological boundaries, glacier hypsometry and accumulation area ratio have no significant effect on the likelihood that a glacier is of surge-type.

A multivariate logit regression model was developed in order to analyse the independent and combined effects of explanatory variables on the incidence of glacier surging in Svalbard. The logit analysis allows the combined analysis of continuous and categorical explanatory variables and the identification of the independent effects of variables whilst controlling for the confounding effects of other variables. Using an iterative interactive method, a so-called optimal multivariate model was obtained, giving the highest reduction in model deviance and explaining most of the variance in the data. This optimal multivariate model shows that of the glacial and geological variables tested, glacier length, surface slope, lithology, geological age and aspect of the ablation area cause a significant reduction in the model deviance. The relatively high parameter estimates for glacier length, surface slope and the lithology category 'shale and mudstone' indicate that long glaciers with steeper slopes, overlying fine grained sedimentary lithologies of geological age younger than 360 Ma have the highest probability of being surge-type. These factors are inferred to control surging. The positive relationship between glacier length and surging and sedimentary lithologies is consistent with findings from previous research (Clarke *et al.*, 1986; Hamilton and Dowdeswell, 1996).

For a subset of 137 glaciers for which thermal regime is known by means of radio-echo sounding or direct temperature measurements, a separate optimal multivariate model was fitted. This indicates that glaciers with a polythermal regime have a higher likelihood of being of surge-type than glaciers with other thermal regimes.

The contributions of individual glaciers to the statistical model was explored through a residual analysis of fitted values of these glaciers. This residual analysis was used to isolate 'outliers' in the data and to spot unusual surge-type and normal glaciers. The model performance of 13 of the 372 normal glaciers was poor, giving fitted values indicating that the glacier was likely to be of surge-type. Examination of these glaciers indicated that seven of these should indeed be re-classified as surge-type. The model performance for 55 of the 132 surge-type glacier in the dataset was poor as these were predicted not to be of surge-type. Some of these might have been misinterpreted to surge, but the others might have characteristics that are different from that of the majority of surge-type glaciers and have characteristics that are ascribed to normal glaciers. Although simple analysis of these glaciers could not elucidate specific surge related characteristics of these, detailed analysis of these uncommon surge-type glaciers might reveal further controls on surging. The findings from this residual analysis indicate that the model can not only be used to identify controls on surging, but can also be used to predict individual surge-

type glaciers that were not classified before as being of surge-type, and locate 'uncommon' surge-type glaciers that are not well grasped by the general statistical model. As the prediction of surge-type glaciers by the logit model leads to a much higher percentage of detected surge features than a random aerial photograph interpretation, it seems that the criteria used in the model are indeed related to surging. Hence, these logit models can be used as a predictive tool for glacier surging.

The surge history and behaviour of Sortebræ, a large tidewater glacier complex in East Greenland was analysed and compared to other glacier surges in order to identify possible groups of surge-type glaciers and surge behaviour and to add information to our knowledge of the surge behaviour in this region. Only four other East Greenland glaciers have recorded surges, whereas an additional 70 have been classified as surge-type. The first known surge in the Sortebræ's glacier system took place between 1933 and 1943 in its western unit and the second known surge occurred between 1992 and 1995 in its main flow unit. Quantitative measurements on this most recent surge were made using multi-model photogrammetric equipment. The 1990s surge affected the lower 50 km of Sortebræ over an area of approximately 335 km^2. Over a period of less than 2 years the tide-water front advanced 4-5 km. Numerous tributaries were sheared off and moraine loops were elongated, while large turbid lakes appeared in the marginal shear zones. The crevasse patterns on Sortebræ are typical for glaciers in surge. Crevasse types include transverse, concentric and longitudinal crevasses in the upper and middle basins; and chaotic crevassing and ice rifts with individual heights of tens of metres in the lower basin. During surge, the ice velocity increased approximately ten-fold and is in the order of kilometres per annum. Measurements of surface depression (up to 219 m) and uplift (up to 74 m) indicate that the total volume displacement as a result of the surge was 18.6±0.4 km^3. This resulted in a calving surplus of 11.7±0.7 km^3, equivalent to a calving flux of 2.3±0.1 to 5.9±0.4 $km^3\ a^{-1}$. Sortebræ has a quiescent phase of at least 60 years and a surge phase of 2-4 plus years. The thermal regime of the glacier is unknown but some glaciers in its vicinity are polythermal. Sortebræ overlies a potentially deformable bed, at least in its lower reaches. The surge duration and environmental setting of Sortebræ suggests that the surge mechanisms might be similar to those of Svalbard surge-type glaciers.

The specific conclusions of the research presented in this thesis can be summarised as follows:

- After reclassification of the glaciers, 145 of the 504 glaciers in the Svalbard database are classified as surge-type. This is about 14% of the total glacier population in Svalbard and these surge-type glaciers cover approximately 50% of the total glaciated area of the archipelago. This percentage is much lower than previously published figures on glacier

surging in Svalbard (e.g. Liestøl, 1969 Jania, 1988; Lefauconnier and Hagen, 1991; Hamilton, 1992).

- The factors that have been identified to control surging in Svalbard suggest that the surge mechanism in this region is most likely related to a soft deformable bed in which the thermal regime could have a regulatory effect (e.g. Clarke *et al.*, 1984; Mooers, 1990; Murray *et al.*, in review). The linked-cavity surge mechanism (Kamb, 1987) is found not to be valid surge mechanism in Svalbard, given that the criteria low slope and Fowler's index are not found to be significant parameters in distinguishing surge-type glaciers from normal glaciers in this region. The prevalence of surge-type glaciers overlying fine-grained sedimentary lithologies is consistent with the findings of Boulton and Jones (1979), Boulton (1996) and Tulaczyk *et al.* (1998) stating that a fine-grained unconsolidated substrate underlain by a relatively impermeable bedrock is conducive for the developments of flow instabilities and fast flow.

- The likelihood that a glacier is of surge-type increases with glacier length, both for glacier in Svalbard and in the Yukon Territory. Although longer glaciers are more likely to cross geological boundaries, neither type nor direction nor number of geological boundaries has been found significantly related to the distribution of surge-type glaciers in Svalbard. Long glaciers could have larger glacier depths than short glaciers and it is suggested that glacier thickness is a control on the thermal regime of a glacier: thick glacier have been suggested to have a polythermal regime while thin glaciers are cold throughout. A polythermal regime could create conditions that enhance surge behaviour. However, it is not clear if a polythermal regime is a cause of or a result of surge behaviour. Furthermore, a longer transport distance of glacial debris could affect the composition and properties of the subglacial bed, hence could create subglacial conditions that facilitate flow instabilities. Additionally, an innovative physical explanation for length being a primary control of glacier surging could be a length-related attenuation of longitudinal stresses: stress distributions in longer glaciers could affect the overall dynamic behaviour in such a way that either flow instability or restriction in outflow is enhanced in these glaciers.

- When data is available on maximum elevation, median elevation and minimum elevation of glaciers, an approximate glacier hypsometry curve can be obtained, as well a measure for altitude skewness (Etzelmüller and Sollid, 1997). Using this approximate hypsometry in combination with equilibrium line altitude, the accumulation area ratio can be calculated, thus giving a measure for glacier health. Testing these parameters on the incidence of glacier surging in Svalbard, no mass balance related control on glacier surging could be

established. Therefore, no foundation of a balance flux control on glacier surging as postulated by Budd (1975) was ascertained. This null-finding could however be a result of the crude measure for mass balance related data in this study.

- The data on glacier surging in East Greenland give the impression that surge behaviour in this region is similar to that occurring in Svalbard rather than to that observed in other cluster regions of surge-type glaciers. However, there is not enough accurate data to support this hypothesis and accurate data on onset and termination of surges as well as propagation of surges in Greenland through field or remote sensing measurements is necessary to test this hypothesis.

- From observations on the interaction of flow units in the Sortebræ complex and from the possible controls on glacier surging it is concluded that restriction in outflow could control the surge potential of glaciers. This finding is in agreement with Clarke *et al.* (1984), postulating that downstream resistance to sliding is the cause for surge-type glaciers to have an unstable flow behaviour.

9.2 Suggestions for further research

The research in this thesis suggests that specific combinations of glacier and environmental attributes control glacier surging. It is however plausible that these controls are local controls and that the surge controls in other regions are of a different type, on the condition that more than one surge mechanism exists for different regions. Because the surge behaviour of glaciers in East Greenland has been found similar to the surge behaviour common in Svalbard, it would first of all be necessary to investigate if the surge controls in these two regions are of the same kind. Therefore, a similar multivariate logit analysis could be performed for a cluster region of surge-type glaciers in East Greenland. Furthermore, the analysis could be expanded to other cluster regions of surge-type glaciers.

Geological variables were used in this thesis as an alternative to physical properties of the substrate. This method is obviously too inexact to fully represent possible controls on ice-bed interaction, including substrate rheology, subglacial hydrology and basal thermal regime. Improvements in data representing subglacial conditions could therefore include for example (approximate) average conductivities, porosities and water storage capacities (e.g. Freeze and Cherry, 1979; Marshall *et al.*, 1996) and measures for bed roughness, thermal conductivity and effective viscosity (e.g. Murray, 1997). Similarly, improvements could be made on mass balance related attributes. For example, instead of using approximate hypsometries and

therefore inaccurate measures for accumulation area ratio the hypsometry of glaciers could be established more accurately using DEMs and automated methods. Other suggestions for expanding the number of tested attributes and for improvements to the existing data are assigning a measure for the complexity of the glacier system (e.g. the higher the circumference:area ratio the more complex the glacier system is) and to include accurate surface and bed profiles for glaciers for which radio-echo sounding data are available. Further, some aspects of planned research for this thesis was hampered by a lack of (accurate) data. For example, temporal variations in surge behaviour are not adequately studied (e.g. Muller and Fleisher, 1995; Lawson, 1996), mainly because of the time scale at which these are occurring being longer than the time period of detailed observation. Moreover, systematic collection of certain data is time consuming and is left for future research.

Although the method of multivariate logit regression has some advantages to previously used methods, the discussion in Section 8.4 clarifies that there are several drawbacks to the method. By using other data analysis methods capable of handling a mixture of attribute data, it can be established to which extent the attributes that have been detected as characteristic for surge-type glaciers, are actual (possible) controls on glacier surging or if these are a result of the model structure and link functions. For example, techniques which are not bounded by link functions, nor by data distribution are neural networks, fuzzy logic models and data retrieval systems. These techniques have been successfully used to for example forecast avalanches, flooding and response of a subglacial drainage system (e.g. Purves and Sanderson, 1998; Corne *et al.*, in press), but the drawback of these models is that they are generally of a 'black box' type. It is therefore doubtful if the underlying primary controls on glacier surging will emerge from this type of analysis. Another technique that can be used to differentiate characteristics of surge-type glaciers from that of normal glaciers is a scaling method (Bahr, 1997). According to Bahr (1997) the global distribution of glacier properties can be described as relationships between the area distribution and other properties (for example length, average width, volume and mass balance characteristics of a glacier). Using scaling analysis, these relationships have been described as simple power laws. Assuming we can distinguish between the populations of surge-type glaciers and non-surge-type glacier we would expect these power laws to be different for the two populations. If it could be established that scaling up laws are different for surge-type glaciers than for non-surge-type glaciers then evaluation of the determined scaling up laws could suggest further controls on surging. In addition, explorative and predictive spatial (point) patterns analysis into the distribution of surge-type glaciers may reveal additional environmental controls on surging. It is essential to find where surge-type glaciers are clustered relative to the glacier population and relative to subsets (e.g. small glaciers, large glaciers, glaciers overlying specific bedrock) of the glacier population. Furthermore, research into systematic differences in

surge behaviour and relating these differences to environmental conditions and/or glacier morphology could aid the understanding of controls on glacier surging.

The 1990s surge of Sortebræ is, after Storstrømmen (Reeh *et al.*, 1994; Mohr *et al.*, 1998), the best recorded surge in East Greenland. Still, for a thorough analysis of this surge certain essential data are missing, leaving a number of phenomena unexplained and a large number of questions open. For example, the waves appearing on the surface of one of Sortebræ's upper basins after the surge (see Section 7.5.8) require further attention. Although these could be the result of kinematic waves travelling downglacier during the surge and clearly suggest a specific longitudinal strain rate distribution over the glacier, it is not entirely clear what the associations between these waves and the ice flow dynamics are. A detailed analysis of crevasse patterns could help reconstructing the tectonic processes that took place during the Sortebræ surge (e.g. Sharp *et al.*, 1988; Hodgkins and Dowdeswell, 1994). Further, accurate measurement of surface velocity during quiescence and surge would give an indication of the velocity imbalance of the glacier, and, together with accumulation data, would enable us to calculate the recovery time of the glacier. From these data further information about strain rate distribution could be obtained as well (e.g. McMeeking and Johnson, 1986). Velocity measurements and crevasse patterns could for example be obtained using remotely sensed data (e.g. Dwyer, 1993; Rolstad *et al.*, 1997; Mohr *et al.*, 1998). From these, a more accurate estimate of the timing of surge initiation and termination could be obtained as well.

Although the field- and remote sensing analysis of surge-type glaciers is still in the increase, specific studies on environmental controls on surging are sparse. There are a number of objectives that should ideally be addressed while studying the dynamics of (surge-type) glaciers.

1. Detailed study of the group of irregular or 'unusual' surge-type glaciers identified through the residual analysis in this study could reveal further controls on surging. These studies could involve comparative studies of surge-type glaciers on for example similar substrate but with different dimensions or climatic conditions. For example, surge-type glaciers in East and West Greenland overlie similar Tertiary basalts (Weidick, 1988), but exhibit differences in surge behaviour. Differences in, for example, glacier size, thermal regime or local climate could play a role in determining the ultimate properties of the substrate and hence could explain observed differences in surge behaviour.
2. Apart from concentrating on finding mechanisms that cause flow instability, as described in Chapter 2 of this thesis, it could be necessary to ascertain what causes the restriction in outflow that is characteristic of surge-type glaciers. From a discussion of possible controls on restriction of outflow in section 2.1.12 (Chapter 2), clearly a large number of possible mechanisms related to restriction of outflow have been proposed, including mechanisms of

increased (local) friction, blocking and obstructing. Specific field studies should be undertaken to what extent glacier flow is controlled by local variations in these mechanisms that possibly obstruct glacier flow. A systematic analysis of velocity imbalance (difference between balance velocity and actual velocity) could for example lead to a proxy dataset on degree of outflow restriction. From these data, specific glaciers could be identified for field analysis.

3. The research in this thesis could not establish relationships between geological boundaries and surge potential. It would be of general interest in glacier dynamics studies to establish what, if any, the direct effects of changes in subglacial lithology on glacier dynamics are. Although several studies have been performed to the effect of a glacier flowing over different lithologies and of transport distance on the englacial sediment content and character of the basal ice layer (e.g. Boulton, 1970; Dreimanis and Vagnes, 1972; Sharp *et al.*, 1994), no direct measurements exist of processes at the transition of one type of substrate to the other. Boulton and Paul (1976) theorised that transitions from one type of substrate to another would affect the gradient and height of the piezometric surface, but no field measurements have confirmed this hypothesis. The main problem of such field studies was summarised by Boulton and Jones (1979): for the present glaciers we do not exactly know what the subglacial geological conditions and for past glaciers for which the substrate is exposed, we have no exact information on the former ice profile. However, since then, technical progress has made it possible to measure to a certain extend what is underneath the present ice covers (e.g. Richards, 1988; Blake *et al.*, 1994; Porter, 1997; Smith, 1997; Tulaczyk, 1999). Studies to into flow instabilities could focus on the detection of changes in physical processes (e.g. water pressure, decoupling, basal drag) measurable at the transition of one type of substrate to another. Do subglacial changes directly result in changes in the (local) dynamic behaviour glaciers? To what extent are possible effects of lithological boundaries on for example water pressure dampened out by a layer of unconsolidated sediments between the rock and the glacier bed (e.g. Boulton, 1996)? Further, medial moraines are a prominent feature of surge-type glaciers as is a higher than average englacial debris content. To what extent is englacial moraine material affecting glacier flow: what are the rheological consequences of the presence of this material (e.g. Souchez and Lorrain, 1991; Hambrey *et al.*, 1999)? These aspects of the processes at the ice-bed interface and of englacial glacier dynamics in respect to glacier surging need further attention.
4. It has been suggested in this thesis that the length control on surging could be explained by the distance related attenuation of longitudinal stresses (e.g. Kamb and Echelmeyer, 1987). To test this hypothesis it could be investigated whether longitudinal stress and stress gradients are a function of glacier length and if pushing and pulling power increases with glacier length (e.g. Hughes, 1992; Fountain and Walder, 1998).

References

Ahlmann, H.W., 1948. Glaciological research on the North Atlantic coasts. *R.G.S. Research Series* **1**, 80 pp.

Aitkin, M., Anderson, D., Francis, B., and Hinde, J., 1989. Statistical modelling in GLIM. Oxford University Press, Oxford.

Alley, R.B., 1989. Water-pressure coupling of sliding and bed deformation: II. Velocity-depth profiles. *J. Glaciol.* **35** (119), 119-129.

Alley, R.B., 1991. Deforming-bed origin for the southern Laurentide till sheets? *J. Glaciol.* **37** (125), 67-76.

Alley, R.B., 1992. Flow law hypotheses for ice-sheet modeling. *J. Glaciol.* **38** (129), 245-256.

Alley, R.B., 1993. In search of ice-stream sticky spots. *J. Glaciol.* **39** (133), 447-454.

Alley, R.B., Blankenship, D.D., Rooney, S.T., and Bentley, C.R., 1989. Water-pressure coupling of sliding and bed deformation: III. Applications to the Ice Stream B, Antarctica. *J. Glaciol.* **35** (119), 130-139.

Alley, R.B., and MacAyeal, D.R., 1994. Ice-rafted debris associated with binge/purge oscillations of the Laurentide Ice Sheet. *Paleoceonography* **9** (4), 503-511.

Andrews, J.T., 1972. Glacier power, mass balances, velocities and erosional potential. *Z. Geomorphologie*, NF **13**, 1-17.

Andrews, J.T., 1975. Glacial systems: an approach to glaciers and their environment. Duxbury Press, Massachusetts, 191 pp.

Anonymous, 1986. Alaska glacier seals fate of fiord wildlife. *Nature* **324**, 5.

Atkinson, P., Jiskoot, H., Massari, R., and Murray, T., 1998. Generalized linear modelling in geomorphology. *Earth Surf. Process. Landforms.* **23**, 1185-1195.

Bahr, D.B., 1997. Global distribution of glacier properties: A stochastic scaling paradigm. *Water Resources Research* **33** (7), 1669-1679.

Bahr, D.B., and Dyurgerov, M.B., 1999. Characteristic mass-balance scaling with valley glacier size. *J. Glaciol.* **45** (149), 17-21.

Bahr, D.B., Pfeffer, T., Sassolas, C., and Meier, M.F., 1998. Response time of glaciers as a function of size and mass balance: I Theory. *J. Geophys. Res.* **103** (B5), 9777-9782.

Bamber, J.L., 1987. Internal reflecting horizons in Spitsbergen glaciers. *Ann. Glaciol.* **9**, 5-10.

Bamber, J.L., 1988. Notes on the Svalbard radio echo sounding database. 19 pp.

Bamber, J.L., 1989. Ice/bed interface and englacial properties of Svalbard ice masses deduced from airborne radio echo-sounding data. *J. Glaciol.* **35** (119), 30-37.

Bamber, J.L., and Dowdeswell, J.A., 1990. Remote-Sensing studies of Kvitøyjøkulen, and ice cap on Kvitøya, north-east Svalbard. *J. Glaciol.* **36** (122), 75-81.

Baranovski, S., 1977. The subpolar glaciers of Spitsbergen seen against the climate of this region. *Acta Universitatis Wratislaviensis* **410**, 111 pp.

Bauer, A., 1968. Missions aériennes de reconnaissance au Groenland 1957-1958. Observations aériennes et terrestres, exploitation des photographies aériennes, détermination des vitesses des glaciers vêlant

dans Disko Bugt et Umanak fjord. E.G.I.G. 1957-1960 Vol. 2 No. 1, *Meddelelser om Grønland* **173** (3), 116 pp.

Bindschadler, R., 1982. A numerical model of temperate glacier flow applied to the quiescent phase of a surge-type glacier. *Glaciol.* **28** (99), 239-265.

Bindschadler, R., 1983. The importance of pressurized subglacial water in separation and sliding at the glacier bed. *Glaciol.* **29** (101), 3-19.

Bindschadler, R., Harrison, W.D., Raymond, C.F. and Gantet, C., 1976. Thermal regime of a surge-type glacier. *J. Glaciol.* **16** (74), 251-259.

Bindschadler, R., Harrison, W.D., Raymond, C.F. and Crosson, C., 1977. Geometry and dynamics of a surge-type glacier. *J. Glaciol.* **18** (79), 181-194.

Björnsson, H., 1998. Hydrological characteristics of the drainage system beneath a surging glacier. *Nature* **295**, 771-774.

Björnsson, H., Gjessing, Y., Hamran, S-E., Hagen, J.O., Liestøl, O., Pálsson, F., and Erlingsson, B., 1995. The thermal regime of sub-polar glaciers mapped by multi-frequency radio-echo sounding. *J. Glaciol.* **42** (140), 23-32.

Blake, E.W., Fischer, U.H., and Clarke, G.K.C., 1994. Direct measurements of sliding at the glacier bed. *J. Glaciol.* **40** (136), 595-599.

Blatter, H., Clarke, G.K.C., and Colinge, J., 1998. Stress and velocity fields in glaciers: Part II. Sliding and basal shear stress distribution. *J. Glaciol.* **44** (148), 457-466.

Booij, M., Leijnse, A., Hadorsen, S., Heim, M., and Rueslåtten, H., 1998. Subpermafrost Groundwater Modelling in Ny-Ålesund, Svalbard. *Nordic Hydrology* **29** (4/5), 385-396.

Boulton, G.S., 1970. On the origin and transport of englacial debris in Svalbard. *J. Glaciol.* **9** (56), 213-229.

Boulton, G.S., 1971. Till genesis and fabric in Svalbard, Spitsbergen. *In:* Goldthwait, R.P. (ed.), Till: a symposium, Ohio State University Press, 41-72.

Boulton, G.S., 1979. Processes of glacier erosion on different substrata. *J. Glaciol.* **23** (89), 15-38.

Boulton, G.S., 1987. A theory of drumlin formation by subglacial sediment deformation. *In:* Menzies, J., and Rose, J. (eds.): Drumlin Symposium. Balkema, Rotterdam, 25-55.

Boulton, G.S., 1996. Theory of glacial erosion, transport and deposition as a consequence of subglacial sediment deformation. *J. Glaciol.* **42** (140), 43-62.

Boulton, G.S., and Paul, M.A., 1976. The influence of genetic processes on some geotechnical properties of glacial tills. Quarterly Journal of Engineering Geology **9**, 157-194.

Boulton, G.S., Dent, D.I., and Morris, E.M., 1974. Subglacial shearing and crushing, and the role of water pressures in tills from south-east Iceland. *Geografiska Annaler* **56A** (3-4), 135-145.

Boulton, G.S., and Jones, A.S., 1979. Stability of temperate ice caps and ice sheets resting on beds of deformable sediment. *J. Glaciol.* **24** (90), 29-43.

Boulton, G.S., and Hindmarsh, R.C.A., 1987. Sediment deformation beneath glaciers: rheology and geological consequences. *J. Geophys. Res.* **92** (B9), 9059-9082.

Boulton, G.S., and Dobbie, K.E., 1993. Consolidation of sediments by glaciers: relations between sediment geotechnics, soft-bed glacier dynamics and subglacial ground-water flow. *J. Glaciol.* **39** (131), 26-44.

Boulton, G.S., Caban, P., and van Gijssel., 1995. Groundwater flow beneath ice sheets: Part I – Large scale patterns. *QSR* **14**, 545-562.

Braithwaite, R.J. and Müller, F., 1980. On the parameterization of glaciers equilibrium line altitude. IAHS-AISH **126**, 263-271.

Brooks, C.K., 1979. Geomorphological observations at Kangerlugssuaq, East Greenland. *Greenland Geoscience* **1**, 21 pp.

Brown, J., Ferrians, O.J., Jr., Heginbottom, J.A., and Melnikov, E.S., 1997. Circum-Arctic map of permafrost and ground-ice conditions. U.S.G.S. Circum-Pacific Map Series: Map CP-45, 1 sheet.

Bruce, R.H., Cabrera, G.A., Leiva, J.C., and Lenzano, L.E., 1987. The 1985 surge and ice dam of Glaciar Grande del Nevado sel Plomo, Argentina. *J. Glaciol.* **33** (113), 131-132.

Budd, W.F., 1970. Ice flow over bedrock perturbations. *J. Glaciol.* **9** (55), 29-48.

Budd, W.F., 1975. A first model for periodically self-surging glaciers. *J. Glaciol.* **14** (70), 3-21.

Budd, W.F., and Warner, R.C., 1996. A computer scheme for rapid calculations of balance-flux distributions. *Ann. Glaciol*. **23**, 21-27.

Chinn, T.J.N., 1989. Glaciers of New Zealand. *In:* R.S. Williams, Jr., and J.G. Ferrigno (eds.). Satellite image atlas of glaciers of the world: Irian Jaya, Indonesia and new Zealand. *USGS Professional Paper* **1386-H**, 23-48.

Clapperton, C.M., 1975. The debris content of surging glaciers in Svalbard and Iceland. *J. Glaciol.* **14** (72), 395-406.

Clarke, G.K.C., 1976. Thermal regulation of glacier surging. *J. Glaciol.* **16** (74), 231-250.

Clarke, G.K.C., 1987a. Fast glacier flow: ice streams, surging, and tidewater glaciers. *J. Geophys. Res.* **92** (B9), 8835-8841.

Clarke, G.K.C., 1987b. Subglacial till: A physical framework for its properties and processes. *J. Geophys. Res.* **92** (B9), 9023-9036.

Clarke, G.K.C., 1991. Length, width and slope influences on glacier surging. *J. Glaciol.* **37** (126), 236-246.

Clarke, G.K.C., and Jarvis, G.T., 1976. Post-surge temperatures in Steele glacier, Yukon Territory, Canada. *J. Glaciol.* **16** (74), 261-268.

Clarke, G.K.C., Nitsan, U., and Paterson, W.S.B., 1977. Strain heating and creep instability in glaciers and ice sheets. *Reviews of Geophysics and Space Physics* **15** (2) 235-247.

Clarke, G.K.C., Collins, S.G., and Thompson, D.E., 1984. Flow, thermal structure, and subglacial conditions of a surge-type glacier. *Can. J. Earth. Sc.* **21**, 232-240.

Clarke, G.K.C., Schmok, J.P., Ommanney, C.S.L. and Collins, S.G., 1986. Characteristics of surge-type glaciers. *J. Geophys. Res.* **91** (B7), 7165-7180.

Clarke, G.K.C., and Blake, E.W., 1991. Geometric and thermal evolution of a surge-type glacier in its quiescence state: Trapridge Glacier, Yukon Territory, Canada, 1969-89. *J. Glaciol.* **37** (125), 158-169.

Clayton, L., Mickelson, D.M., and Attig, J.W., 1989. Evidence against pervasively deformed bed material beneath rapidly moving lobes of the southern Laurentide Ice Sheet. *Sedimentary Geology* **62**, 203-208.

Collins, S.G., 1972. Survey of the Rusty Glacier area, Yukon Territory, Canada, 1967-70. *J. Glaciol.* **11** (62), 235-250.

Colvill, A.J., 1984. Some observations on glacier surges, with notes on the Roslin glacier, East Greenland. *In*: Miller, K.J. (ed.). The International Karakoram Project. Vol I. Proceedings of the International Conference held at Quaid-i-Azam, Islamabad, Pakistan. Cambridge University Press, 64-75.

Conway, W.M., 1898. An exploration in 1897 of some of the glaciers of Spitsbergen. *The Geographical Journal* **12**, 137-158.

Corne, S., Murray, T., Openshaw, S., See, L., and Turton, I., in press. Using computational intelligence techniques to model subglacial water systems. To appear in *Journal of Geographical Systems*.

Corte, A.E., 1980. Glaciers and glaciolithic sytems of the central Andes. *IAHS-AISH Publ.* **126**, 11-24.

Crawley, M.J., 1993. *GLIM for ecologists. Methods in Ecology*. Blackwell Scientific Publications. 379 pp.

Croot, D.G., 1988. Glaciotectonics and surging glaciers: A correlation based on Vestspitsbergen, Svalbard, Norway. *In:* Croot, D.G. (ed.): Glaciotectonics: forms and processes. A.A. Balkema, 49-62.

Davis, J.C., 1986. *Statistics and data analysis in geology*. Second edition. John Wiley and sons, 646 pp.

Davis, J.L., Halliday, J.S., and Miller, K.J., 1973. Radio echo sounding on a valley glacier in East Greenland. *J. Glaciol.* **12** (64), 87-91.

De Geer, G., 1900. Om östra Spitsbergens glaciation under istiden. *Geol. Fören.* Stockholm Förh. **22** (5), 427-436.

De Geer, G., 1910. Guide de l'excursion au Spitzberg. XIe Congrès Géologique Internationale, Stockholm. 23 pp.

Dolgoushin, L.D. and Osipova, G.B., 1975. Glacier surges and the problem of their forcasting. *IAHS-AISH Publ.* **104**, 292-304.

Dowdeswell, J.A., 1986. Drainage-basin characteristics of Nordaustlandet ice caps, Svalbard. *J. Glaciol.* **32** (110), 31-38.

Dowdeswell, J.A., 1989. On the nature of Svalbard icebergs. *J. Glaciol.* **35** (120), 224-234.

Dowdeswell, J.A., 1996. Glaciers in the High Arctic and recent environmental change. *In:* Wadhams, P., Dowdeswell, J.A., and Schofield, A.N. (eds.). *The Arctic and Environmental Change.* Royal Society, Gorden and Breach, United Kingdom, 121-146.

Dowdeswell, J.A., Drewry, D.J., Liestøl, O., and Orheim, O., 1984a. Airborne radio echo sounding of sub-polar glaciers in Spitsbergen. *Norsk Polarinstitutt Skrifter* **182**, 41 pp.

Dowdeswell, J.A., Drewry, D.J., Liestøl, O., and Orheim, O., 1984b. Radio echo-sounding of Spitsbergen glaciers: problems in the interpretation of layer and bottom returns. *J. Glaciol.* **30** (104), 16-21.

Dowdeswell, J.A., and McIntyre, N.F., 1987. The surface topography of large ice masses from landsat imagery. *J. Glaciol.* **33** (113), 16-23.

Dowdeswell, J.A., and Collin, R. L., 1990. Fast-flowing outlet glaciers on Svalbard ice caps. *Geology* **18**, 778-791.

Dowdeswell, J.A., Hamilton, G.S., and Hagen, J.O., 1991. The duration of the active phase on surge-type glaciers: contrasts between Svalbard and other regions. *J. Glaciol.* **37** (127), 338-400.

Dowdeswell, J.A., Hodgkins, R., Nuttall, A.-M., Hagen, J.O., and Hamilton, G.S., 1995. Mass balance changes as a control on the frequency and occurrence of glacier surges in Svalbard, Norwegian High Arctic. *Geophysical Research Letters* **22** (21), 2909-2912.

Dowdeswell, J.A., and Bamber, J., 1995. On the glaciology of Edgeøya and Barentsøya, Svalbard. *Polar Research* **14** (2), 105-122.

Dowdeswell, J.A., and Nuttall, A.-M., 1996. Investigations of glacier surges: measurements and modelling of ice dynamics in Svalbard, European Arctic. Aberystwyth Centre for Glaciology Report **96-2**. Final Report European Union Environment Programme Grant EN5V-CT93-0299, 151 pp.

Dowdeswell, J.A., and 10 others, 1997. The mass balance of Circum-Arctic glaciers and recent climate change. University of Washington Article QR971900, 1-13.

Dowdeswell, J.A., and Williams, M., 1997. Surge-type glaciers in the Russian High Arctic identified from digital satellite imagery. *J. Glaciol.* **43** (145), 489-494.

Dowdeswell, J.A., Unwin, B., Nuttall, A.-M., Wingham, D.J., 1999. Velocity structure, flow instability and mass flux on a large Arctic ice cap from satellite radar interferometry. *Earth and Planetary Science Letters* **167**, 131-140.

Downs, P.W., 1995. Estimating the probability of river channel adjustment. *Earth Surf. Process. Landforms.* **20**, 687-705.

Dreimanis, A., and Vagners, U.J., 1972. The effect of lithology upon texture of till. *In:* Goldwaith, R.P. (ed.): Glacial deposits. *Benchmark Papers in Geology* **21**, Dowden, Hutchinson & Ross, Inc., 86-102.

Drewry, D.J., 1986. *Glacial geologic processes.* Edward Arnold Publishers Ltd., London. 276 pp.

Drewry, D.J., and Liestøl, O., 1985. Glaciological investigations of surging ice caps in Nordaustlandet, Svalbard, 1983 *Polar Record* **22** (139), 357-378.

Dueholm, K.S., and Coe, J.A., 1989. GEOPROGRAM. Program for geologic photogrammetry. *Compass* **66** (2), 59-64.

Dueholm, K.S., 1992. Geologic photogrammetry using small-frame cameras. *Rapp. Grønlands geol. Unders*. **156**, 7-17.

Dueholm, K.S., and Pedersen, A.K., 1992. The application of multi-model photogrammetry in geology - status and development trends. *Rapp. Grønlands geol. Unders*. **156**, 69-72.

Dwyer, J.L., 1993. Monitoring characteristics of glaciation in the Kangerlugssuaq Fjord Region, East Greenland, using Landsat data. Unpublished M.Sc. thesis, Univ. of Colorado, 238 pp.

Dyurgerov, M.B., and Bahr, D.B., 1999. Correlations between glacier properties: finding appropriate parameters for global glacier monitoring. *J. Glaciol.* **45** (149), 9-16.

Dyurgerov, M.B., Ayzin, V.B., and Buynitskiy, A.B., 1985. Mass accumulation in the accumulation area of Medvezhiy glacier during its quiescent period. *Mater. Glyatsiologicheskikh Issled. Khronika* **54**, 131-135.

Echelmeyer, K.A. and Kamb, B., 1987. Glacier flow in a curving channel. *J. Glaciol.* **33** (115), 281-292.

Echelmeyer, K., Butterfield, R. and Cuillard, D., 1987. Some observations on a recent surge of Peters Glacier, Alaska, U.S.A. *J. Glaciol.* **33** (115), 341-445.

Echelmeyer, K., and Wang Zhongxiang, 1987. Direct observations of basal sliding and deformation of basal drift at sub-freezing temperatures. *J. Glaciol.* **33** (113), 83-98.

Engelhardt, H., and Kamb, B., 1988. Basal sliding of Ice Stream B, West Antarctica. *J. Glaciol.* **44** (147), 223-230.

Engeset, R.V., and Weydahl, D.J., 1998. Analysis of glaciers and geomorphology on Svalbard using multitemporal ERS-1 SAR images. *IEEE Transactions on Geoscience and Remote Sensing* **36** (6), 1979-1887.

Etzelmüller, B., and Sollid, J.L., 1997. Glacier geomorphology - and approach for analyzing long-term glacier surface changes using grid-based digital elevation models. *Ann. Glaciol.* **24**, 135-141.

Fatland, D.R., and Lingle, C.S., 1998. Analysis of the 1993-95 Bering Glacier (Alaska) surge using differential SAR interferometry. *J. Glaciol.* **44** (148), 532-546.

Ferrigno, J.G. and Williams Jr, R.S., 1980. Satellite Image Atlas of glaciers. *IAHS Publ.* **126**, 333-341.

Finsterwalder, S., 1897. Der Vernagtferner: Seine Geschichte und seine Vermessung in der Jaren 1888 und 1889. Wissenschagtliche Ergänzungshefte zur Zeitschrift des D.U.Ö. Alpenvereins, 41, 65-67, 85.

Fischer, U.H., Clarke, G.K.C., and Blatter, H., 1999. Evidence for temporally varying ‘‘sticky spots’’ at the base of Trapridge Glacier, Yukon Territory, Canada. *J. Glaciol.* **45** (150), 352-360.

Fleisher, P.J. Muller, E.H., Cadwell, D.H., Rosenfeld, C.L., Bailey, P.K., Pelton, J.M., and Puglesi, M.A., 1995. The surging advance of Bering Glacier, Alaska, U.S.A.: a progress report. *J. Glaciol.* **41** (137), 207-213.

Fountain, A.G., and Walder, J.S., 1998. Water flow through temperate glaciers. *Reviews of Geophysics* **36** (3), 299-328.

Fowler, A.C., 1987a. A theory of glacier surges. *J. Geophys. Res.* **92** (B9), 9111-9120.

Fowler, A.C., 1987b. Sliding with cavity formation. *J. Glaciol.* **33** (115), 255-267.

Fowler, A.C., 1989. A mathematical analysis of glacier surges. *SIAM J. Appl. Math*. **49** (1), 246-263.

Fowler, A.C., 1997. Sliding, drainage and subglacial geomorphology. *EISMINT Summerschool Lecture Notes*, 1-20.

Fowler, A.C., and Walder, 1993. Creep closure of channels in deforming subglacial till. *Proc. R. Soc. London, Ser. A* (441), 17-31.

Fowler, A.C., Björnsson, H., Murray, T., and Collins, D. (eds.), 1994. Report of the EISMINT workshop on basal processes. Iceland, 23-30 August 1993, 31 pp.

Fowler, A.C. and Johnson, C., 1995. Hydraulic run-away: a mechanism for thermally regulated surges of ice sheets. *J. Glaciol.* **41** (139), 554-561.

Francis, B., Green, M. and Payne, C., 1993. *GLIM4: The Statistical System for Generalized Linear Interactive Modelling*. Clarendon Press, Oxford, 821 pp.

Freeze, R.A. and Cherry, J.A. 1979. *Groundwater*. Prentice-Hall, 604pp.

Furbish, D.J., and Andrews, J.T., 1984. The use of hypsometry to indicate long-term stability and response of valley glaciers to changes in mass transfer. *J. Glaciol.* **30** (105), 199-211.

Gabel-Jørgensen, C.C.A., 1940. 6. og 7. Thule-expedition til Sydøstgrønland 1931-33. Leader: Knud Rasmussen. Report on the expedition. *Meddelelser om Grønland* **106** (1), 268 pp.

Gardner, J.S., and Hewitt, K., 1990. A surge of Bualtar Glacier, Karakoram Range, Pakistan: A possible landslide trigger. *J. Glaciol.* **36** (123), 159-162.

Glasser, N.F., Huddart, D., and Bennett, M.R., 1998. Ice-marginal characteristics of Fridtjovbreen (Svalbard) during its recent surge. *Polar Research* **17** (1), 93-100.

Glazovsky, A.F., Macheret, Yu. Ya., Moskalevsky, M. Yu., and Jania, J., 1991. Tidewater glaciers in Spitsbergen. *In:* Kotlyakov, Ushakov and Glazovsky (eds.): Glacier-Ocean-Atmosphere Interactions. *IAHS Publ.* No. 208, 229-239.

Glazyrin, G.E., 1978. Identification of surging glaciers by morphometric characteristics. *Mater. Glyatsiologicheskikh Issled. Khronika* **33**, 136-137.

Glebova, L.N., Zverkova, N.M., Khromova, T.E., Chernova, L.P., and Narozhny, Yu.K., 1991. Some interactions of regional glacial system elements (*The World Atlas of Snow and Ice Resources* analysis). *In:* Kotlyakov, Ushakov and Glazovsky (eds.): Glacier-Ocean-Atmosphere Interactions. *IAHS Publ.* No. 208, 221-228.

Glen, J.W., 1955. The creep of polychrystalline ice. *Proceeding of the Royal Society of London.* Series A, Vol. **228**, 519-538.

Górski, M., 1997. Seismicity of the Hornsund Region, Spitsbergen: Icequakes and Earthquakes. *Publs. Inst. Geophys. Pol. Ac. Sc.*, **B-20** (308), 76 pp.

Gripp, K., 1929. Glaciologische und geologische Ergebnisse der Hamburgischen Spitsbergen-Expedition 1927. *Abhandlungen des Naturwissenschaftlichen Vereins zu Hamburg*, Band XXII 2.-4. Heft, 249 pp, 162-231.

Haeberli, W., 1986. Factors influencing the distribution of rocky and sedimentary glacier beds. *In*: Vischer, D. (ed.). Hydraulic effects at the glacier bed and related phenomena. International Workshop, 16-19 September 1985, Interlaken, Switzerland. Mitteilungen der VWHG/ETH **90**, 48-49.

Haeberli, W., and Hoelzle, M., 1995. Application of inventory data for estimating characteristics of and regional climate-change effects on mountain glaciers: a pilot study with the European Alps. *Ann. Glaciol.* **21**, 206-212.

Haeberli, W., Hoelzle, M., and Suter, S., 1998. Into the second century of worldwide glacier monitoring: prospects and strategies. *UNESCO Studies and reports in hydrology* **56**, 227 pp.

Hagen, J.O., 1987. Glacier surge at Usherbreen, Svalbard. *Polar Research* **5**, 239-252.

Hagen, J.O., 1988. Glacier surge in Svalbard with examples from Usherbreen. *Norsk geogr. Tiddskr*. **42**, 203-213.

Hagen, J.O., and Liestøl, O., 1990. Long-term mass balance investigations in Svalbard, 1950-88. *Ann. Glaciol.* **14**, 102-106.

Hagen, J.O., Lefauconnier, B., and Liestøl, O., 1991. Glacier mass balance in Svalbard since 1912. *In:* Kotlyakov, Ushakov and Glazovsky (eds.): Glacier-Ocean-Atmosphere Interactions. *IAHS Publ.* No. 208, 313-328.

Hagen, J.O., Liestøl, O., Roland, E., and Jørgensen, T., 1993. Glacier atlas of Svalbard and Jan Mayen. *Meddelelser* **129**, Norsk Polarinstitutt, 140 pp.

Hambrey, M.J., Dowdeswell, J.A., Murray, T., and Porter, P.R., 1996. Thrusting and debris entrainment in a surging glacier: Bakaninbreen, Svalbard. *Ann. Glaciol.* **22**, 241-248.

Hambrey, M.J., Bennett, M.R., Dowdeswell, J.A., Glasser, N.F., and Hyddart, D., 1999. Debris entrainment and transfer in polythermal valley glaciers. *J. Glaciol.* **45** (149), 69-86.

Hamilton, G.S., 1992. Investigations of Surge-Type glaciers in Svalbard. *Unpublished* PhD dissertation, Scott Polar Research Institute, Cambridge, 275 pp.

Hamilton, G.S. and Dowdeswell, J.A., 1996. Controls on glacier surging in Svalbard. *J. Glaciol.* **42** (140), 157-168.

Harrison, W.D., 1972. Reconnaissance of Variegated Glacier: thermal regime and surge behaviour. *J. Glaciol.* **11** (63), 455-456.

Harrison, W.D., Echelmeyer, K.A., Chacho, E.F., Raymond, C.F. and Benedict, R.J., 1994. The 1987-88 surge of West Fork Glacier, Susitna, Alaska, U.S.A. *J. Glaciol.* **40** (135), 241-254.

Hart, J.K., 1998. The deforming bed/debris-rich basal ice continuum and its implications for the formation of glacial landforms (flutes) and sediments (melt-outs). *Quaternary Science Reviews* **17**, 737-754.

Hattersley-Smith, G., 1964. Rapid advance of glacier in Northern Ellesmere Island. *Nature* **201**, 176.

Heinrichs, T.A., Mayo, L.R., Echelmeyer, K.A., and Harrison, W.D., 1996. Quiescent-phase evolution of a surge-type glacier: Black Rapids Glacier , Alaska, U.S.A.. *J. Glaciol.* **42** (140), 110-122.

Hendriksen, N., and Watt, W.S., 1968. Geological reconnaissance of the Scoresby Sund Fjord complex. *Rapp. Grønlands geol. Unders.* **15**, 72-77.

Herzfeld, U.C., and Mayer, H., 1997. Surge of Bering Glacier and Bagley Ice Field, Alaska: an update to August 1995 and an interpretation of brittle deformation patterns. *J. Glaciol.* **43** (145), 427-434.

Hewitt, K., 1969. Glacier surges in the Karakoram Himalaya (Central Asia). *Can. J. Earth Sci.* **6**, 1009-1018.

Hewitt, K., 1998. Recent glacier surges in the Karakoram Himalaya, South Central Asia, http://www.agu.org/eos_elec/ 97106e.html. Accessed: 15/1/99.

Higgins, A.K., 1990. North Greenland glacier fluctuations and calf ice production. *Polarforschung* **60** (1), 1990, 1-23.

Higgins, A.K., and Weidick, A., 1988. The world's northernmost surging glacier? *Zeitschrift für Gletscherkunde und Glazialgeologie* **24** (2), 111-123.

Hjelle, A., 1993. Geology of Svalbard. Norsk Polarinstitutt, Oslo, 162 pp.

Hodgkins, R., 1997. Glacier hydrology in Svalbard, Norwegian High Arctic. *QSR* **16** (9), 957-973.

Hodgkins, R., and Dowdeswell, J.A., 1994. Tectonic processes in Svalbard tide-water glacier surges: evidence from structural geology. *J. Glaciol.* **40** (136), 553-560.

Hoinkes, H.C., 1969. Surges of the Vernagtferner in the Ötztal Alps since 1599. *Can. J. Earth Sci.* **6**, 853-860.

Hooke, R.LeB., Calla, P., Holmlund, P., Nilsson, M., and Stroeven, A., 1989. A 3 year record of seasonal variations in surface velocity, Storglaciären, Sweden. *J. Glaciol.* **35** (120), 235-247.

Hooke, R.LeB., and Iverson, N.R., 1995. Grain-size distribution in deforming subglacial tills: Role of grain fracture. *Geology* **23** (1), 57-60.

Horvath, E.V, 1975. Glaciers of Pamir-Alay. *In:* Field, W.O. (ed.): Mountain glaciers of the northern hemisphere. Volume I. *ACRREL,* 235-265.

Horvath, E.V., and Field, W.O., 1969. References to glacier surges in North America. *Can. J. Earth Sci.* **6**, 845-851.

Hubbard, B., and Hubbard, A., 1998. Bedrock surface roughness and the distribution of subglacially precipitated carbonate deposits: Implications for formation at Glacier de Tsanfleuron, Switzerland. *Earth Surf. Process. Landforms* **23**, 261-270.

Hughes, T., 1992. On the pulling power of ice streams. *J. Glaciol.* **38** (128), 125-151.

Humlum, O., 1992. Geomorphological applications of multi-model photogrammetry. *Rapp. Grønlands geol. Unders.* **156**, 63-67.

Humphrey, N.F., and Raymond, C.F., 1994. Hydrology, erosion and sediment production in a surging glacier: Variegated Glacier, Alaska, 1982-83. *J. Glaciol.* **40** (136), 539-552.

Hutter, K., 1983. *Theoretical glaciology : material science of ice and the mechanics of glaciers and ice sheets.* Series: Mathematical approaches to geophysics. Terra Scientific Pub. Co., Dordrecht, 510 pp.

Hutter, K., 1993. Thermo-mechanically coupled ice-sheet response - cold, polythermal, temperate. *J. Glaciol.* **39** (131), 65-86.

IAHS(ICSI)/UNEP/UNESCO, 1989. World Glacier Inventory. Status 1988. (Haeberli, W., Bösch, H., Scherler, K., Ostrem, G., and Wallén, C.C., eds.).

IAHS(ICSI)/UNEP/UNESCO, 1996. Glacier Mass Balance Bulletin 4 (1994-1995). (Haeberli, W., Hoelzle, M., and Suter, S., eds.), 90 pp.

IAHS(ICSI)/UNEP/UNESCO, 1999. Glacier Mass Balance Bulletin 5 (1996-1997). Haeberli, W., Hoelzle, M., and Suter, S., eds.), 90 pp.

Iken, A., 1981. The effect of the subglacial water pressure on the sliding velocity of a glacier in an idealized numerical model. *J. Glaciol.* **27** (97), 407-421.

Iken, A., and Bindschadler, R.A., 1986. Combined measurements of subglacial water pressure and surface velocity of Findelengletscher, Switzerland: conclusions about drainage system and sliding mechanisms. *J. Glaciol.* **32** (110), 101-119.

Ingólfsson, Ó., Rögnvaldsson, RF., Bergsten, H., Hedenäs, L., Lendahl, G., Lirio, J.M., and Sejrup, H.P., 1995. Late Quaternary glacial and environmental history of Kongsøya, Svalbard. *Polar Research* **14** (2), 123-139.

Iverson, N.R., Hanson, B., Hooke, R.L., and Jansson, P., 1995. Flow mechanics of glaciers on soft beds. *Science* **267**, 80-81.

Jackson, M., and Kamb, B., 1997. The marginal shear stress of Ice Stream B, West Antarctica. *J. Glaciol.* **43** (145), 415-426.

Jania, J., 1988. Dynamic glacial processes in south Spitsbergen (in the light of photointerpretation and photogrammetric research) (Summary). *Katowice*: Uniwersytet Slaski, 256-258.

Jania, J., and Hagen, J.O. (eds.), 1996. Mass balance of Arctic glaciers. *IASC Report No 5*, Sosnowiec-Oslo, 62 pp.

Jania, J., and Glowacki, P., 1996. Is the Hansbreen in South Spitsbergen (Svalbard) a surge-type glacier? *In*: Krawczyk, W.E. (ed.) 23rd Polar Symposium, Sosnowiec, 27-43.

Jania, J., Mochnacki, D., and Gadek, B., 1996. The thermal structure of Hansbreen, a tidewater glacier in southern Spitsbergen, Svalbard. *Polar Research* **15** (1), 53-66.

Jeffries, M.O., 1984. Milne glacier, Northern Ellesmere Island, N.W.T., Canada: a surging glacier? *J. Glaciol.* **30** (105), 251-253.

Jiskoot, H., Boyle, P., and Murray, T., 1998. The incidence of glacier surging in Svalbard: evidence from multivariate statistics. *Computers and Geosciences* **24** (4), 387-399.

Jiskoot, H., Murray, T., Boyle, P., in review. Controls on the distribution of surge-type glaciers in Svalbard. Submitted to the *Journal of Glaciology.*

Jóhannesson, T., Raymond, C., and Waddington, E., 1989. Time-scale for adjustment of glaciers to changes in mass balance. *J. Glaciol.* **35** (121), 355-369.

Jóhannesson, T., and Sigurðsson, O., 1998. Interpretation of glacier variations in Iceland 1930-1995. *Jökull* **45**, 27-34.

Johnson, P.G., 1972. The morphological effects of surges of the Donjek Glacier, St Elias mountains, Yukon territory, Canada. *J. Glaciol.* **11** (62), 227-234.

Josberger, E.G., True, M.A., and Shuchman, R.A., 1994. Determination of surface features on glaciers in Alaska from ERS-1 SAR observations. *In:* Stein, T.L. (ed.): IGARSS '94 Surface and atmospheric remote sensing: technologies, data analysis and interpretation, Volume 4. *IEEE*, 2398-2400.

Joughin, I., Tulaczyk, S., Fahnestock, M., and Kwok, R., 1996. A mini-surge on the Ryder Glacier, Greenland, observed by satellite radar interferometry. *Science* **274** (5285), 228-230.

Joughin, I., Fahnestock, M., Kwok, R., Gogineni, P., and Allen, C., 1999. Ice flow of Humboldth, Petermann and Ryder Gletscher, northern Greenland. *J. Glaciol.* **45** (150), 231-241.

Kamb, B., 1987. Glacier surge mechanisms based on linked cavity configuration of the basal water conduit system. *J. Geophys. Res.* **92** (B9), 9083-9100.

Kamb, B., Raymond, C.F., Harrison, W.D., Engelhardt, H., Echelmeyer, K.A., Humphrey, N., Brugman, M.M. and Pfeffer, T., 1985. Glacier Surge Mechanism: 1982-1983 Surge of Variegated Glacier, Alaska. *Science* **227** (4686), 469-479.

Kamb, B., and Engelhardt, H., 1987. Waves of accelerated motion in a glacier approaching surge: the mini-surges of Variegated Glacier, Alaska. *J. Glaciol.* **33** (113), 27-46.

Kamb, B. and Echelmeyer, K.A., 1987. Stress-gradient coupling in glacier flow: I Longitudinal averaging of the influence of ice thickness and surface slope. *J. Glaciol.* **32** (111), 267-284.

Kasser, P., 1980. On the effect of topographic orientation on the variations in glacier length. . IAHS-AISH **126**, 305-311.

Kirchner, G., 1963. Observations at bore holes sunk through the Schuchert Gletscher in north-east Greenland. *J. Glaciol.* **4** (36), 817-818.

Kirkby, M.J., 1987. Models in geography. *In:* Clark *et al.* (eds.): Horizons in physical geography. Macmillan Education Ltd., 47-61.

Knight, P.G., 1997. The basal ice layer of glaciers and ice sheets. *Quaternary Science Reviews* **16**, 975-993.

Knizhnikov, Yu.F., Osipova, G.B., Tsvetkov, D.G., and Kharkovets, E.G., 1997. Measurements of the movement of surging glaciers by the method of aeropseudoparallaxes (using the Medvezhiy glacier as an example). *Mater. Glyatsiol. Issledovaniy Publ.* **81**, Proceedings of the international symposium 'Seasonal and longterm fluctuations of nival and glacial processes in mountains'. Tasjkent, September 12-19, 1993, 55-60.

Kotlyakov, V.M., 1980. Problems and results of mountain glaciers in the Soviet Union. *IAHS-AISH* **126**, 129-137.

Kotlyakov V.M., and Macheret. Yu.Ya., 1987. Radio-echo sounding of sub-polar glaciers in Svalbard: some problems and results of Soviet studies. *Ann. Glaciol.* **9**, 151-159.

Kotlyakov, V.M., Osipova, G.B., and Tsvetkov, D.G., 1997. Fluctuations of unstable mountain glaciers: scale and character. *Ann. Glaciol.* **24**, 338-343.

Krass, M.S., Larina, T.B., and Macheret, Yu.Ya., 1991. Formation of the thermal regime of subpolar glaciers under climate change. *In:* Kotlyakov, Ushakov, Glazovsky (eds.): Glacier-Ocean-Atmosphere Interactions. *IAHS Publ.* no. 208, 515-525.

Lambeck, K., 1995. Constraints on the Late Weichselian ice sheet over the Barents Sea from observations of raised shorelines. *Quaternary Science Reviews* **14**, 1-16.

Lamplugh, G.W., 1911. On the shelly moraine of Sefström Glacier and other Spitsbergen phenomena illustrative of British glacial conditions. *Proc. Yorks. Geol. Soc.* **XVII**, 216-241.

Landvik, J.Y., Mangerud, J., and Salvigsen, O., 1988. Glacial history and permafrost in the Svalbard area. *In:* Sennesset, K. (ed.) *Permafrost. Fifth International Conference* 2-5 August 1988. Proceedings Volume I, 194-198.

Landvik, J.Y., Hjort, C., Mangerud, J., Möller, P., and Salvigsen, O., 1995. The Quaternary record of eastern Svalbard - an overview. *Polar Research* **14** (2), 95-103.

Larsen, H.C, Brooks, C.K., Hopper, J.R., Dahl-Jensen, T., Pedersen, A.K., Nielsen, T.F.D., and field parties, 1995. The Tertiary opening of the North Atlantic: DLC investigations along the east coast of Greenland. *Rapp. Grønlands geol. Unders.* **165**, 106-115.

Lawson, W., 1996. Structural evolution of Variegated Glacier, Alaska, U.S.A., since 1948. *J. Glaciol.* **42** (141), 261-270.

Lawson, W., 1997. Spatial, temporal and kinematic characteristics of surges of Variegated Glacier, Alaska. *Ann. Glaciol.* **24**, 95-101.

Lefauconnier, B., and Hagen, J.O., 1990. Glaciers and climate in Svalbard: Statistical analysis and reconstruction of the Brøggerbreen mass balance for the last 77 years. *Ann. Glaciol.* **14**, 148-152.

Lefauconnier, B., and Hagen, J.O., 1991. Surging and calving glaciers in Eastern Svalbard. *Norsk Polarinst. Meddel.* **116**, 130 pp.

Leiva, J.C., Lenzano, L.E., Cabrera, G.A., and Suarez, J.A., 1989. Variations of the Rio Plomo glaciers, Andes Centrales Argentinos. *In*: Oerlemans, J. (ed.), *Glacier Fluctuations and Climate Change*, Kluwer Ac. Publ., 143-151.

Liao, T.F., 1994. Interpreting probability models: logit, probit, and other generalized linear models. *Quantitative approaches in social sciences* **07-101**, 87 pp.

Liestøl, O., 1969. Glacier surges in West Spitsbergen. *Can. J. Earth Sc.* **6**, 895-897.

Liestøl, O., 1977. Pingos, springs and permafrost in Spitsbergen. *Norsk polarinstitutt Årbok 1975*, 7-29.

Liestøl, O., 1984. Glaciological work in 1983. *Norsk Polarinstitutt Årbok 1983*, 35-45.

Liestøl, O., 1990. Glaciers in the Kongsfjorden area. *Norsk Polarinstitutt Årbok 1989*, 51-61.

Liestøl, O., 1993. Glaciers of Svalbard, Norway. *In:* Williams, R.S. Jr., and Ferrigno, J.G. (eds.). Satellite image atlas of glaciers of the world: Europe. *USGS Professional Paper* **1386-E**, 127-151.

Liestøl, O., Repp, K. and Wold, B., 1980. Supra-glacial lakes in Spitsbergen. *Norsk geogr. Tiddskr.* **34**, 89-92.

Lingle, C.S., Post, A., Herzfeld, U.C., Molnia, B.F., Krimmel, R.M., and Roush, J.J., 1993. Correspondence. Bering Glacier surge and iceberg-calving mechanism at Vitus Lake, Alaska, U.S.A. *J. Glaciol.* **39** (133), 722-727.

Liu Chaohai and Ding Liangfu, 1986. The newly progress of glacier inventory in Tianshan Mountains.(Abstr.) *J. Glaciology and Geocryology* **8** (2), 170.

Lliboutry, L., 1968. General theory of subglacial cavitation and sliding of temperate glaciers. *J. Glaciol.* **7** (49), 21-58.

Lliboutry, L., 1969. Contribution à la théorie des ondes glaciaires. *Can. J. Earth. Sc.* **6**, 943-873.

Lliboutry, L., 1998. Glaciers of Chile and Argentina. *In:* Williams, R.S., Jr, and Ferrigno, J.G. (eds.), Satellite image atlas of glaciers of the world. *USGS Professional Paper* **1386-I-6**, 141 pp.

Macheret, Yu. Ya., 1981. Forms of glacial relief of Spitsbergen glaciers. *Ann. Glaciol.* **2**, 45-51.

Macheret, Yu. Ya., 1990. Two-layered glaciers in Svalbard. *In:* Arctic Research: Advances and prospects. Proceedings of the conference of Arctic and Nordic countries on coordination of research in the Arctic. Leningrad, December 1988. Part I, 'Nauka', 58-60.

Macheret, Yu. Ya., and Zhuravlev A.B., 1982. Radio echo-sounding of Svalbard glaciers. *J. Glaciol.* **28** (99), 295-314.

Marshall, S.J., and Clarke, G.K.C., Dyke, A.S., and Fisher, D.A., 1996. Geologic and topographic controls on fast flow in the Laurentide and Cordilleran Ice Sheets. *J. Geophys. Res.* **101** (B8), 17827-17839.

Marshall, S.J., and Clarke, G.K.C., 1997. A continuum mixture model of ice stream thermomechanics in the Laurentide Ice Sheet. 1. Theory. *J. Geophys. Res.* **102** (B9), 20599-20613.

Marshall, S.J., and Clarke, G.K.C., 1999. Ice sheet inception: subgrid hypsometric parametrization of mass balance in an ice sheet model. *Climate dynamics* **15** (7), 533-550.

Mazo, A.B., and Salamatin, A.N., 1986. Modelling of surges and climatically induced fluctuations of glaciers. *Mater. Glyatsiologicheskikh Issled. Khronika* **58,** 210-214.

McMeeking, R.M. and Johnson, R.E., 1985. On the analysis of longitudinal stress in glaciers. *J. Glaciol.* **31** (109), 293-302.

McMeeking, R.M. and Johnson, R.E., 1986. On the mechanism of surging glaciers. *J. Glaciol.* **32** (110), 120-132.

Meer, van der, J.J.M., 1992. The De Geer Archive in Stockholm exemplified by the documentation on a late-nineteenth century glacier surge in Spitsbergen. *Sveriges Geologiska Undersökning,* Ser. Ca. **81**, 187-194.

Meier, M.F., 1962. Proposed definitions for glacier mass budget terms. *J. Glaciol.* **4** (33), 252-263.

Meier, M.F., 1965. Glaciers and climate. *In*: Wright, H.E., and Frey, D.G. (eds.). The Quaternary of the United States, Princeton University Press, Princeton, NJ, 795-805.

Meier, M.F. and Post, A., 1969. What are glacier surges? *Can. J. Earth Sci.* **6**, 807-817.

Meier, M.F. and Post, A., 1987. Fast tidewater glaciers. *J. Geophys. Res.* **92** (B9), 9051-9058.

Meier, M.F. and Bahr, D.B., 1996. Counting glaciers: Use of scaling methods to estimate the number and size distribution of the glaciers of the world. *CRELL Special Report* **96**/**27**, 89-94.

Melvold, K. and Hagen, J.O., 1998. Evolution of a surge-type glacier in its quiescent phase: Kongsvegen, Spitsbergen, 1964-95. *J. Glaciol.* **44** (147), 394-404.

Mercer, J.H., 1975. Glaciers of Greenland. *In:* Field, W.O. (ed.): Mountain glaciers of the northern hemisphere. Volume II. *ACRREL,* 755-808.

Miller, M.M., 1973. Enthropy and the self-regulation of glaciers in Arctic and Alpine regions. *In:* Fahey, B.D., and Thompson, R.D. (eds.) Research in Polar and Alpine geomorphology. 3rd Guelph symposium on Geomorphology, 1973. Geo Abstracts, Norwich, 136-158.

Mock, S.J., 1966. Fluctuations of the terminus of the Harald Moltke Bræ, Greenland. *J. Glaciol.* **6** (45), 369-373.

Mohr, J.J., Reeh, N., and Madsen, S.N., 1998. Three-dimensional glacial flow and surface elevation measured with radar interferometry. *Nature* **391**, 273-276.

Molnia, B.F., 1994. The 1993-1994 surge of Bering Glacier, Alaska, Slide Captions. Photographs and Captions by US Geological Survey, 1-4.

Mooers, H.D., 1990. Ice-marginal thrusting of drift and bedrock: thermal regime, subglacial aquifers, and glacial surges. *Can. J. Earth Sci.* **27**, 849-862.

Muller, E.H., and Fleisher, P.J., 1995. Surging history and potential for renewed retreat: Bering Glacier, Alaska, U.S.A. *Arctic and Alpine Research* **27** (1), 81-88.

Murray, T., 1997. Assessing the paradigm shift: deformable glacier beds. *Quaternary Science Reviews* **16**, 995-1016.

Murray, T., and Dowdeswell, J.A., 1992. Water throughflow and the physical effects of deformation on sedimentary glacier beds. *J. Geophys. Res.* **97** (B6), 8993-9002.

Murray, T., Dowdeswell, J.A., Drewry, D.J., and Frearson, I., 1998. Geometric evolution and ice dynamics during a surge of Bakaninbreen, Svalbard. *J.Glaciol.* **44** (147), 263-272.

Murray, T., Stuart, G.W., Miller, P.J., Woodward, J., Smith, A.M., Porter, P.R., and Jiskoot, H., in review. Glacier surge propagation by thermal evolution at the bed. *Submitted to JJR*, 1999.

Ng, F., and Fowler, A., in review. Sediment creep closure of wide channels overlying deformable subglacial till. Submitted to *Journal of Glaciology*

Nielsen, L.E., 1972. The ice-dam, powder-flow theory of glacier surge. *In*: Bushnell, V.C., and Ragle, R.H. (eds.). Icefield Ranges Research Project, Sci. Res. Vol 3. Am. Geogr. Soc, N.Y., 71-74.

Nurkadilov, L.K., Knegai, A.Yu., and Popov, N.V., 1986. Artificial draining of an outburst-dangerous lake at the foot of a surging glacier. *Mater. Glyatsiologicheskikh Issled. Khronika* **58,** 220-221.

Nuttall, A-M., Hagen, J.O., and Dowdeswell, J., 1997. Quiescent-phase changes in velocity and geometry of Finsterwalderbreen, a surge-type glacier in Svalbard. *Ann. Glaciol.* **24**, 249-254.

Ødegard, R.S., Hagen, J.O., and Hamran, S.E., 1997. Comparison of radio echo-sounding (30-1000 MHz) and high-resolution borehole-temperature measurements at Finsterwalderbreen, southern Spitsbergen, Svalbard. *Ann. Glaciol.* **24**, 262-267.

Oerlemans, J., 1989. On the response of valley glaciers to climatic change. *In*: Oerlemans, J. (ed.), *Glacier fluctuations and climate change*, Kluwer Academic Publishers, 353-371.

Oerlemans, J., 1996. Modelling the response of valley glaciers to climatic change. *In:* Boutron, C. (ed.). Physics and chemistry of the atmospheres of the Earth and other objects of the solar system. ERCA Volume 2, Chapter III, 91-123.

Ohmura, A., and Reeh, N., 1991. New temperature and accumulation maps for Greenland. *J. Glaciol.* **37** (125), 140-148.

Olesen, O.B., and Reeh, N., 1969. Preliminary report on glacier observations in Nordvestfjord, East Greenland. *GGU Report* **21**, 41-53.

Olesen, O.B., and Reeh, N., 1973. Glaciological observations in the south-western Scoresby Sund region. A preliminary report. *GGU Report* **58**, 49-54.

Ommanney, C.S.L., 1980. The inventory of Canadian glaciers: procedures, techniques, progress and applications. *IAHS-AISH* **126**, 35-44.

Ommanney, C.S.L., Clarkson, J., and Strome, M.M., 1973. Information booklet for the inventory of Canadian glaciers, *Glacier inventory note* **4**, Inland Waters Directorate, Environment Canada, Ottawa, Ont., 1-7.

Osipova, G.B., Tsvetkov, D.G., Bondareva, O.A., and Morozov, V.Yu., 1990. On the possibilities of aerotopographic monitoring of surging glaciers. *Mater. Glyatsiologicheskikh Issled. Khronika* **68,** 149-156.

Osipova, G.B., and Tsvetkov, D.G., 1991. Kinematics of the surface of a surging glacier (comparison of the Medvezhiy and Variegated Glaciers). *In:* Kotlyakov, Ushakov and Glazovsky (eds.): Glacier-Ocean-Atmosphere Interactions. *IAHS Publ.* No. 208, 345-357.

Palmer, A.C., 1972. A kinematic wave model of glacier surges. *J. Glaciol.* **11** (61), 65-72.

Paterson, W.S.B, 1994. The physics of glaciers. Third edition, Oxford etc., Pergamon Press, 480 pp.

Pedersen, A.K., and Dueholm, K.S., 1992. New methods for the geological analysis of Tertiary volcanic formations on Nuussuaq and Disko, central West Greenland, using multi-model photogrammetry. *Rapp. Grønlands geol. Unders*. **156**, 19-34.

Pedersen, A.K., and field party, 1995. Stereo-photography along the continental margin of East Greenland, 66ºN-70ºN. *http://www.dlc.ku.dk/DLC_docs/95-Documents/EG.html*. Accessed 11/6/99.

Pedersen, A.K., Watt, M., Watt, W.S., and Larsen, L.M., 1997. Structure and stratigraphy of the Early Teriary basalts of the Blosseville Kyst, East Greenland. *Journal of the Geological Society, London* **153**, 565-570.

Pillmore, C.L., Dueholm, K.S., Jepsen, H.F., and Schuch, C.H., 1981. Computer-assisted photogrammetric mapping system for geologic studies – a progress report. *Photogrammetria* **36**, 159-171.

Pollack, H.N., Hurter, S.J., and Johnson, J.R., 1993. Heat flow from the earth's interior: analysis of the global data set. *Reviews of Geophysics* **31**(3), 267-280.

Porter, P.R., 1997. *Glacier surging: subglacial sediment deformaton and ice-bed coupling.* Unpublished PhD thesis, School of Geography, University of Leeds, 235 pp.

Porter, P.R., Murray, T., and Dowdeswell, J.A., 1997. Sediment deformation and basal dynamics beneath a glacier surge front: Bakaninbreen, Svalbard. *Ann. Glaciol.* **24**, 21-26.

Post, A., 1967. Effects of the March 1964 Alaska earthquake on glaciers. *USGS Prof. Pap.* **544-D**, 42 pp

Post, A., 1969. Distribution of surging glaciers in western North America. *J. Glaciol.* **8** (53), 229-240.

Post, A., 1972. Periodic surge origin of folded medial moraines on Bering piedmont glacier, Alaska. *J. Glaciol.* **11** (62), 219-226.

Post, A., and LaChapelle, E., 1972. *Glacier Ice*. The Mountaineers, Seattle, 110 pp.

Purves, R.S., and Sanderson, M., 1998. A methodology to allow avalanche forcasting on an information retrieval system. *Journal of Documentation* **54 (**2), 198-209.

Radok, U., Jenssen, D., and McInnes, 1987. On the surging potential of polar ice streams. Antarctic surges - a clear and present danger? Report for the US Dept. of Energy. *DOE/ER/60197-H1*. 1, 57 pp.

Ramberg, H., 1964. Note on model studies of folding of moraines in piedmont glaciers. *J. Glaciol.* **5** (38), 207-218.

Raymond, C.F., 1980. Temperate valley glaciers. *In:* Colbeck, C.S. (ed.): Dynamics of snow and ice masses. AP Inc., 79-139.

Raymond, C.F., 1987. How do glaciers surge? A review. *J. Geophys. Res.* **92** (B9), 9121-9134.

Raymond, C.F., and Malone, S., 1986. Propagation of strain anomalies during mini-surges of Variegated Glacier, Alaska, U.S.A. *J. Glaciol.* **32** (111), 178-191.

Raymond, C.F., Jóhannesson, T., and Pfeffer, T., 1987. Propagation of a glacier surge into stagnant ice. *J. Geophys. Res.* **92** (B9), 9037-9049.

Raymond, C.F., and Harrison, W.D., 1988. Evolution of Variegated Glacier, Alaska, U.S.A., prior to its surge. *Glaciol.* **34** (117), 154-169.

Reeh, N., Bøggild, C.E. and Oerter, C., 1994. Surge of Storstrømmen, a large outlet glacier from the Inland Ice of North-East Greenland. *Rapp. Grønlands geol. Unders.* **162**, 201-209.

Repp, K., 1988. The hydrology of Bayelva, Spitsbergen. *Nordic Hydrology* **19**, 259-286.

Richards, M.A., 1988. Seismic evidence for a weak basal layer during the 1982 surge of Variegated Glacier, Alaska, U.S.A. *J. Glaciol.* **34** (116), 111-120.

Rivera, A., Aravena, J.C., and Casassa, G., 1997. Recent fluctuations of Glaciar Pío XI, Patagonia: Discussion of glacial surge hypothesis. *Mountain Research and Development* **17** (4), 309-322.

Robin, G. de Q., 1955. Ice movement and temperature distribution in glaciers and ice sheets. *J. Glaciol.* **2** (18), 523-532.

Robin, G. de Q., 1969. Initiation of glacier surges. *Can. J. Earth. Sc.* **6**, 919-928.

Robin, G. de Q., and Weertman, J., 1973. Cyclic surging of glaciers. *J. Glaciol.* **12** (64), 3-17.

Rolstad, C., Amlien, J., Hagen, J-O., and Lundén, B., 1997. Visible and near-infrared digital images for determination of ice velocities and surface elevation during a surge on Osbornebreen, a tidewater glacier in Svalbard. *Ann. Glaciol.* **24**, 255-261.

Röthlisberger, H., 1969. Evidence for a glacier surge in the Swiss Alps. *Can. J. Earth. Sc.* **6**, 867-873.

Röthlisberger, H., 1972. Water pressure in intra- and subglacial channels. *J. Glaciol.* **11** (62), 177-203.

Röthlisberger, H., and Iken, A., 1971. Plucking as an effect of water pressure variations at the glacier bed. *Ann. Glaciol.* **2**, 57-62.

Rototayev, K.P., 1986. Problems of diagnostics, statistical analysis and classification of instabilities in glacier dynamics. *Mater. Glyatsiologicheskikh Issled. Khronika* **58,** 205-209.

Rucklidge, J., 1966. Observations of hollows in the snow surface of Torv Gletscher, East Greenland. *J. Glaciol.* **6** (45), 446-449.

Rundquist, D.C., Collins, S.G., Barnes, R.B., Bussom, D.E., Samson, S.A., and Peake, J.S., 1978. The use of Landsat information for assessing glacier inventory parameters. *IAHS-AISH* **126**, 321-329.

Rutishauser, H., 1971. Observations on a surging glacier in East Greenland. *J. Glaciol.* **10** (59), 227-236.

Rutter, N.W., 1969. Comparison of moraines formed by surging and normal glaciers. *Can. J. Earth. Sc.* **6**, 991-999.

Salvigsen, O., Adrielson, L., Hjort, C., Kelly, M., Landvik, J.Y., and Ronnert, L., 1995. Dynamics of the last glaciation in eastern Svalbard as inferred from glacier-movement indicators. *Polar Research* **14** (2), 141-152.

Sauber, J., Plafker, G., and Gipson, J., 1995. Geodetic measurements used to estimate ice transfer during Bering Glacier surge. *Eos* **76** (29), 289-290.

Schumskii, P.A., 1964. *Principles of structural glaciology: The petrography of fresh-water ice as a method of glaciological investigation.* Dover Publications, Inc., New York, 497 pp.

Schweizer, J., and Iken, A., 1992. The role of bed separation and friction in sliding over an undeformable bed. *J. Glaciol.* **38** (128), 77-92.

Schwitter, M.P., and Raymond, C.F., 1993. Changes in the longitudinal profiles of glaciers during advance and retreat. *J. Glaciol.* **39** (133), 582-590.

Schytt, V., 1969. Some comments on glacier surges in Eastern Svalbard. *Can. J. Earth. Sc.* **6**, 867-873.

Sclater, J.G., Jaupart, C., and Galson, D., 1980. The heat flow through oceanic and continental crust and the heat loss of the earth. *Review of Geophysics and Space Physics* **18** (1), 269-311.

Sharp, M., 1985. "Crevasse-fill" ridges-a landform type characteristic of surging glaciers. *Geogr. Ann.* **67A** (3-4), 213-220.

Sharp, M., 1988a. Surging glaciers: behaviour and mechanisms. *Progress in Physical Geography* **12** (4), 349-370.

Sharp, M., 1988b. Surging glaciers: geomorphic effects. *Progress in Physical Geography* **12** (4), 533-559.

Sharp, M., Lawson, W., and Anderson, R.S., 1988. Tectonic processes in a surge-type glacier. *J. Struct. Geol.* **10** (5), 499-515.

Sharp, M., Jouzel, J., Hubbard, B., and Lawson, W., 1994. The character, structure and origin of the basal ice layer of a surge-type glacier. *J. Glaciol.* **40** (135), 327-340.

Shih Ya-feng, Hsieh Tze-chu, Cheng Pen-hsing and Fei Ching-shen, 1980. Distribution, features and variations of glaciers in China. *IAHS-AISH Publ.* **126**, 111-116.

Siegel, E., Dowlatabadi, H., and Small, M.J., 1995. A probabalistic model of ecosystem prevalence. J. Biogeogr. 22, 875-879.

Siegert, M.J., and Dowdeswell, J.A., 1995. Numerical modelling of the late Weichselian Svalbard-Barents sea ice sheet. *Quaternary Research* **43**, 1-13.

Simpson, 1951, E.H., The interpretation of interaction in contingency tables. *Journal of the Royal Statistical Society* **2**, 238-241.

Smith, A.M., 1997. Basal conditions on Rutford Ice Stream, West Antarctica, from seismic observations. *J. Geophys. Res.* **102** (B1), 543-552.

Smolyarova, N.A., 1987. Statistical analysis of interrelations of the main properties of glaciers. *Mater. Glyatsiologicheskikh Issled. Khronika* **59**, 146-149.

Souchez, R.A., and Lorrain, R.D., 1991. Ice composition and glacier dynamics. Springer-Verlag, 207 pp.

Squires, G.L., 1976. *Practical Physics –2/e*. McGraw-Hill Book Company (UK) Ltd, 224 pp.

Stacey, F.D., 1992. *Physics of the earth.* Brookfield Press, Australia, 513 pp.

Stanley, A.D., 1969. Observations of the surge of Steele Glacier, Yukon Territory, Canada. *Can. J. Earth Sci.* **6**, 819-830.

Sturm, M., 1987. Observations on the distribution and characteristics of potholes on surging glaciers. *J. Geophys. Res.* **92** (B9), 9015-9022.

Sugden, D.E., and John B.S., 1976. *Glaciers and Landscape. A geomorphological approach.* Edward Arnold, 176 pp.

Tangborn, W., 1999. Mass balance, runoff and internal water storage of the Bering Glacier, Alaska (1950-96), a preliminary report. *http://www.hymet.com/bering.htm.* Accessed: 28/8/99.

Tarr, R.S., and Martin, L., 1914. Alaskan Glacier studies of the NGS, Prince William Sound and Lower Copper River Regions. The Nat. Geogr. Soc., Washington, 498 pp.

Thomsen, Th., and Weidick, A., 1992. Climate change impact on northern water resources in Greenland. *In:* Prowse, T.D., Ommanney, C.S.L., and Ulmer, K.E. (eds.). 9th International Northern Research Basins Symposium/Workshop, Canada, 1992. NHRI Symposium No. 10, 749-781.

Thorarinsson, S., 1969. Glacier surges in Iceland with special reference to the surges of Bruárjökull. *Can. J. Earth. Sc.* **6**, 875-882.

Troitsky, L.S., 1981. The history of the glaciation of Svalbard. *Polar Geography and Geology* **5** (2), 57-81.

Tulaczyk, S., 1999. Ice sliding over weak, fine-grained tills: Dependence of ice-till interactions on till granulometry. *In:* Mickelson, D.M., and Attig, J.W. (eds.): Glacial processes past and present. Geological Society of America. Special Paper **337**, 159-177.

Tulaczyk, S., Kamb, B., Scherer, R.P., and Engelhardt, H.F., 1998. Sedimentary processes at the base of a West Antarctic ice stream: constraints from textural and compositional properties of subglacial debris. *Journal of Sedimentary Research* **68** (3), 487-496.

Uno, T., Sugii, T., Hayashi, M., 1994. Logit model for river levee stability evaluation considering the flood return period. Structural Safety 14, 81-102.

USGS, 1994. Satellite Image Atlas of Glaciers of the World. USGS Fact Sheet 009-94. *http://geochange.er.usgs.gov/pub/info/facts/atlas/.* Accessed: 9/9/99.

Van der Wateren, F.M., 1995. Structural geology and sedimentology of push moraines: Processes of soft sediment deforrmation in a glacial environment and the distribution of glaciotectonic styles. *Meded. Rijks Geol. Dienst* **54**, 168 pp.

Vaughan, D.G., 1993. Relating the occurrence of crevasses to surface strain rates. *J. Glaciol.* **39** (132), 255-266.

Wadhams, P., 1981. The ice cover in the Greenland and Norwegian seas. *Rev. Geophys. Space Phys.* **19** (3), 345-393.

Wake, C.P., and Searle, M.P., 1992. Rapid advance of Pumarikish Glacier, Hispar Glacier Basin, Karakoram Himalaya. *J. Glaciol.* **39** (131), 204-206.

Walder, J.S., 1982. Stability of sheet flow of water beneath temperate glaciers and implications for glacier surging. *J. Glaciol.* **28** (99), 273-293.

Walder, J.S., and Hallet, B., 1979. Geometry of former subglacial water channels and cavities. *J. Glaciol.* **23** (90), 335-346.

Wang Wenying, Huang Moahuan, and Chen Jianming, 1984. A surging advance of Balt Bare glacier, Karakoram mountains. *In:* Miller, K.J. (ed.). The International Karakoram Project. Vol I. Proceedings of the International Conference held at Quaid-i-Azam, Islamabad, Pakistan. Cambridge University Press, 76-83.

Weertman, J., 1967. Sliding of nontemperate glaciers. *J. Geophys. Res.* **72** (2), 521-523.

Weertman, J., 1969. Water lubrication mechanism of glacier surges. *Can. J. Earth Sci.* **6**, 929-942.

Weertman, J., 1979. The unsolved general glacier sliding problem. *J. Glaciol.* **23** (89), 97-115.

Weidick, A., 1983. Location of two glacier surges in West Greenland. *Rapp. Grønlands geol. Unders.* **120**, 100-104.

Weidick, A., 1984. Studies of glacier behaviour and glacier mass balance in Greenland - A review. *Geografiska Ann.* **66A** (3), 183-195.

Weidick, A., 1988. Surging Glaciers in Greenland- a status. *Rapp. Grønlands geol. Unders.* **140**, 106-110.

Weidick, A., 1995. Satellite image atlas of glaciers of the world: Greenland. (Edited by Williams, R.S., Jr, and Ferrigno, J.G.), *USGS Professional Paper* **1386-C**, 141 pp.

Weidick, A., Bøggild, C.E., and Knudsen, N.T., 1992. Glacier inventory and atlas of West Greenland. *Rapp. Grønlands geol. Unders.* **158**, 194 pp.

Wellman, P., 1982. Surging of Fisher Glacier, Eastern Antarctica: Evidence from geomorphology. *J. Glaciol.* **28** (98), 23-28.

Wilbur, S.C., 1988. Surging versus nonsurging glaciers: a comparison using morphometry and balance. *Unpublished* MSc. thesis, University of Alaska, Fairbanks, 113 pp.

Williams, R.S., Jr., 1983. Satellite glaciology of Iceland. *Jökull* **33**, 3-12.

Woodward, J., Sharp, M., and Arendt, A., 1997. The influence of superimposed-ice formation on the sensitivity of glacier mass balance to climate change. *Ann. Glaciol.* **24**, 186-190.

Wright Locke, C., 1981. Pictorial records of glaciers. Report **GD-10**. World Data Center A for Glaciology, 39-53.

Wrigley, N., 1985. *Categorical data analysis for geographers and environmental scientists*. Longman Inc., New York, 392 pp.

Zhang Wenjing, 1992. Identification of glaciers with surge characteristics on the Tibetan Plateau. *Ann. Glaciol.* **16**, 168-172.

Appendix I

30 RANDOMLY SELECTED GLACIERS TESTED ON SURGE EVIDENCE							
Glacier ID	***Glacier name***	***Fitted value***	***Glacier type***	***Frontal Type***	***Length [km]***	***Longitude North***	***Latitude East***
133 16	Svalbreen[1]	0.32	valley	confluent	13	77º 40' 00"	16º 35' 00"
151 08	NE Buchananisen[1]	0.11	uncertain	piedmont	3.0	78º 40' 00"	10º 59' 00"
115 03	Perseibreen[2]	0.41	valley	calving	11.5	77º 28' 00"	17º 26' 00"
143 15	Hellefonna NW[2]	0.21	outlet	normal	5.0	78º 11' 06"	17º 33' 30"
134 13	Vallåkrabreen[2]	0.28	valley	normal	11	77º 52' 00"	17º 08' 30"
147 05	Gufsbreen[2]	0.02	valley	normal	4.8	78º 51' 48"	14º 50' 00"
155 12	Conwaybreen[2]	0.30	valley	calving	16.6	79º 00' 00"	12º 45' 00"
167 10	Eddabreen[2]	0.16	valley	normal	8.6	79º 16' 00"	14º 50' 00"
167 12	Binnebreen[2]	0.04	valley	normal	4.7	79º 16' 42"	15º 12' 00"
174 04	Moltkebreen[2]	0.10	outlet	calving	10.0	78º 57' 00"	19º 52' 00"
221 03	Ericabreen[2]	0.04	outlet	normal	8.5	79º 30' 06"	21º 15' 12"
311 24	[2]	0.05	outlet	normal	5.5	77º 34' 24"	22º 01' 06"
113 02	Daudbreen[3]	0.05	valley	normal	3.6	78º 05' 06"	18º 47' 00"
113 12	Passbreen[3]	0.17	valley	normal	7.5	78º 01' 18"	17º 58' 30"
115 07	Bellingbreen[3]	0.29	valley	confluent	6.4	77º 18' 36"	17º 17' 00"
123 04	Vitkovskibreen[3]	0.09	valley	normal	9.0	76º 45' 42"	16º 16' 00"
135 16	Oppdalsbreen[3]	0.33	valley	confluent	4.9	78º 05' 24"	17º 28' 00"
142 12	Rieperbreen[3]	0.11	outlet	normal	4.0	78º 07' 06"	16º 07' 00"
146 08	Robertsonbreen[3]	0.01	valley	normal	3.7	78º 47' 12"	15º 58' 00"
156 03	Flakbreen[3]	0.06	valley	normal	3.8	79º 10' 18"	11º 58' 30"
156 07	Tinayrebreen[3]	0.24	outlet	calving	15.7	79º 12' 12"	12º 26' 00"
158 06	Marstrandbreen[3]	0.04	valley	calving	4.6	79º 40' 00"	11º 26' 30"
162 08	Emmabreen[3]	0.23	valley	calving	7.1	79º 33' 00"	12º 14' 00"
173 02	Sven Ludvigbreen[3]	0.33	outlet	calving	10.5	79º 23' 12"	18º 44' 00"
173 09	Loderbreen[3]	0.23	valley	calving	6.5	79º 12' 06"	18º 46' 30"
174 01	Vaigattbreen[3]	0.45	outlet	calving	10.8	79º 07' 00"	19º 30' 00"
211 04	[3]	0.15	outlet	calving	23.0	79º 52' 24"	26º 34' 18"
252 02	Nilsenbreen[3]	0.41	outlet	calving	43.0	80º 02' 24"	25º 11' 06"
312 02	[3]	0.07	outlet	normal	4.0	77º 33' 00"	21º 10' 18"
313 05	Blåisen N[3]	0.02	outlet	normal	3.1	78º 03' 30"	21º 52' 06"

Thirty randomly selected glaciers, initially classified as non-surge-type, with fitted values below 0.5 that were used as control set for testing whether any detailed aerial photograph interpretation would lead to the detection of a large number of new surge-type glaciers. Details about this test and conclusions are presented in Chapter 6 (Section 6.5).

[1]*Glaciers with diagnostic surge evidence that were reclassified as surge-type (2).*

[2]*Glaciers that may be of surge-type but have only one or two possibly surge related features but lacking diagnostic surge evidence and remained therefore classified as normal (10).*

[3]*Glaciers without surge features that are almost certainly of normal type (18).*

Appendix II

This appendix contains an explanation to the table headings of the data on 504 glaciers in the electronic database that can be found on the floppy disk in the back pocket of this thesis. Most of these data are from the *Glacier Atlas of Svalbard and Jan Mayen* (Hagen *et al.*, 1993), in which full details and an accuracy evaluation of these data are given. Below I indicate data from Hagen et *al.* (1993) with an asterisk*, and where these have been transformed for modelling purpose with a double asterisk**. After the explanation of the table headings in the database follows a table explaining the full geological classification used in the database.

THE FLOPPY DISK CONTAINS THE FOLLOWING FILES:

1. ***sval504.xls*** Attribute data of the 504 Svalbard glaciers used in in the data analysis presented in Chapters 5 and 6 of this thesis. File in Microsoft Excel97 format
2. ***sval504.txt*** As *sval504.xls* but in Tab delimited text format (ASCII)
3. ***readme.doc*** Explanation to the data in the tables in *sval504.xls* and *sval504.txt* as given below. File in Word97 format
4. ***readme.txt*** As *readme.doc* but in ASCII format.

EXPLANATION TO THE DATA ON 504 SVALBARD GLACIERS IN THE ELECTRONIC DATABASE ON THE FLOPPY DISK IN POCKET

*	**ID**	A five digit glacier identification number. The first three digits indicate the drainage basin number, the last two the glacier number counted counter-clockwise in that drainage basin. For details and maps see Hagen *et al.* (1993).
*	**NAME**	The (abbreviated) name of the glacier unit (when available)
	S	Surge index: 0=normal glacier, 1=surge-type glacier
	SNEW	Updated surge index: 0=normal glacier, 1=surge-type glacier
	CHECKED	Surge evidence verified by means of aerial photograph interpretation 0=glacier not checked on surge evidence, 1=glacier checked on surge evidence.
**	**LAT N**	Latitudinal location of approximate centre of the glacier unit given in degrees and tenths of degrees North
**	**LON E**	Latitudinal location of approximate centre of the glacier unit given in degrees and tenths of degrees East
*	**C1**	Glacier type: 0=uncertain, 1=ice sheet, 2=ice field, 3=ice cap, 4=outlet glacier, 5=valley glacier, 6=mountain glacier, 7=glacieret or snowfield
*	**C2**	Glacier form: 0=uncertain, 1=more than one composite firn area, 2=one composite firn area, 3=single firn area, 4=cirque glacier, 5=ice apron
*	**C3**	frontal characteristic: 0=normal terminating on land, 1=piedmont, 2=expanded foot, 3=lobed, 4=calving, 5=confluent

TABLE CONTINUED OVERLEAF →

		(CONT.)
**	**AC**	Aspect of accumulation area in octants, numbered clockwise, N=1, NE=2, *etc*.
**	**AB**	Aspect of ablation area in octants, numbered clockwise, N=1, NE=2, *etc*.
*	**AREA**	area of glacier [km^2]
*	**LENGTH**	length of centre flowline [km]
	WIDTH	average glacier width (area/length) [km]
*	**MAX**	elevation at the head of the glacier [m above sea level]
*	**MED**	elevation of contourline which divides the glacier area into two equal parts [m above sea level]
*	**MIN**	lowest elevation of the glacier terminus [m above sea level]
*	**ELA**	equilibrium line elevation [m above sea level]
	SPAN	elevation span (max-min) [m]
*	**VOLUME**	Estimated glacier volume [km^3] (see Hagen *et al.* (1993) for empirical formulae)
	SLOPE	Angle of average surface slope [degrees]
	FOWLER	Fowler's index
	HI	Hypsometry index (=(max-med):(med-min)): HI>1 bottom-heavy glacier, HI<1 top heavy glacier, HI~1 equidimensional glacier
	AAR	Accumulation area ratio (accumulation area:total area)
	ACC AREA	Accumulation area (AAR times total area) [km^2]
	IRH	Measure for thermal regime: 1=unknown (no RES data available), 2=without continuous internal reflection horizon (cold glacier), 3=with continuous reflection horizon (polythermal glacier)
	BEDROCK	Petrological category, 1=igneous, 2=metamorphic, 3=sedimentary (see overleaf)
	LITHOLOGY	Lithology type (see next page)
	PREFIX	Prefix for lithology type (see next page)
	LAYERS	Layers or inclusion in lithology type (see next page)
	GEOL.AGE	Geological age of lithology underlying the glacier: 1=Precambrian, 2=Devonian, 3=Carboniferous, 4=Permian, 5=Triassic, 6=Jurassic, 7=Cretaceous, 8=Tertiary, 9=Quaternary
	B. TYPE	Type of geological boundary in direction of ice flow: 0=none or unknown, 1=igneous-igneous, 2=igneous-metamorphic, 3=igneous sedimentary, 4=metamorphic-igneous, 5=metamorphic-metamorphic, 6=metamorphic-sedimentary, 7=sedimentary-igneous, 8=sedimentary-metamorphic, 9=sedimentary-sedimentary
	B. DIR	Direction of geological boundary in respect to ice flow: 0=unknown or no boundaries, 1=perpendicular, 2=parallel, 3=oblique
	B. NUMB	Number of geological boundaries crossed by the glacier: 0=none, 1=one, 2=more than one

FULL GEOLOGICAL CLASSIFICATION						
1 ***Petrological category***		**2** ***Lithology***	**3** ***Prefix***	**4** ***Layers or inclusions***		**5** ***Age***
1 igneous	0	undefined	undefined	Undefined	1	Pre/Cambrian
	1	granite	granitic	Granite	2	Devonian
	2	basalt	with basalt	Basalt	3	Carboniferous
	3	gabbro	carbonate/dolomite	Gabbro	4	Permian
	4	intrusive		Intrusive	5	Triassic
	5	diorite		Diorite	6	Jurassic
	6	porphyric			7	Cretaceous
	7				8	Tertiary
	8				9	Quaternary
2 metamorphic	0	undefined	undefined	undefined		
	1	quartzite	quartzitic	quartzite		
	2	schist/phyllite	schist (phyllitic)	schist (phyllitic)		
	3	amphibolite	amphibolitic	amphibolite		
	4	migmatite	migmatite	migmatite		
	5	diamictite	diamictite	diamictite		
	6	gneiss	gneiss	gneiss		
	7	marble	marble	marble		
	8			metamorphic mixed		
3 sedimentary	0	undefined	undefined	undefined		
	1	sandstone	coarse/shelly/sandy	sandstone/quarzite		
	2	siltstone	silty	siltstone		
	3	shale/mudstone	muddy/shaly	shale		
	4	limestone/carbonate/dolomite	carbonate-rich	limestone/carbonate		
	5	conglomerate	conglomerate	conglomerate		
	6	coal	coaly	coal		
	7	chert		coal+shales		
	8	tillite		siltstone+shales		
	9	marine		sand+siltstone		

The digits in this geological classification are read in sequence, starting from the petrological category. For example: a glacier with digits 31263 overlies a silty sandstone with coal layers of Carboniferous age.For the simple lithology one could use only the first two digits, which differentiates between 25 lithology types.

Appendix III

LIST OF PUBLICATIONS

Refereed international journals

Atkinson, P., Jiskoot, H., Massari, R., and Murray, T., 1998. Generalized linear modelling in geomorphology. *Earth Surf. Process. Landforms.* **23**, 1185-1195.

Jiskoot, H., Boyle, P., and Murray, T., 1998. The incidence of glacier surging in Svalbard: evidence from multivariate statistics. *Computers and Geosciences* **24** (4), 387-399.

Jiskoot, H., Murray, T., Boyle, P., in press. Controls on the distribution of surge-type glaciers in Svalbard. *Journal of Glaciology.*

Murray, T., Stuart, G.W., Miller, P.J., Woodward, J., Smith, A.M., Porter, P.R., and Jiskoot, H., in review. Glacier surge propagation by thermal evolution at the bed. *Submitted to Journal of Geophysical Research*, July 1999.

Conference proceedings

Jiskoot, H., Boyle, P., and Murray, T., 1996. Statistical modelling of the incidence of glacier surging in Svalbard. *Proceedings of the 1st International Conference on Geocomputation Volume II*, School of Geography, University of Leeds, 17-19 September 1996., 454-467.

Jiskoot, H., Boyle, P., and Murray, T., 1997. Factors controlling glacier surging: probability and residual analysis of a glacier population in Svalbard, High Arctic. AGU Fall Meeting, December 8-12, 1997. *Supplement to Eos, Transactions, AGU* **78** (46), F253.

Jiskoot, H., Pedersen, A.K., and Murray, T., 1999. Characteristics of the 1990s surge of Sortebræ, East Greenland, analysed with multi-model photogrammetry. AGU Fall Meeting, December 13-17, 1999. *Supplement to Eos, Transactions, AGU* **80** (46), F355.